Universidade de Aveiro Departamento de Ciências Médicas
2016

Joana Vieira da Silva

Proteínas do espermatozoide como alvos para contraceção e biomarcadores de fertilidade

Sperm proteins as targets for contraception and fertility biomarkers

Universidade de Aveiro Departamento de Ciências Médicas
2016

Joana Vieira da Silva

Proteínas do espermatozoide como alvos para contraceção e biomarcadores de fertilidade

Sperm proteins as targets for contraception and fertility biomarkers

Tese apresentada à Universidade de Aveiro para cumprimento dos requisitos necessários à obtenção do grau de Doutor em Biomedicina, realizada sob a orientação científica da Doutora Margarida Fardilha, Professora Auxiliar Convidada do Departamento de Ciências Médicas da Universidade de Aveiro e do Doutor José Fernando Mendes, Professor Catedrático do Departamento de Física da Universidade de Aveiro

Este trabalho é financiado por Fundos FEDER através do Programa Operacional Factores de Competitividade – COMPETE e por Fundos Nacionais através da FCT – Fundação para a Ciência e a Tecnologia no âmbito do projeto «PTDC/DTP-PIC/0460/2012»; da bolsa individual « SFRH/BD/81458/2011»; e do Instituto de Biomedicina – iBiMED «UID/BIM/04501/2013».

Dedico este trabalho aos meus pais, Clara e Armando, e ao Miguel.

o júri

presidente

Professor Doutor Carlos Fernandes da Silva
professor catedrático do Departamento de Educação e Psicologia da Universidade de Aveiro

Professor Doutor António Luís Mittermayer Madureira Rodrigues Rocha
professor catedrático do Instituto de Ciências Biomédicas Abel Salazar da Universidade do Porto

Professor Doutor José Fernando Ferreira Mendes
professor catedrático do Departamento de Física da Universidade de Aveiro

Professora Doutora Maria de Lourdes Gomes Pereira
professora associada com agregação do Departamento de Biologia da Universidade de Aveiro

Professor Doutor Duarte Luís Pignatelli Dias de Almeida
professor afiliado da Faculdade de Medicina da Universidade do Porto

Professor Doutor Carlos Pedro Fontes Oliveira
professor afiliado do Instituto de Ciências Biomédicas Abel Salazar da Universidade do Porto

Professora Doutora Margarida Sâncio da Cruz Fardilha
professor auxiliar convidada do Departamento de Ciências Médicas da Universidade de Aveiro

Doutor Marco Aurélio Gouveia Alves
Investigador do Centro de Investigação em Ciências da Saúde, Universidade da Beira Interior

agradecimentos

À minha orientadora, Margarida Fardilha, por ter sido bem mais que uma orientadora ao longo destes anos. Por me desafiar e proporcionar todas as oportunidades que estão ao seu alcance. Obrigada pela franqueza e confiança que sempre depositou em mim. É um prazer trabalhar com uma das pessoas mais íntegras e altruístas que alguma vez conheci.

Ao meu co-orientador, Professor José Fernando Mendes, pela constante disponibilidade. Por colocar ao meu alcance todas as ferramentas necessárias para a realização deste projeto. *To his research group, I3N, thank you for everything you taught me, with an unparalleled patience. Especially to Sooyeon Yoon, I couldn't have done it without you.*

To John Howl and Sarah Jones from the Molecular Pharmacology Group at the University of Wolverhampton. Thank you for your exceptional contribution to this work. I truly appreciate your hospitality and enthusiasm. If not for you, sperm cells would still be able to swim!

A todos os meus colegas do Laboratório de Transdução de Sinais. Em especial à Maria e à Juliana, que se tornaram bem mais do que colegas de trabalho, a vossa amizade foi uma das melhores partes destes anos. Ao Luís Korrodi por ser o melhor orientador (não oficial) à face da terra. À Bárbara pela incansável ajuda com os “números”.

Aos meus amigos, em especial à Joana Oliveira, à Ritinha, ao Igor e ao Hélder, por tudo o que partilhamos ao longo destes anos. Ao Edgar, por ser como família para mim. À Joana Rocha, por me lembrar todos os dias que, independentemente daquilo que nos rodeia, temos o livre arbítrio de escolher quem queremos ser.

A toda a minha (grande) família por estar sempre presente. Em especial aos meus avós e padrinhos, não existem palavras para agradecer o vosso incansável apoio e carinho.

À Gui, por mesmo longe estar sempre tão perto.

Ao Miguel, *you can´t do everything, but I know you do anything for me*.

Aos meus pais. Por me terem ensinado que estamos constantemente a ser postos à prova, mas que as pessoas são muito mais que notas, pontuações e graus. Por nunca me terem feito sentir que tinha que corresponder a qualquer expectativa e nunca se terem importado se seria advogada, bombeira ou cientista. Mas sim, se perseguia os meus sonhos com integridade, persistência e entusiasmo. Muito, muito obrigada por tudo.

palavras-chave

(in)fertilidade e contracepção masculina, espermatozoide, transdução de sinais, interacções proteína-proteína, fosfoproteína fosfatase 1, proteína precursora amilóide.

resumo

O elevado número de gravidezes indesejadas a nível mundial (~41%) reflete a necessidade premente de novos métodos contracetivos. Para já, os contracetivos masculinos estão limitados ao preservativo, ao coito interrompido e à vasectomia dado que ainda não existem métodos farmacológicos disponíveis. Por outro lado, nos países desenvolvidos, 15% dos casais são inférteis e, em metade dos casos, as causas estão relacionadas com fatores masculinos, sendo a infertilidade idiopática o tipo mais comum de infertilidade masculina. Os principais objetivos deste trabalho consistiram em (1) identificar, caracterizar e modular alvos não-hormonais para a contraceção masculina; e (2) estabelecer um conjunto de biomarcadores para avaliar a fertilidade masculina. No que toca à identificação de alvos para a contraceção masculina, foi dada especial atenção a duas proteínas e aos seus interactors: a fosfoproteína fosfatase 1 (PPP1) e a proteína percursora amilóide (APP). Caracterizámos o interactoma da subunidade catalítica gama 2 da PPP1 (PPP1CC2), uma isoforma específica do testículo e espermatozoide. Demonstrando, pela primeira vez, a interação entre a PPP1CC2 e a *A-kinase anchor protein 4* (AKAP4), uma proteína expressa especificamente no testículo essencial para a motilidade do espermatozoide, e o potencial desse complexo como alvo contracetivo. A motilidade do espermatozoide foi, então, modulada eficazmente recorrendo a *cell penetrating peptides* (CPPs) como sistemas de transporte intracelular de sequências peptídicas direcionadas para padrões únicos de interações proteicas. Um outro interactor da PPP1CC2, a *several ankyrin repeat protein variant 2* (SARP2), foi também caracterizado em testículo e espermatozoide. Descrevemos ainda, o interactoma da APP em testículo e espermatozoide humano sendo que a nossa abordagem permitiu a identificação de novos interactores e o reconhecimento de interactores-chave na fertilidade masculina, particularmente na interação espermatozoide-oócito, o que representa um potencial mecanismo alvo para a contraceção masculina. Identificámos diversas proteínas sinalizadoras cuja atividade se correlaciona com parâmetros seminais distintos, tendo o potencial para integrar uma plataforma de diagnóstico que poderá ter várias aplicações: explicar situações de infertilidade idiopática; explicar o insucesso de técnicas de procriação medicamente assistida (PMA) ou abortos de repetição; auxiliar a escolha da técnica de PMA mais apropriada; avaliar a eficácia de intervenções médicas; e clarificar os mecanismos responsáveis pela deterioração da qualidade dos espermatozoides associada com a idade. Para além do potencial para integrar um painel de biomarcadores, essas proteínas permitiram o reconhecimento de vias de sinalização responsáveis por regular funções específicas do espermatozoide que podem ser utilizadas com fins terapêuticos.

keywords

male (in)fertility and contraception, spermatozoa, signal transduction, protein-protein interactions, phosphoprotein phosphatase 1, amyloid precursor protein.

abstract

The large number of unintended pregnancies worldwide (~41%) highlights the need for new contraceptive methods. Still, male contraceptive methods are limited to condoms, withdrawal or vasectomy as, currently, no pharmaceutical contraceptive agents exist for men. In contrast, in developed countries, infertility affects 15% of couples attempting to conceive and in half of these cases the cause is related to male reproductive issues. Moreover, idiopathic infertility remains the most common type of male infertility.

The main goals of this work were to (1) identify, characterize and modulate non-hormonal targets for male contraception; and (2) establish a biomarker “fingerprint” to assess male fertility. Concerning the identification of targets for male contraception, particular attention was given to two distinct proteins and its interacting partners: phosphoprotein phosphatase 1 (PPP1) and amyloid precursor protein (APP). We characterized the interactome of PPP1 catalytic subunit gamma 2 (PPP1CC2), a testis-enriched/sperm-specific PPP1 isoform, in human testis/spermatozoa. We demonstrated for the first time the interaction between PPP1CC2 and A-kinase anchor protein 4 (AKAP4), a testis-specific protein essential for sperm motility, in human spermatozoa and the potential of the complex as a contraceptive target. Sperm motility was then successfully modulated by specific protein complex disruption using cell-penetrating peptides (CPPs) as a drug intracellular delivery system. Herein, we demonstrated for the first time the potential of CPPs to deliver peptide sequences that target unique protein-protein interactions in spermatozoa. Another PPP1CC2 interacting protein – several ankyrin repeat protein variant 2 (SARP2) – was also characterized in testis and spermatozoa. Moreover, we provided the first report on APP interactome in human testis/spermatozoa and our approach allowed the identification of novel interactions and the recognition of key APP interacting proteins for male reproduction, particularly in sperm-oocyte interaction, which represent a potential mechanism for male contraception modulation.

We identified several signaling proteins that showed a high degree of differential activity in spermatozoa samples with distinct seminal parameters and have the potential to integrate a diagnostic array, which may have several applications: explain idiopathic infertility, failure in assisted reproductive techniques (ART) or repeated abortion; choice of the appropriate ART; assess the efficacy of medical interventions; and clarify the mechanisms responsible for age-dependent declines in spermatozoa quality. Besides the potential to integrate a biomarker "fingerprint" to assess sperm quality, those proteins allowed the recognition of the signaling pathways accountable for regulating specific spermatozoa functions that by future modulation could serve for therapeutic proposes.

Table of Contents

Table of Figures

Table of Tables

A. General Introduction and Aims

1. Male Reproductive System

The male reproductive system consists of two testes, a system of genital ducts, the accessory glands and the penis. This system produces spermatozoa (spermatogenesis) and male sex hormones (steroidogenesis) and delivers the male gametes into the female reproductive tract.

1.1. Testis

Testes are oval structures housed in separate compartments within the scrotum (Figure A.1 A). The testicular parenchyma is composed of highly convoluted seminiferous tubules (1 to 3 in each lobe) where the production of spermatozoa occurs, and by interstitial tissue that surrounds the tubules, containing the Leydig cells that secrete testosterone (Figure A.1 B). The seminiferous epithelium is composed of sustentacular Sertoli cells and a stratified layer of developing male germ cells (spermatogonia, spermatocytes, and spermatids; see section 2.3.2.1.) [1,2].

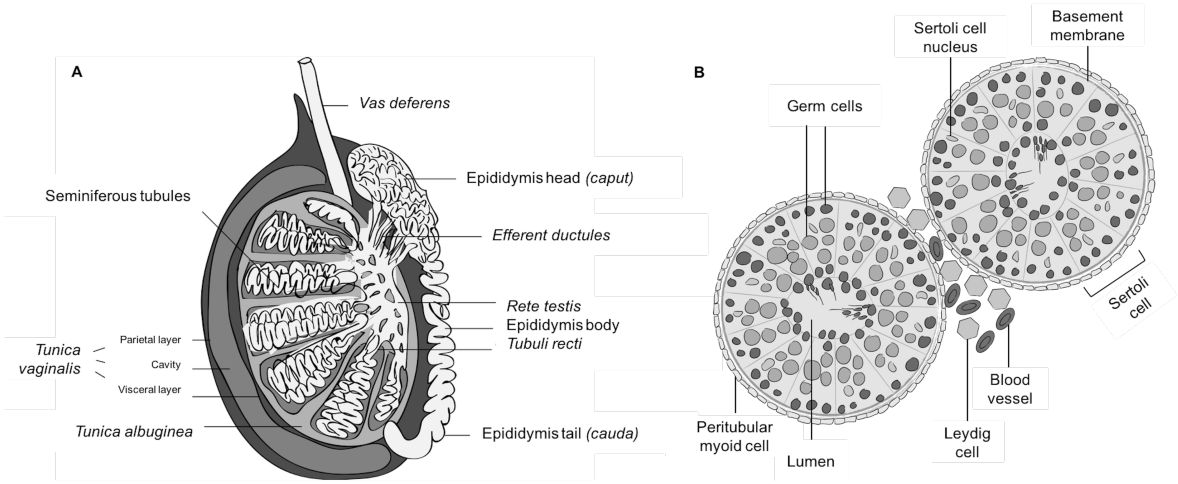

Figure A.1 - Testis (A) Cross-section showing the location of the seminiferous tubules, the vas deferens and the epididymis. (B) Schematic cross-section of a testicular tubule, illustrating the germ cells at different stages of maturation embedded in somatic Sertoli cells (outlined). Leydig cells are present in the interstitium. Maturing sperm are shown in the lumen of the tubules.

1.1.1. Sertoli Cells – The supporting cells

Sertoli cells provide the structural organization of the seminiferous tubules [3]. These cells do not replicate after puberty and their number determines the testicular size, germ cell numbers and spermatozoa output [4,5]. Sertoli cells are involved in (i) mechanical support and nutrition of germ cells, (ii) paracrine regulation of male germ cell proliferation and differentiation by secretion of regulatory proteins, including growth factors and hormones, (iii) phagocytosis, (iv) steroid hormone synthesis and metabolism, and (v) maintenance of the integrity of the seminiferous epithelium by establishing the blood-testis barrier [5]. The adjacent Sertoli cells establish tight junctions forming the blood-testis barrier, dividing the seminiferous tubule into two compartments:

the basal containing the stem cells and the pre-meiotic cells (spermatogonia) and the adluminal including the meiotic (spermatocytes) and the post-meiotic (round and elongating spermatids) cells; thus protecting the differentiating germ cells from an immune response [6].

1.1.2. Leydig Cells – The interstitial cells

Leydig cells lie within the intertubular region of the testis and are found adjacent to the blood vessels, reflecting their endocrine function. They are responsible for testosterone production, which is essential for spermatogenesis. In most species there are two generations of Leydig cells [7–9]. A fetal generation under the stimulation of human Chorionic Gonadotropin (hCG) results in the production of testosterone during gestation in humans. These cells decrease in number and are lost from the intertubular space around twelve months of age [10]. The adult generation of Leydig cells in humans results from Luteinizing Hormone (LH) stimulation which starts at puberty [11].

1.2. Genital ducts

A system of genital ducts conveys the spermatozoa and the fluid that composes semen to the outside. The seminiferous tubules are connected by short straight tubules, the *tubuli recti*. From here, spermatozoa enter the *ductuli efferentes* that lead into the epididymis and then the *vas deferens*, where the seminal vesicle empties its secretions. The continuation of the duct, known as ejaculatory duct, enters the prostatic gland, which delivers its secretory product. Both ejaculatory duct (right and left) empty into the urethra, which conveys semen to the outside.

1.2.1. Epididymis

The human epididymis is a long convoluted tubule that serves as a conduit for the transport of spermatozoa from the testis to the *vas deferens* and is the site where spermatozoa mature and acquire progressive motility (see section 2.4.1.) and fertility [12]. Additionally, the epididymis has a role in: reabsorption of fluid from seminiferous tubules, elimination of defective male gametes, and sperm protection against oxidative damage [12,13]. The epididymis can be divided into three major segments – caput (head), corpus (body) and cauda (tail) [14].

The adult epididymis consists of a pseudostratified columnar epithelium of several cell types: principal (80%), basal, clear, narrow, apical and halo cells (Figure A.2). The principal cells are columnar with non-motile cilia and are responsible for most of the proteins secreted into the luminal fluid. Narrow and apical cells are found predominantly in the proximal and mid region of the caput, whereas the rest are present along the epididymis. Clear cells are also endocytic cells and together with the apical cells could be responsible for the endocytosis of proteins from the lumen.

The shorter, pyramid-shaped cells called basal cells lie under the principal cells and do not have access to the luminal compartment, nevertheless they may regulate the functions of the principal cells. Halo cells appear to be the primary immune cells of the epididymis. Principal cells form tight junctions to create an immunoprotective site within the epididymal lumen necessary for sperm maturation that is called blood-epididymis barrier [15].

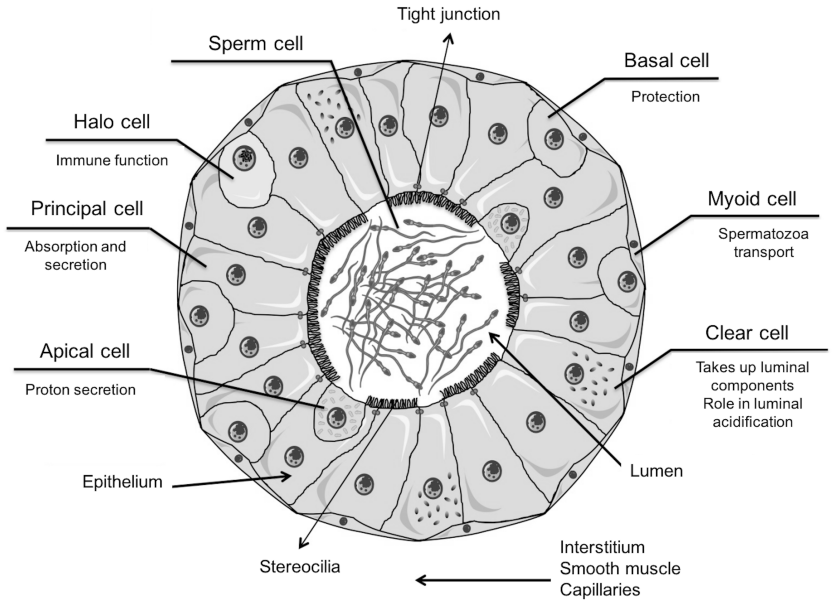

Figure A.2 - Schematic representation of a cross-section of the mammalian epididymis. Adapted from [14,16].

The epididymal environment (extracellular milieu, also called epididymal fluid) is certainly the most sequentially modified and complex milieu of the body in which spermatozoa are bathed for the duration of the transit (in average from 3 to 11 days in humans) through this environment [17]. The epididymal fluid consists of water, inorganic ions, small organic molecules, and organic macromolecules (proteins) [17,18].

1.3. Spermatozoa

Germ cells divide and differentiate from spermatogonia to spermatozoa through a process that occurs in seminiferous tubules of the testis, designated spermatogenesis (see section 2.3.2.1.). In humans, the release of spermatozoa occurs in the early stages of puberty at approximately 13.5 years of age, and spermatogenesis continues throughout life [19].

1.3.1. Spermatozoa structure

Sperm may be divided into two regions, the head and the flagellum (Figure A.3). Both are covered by the plasma membrane. The head comprises a nucleus, in which the DNA condensing core and linker histones have been partially replaced during spermiogenesis by protamines, positively charged DNA proteins that enable nuclear hypercondensation [20,21]. In humans, sperm chromatin is tightly packaged by protamines, but up to 4% of the DNA remains packaged by histones [22]. The histone-bound DNA sequences are less tightly compacted and are correlated with early embryo development [22]. Infertile men have a higher sperm histone to protamine ratio when compared with fertile controls [23]. The nucleus is covered by a reduced nuclear envelope, from which the nuclear pore complexes have been removed during spermiogenesis, except for the redundant nuclear envelopes (RNEs) found in some species at the base of the sperm nucleus [24]. Sperm nucleus is protected by the perinuclear theca, forming a rigid shell composed of disulfide (SS) bond-stabilised structural proteins combined with various other proteins [25]. The acrosome is a Golgi-derived structure that covers the anterior half to two thirds of the head [26]. The inner and outer acrosomal membranes hold inside a dense acrosomal matrix containing the proteases that are believed to digest a fertilization slit in the zona pellucida [27]. The equatorial segment is a folded-over complex of perinuclear theca, inner and outer acrosomal membranes, which carries receptors involved in the initial binding of the sperm to the oocyte plasma membrane. The postacrosomal sheath is believed to contain a complex of sperm borne, oocyte-activating factors (including phospholipase C ζ, PLCζ).

The flagellum provides a motile force for the spermatozoon, which is based upon a 9 plus 2 arrangement of microtubules within the flagellar axoneme [28]. Inner and outer dynein arms project from each of the outer doublets, these arms being responsible for generating the motive force of the flagellum. Nine radial spokes, each deriving from one of the outer microtubular doublet pairs, extend inwards towards the central pair in a helical fashion [29]. The flagellum can be divided in connecting piece, midpiece, principal piece and endpiece. From the remnant of the centriole at the connecting piece the axoneme extends throughout the length of all subdivisions of the sperm flagellum. The mid-piece presents nine outer dense fibers (ODFs) surrounding each of the nine outer axonemal microtubule doublets, and a mitochondrial sheath (MS) that encloses the ODFs and the axoneme. While the MS is restricted to the mid-piece, the ODFs extend into the principal piece of the flagellum. The end of the mid-piece and the beginning of the principal piece are marked by the annulus [30]. At the start of the principal piece, the MS terminates and two of the ODFs are replaced by two longitudinal columns of fibrous sheet (FS). The most abundant protein present in the FS is A-kinase anchor protein 4 (AKAP4), a PKA-anchoring testis-specific protein [31]. The FS columns run the length of the principal piece and are stabilized by circumferential ribs that

surround the ODFs. The FS is the only structure that is restricted to the principal piece. The end-piece is the short terminal portion of the flagellum and has only the axoneme surrounded by the plasma membrane [30]. While the axoneme is highly conserved in ciliated eukaryotic cells, the ODFs, MS and FS are accessory structures that are exclusive to mammalian spermatozoa [30].

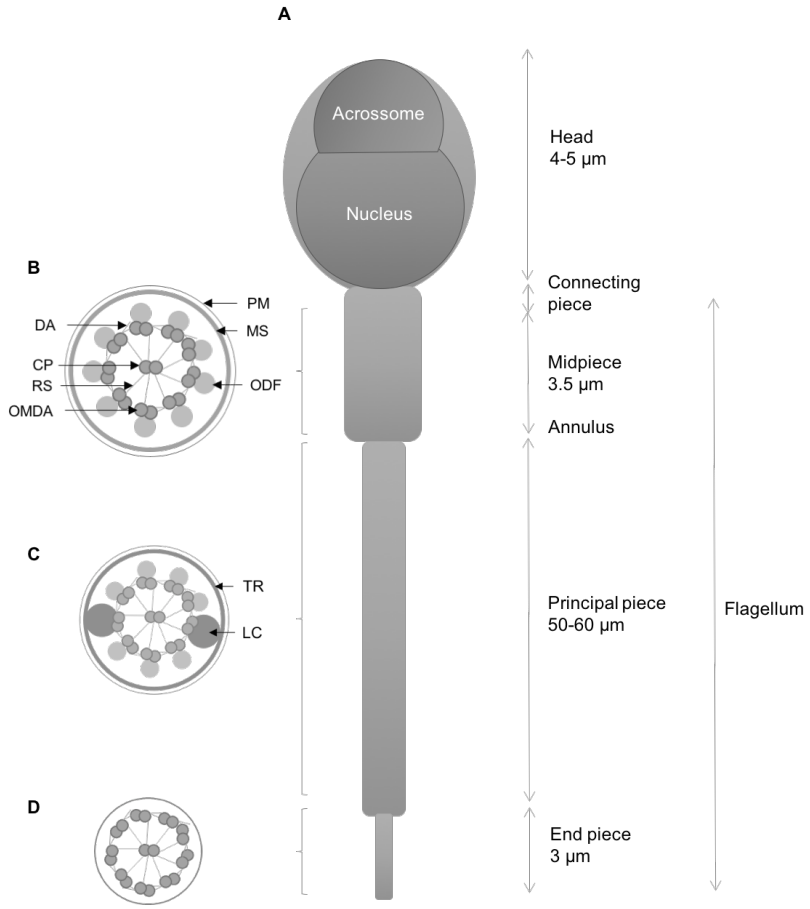

Figure A.3 - Schematic representation of the mammalian spermatozoa and the ultrastructure of the flagellum. (A) Mammalian spermatozoa flagellum is divided structurally into four areas: the connecting piece, mid-piece, principal piece and end-piece. The end of the mid-piece and start of the principal piece are demarcated by the annulus. (B) Cross-section through the mid-piece showing the plasma membrane (PM) and mitochondrial sheath (MS) surrounding the nine outer dense fibres (ODFs). Within the ODFs are the components of the axoneme; the nine outer microtubule doublets of the axoneme (OMDA) with associated dynein arms (DA) and radial spokes (RS) and the central pair of microtubule doublets (CP). (C) Cross-section through the principal piece showing the PM surrounding seven ODFs. The ODFs 3 and 8 have been replaced by the two longitudinal columns of the fibrous sheath (LC). The two columns are connected by transverse ribs (TR). The axonemal components are unchanged. (D) Cross-section through a representative segment of the end-piece showing the PM surrounding the axoneme. Adapted from [16]

1.3.2. Epididymal maturation and storage

In mammals, testicular spermatozoa are immotile and incapable of fertilizing the oocyte. During epididymal transit, spermatozoa are subjected to a sequentially changing environment where their function is modified as they undergo complex membrane remodeling and protein acquisition [14]. Such properties acquired during maturation include progressive motility (see section 2.4.1.). The changes that occur in spermatozoa during the epididymal transit are related to protein exchanges

with the epididymal lumen or with modifications of the protein repertoire (e.g. post-translational modifications, PTMs). Epididymosomes are the key players in the protein exchange process between epididymal lumen and spermatozoa thereby protecting the proteins against the luminal proteases [17]. Several epididymosomal proteins that are transferred to spermatozoa have functions related to immunological protection, sperm motility (see section 2.4.1.) or as decapacitation factors [17,18].

The cauda region in many mammals acts as a site for sperm storage until ejaculation. The human epididymis does not present such clearly defined sections in comparison to other species and lacks a pronounced cauda region decreasing the storage capacity [14]. In humans, the sperm number after ejaculation can increase from 50 millions after 1 day to 300 millions after 10 days of abstinence. Beyond this time ejaculate sperm numbers remain constant as the epididymis is filled and sperm start to enter in the urine [17].

1.4. Ejaculation and seminal components

Ejaculation results from a coordinated contraction of the smooth muscle surrounding the epididymis cauda and *vas deferens* [32]. During ejaculation sperm cells are suspended in seminal plasma, which originates from the accessory sex glands (seminal vesicles, prostate, Cowper and Littre glands) [33]. The seminal vesicles provide the majority of ejaculate volume rich in bicarbonate, prostaglandins, antioxidants, fructose, ascorbic acid, as well as, seminogelin I and II [34]. Approximately 5% of the ejaculate results from secretions from the Cowper (bulbourethral) and Littre glands. The prostate provides secretions with zinc, citric acid, prostate specific antigen (PSA) and choline. PSA helps to liquefy the semen following ejaculation as it degrades Semenogelin (I and II) [34]. The epithelial cells lining the prostate also secrete small membrane-bound vesicles called prostasomes. Prostasomes contain over 400 proteins [35] and are capable of undergoing hydrophobic fusion with sperm transferring their contents into the cell [36,37]. The presence of prostasomes has been associated with beneficial effects on sperm motility [38,39]. A small contribution is made from epididymal fluid containing carnitine inositol and potassium.

2. Protein-Protein Interactions - no protein is an island

2.1. PPI determination, databases, networks and modulation

Cells use different mechanisms, such as PTMs and protein-protein interactions (PPIs), to regulate its signal cascades [40]. Phosphorylation is one of the most common PTMs and it functions by inducing conformational changes in a target protein or changing the accessibility between enzyme and interacting protein [41].

PPIs are defined as physical contacts with molecular docking between proteins that occur in living organism and can be defined as permanent or transitory. The transient interactions would form signaling pathways while permanent interactions will form a stable protein complex. Stable protein assemblies include macromolecular protein complexes and cellular machines, such as ATP synthase (eight different proteins in mammals) or cytochrome oxidase (13 proteins in mammals). Another essential element for defining PPIs is the biological context. Not all possible interactions will occur in any cell at any time. Instead, interactions depend on cell type, cell cycle phase, development stage, environmental conditions, protein modifications (e.g., phosphorylation), presence of cofactors, and presence of other binding partners. PPIs can (i) change the kinetic properties of enzymes; (ii) act as a general mechanism to allow for substrate channeling; (iii) construct a new binding site for small effector molecules; (iv) inactivate or suppress a protein activity; (v) modify the specificity of a protein for its substrate through interaction with distinct binding partners; (vi) serve a regulatory role in either upstream or downstream level [42].

Within the last years a large amount on PPI has been obtained both by *in vitro* (e.g. coimmunoprecipitation) and *in vivo* (e.g. Yeast two-hybrid, see section 2.2.) high-throughput and small technologies, as well as, *in silico* approaches (e.g. domain-pairs-based sequence approach) [43].

The massive quantity of PPI data being generated on the last decades has led to the creation of biological databases in order to organize this data. A comparison of the main databases and repositories that include protein interactions is shown in Table A.1.

Table A.1 - Main public PPI databases: (i) primary databases, which include PPIs from large- and small-scale (Lsc and Ssc) experimental data that are usually obtained from curation of research articles; (ii) meta-databases, which include PPIs derived from integration and unification of several primary repositories; and (iii) prediction databases, which include PPIs from experimental analyses together with predicted PPIs obtained from the analyses of heterogenous biological data. PPI databases containing only yeast and microbial data were excluded (adapted from [44]).

Primary DB	Full name	URL	PPI sources	Species	Type of MI	R
BIND	Biomolecular Interaction Network Database	http://bond.unleashedinformatics.com/Action	Ssc & Lsc published studies (literature-curated)	All	PPIs and others	[45]
BioGRID	Biological General Repository for Interaction Datasets	http://thebiogrid.org		All	PPIs and others	[46]
DIP	Database of	http://dip.doe-		All	Only PPIs	[47]

	Interacting Proteins	mbi.ucla.edu/dip/Main.cgi				
HPRD	Human Protein Reference Database	http://www.hprd.org		Human	Only PPIs	48
IntAct	IntAct Molecular Interaction Database	http://www.ebi.ac.uk/intact/		All	PPIs and others	42
MINT	Molecular INTeraction database	http://mint.bio.uniroma2.it/mint		All	Only PPIs	42
MIPS-MPPI	Mammalian Protein-Protein Interaction Database	http://mips.helmholtz-muenchen.de/proj/ppi/	Ssc published studies (literature-curated)	Mammalian	Only PPIs	42
Meta DB	Full name	URL	PPI sources	Species	Type of MI	R
APID	Agile Protein Interaction DataAnalyzer	http://bioinfow.dep.usal.es/apid/	BIND, BioGRID, DIP, HPRD, IntAct, MINT	All	Only PPIs	42
HIPPIE	Human Integrated Protein-Protein Interaction rEference	http://cbdm.mdc-berlin.de/tools/hippie/	BioGRID, DIP, HPRD, IntAct, MINT, BIND, MIPS, manually selected studies	Human	Only PPIs	49
PINA	Protein Interaction Network Analysis platform	http://csbi.ltdk.helsinki.fi/pina/	BioGRID, DIP, HPRD, IntAct, MINT, MPact	All	Only PPIs	42
Prediction DB	Full name	URL	PPI sources	Species	Type of MI	R
MiMI	Michigan Molecular Interactions	http://mimi.ncibi.org/MimiWeb/	BIND, BioGRID, DIP, HPRD, IntAct, nonPPI data	All	PPIs and others	42
PIPs	Human PPI Prediction database	http://www.compbio.dundee.ac.uk/www-pips/	BIND, DIP, HPRD, OPHID, nonPPI data	Human	PPIs and others	42
OPHID	Online Predicted Human Interaction Database	http://ophid.utoronto.ca/	BIND, BioGRID, HPRD, IntAct, MINT, MPact, nonPPI data	Human	PPIs and others	42
STRING	Known and Predicted Protein-Protein Interactions	http://string.embl.de/	BIND, BioGRID, DIP, HPRD, IntAct, MINT, nonPPI data	All	PPIs and others	42
UniHI	Unified Human Interactome	http://www.mdc-berlin.de/unihi/	BIND, BioGRID, DIP, HPRD, IntAct, MINT, nonPPI data	Human	PPIs and others	42

DB, database; MI, molecular interaction; R, reference.

PPI networks are defined as the networks of protein complexes formed by biochemical events and/or electrostatic forces and that serve a distinct biological function as a complex [50]. Several bioinformatic tools have been developed to represent and explore such PPI networks, such as the Cytoscape, an open-source bioinformatics software platform for visualizing molecular interaction networks and biological pathways and for integrating these networks with annotations and other types of data [51].

In the past two decades PPI have emerged as promising drug targets, and the field is now evolving fast. Several approaches have been used to modulate PPIs [52], in particular those based on the use of small organic molecules, either derived from natural compounds or from organic synthesis (for review see [53–55]). However, the large contact surfaces involved in PPIs, the fact that these protein–protein interfaces are generally flat and often lack the grooves and pockets present on the surfaces of proteins that bind to small molecules represent considerable weaknesses to the use of this approach [54]. Alternatively recombinant proteins/antibodies, and peptides, which can explore larger surfaces, may represent excellent PPI modulators. Peptides in particular present several advantages: (1) adaptability to large surfaces due to their flexibility; (2) easy modularity, which increases structural diversity allowing for higher selectivity and potency; (3) they accumulate only to a minor extent in tissues; and (4) biocompatibility, which means low toxicity in humans [56]. However, peptides are hard to convert into oral drugs, as typically they are not metabolically stable undergoing rapid removal by hepatic and renal clearance, they do not cross physiological barriers easily and they have poor oral bioavailability as they present low stability against degradation by proteolytic enzymes of the digestive system and blood plasma. Fortunately peptides can be easily synthetized and modified to improve their stability, permeability and bioavailability.

Cell-penetrating peptides (CPPs) are reliable vehicles for the intracellular delivery of therapeutic agents. CPPs are short peptide sequences (up to 30 amino acids in length) that can pass through the cellular membrane and deliver different types of cargo. The identification of intrinsically bioactive CPPs emphasizes the tremendous clinical potential of CPP technologies [57,58]. The first described CPPs included penetratin and Tat peptides, cationic stretches of amino acids identified in the primary sequences of both insect- and virally-encoded transcription factors, respectively. These polycationic CPP motifs confer their native proteins the capacity to cross biological membranes to fulfill their role as transcriptional activators. Similar CPP sequences have been also identified in several human proteins [59]. Recently Jones and colleagues demonstrated that CPPs are able of translocate into the sperm cell without affecting its viability and motility [60]. In terms of clinical applications, CPP can potentially be used to deliver a wide range of therapeutic moieties, including small molecules, oligonucleotides and proteins. CPP internalization may be achieved by both direct plasma membrane translocation and energy-dependent endocytotic mechanisms.

2.2. The power of the yeast two-hybrid system in the identification of novel drug targets: building and modulating PPP1 interactomes

Joana Vieira Silva, Maria João Freitas, Juliana Felgueiras and Margarida Fardilha

Laboratory of Signal Transduction, Department of Medical Sciences, Institute of Biomedicine – iBiMED, University of Aveiro, 3810-193 Aveiro, Portugal.

Corresponding author: Margarida Fardilha, Departamento de Ciências Médicas, Universidade de Aveiro, Campus Universitário de Santiago, Agra do Crasto – Edifício 30, 3810-193 Aveiro, Portugal. T: +351-918143947. E: mfardilha@ua.pt

Silva JV, Freitas MJ, Felgueiras J, Fardilha M. The power of the yeast two-hybrid system in the identification of novel drug targets: building and modulating PPP1 interactomes. Expert Review of Proteomics. 2015; 12(2):147-58. doi: 10.1586/14789450.2015.1024226.

2.2.1. Abstract

Since the description of the yeast two-hybrid (Y2H) method, it has become more and more evident that it is the most commonly used method to identify protein-protein interactions (PPIs). The improvements in the original Y2H methodology in parallel with the idea that PPIs are actually promising drug targets, offer an excellent opportunity to apply the principles of this molecular biology technique to the pharmaceutical field. Additionally, the theoretical developments in the networks field make PPI networks very useful frameworks that facilitate many discoveries in biomedicine. This review aims to highlight the relevance of the Y2H in the determination of PPIs, specifically Phosphoprotein Phosphatase 1 (PPP1) interactions, and its possible outcomes in pharmaceutical research.

2.2.2. Introduction

The yeast two-hybrid system (Y2H) was first described by Fields and Song in 1989 [61] and since its discovery it has been intensively used to search for novel protein-protein interactions (PPIs). In fact, the Y2H system rapidly turned into the most used method to study PPIs, being a major contributor to PPIs databases. In spite of the clear progress enabled by the introduction of the Y2H, the initial system presented several limitations. For instance, the Y2H does not reflect *in vivo* spatial or temporal context of the interactions and all the interactions are forced to occur in the yeast nucleus. Improvements on the original method not only overcame major limitations of the original Y2H system, but also expanded its applications: high-throughput Y2H can now be used to study complex protein interactomes, as well as other types of molecular interactions, such as protein-DNA and protein-RNA interactions. More recently, high-throughput Y2H has been applied in the screening of small molecule libraries to identify molecules capable of modulating a particular PPI or, conversely, to identify, from a group of interactions, the one that is targeted by a specific molecule. Progress on network medicine also contributed to the empowerment of the Y2H system. Interactome networks allow the attribution of spatial or temporal context, essential to identify regulatory networks of specific-cell types and recognize key protein complexes for a particular biological process. Here we will address the panoply of variations and applications of the Y2H system and its vast contribution to the discovery of PPIs and the study of interactomes. We will particularly focus our attention on the use of Y2H system in drug discovery. To emphasize the usefulness of the method, we will demonstrate how the Y2H contributed to the identification of phosphoprotein phosphatase 1 (PPP1) interactome and its potential application in the discovery of PPP1 complexes-modulating drugs.

2.2.3. Yeast Two-Hybrid system: a useful system to the unraveling of molecular interactions

The original Y2H method, established by Stanley Fields and Ok-Kyu Song in 1989 [61], used the reconstitution of the GAL4 transcription factor of the *Saccharomyces cerevisiae* to assay for PPIs. The function of GAL4, like other eukaryotic transcription factors, requires the physical bound (though not covalent) between a DNA-binding domain (DBD) and an activation domain (AD). Based on this, Fields and Song fused one protein of interest, the "bait", to the DBD of the GAL4 and the other, the "prey", was expressed as a fusion to the AD. As a consequence of the interaction between bait and prey proteins, the GAL4 transcription factor reassembled and induced the transcription of the *lac*Z reporter gene, resulting in a turning-blue phenotype in the presence of the substrate X-gal [61]. The general scheme of the Y2H is depicted in Figure A.4.

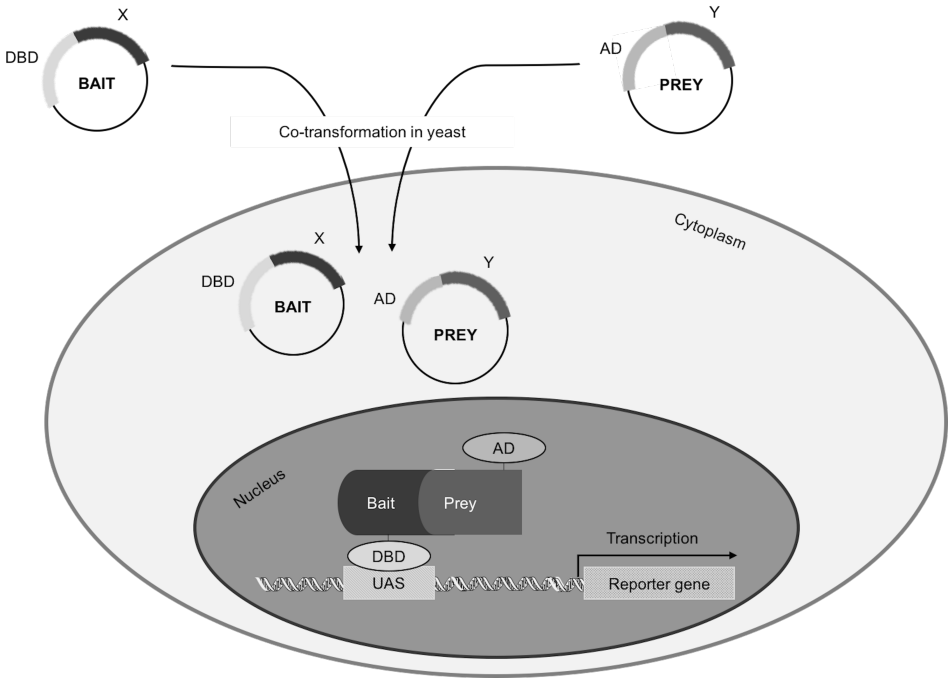

Figure A.4 - Schematic representation of the Y2H system. Two plasmids are constructed: the bait, which encodes the protein of interest (X) fused with the DNA-binding domain (DBD) of a transcription factor, and the prey, which encodes the potential interacting-protein (Y) fused with an activation domain (AD). The plasmids are co-transformed into an appropriate yeast strain where the hybrids—bait and prey—are expressed. Within the nucleus of the recipient cell, the DBD binds the upstream activating sequence (UAS). If the interaction of proteins X and Y occurs, the close proximity between DBD and AD leads to the activation of the transcription of the reporter gene.

The Y2H system rapidly became a versatile method for the study of binary protein interactions, since it offers significant advantages when compared with other biochemical methods (Figure A.5). To further improve the method, a number of adaptations (e.g. different options for DBD, AD, and reporter gene revised in [62]) were introduced in order to overcome the drawbacks of the original system (Figure A.5), and several variants were developed to extend the number of molecular interactions covered (Figure A.5).

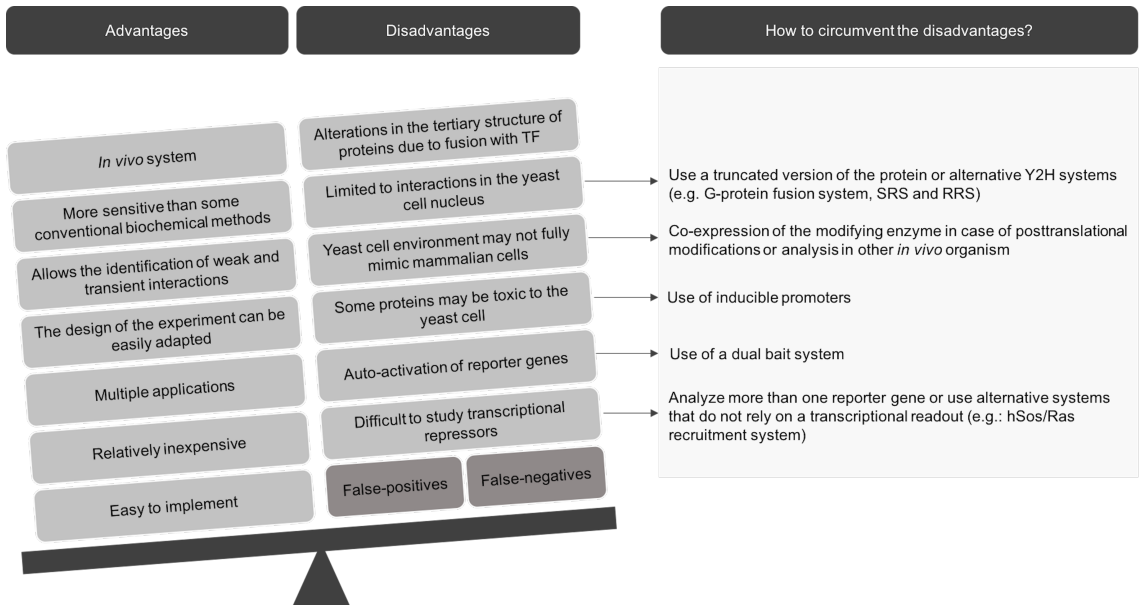

Figure A.5 - Advantages and disadvantages of Y2H system. The disadvantages of the conventional Y2H system may lead to false-positive or false-negative results. However, several adaptations can be made to the traditional method in order to circumvent the majority of the problems.

Additional information on the variants of the Y2H can be consulted in several review articles (e.g. [62,63]). The Y2H method has also been modified for large-scale screenings, using either the library screening or the matrix approaches. Most commonly, yeast cells expressing the bait protein are transformed with a library of cDNA molecules fused to AD (library screening approach). On the other hand, a given set of yeast cells expressing the bait protein can be screened against a specific set of yeast cells expressing the prey protein (matrix approach) (further details on [64]). These mated improvements culminate in a wide range of applications for the Y2H and its variants, including the study of several types of molecular interactions (e.g. PPIs, RNA-protein, DNA-protein, and small molecule-protein interactions), as well as the study of PPIs in various subcellular compartments (e.g. nuclear, membrane, cytosol).

The application of the Y2H system in drug discovery is a recent but very promising phenomenon, as further discussed below. Several variants of the method have been particularly adapted aiming pharmacological studies, including the reverse Y2H screening and the yeast three-hybrid. An in-depth understanding of the vital contribution of the Y2H system for unravelling interactomes and driving drug discovery will be provided in the next section.

2.2.4. Yeast Two-Hybrid system: 25 years of contribution

Since the Y2H system development, 25 years ago [61], its contribution to identify new protein interactions is indisputable. In fact, the Y2H system evolved into one of the most popular tools in biology and the number of interactions identified by this method is in the order of the thousands. The high-throughput Y2H screening was the most significant improvement of this technique, since it allows the mapping of thousands of protein interactions in a short period of time. Several proteomes have been characterized by this method, ranging from complete organism to disease-specific interactomes [91–93]. The significant contribution made by the Y2H system to PPIs databases reflects the utmost importance of this technique. It is estimated that around 50% of the interactions described in Pubmed resulted from Y2H screenings [92]. Moreover, from 1990 to 2007, the number of high confidence binary interactions identified using this method increased exponentially [94]. A search in BIND, BioGrid, DIP, HPRD, IntAct and MINT databases (30/10/2014) also revealed that 22% of *Homo Sapiens* PPIs were identified using Y2H methods. Nowadays, the Y2H system is probably the most commonly used technique for the detection of PPIs [95].

2.2.4.1. Unraveling organism interactomes

Since the human genome was sequenced in 2001 [96], revealing the complete proteome and interactome of the Homo sapiens has become the main goal to understand human physiology. However, Stumpf et al. estimated that the human interactome contains a range of 130 000 to 650 000 binary interactions, and being, therefore, too complex to map [97]. Over the last two decades, the interactome of several species far less complex than the human was identified due to the Y2H [95]. For example, in 1994 Finley et al. tested 14 Drosophila melanogaster open reading frames (ORF) and identified 19 interactions [98]. Today, complete or almost complete interactomes are described for several organisms. The first interactome to be described was the Saccharomyces cerevisiae, in 2000 [99,100], followed by the Drosophila melanogaster [101] and the Helicobacter pylori [102]. More recently, Simonis et al. completed the Caenorhabditis elegans interactome [103]. In 2005 Stelzl et al. and Rual et al. characterized part of the human interactome. While Rual et al. identified around 2 800 interactions, 300 of which were new, Stelzl et al. identified 3186 interactions, mostly all of them new. Interestingly, the overlap between datasets is small—from the proteins identified, only 16% were common to both datasets [50,104]. From the common proteins, only 15% of the interactions were detected in both interactomes. Even though both interactomes were obtained by Y2H, the experimental procedures differed and this may explain the different results obtained from both scans [105]. In addition to describing organism interactomes, the Y2H allowed the characterization of subcellular components or entire signaling pathways. For instance, in 2001, the metozoan 26S

proteosome was mapped, confirming several interactions reported previously, but also revealing novel interactions [106]. Additionally, Colland et al. characterized the Transforming Growth Factor beta (TGFβ) signaling pathways. This work demonstrated that the use of the Y2H technique is not restricted to the determination of the interactome of a specific protein [107].

2.2.4.2. Unraveling pathophysiological mechanisms

Bacterial and viral infections are a growing concern for the World Health Organization [108]. However, our knowledge on the infection mechanisms is still patchy and identifying potential key interactions can help elucidating the mechanisms behind pathogen-human interaction [50]. For that purpose, the interactome of several pathogens, such as *Campylobacter jejuni,* Human cytomegalovirus and the Human Immunodeficiency virus have been recently described [102,109–111]. Furthermore, it is essential to identify and analyze interactions between host and pathogens to better characterize the pathophysiologic mechanisms of viruses and bacteria. In 2010, Dyer *et al*. mapped the protein interactions between human cells and three pathogens: *Bacillus anthracis*, *Francisella tularensis* and *Yersinia pestis*, which cause anthrax, lethal acute pneumonic disease and bubonic plague, respectively [112].

2.2.4.3. Protein interactomes

As previously mentioned, the Y2H is the main technique used to identify PPIs. Numerous protein-specific interactomes are described in the literature, most of which were characterized by the Y2H system [92]. In the last year, at least six protein-specific interactomes were characterized using this system [113]. The characterization of protein-specific interactomes allows researchers to infer on the physiological role of the targeted proteins. For example, Katsogiannou *et al*. characterized the Hsp27 interactome, revealing new potential roles for Hsp27 in DNA repair and alternative splicing [114]. The Y2H technique proved to be particularly critical in the comprehension of PPP1 molecular roles. Over the past two decades, it has become evident that the key to understand the regulation and versatility of this major serine/threonine protein phosphatase lies on the identification of its multiple targeting/regulatory subunits, known as PPP1-interacting proteins (PIPs). From this point on, we will discuss the role of the Y2H technique in the characterization of PPP1 interactomes. Furthermore, the potential of PPP1 complexes as new drug targets will also be addressed.

2.2.5. Yeast Two-Hybrid contribution to unravel the Phosphoprotein Phosphatase 1 Interactome

Phosphoprotein phosphatase 1 (PPP1) is estimated to catalyze about a third of all protein dephosphorylation reactions in eukaryotic cells [115]. PPP1 catalytic subunit (PPP1C) is encoded by

three different genes giving rise to PPP1CA, PPP1CB and PPP1CC isoforms. After transcription, PPP1CC undergoes tissue-specific splicing, originating a ubiquitous isoform, PPP1CC1, and a testis-enriched and sperm-specific isoform, PPP1CC2 [116]. It has already been shown that PPP1 isoforms are expressed in a wide variety of mammalian cells [117,118]. PPP1CA is predominantly expressed in brain and was found to be ubiquitous in all tissues except in skeletal and heart muscles. PPP1CB has higher levels in liver and kidney and is also ubiquitous in all tissues except in skeletal muscle in which it is presented in low but detectable amounts. PPP1CC1 is present in higher levels in brain, small intestine and lung and was not detectable in heart and spleen. Finally, PPP1C2 is the isoform in higher amount in testis and spermatozoa [117,119]. Although most studies had not directly addressed the significance of the distinct isoforms *in vivo*, data shows that they have distinct subcellular localizations [120,121]. In the nucleus, PPP1CC1 accumulates in the nucleolus in association with RNA, whereas PPP1CA is primarily found in the nucleoplasm [121] and PPP1CB localizes to non-nucleolar whole chromatin [120]. During mitosis, PPP1CA localizes to the centrosome, PPP1CC1 is associated with microtubules of the mitotic spindle and PPP1CB is strongly associated with chromosomes [120]. This implies differences in their specificity to interact with specific targeting subunits and, therefore, to incorporate distinct signaling complexes [122]. In brain, the different PPP1C isoforms were shown to be present in distinct regions and also revealed specific subcellular localization [116,123,124]. All four isoforms are expressed in mammalian testis [125,126]. However, their cellular and subcellular distributions differ. PPP1CC2 is predominantly localized in post-meiotic cells, in the cytoplasm of secondary spermatocytes, round spermatids and elongated spermatids [125,126]. *Ppp1cc* gene deletion in mouse testis causes loss of both isoforms (PPP1CC1 and PPP1CC2) and results in male infertility due to impaired spermatogenesis [127]. Recently, Sinha *et al*. confirmed that the spermatogenic defects observed in the global *Ppp1cc* knockout mice were due to compromised functions of PPP1CC2 in meiotic and postmeiotic germ cells [126]. The mammalian PPP1C isoforms exist within the cell associated with multiple regulatory proteins, the PIPs, which determine its enzymatic activity, substrate specificity and subcellular localization [128]. The different cellular and subcellular localizations suggest that each PPP1C isoform interacts with a different set of substrates. Consequently, PPP1C isoforms are involved in distinct signal transduction pathways, in different cells and even in different cell regions. The key to understand PPP1 regulation in different cellular processes lies on the identification and characterization of its interacting partners [129]. Additionally, the identification of the cellular compartment-specific interactome may help to understand PPP1 precise regulation [130]. The majority of known PIPs contain a variant of a motif commonly referred to as the RVxF motif, which binds as an extended beta strand to a hydrophobic groove of PPP1 (away from the catalytic

site) [131–134]. Beside the PPP1 docking motifs, PIPs do not show any obvious structural similarity [135]. Classical biochemical approaches and Y2H screens have identified most PIPs [136].

2.2.5.1. PPP1 interactome in brain

Esteves *et al*. took an in-depth survey to identify specific PPP1CA, PPP1CC1 and PPP1CC2 interactors in human brain using a high-throughput Y2H approach [137,138]. Sixty-six proteins were documented to bind PPP1CA, from which 39 had never been associated with this phosphatase. A search in PIP databases was also performed to complement the approach and a total of 246 interactions were described [138]. When using PPP1CC1, PPP1CC2 or PPP1CC2 C-terminus as baits, 52, 141 and 4 PIPs were identified, respectively [137]. From the proteins identified that bind to PPP1CC1, the most abundant clones corresponded to previously characterized PIPs, including the apoptosis-associated tyrosine kinase (AATK), the tumor suppressor p53-binding protein 2 (TP53BP2) and Taperin (TPRN). Novel PPP1CC1 interactors, such as cysteine/serine rich nuclear protein 1 (CSRNP1), were also identified. Several novel PPP1CC2 interactors were also recognized, namely COPS5 and PINK [137]. One of the novel PPP1 regulators isolated in three independent Y2H screens was the nuclear membrane protein lamina associated polypeptide 1B (LAP1B), which interacts with the DYT1 dystonia protein torsinA [139].

2.2.6. PPP1 Interactome in Testis

Given the relevance of the testis/sperm-enriched variant PPP1CC2 in sperm motility and spermatogenesis, Fardilha *et al*. performed Y2H screens from a human testis cDNA library, using as baits different PPP1C isoforms (PPP1CC1, PPP1CC2 and PPP1CC2-specific C-terminus), to characterize the human testis PPP1 interactome [140]. They reported the identification of 77 different proteins, some of them unique to a particular bait. Thirty-five proteins were found to exclusively bind PPP1CC2-specific C-terminus, meaning that they could reflect the PPP1CC2 isoform specificity [140]. One of the novel interactors identified, TCTEX1D4, was recently characterized in human spermatozoa [141,142]. As suggested by Dominguez and co-workers some PIPs interact with the flexible C-terminus of PPP1 to mediate isoform specificity [135]. Y2H screenings conducted using a mouse testis expression library and PPP1CC2 as bait allowed the identification of isoform-specific interactors such as endophilin B1t, a testis enriched isoform of the somatic endophilin B1a, and the spermatogenic zip protein (Spz1) [143,144]. Both endophilin B1t and Spz1 do not interact with other PPP1C isoforms or with a truncated PPP1CC2 mutant lacking the unique C-terminus [143,144].

2.2.6.1. Other PPP1 interactions identified using the Yeast Two-Hybrid system

PPP1 has been implicated in the regulation of the cardiac function. Chen *et al*. conducted a search for proteins capable of interacting with PPP1CA in human heart using the Y2H methodology and identified a novel heart/testis-specific PIP named heart protein phosphatase 1-binding protein (Hepp1) [145]. A 3T3-L1 adipocyte cDNA library was screened with PPP1CA as bait and a novel PIP, homologous with the myosin phosphatase targeting subunit (MYPT) family, was identified - MYPT3 [146]. The Y2H also allowed to recognize that Bcl-2 and Bad interact with PPP1CA [147] and that the binding of the pre-mRNA splicing factor SIPP1 to PPP1 involves the RVxF motif [148]. The apoptosis-associated tyrosine kinase (AATYK) interaction with PPP1 and the relevance of a PPP1 docking motif was demonstrated by Y2H [149]. The dephosphorylation of one of the six subunits of the origin recognition complex (Orc2) by PPP1 promotes the binding of the complex to chromatin. Orc2 physical interaction with the distinct PPP1C isoforms (PPP1CA, PPP1CB and PPP1CC) was identified by Y2H [150]. Additionally, the Y2H technique was used to prove that the interaction of Orc2 with PPP1C isoforms occurred through a variation of the RVxF motif (119-KSVSF-123), by generating Orc2 mutants that contained a deletion of the binding motif [150]. Nucleolar protein with MIF4G domain 1 (NOM1), which was the first PIP identified as being involved in targeting PPP1 to the nucleolus, was identified as an interactor in a Y2H screening. The Y2H technique was also used to characterize the Sds22-PPP1-I3 complex and to demonstrate that PPP1 is strictly controlled by both inhibitors, Sds22 and I3 [151]. Phostensin, a PPP1 F-actin cytoskeleton targeting subunit, was also identified as a PIP by Y2H, supporting the role of PPP1 in the modulation of actin rearrangements [152]. PPIs are a recent but promising class of drug targets. As demonstrated above, PPP1-PIPs complexes are essential regulatory components in signaling cascades involved in a wide range of cellular function. An attractive approach to modulate PPP1 activity is to target specific interfaces between PPP1 and tissue/event-specific PIPs, disrupting their interaction. Thus, the Y2H system became essential not only to construct PPP1 interactome in different cell and tissue types, but also to screen for drugs that modulate PPP1/PIPs complexes.

2.2.7. Yeast Two-Hybrid in drug screening

Drug discovery paradigm was forced to change in the post-genomic era—from protein-focused to pathway-centered. Instead of looking to the usual suspects (e.g. G protein coupled receptors and kinases), researchers and pharmaceutical industries invested in the huge amount of data retrieved from high-throughput proteome analyses, which include Y2H approaches (revised in [93]). Constructing disease-specific PPI networks allows the identification of key proteins or protein complexes more prone to be druggable. For example, developing an Y2H screen in which the bait is a well-known disease-related protein drives the construction of specific disease-related networks,

thereby identifying promising PPIs. A drug screen approach based on the high-throughput Y2H can then be used to test drug libraries and identify compounds that modulate previously retrieved PPIs. For instance, p53 is mutated in approximately 50% of all human cancers. A search for p53 interactors using the Y2H method allowed the identification of many partners and the building of the p53 interactome [153]. One of the interactions identified, p53/MDM2, was further validated and a drug screen for the inhibition of the complex was performed allowing the identification of nutlins. These molecules induce p53 activation and apoptosis of cancer cells, since binding of MDM2 to p53 inhibits p53 activity [154]. Another option is to use a wide proteome approach, in which several proteins associated with a certain disease are used as baits. Lim *et al.* identified the interactors of 20 proteins that have been proved to be involved in the pathophysiology of Ataxia [155]. PPI network analysis showed that the interactors form network modules suggesting that they function in a combined way. Finally, in a non-specific way, large scale PPIs can be obtained by performing Y2H methodology using thousands of baits to screen libraries [50,104]. Bioinformatic analysis of the results allows the identification of disease-related interactions and the proposal of putative drug targets.

Independently of the number of baits used or the particular goal behind the high-throughput Y2H performed, the result is always a collection of binary interactions. Consequently, it is possible to build protein networks and to identify promising protein complexes that can be subsequently subjected to a large-scale drug screen (also based in the Y2H). The drug targeting of protein complexes has much to grow and, accordingly, screening systems based on the Y2H methodology are still being improved. For instance, the mammalian Y2H is being used for high-throughput drug screening. Comparing to the yeast environment, mammalian cells are more permeable, support appropriate folding, as well as co-factors and post-translational modifications that are essential for proper PPIs and adequate drug action. The mammalian Y2H was used to identify small molecules that disrupt the p53/MDM2 complex. The compound library consisted of 3840 compounds and SL-01, besides nutlin-3, was shown to activate p53 pathway and induce growth arrest in tumor cells [156]. There are many other examples that show the power of Y2H in the screening of drugs that target specific PPIs [92,93,157]. Furthermore, it is expected that Y2H systems continue to be the reference method to identify PPIs and that, in the near future, they also turn into one of the most used methods to identify modulators of PPIs.

2.2.7.1. PPP1 complexes as therapeutic targets

As previously stated, a great number of PPP1 interactors were identified using Y2H screenings. The diversity of the interactors is astonishing and the associated functions are diverse: from cytoskeleton organization and cell cycle control to apoptosis (revised in [129]). Consequently, many disorders may arise from abnormalities in the PPP1 regulators or in the complexes themselves. This

fact highlights the relevance of unravelling novel therapeutic drugs that target PPP1 holoenzymes and/or a specific regulator in certain pathophysiological conditions. Targeting PPP1 complexes has already been successfully accomplished using alternative methods. Salubrinal has been identified in a screen for small molecules that protect cells from endoplasmic reticulum (ER) stress. Salubrinal is a selective inhibitor of cellular complexes that dephosphorylates the eukaryotic eIF2alpha, thereby blocking eIF2alpha dephosphorylation, mediated by a Herpes simplex virus protein, and inhibiting viral replication [158]. In fact, it does so by acting on the PPP1-GADD34 complex, which was identified by the Y2H system and was found activated during ER stress. Trichostatin A (TSA) is used in the treatment of glioblastoma and prostate cancer cells through the inhibition of histone deacetylases (HDACs) by disrupting PPP1-HDAC6 complex [159] a complex also detected by the Y2H methodology. In both cases, the screen for small molecules was performed without taking into consideration the PPP1 complexes *a priori*. Nevertheless, those studies allowed to demonstrate the relevance of PPP1 complexes as druggable entities. The tendency, in the field of PPP1 research, is to perform high-throughput screens directed for drugs that modulate PPP1 complexes. A critical example of the importance of modulating PPP1 complexes is the spermatozoon, a specialized cell incapable of genetic expression. Any functional alteration depends essentially on protein post-translational modifications (e.g., protein phosphorylation) or mechanisms based on the disruption or formation of protein complexes providing a key general mechanism for regulating vital sperm functions. As mentioned before, PPP1CC2 is a testis-enriched and sperm-specific PPP1C isoform, essential in sperm motility. PPP1CC2 activity is associated with immotile spermatozoa in the *caput* of epididymis. However, in the *cauda* of the epididymis, PPP1CC2 activity is lower and spermatozoa are motile [160].

We proposed that PPP1CC2 is progressively inhibited along the epididymis and consequently the spermatozoa acquire motility [161]. Two of the inhibitors possibly involved in this mechanism are PPP1R2P3 and SARP2, both sperm-enriched proteins that were first identified as PPP1 interactors by the Y2H methodology [140]. Sperm-specific PPP1 complexes are challenging pharmacological targets for reversible male contraception. PPIs disruption can be achieved using synthetic peptides that mimic the interaction site or a peptide with higher affinity to the interaction site [162]. Interestingly, most PPP1 inhibitors present a small motif (RVxF) that interacts with PPP1. A few *in vitro* studies used synthetic peptides (based in the RVxF motif) to disrupt the PPP1-inhibitor complex [163]. However, the modulation of human spermatozoa physiology by synthetic peptides that disrupt PPP1-inhbitor complexes was never accomplished. A major issue in addressing sperm protein complexes is the bioavailability and translocation through the sperm membrane. A viable option is to use Cell Penetrating Peptides (CPPs) that are able to carry small peptides into specific

compartments of human spermatozoa, without affecting viability, mobility or morphology of cells [60].

In conclusion, a great amount of PPP1 complexes are actually known, mainly due to Y2H screens [129,137,138,140], and may be tested as therapeutic targets in many pathological conditions. Following the boom of drugs that target G protein coupled receptors and kinases is now time to target protein phosphatases, in particular PPP1, through its regulators, and improve the therapeutic options.

2.2.8. Conclusion

The recent revolution of the various omics, specifically proteomics, allowed the identification of a huge collection of PPIs that turned out to be attractive therapeutic targets. Furthermore, the development of systems biology endorsed a more accurate reflection of the protein complexes biological reality. The identification of drugs capable of modulating known protein complexes, using high-throughput methodologies, changed the paradigm of drug discovery which was previously based on phenotype alterations. Much of what is currently known concerning PPIs and protein complex modulating drugs is due to the Y2H method and its high-throughput variations. It is expected that now, more than ever, with the advances in technology, the Y2H will be improved and will be an essential tool for drug discovery.

2.3. Phosphoprotein Phosphatase 1 Complexes in Spermatogenesis

Joana Vieira Silva, Maria João Freitas and Margarida Fardilha

Laboratory of Signal Transduction, Department of Medical Sciences, Institute of Biomedicine – iBiMED, University of Aveiro, 3810-193 Aveiro, Portugal.

Corresponding author: Margarida Fardilha, Departamento de Ciências Médicas, Universidade de Aveiro, Campus Universitário de Santiago, Agra do Crasto – Edifício 30, 3810-193 Aveiro, Portugal. T: +351-918143947. E: mfardilha@ua.pt

Silva JV, Freitas MJ, Fardilha M. Phosphoprotein phosphatase 1 complexes in spermatogenesis. Current Molecular Pharmacology. 2014; 7(2):136-46.

2.3.1. Abstract

The major post-translational modification in eukaryotes is protein phosphorylation, which mediates responses to signals in a myriad of cellular processes. Not surprisingly, many steps in spermatogenesis involve the concerted action of the protein (de)phosphorylation key players, kinases and phosphatases. Phosphoprotein phosphatase 1 catalytic subunit (PPP1C), an evolutionarily conserved Ser/Thr-protein phosphatase, catalyzes the majority of eukaryotic protein dephosphorylation reactions. Three genes, PPP1CA, PPP1CB and PPP1CC, encode four PPP1C isoforms, PPP1CA, PPP1CB, PPP1CC1, and PPP1CC2. After transcription, PPP1CC undergoes tissue-specific splicing, originating a ubiquitously expressed isoform, PPP1CC1 and a testis-enriched and sperm-specific isoform, PPP1CC2 which is essential for completion of spermatogenesis. Highly similar PPP1C isoforms – PPP1CA and PPP1CB – are capable of compensating the loss of Ppp1cc in every tissue except in testis. PPP1C cellular functions depend on the complexes it forms with PPP1C Interacting Proteins (PIPs), which together with the different catalytic subunits, account for PPP1C specificity. This review will focus on the role of the major serine/threonine phosphatase – PPP1C and its holoenzymes in spermatogenesis. Furthermore, current challenges on the protein phosphatases field as targets to male contraception will be addressed.

2.3.2. Introduction

2.3.2.1. Spermatogenesis

Spermatogenesis is a complex process by which a diploid spermatogonium develops into a highly specialized haploid male gamete, the spermatozoon that is capable of fertilizing an oocyte and produce an embryo [164]. The spermatogenic process involves mitotic and meiotic divisions, as well as extensive cell morphological alterations. In humans, spermatogenesis takes approximately 74 days [165]. However, Misell et al. (2006) have shown through the use of ingested $^{2}H_2O$ that spermatogenesis can take much less time than previously suspected, 64±8 days (range 42-76) and that the duration is highly variable among individuals [166]. This process can be divided in: (I) self-renewal and differentiation of spermatogonia, (II) meiosis (III) spermiogenesis and (IV) spermiation. In the phase I spermatogonial stem cells self-renew and differentiate through mitosis producing different cell populations. In humans, four types of spermatogonias have been identified, A long, A dark, A pale and B [167–169]. Type B spematogonia divide mitotically originating primary spermatocytes [167]. Phase II, or spermatocytogenesis, is the meiotic phase in which primary spermatocytes undergo two meiotic cycles giving rise to haploid spermatids. During this process a new genome is built through chromosome pairing, crossover, and genetic exchange. Phase III, or

spermiogenesis, is the development and differentiation of the spermatid into a spermatozoon. During this process there is the formation and development of the acrosome and flagellum, condensation of the chromatin and major substitution of the histones by protamines, reshaping of the nucleus and removal of the cytoplasm so that the spermatid can be released to the tubule lumen during spermiation [167,170].

Spermatogenesis is regulated through the hypothalamic-pituitary-gonadal axis. It is thus initiated by the release of gonadotropin-releasing hormone (GnRH) in the hypothalamus, which signals the pituitary to release follicle-stimulating hormone (FSH) and luteinizing hormone (LH) to the blood stream that will eventually reach the testis. FSH acts on Sertoli cells and directly regulates sperm output by controlling the expansion of pre-meiotic germ cells, being mainly responsible for spermatogenesis. LH acts on Leydig cells inducing the release of androgens which maintain a male phenotype and stimulate sexual organs, being mainly responsible for steroidogenesis [171]. Closing the loop, androgens also have a role as a feedback molecule on the hypothalamus.

The hormonal regulation of spermatogenesis and other stimuli induce a series of alterations into appropriate receptors that are transduced into the interior of the cells by means of post-translational modifications, mainly (de)phosphorylations. Protein phosphorylation is a post-translational modification that allows the regulation of many cellular processes. It is accomplished by the concerted action of protein kinases and protein phosphatases that insert or remove, respectively, the γ-phosphate of ATP into the target amino acid, making protein phosphorylation a reversible process. In eukaryotic cells, most phosphorylation events occur in serine or threonine residues and, to a lesser extent in tyrosine residues [172]. Several kinases and also (although much less) phosphatases have been identified as having a coordinating role on the molecular and cellular events that take place during spermatogenesis.

The importance of protein kinases in spermatogenesis is reflected in infertility phenotypes observed when knocked out. Cyclins are crucial regulators of the cell cycle that are modulated by CDK (cyclin dependent kinases) and dephosphorylated by CDC25 (cell division cycle 25) family members, which are dual specificity phosphatases (phosphatases capable of dephosphorylating Ser, Thr and Tyr residues). Mice which lack cyclins A1 are sterile due to a failure of cyclin B-CDK1 activation and subsequent meiotic arrest [173]. Interestingly, fertility is not affected in mice lacking CDC25 [174] suggesting a compensatory mechanism. CDK16, previously called an orphan kinase since its putative cyclin partner was unknown, is present in postmeiotic spermatids [175,176] and, analysis of the correspondent knockout mouse showed that CDK16 is essential for the completion of spermatogenesis [177]. Other cell cycle related kinases have been linked to spermatogenesis: Aurora kinase C is highly expressed in testis [178,179] and Polo-like kinase 2 and 3 bind calcium and

integrin binding 1 (CIB1) [180]. All these proteins are essential to male fertility and this data clearly indicates that cyclins/CDK complexes are crucial to the regulation of spermatogenesis and consequently to fertility.

Many components of the MAPK pathway have been shown to be expressed during spermatogenesis. ERK1/2 are present in all stages of mouse spermatogenesis and in rat Sertoli cells [181]. ERK participates in the modulation of DNA condensation and in the nucleus/cytoplasm translocation of Sam68, an RNA-binding protein during meiosis [181]. Furthermore, mice lacking JLP (JNK-associated leucine zipper protein), a scaffold protein for JNK and p38, were shown to be subfertile [182].

FSH and LH induce Protein Kinase A (PKA) activation that is crucial for male germ cell development. The different PKA subunits (RIα, RIIα, Cα1 and Cα2) are differentially expressed during spermatogenic development [183]. Mice lacking functional Cα1 and Cα2 have normal sperm counts [184], suggesting that the presence of active PKA in developing spermatogonia and spermatids is not essential for sperm production and differentiation. Nevertheless, the knockout mice for Cα2 (the only Cα isoform present in sperm), could not fertilize the egg, since capacitation was impaired. Sperm motility parameters were also altered, suggesting that Cα2 is required for vigorous sperm motility, consistent with the hypothesis that phosphorylation of flagellar proteins mediated by PKA induces ATP-dependent motor activity [185].

Although much has been described about the hormones and growth factors, as well as about many signaling cascades that control specific mechanisms of the spermatogenesis (mediated by the kinases), less is known about the contribution of protein phosphatases in spermatogenesis. In this chapter, we will address, specifically, PPP1C (Phosphoprotein Phosphatase 1) and its PIPs (PPP1C Interacting Proteins) on this process.

2.3.2.2. Phosphoprotein Phosphatase 1 (PPP1)

Protein phosphatases are divided into four superfamilies, according to structural conservation and mechanism of action [186,187]: the protein tyrosine phosphatase superfamily, which comprises the classical and non-classical receptor protein tyrosine phosphatases and the dual-specificity protein phosphatases, which dephosphorylate tyrosine but also serine and threonine residues; the haloacid dehalogenase superfamily of hydrolases which includes some protein serine/threonine/tyrosine phosphatases; the metal-dependent protein phosphatases superfamily; and the phosphoprotein phosphatases (PPP) superfamily which dephosphorylates serine and threonine residues. With such a broad family, PPPs are responsible for more than 90% of all the dephosphorylations that occur in

a cell. PPPs superfamily includes PPP1 to PPP7 and while all of the family members share high homology in the catalytic domains, they differ in their N- and C-terminal [188–194].

Phosphoprotein phosphatase 1 catalytic subunit, PPP1C (also known as phosphorylase phosphatase) was first identified as the enzyme that converted phosphorylase *a* into phosphorylase *b*. Since its discovery, many roles have been attributed to PPP1C in the regulation of important cellular events. PPP1C has been involved in the regulation of the glycogen metabolism; cell cycle; and sperm motility [129]. In mammals, PPP1C is coded by three genes (*PPP1CA*, *PPP1CB* and *PPP1CC*). The *PPP1CC* gene undergoes tissue-specific splicing, giving rise to a ubiquitously expressed isoform, PPP1CC1, and a testis-enriched and sperm-specific isoform, PPP1CC2. The difference between these isoforms resides strictly in the C-terminal [129].

2.3.2.3. PPP1 Complexes

PPP1 isoforms share more than 90% aminoacid identity. Moreover, the catalytic subunit is identical in all isoforms and significantly similar to PPP2A and PPP2B. The few differences between PPP1C isoforms are localized to the N and C terminus. In contrast, there are 10 times less serine/threonine protein phosphatases than their counter parts protein kinases [195]. The difference observed is explained by the diverse evolutionary strategy used by the two classes of enzymes. While kinases evolved through gene duplication, protein phosphatases and, specifically PPP1C, diversified by binding to different protein regulators and thus forming many holoenzymes. Indeed, PPP1 exists in the cell as an oligomeric complex in which the PPP1C subunit binds to one or two regulatory subunits known as PPP1 Interacting Proteins, PIPs, that modulate its cellular localization, substrate specificity and also activity [172,196,197]. The different isoforms of the PPP1C also add to the diversity [161]. All things considered, the lack of phosphatase genetic diversity is compensated with the high diversity of phosphatases' complexes.

To date more than 200 PIPs have been identified and they can be divided into PPP1C inhibitors, substrates, substrate-specifiers and targeting-subunits [196]. The binding of PIPs to PPP1C is mediated by short amino acid motifs [128,133] and about 10 have already been described. Each PIP may contain only one or a combination of them. For example, the best known PPP1C binding motif, the RVxF, is present in about 90% of all known PIPs and is thought to be the anchor for subsequent interactions [198]. Even more interesting, is the fact that some PIPs are PPP1 isoform specific. The fact that PPP1 isoforms differ at their N- and C terminal can explain this specificity. Indeed, MYPT1 can only interact with the PPP1CB C-terminus [135]; Neurabin-1 (PPP1R9a) and Repo-man (CDCA2) bind preferentially to PPP1CC1. Also, Spz1 and Endophilin B1t can only interact with the testis-specific isoform PPP1CC2 [143,144].

Most PIPs form a unique and stable complex with PPP1C by combining multiple binding motifs – this property led to the concept of the existence of a PPP1C-binding code [133,199]. This code is universal, specific, degenerate, nonexclusive and dynamic [198]. It is universal since the PPP1C binding motifs are conserved along evolution; specific since a PPP1C binding motif does not bind to any related Phosphatase; the amino acids in the binding motifs may have some flexibility which generates different binding affinities among different PIPs; non-exclusive since binding to a PIP does not exclude binding to a second PIP if the binding motif is different; finally, the code is dynamic since there is molar excess of PIPs in comparison to PPP1C, which allows for PPP1C-PIP interaction to be subjected to regulation, for instance by PIP's phosphorylation [198].

Thus, depending on the PIP that is bound to PPP1C, the complex formed is involved in a specific cellular task [129]. For example, the Retinoblastoma protein (Rb) is dephosphorylated when associated with PPP1C, being converted into a E2F transcription factor inhibitor and thus inhibiting G1-S transition [200]. The protein GADD34 targets PPP1C to the endoplasmic reticulum where they both regulate the initiation of protein translation in mammalian tissues by dephosphorylation of eIF-2α [201]. PPP1R2 binds and inhibits PPP1CC2 but when PPP1R2 is phosphorylated by GSK3 the activity of PPP1CC2 is restored. We have recently proposed that a novel isoform of PPP1R2, PPP1R2P3, that cannot be phosphorylated by GSK3, is a PPP1CC2 irreversible inhibitor in caudal sperm [202]. The recent unravelling of many properties of the binding pattern between PPP1C and its PIPs allowed the development of small molecules that can disrupt the non-covalent interactions that keep protein complexes together, with a high degree of selectivity [198]. These small molecules can have an important role in research or, even more promising, a therapeutic potential to treat diseases where proteins in general or pools of proteins are hyper-phosphorylated [129,203]. Indeed, it was shown that Guanabenz, an α2-adrenergic antagonist anti-hypertensive agent, inhibits the interaction of PPP1C and GADD34 by binding to GADD34. Therefore, Guanabenz has the potential to treat protein folding diseases since GAD34-PPP1C is involved in the modulation of endoplasmic reticulum-stress through eIF-2α dephosphorylation [204].

2.3.3. Role of PPP1C Isoforms in Spermatogenesis

The fact that PPP1CC2 is enriched in testis and specific to spermatozoa suggested an essential role of this protein in spermatogenesis and spermatozoa physiology. Indeed, PPP1CC2 critical role in spermatogenesis was first observed in the *Ppp1cc* null male mice [127]. Ppp1cc knockout is not lethal and female mice present a normal phenotype. Male mice, however, are infertile, despite the normal testosterone levels and sexual behavior. A closer look upon the testis revealed alterations in spermatogenesis, namely the breakdown of the transition between round and elongated spermatocytes and a great loss of germ cells, especially spermatids. There is also a generalized lack

of spermatozoa that appears to stem from generalized apoptosis throughout the layers of the seminiferous epithelium instead of a localized apoptosis in the epithelium adjacent to the basement membrane [125,127]. Sertoli cells are also affected in the *Ppp1cc* null mice: their nuclei is displaced from the basement membrane, suggesting a polarity loss [127,205].

The most severe phenotype of Ppp1cc deletion is found in spermatids. Most round spermatids present severe abnormalities that hint a meiotic failure, such as large nuclei and multiple acrosomes, whereas the elongated spermatids display a multinucleated conjoined twin phenotype. The few condensing spermatids observed present histones instead of protamines for DNA packing in sperm head [127]. This may result from abnormal chromatin packing and condensation in earlier germ cells [206].

As a result of defective spermatogenesis, the epididymis of *Ppp1cc* null mice is virtually devoid of spermatozoa. Occasionally, germ cells can be observed, predominantly abnormal round spermatids and pachytene spermatocytes [125,127]. Plus, the few spermatozoa observed show a wide range of head, mitochondrial sheath and midpiece defects, with the mitochondrial sheath being the most affected structure and being loosely arranged when it is not absent altogether. The head presents a round shape instead of the usual sickle shaped head, characteristic of mouse spermatozoa and a disorganized layer of outer denser fibers [125,127]. Also the manchette, a transient organelle composed of numerous microtubules that assist in tail formation, does not involve the spermatid nucleus and there is a reduced quantity of β-tubulin in this organelle [207]. The numerous defects in the *Ppp1cc* knockout seminiferous epithelium suggest a pleiotropic role PPP1CC2 in germ cell development morphogenesis and flagellar integrity [125,127].

As always, the characterization of the phenotype of *Ppp1cc* null mice answered some questions, but it also uncovered others. Since *Ppp1cc* knockout eliminates both PPP1CC1 and PPP1CC2, the phenotype observed can result from the absence of one or both isoforms. To address this question, Soler *et al* expressed PPP1CC2 in *Ppp1cc* null mice and determined if fertility is restored. PPP1CC2 expression prevented generalized apoptosis and restored spermatozoa concentration to normal levels. However, some impairments of *Ppp1cc* null mice persist: mitochondrial sheath presents gaps in proximal and distal ends, epidydimal spermatozoa head fold back at the connecting piece with an angle at 180 degrees and all spermatozoa are immotile [207]. In sum, transgenic expression of PPP1CC2 rescued spermatogenesis but not fertility. This could be the result of insufficient quantity of PPP1CC2; incorrect spatio-temporal PPP1CC2 expression; necessity of PPP1CC1 expression or a combination of all [207].

In 2012, Sinha *et al* restored fertility in Ppp1cc null mice [208]. This was possible by using either the *Ppp1cc* endogenous promoter or the testicular germ cell specific promoter (PKG2) to express

PPP1CC2 in sperm germ cells. The most relevant findings were that transgenic expression of PPP1CC2 rescued spermatogenesis but not fertility. If 50% was not reached, high percentages of morphological defective spermatozoa were observed. Curiously, PPP1CC2 appears to have a stoichiometric relationship with its interactors/substrates in testis, since decreasing levels of PPP1CC2 expression is associated with increasing morphologic abnormalities [208]. On the other hand, mice with three genes for PPP1CC2 (overexpression of PPP1CC2) in testis were fertile and spermatozoa concentration, morphology and motility were indistinguishable from wild type. Interestingly, *Ppp1cc2* mRNA levels were drastically increased while protein levels resembled wild type. This suggests a post-transcriptional regulating mechanism for PPP1CC2 levels.

To better understand the role of PPP1 isoforms in spermatogenesis, the localization of each isoform was determined by Chakrabarti *et al* and Sinha *et al*. In testis, PPP1CC1 and PPP1CA are expressed in spermatogonia, pre-meiotic cells and testicular somatic cells (Sertoli and Leydig cells) [126]. PPP1CB is present through all stages of spermatogenesis in about the same levels, except in fully mature spermatozoa where it is absent [126]. PPP1CC2 is localized in post-meiotic cells, predominantly in the cytoplasm of secondary spermatocytes, round spermatids and elongated spermatids. There is a week signal in spermatogonia, pachytene, peritubular cells and interstitial cells [125,126]. Figure A.6 shows the cellular localization of PPP1 isoforms through spermatogenesis.

PPP1 is without a doubt essential in spermatogenesis. PPP1CC2 is the only PPP1 isoform present in post-meiotic cells. In addition, PPP1CC2 has a unique 22 amino acid C-terminal and is a mammal specific protein suggesting a significant function in spermatogenesis and spermatozoa in these species [125,126].

In vertebrates, PPP1 isoform ablation is usually compensated by other PPP1 isoforms [122]. However, when *Ppp1cc* gene is disrupted in mammals, a deficient spermatogenesis is observed resulting in male sterility, despite an increased compensatory expression of PPP1CA and PPP1CB [125]. This phenotype can result from the disruption key complexes, involving the mammalian testis-specific and sperm-enriched isoform PPP1CC2 and other testis-specific proteins. Besides, some of these proteins only interact with PPP1CC2, which seems to indicate that in mammals a new system is in place involving PPP1CC2 [202].

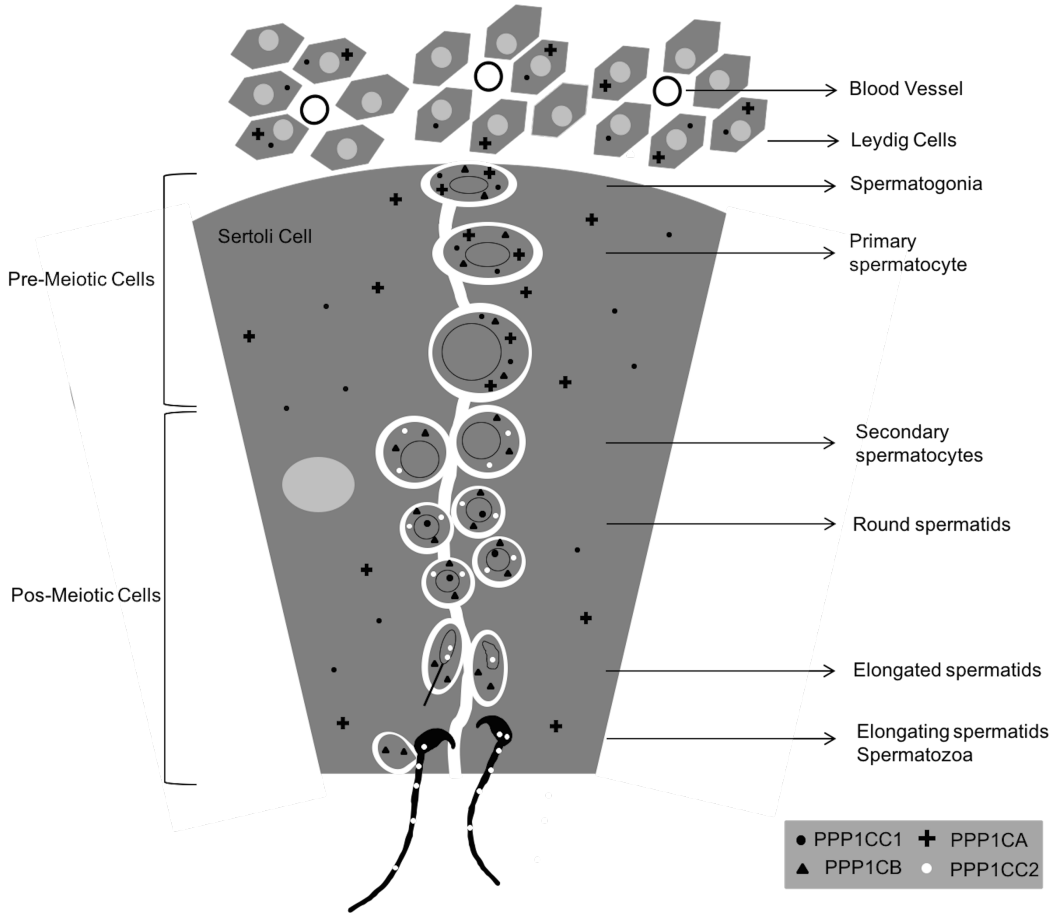

Figure A.6 - PPP1C isoforms localization in mouse testis. PPP1CC1 and PPP1CA are expressed in spermatogonia, pre-meiotic cells and testicular somatic cells (Sertoli and Leydig cells). PPP1CB is localized through the spermatogenesis except fully mature spermatozoa. PPP1CC2 is localized in post-meiotic cells, mainly in the cytoplasm of secondary spermatocytes, round spermatids and elongated spermatids. The expression level of each PPP1 isoform is not reflected in the image.

2.3.4. PPP1 complexes in spermatogenesis

PIPs, structurally unrelated proteins that control PPP1 localization, activity and substrate specificity, show an exceptional diversity and specificity in testis [133]. To this date, a large number of PIPs have been shown to interact with PPP1CC2 in testis and to be involved in spermatogenesis. These include, for instance Spz1, which interact specifically with the PPP1CC2 isoform and PPP1R42that has the ability to interact with multiple PPP1C isoforms.

SPZ1

The spermatogenic zip protein 1 (Spz1) is a member of the basic helix-loop-helix family of transcription factors, a family that has been associated with tissue-specific developmental processes, being highly expressed in testis and epididymis [209,210]. Spz1 was identified by Yeast two-hybrid as a specific binding partner of PPP1CC2 isoform in testis, demonstrated by the loss of interaction on deletion of the unique C-terminus of PPP1CC2 [143]. Despite the presence of a

degenerate RVxF motif, Spz1 does not interact with PPP1CA and PPP1CC1 isoforms [143]. In testis, Spz1 localizes in the cytoplasm of condensing spermatids, which is consistent with the expression of PPP1CC2 in those cells [125,209]. Spz1 localization is grossly abnormal in the testis of the *Ppp1cc* knockout mice, where elongating spermatids are mostly absent. Still, a lack of Spz1 expression is evident in those few tubules where clusters of elongating spermatids are present, which may indicate that the stability of the Spz1 in the cytoplasm is affected by loss of PPP1CC2 [143]. Spz1 was also shown to specifically inhibit PPP1CC2 isoform activity towards phosphorylase *a*. This fact does not exclude the possibility that Spz1 may increase PPP1CC2 activity toward other substrates [143].

Spz1 overexpression in testis leads to dysfunctional spermatogenesis with increased proliferation and apoptosis of germ cells [211]. Moreover, Spz1 overexpression also results in considerable anomalies during late stages of spermatogenesis, since the developing spermatids that survive meiosis show gross morphological defects [211]. Overexpression of Spz1 and loss of PPP1CC in the testis show similarities concerning increased apoptosis and morphological defects in elongating spermatids, suggesting a possible functional relationship between those two proteins.

Endophilin B1t

Endophilin B1t is a splice variant of endophilin B1 (SH3GLB1, SH3 domain GRB2-like endophilin B1) which lacks the last 10 amino acids from the C-terminus [144,212]. Endophilin B1t interacts specifically with PPP1CC2 isoform and, in spite of the presence of a canonical RVxF motif near the N-terminus, does not interact with PPP1CA or with PPP1CC2 mutant lacking the unique C-terminus. In contrast, the somatic endophilin B1 does not interact with any PPP1 isoform [144]. Furthermore, endophilin B1t is able to inhibit PPP1CC2 activity toward phosphorylase a while having little effect on PPP1CA activity [144]. Endophilin B1 isoforms present two kinds of protein distribution in seminiferous tubules: uniform/diffuse cytoplasmic staining (in spermatocytes in some tubules and in elongating spermatids in other tubules) and punctate staining at cell membranes (condensing spermatids). In *Ppp1cc* mutant testis the punctate staining disappears almost completely and only the diffuse pattern is retained [144]. Endophilin involvement in the endocytic pathway, its relationship with PPP1CC2 and the phenotype in the *Ppp1cc* mutant may indicate a role in germ cell release from the seminiferous epithelium [144].

DDOST

The dolichyl-diphosphooligosaccharide−protein glycosyltransferase 48 kDa subunit (DDOST) was identified as a PPP1CC2 interacting protein by tandem affinity purification in transgenic mouse embryonic stem cells [213]. Though DDOST ability to bind to other PPP1 isoforms has not yet been tested, it contains a classical PPP1 binding RVxF motif. This PIP catalyzes the transfer of high-

mannose oligosaccharides to nascent polypeptide chains across the membrane of the endoplasmic reticulum (ER) and it plays a non-catalytic role in the assembly of the oligosaccharyltransferase (OST) complex [214,215]. DDOST localizes in a range of spermatogenic cell types and shows a prominent punctate localization to the nuclear envelope that is especially prevalent in spermatocytes. This is consistent with the localization of DDOST in the rough ER (RER) and with the fact that the spermatocyte nuclei are known to be covered by a layer of RER [213,216]. Even in late elongating spermatids and mature spermatozoa, a smaller but significant amount of DDOST remains present around the nucleus. These facts support a potential role in spermatogenesis/spermiogenesis. DDOST localization in testis is unaffected by the loss of PPP1CC2, suggesting that it may function as a substrate target, directing PPP1CC2 to the nuclear envelope [213]. Moreover, DDOST and other members of the OST complex have been identified in the membrane of human and mouse spermatozoa, which may indicate a putative role in sperm-oocyte interaction [217].

TSKS/ TSSK1

The testis-specific serine/threonine-protein kinase 1 (TSSK1) is essential for spermatogenesis and interacts with PPP1CC2 in testis [218–220]. TSSK1 is only expressed in post-meiotic spermatids [221], being essential for spermiogenesis as demonstrated by the dysregulation caused by targeted deletion of the two genes *Tssk1* and *Tssk2* [220]. This knockout phenotype is distinct in terms of severity from the *Ppp1cc* phenotype which is consistent with a requirement for *Ppp1cc* earlier than Tssk1/2 in spermatogenesis. However, the peak of PPP1CC2 levels in the testis overlaps with that of TSSK1/2 and both knockouts present some similarities such as defects in the organization of the mitochondrial sheaths and reduction in the number and motility of spermatozoa [127,220], suggesting a functional link between PPP1CC2 and TSSK1 late in spermatogenesis. Recently, it was demonstrated that the interaction between PPP1CC2 and TSSK1 in testis is mediated by testis-specific serine/threonine kinase substrate (TSKS) [219]. TSKS, a TSSK1/2 substrate, also displays a post-meiotic expression pattern and is localized to the centrioles of human spermatozoa [222]. TSKS was firstly associated with PPP1 by bioinformatics and then the interaction with PPP1CA was validated *in vitro* [134]. Additionally, the interaction between PPP1CC2 and TSKS is mediated through an RVxF docking motif, that once phosphorylated in testis prevents the interaction with PPP1CC2 [219]. TSSK1 and TSKS have been suggested to play a role in the formation and function of chromatoid body derived structures in elongating spermatids [220] and has been suggested that they function upstream of PPP1CC2 [219]. The haploinsufficiency of TSSK1 and TSKS and their binding to PPP1CC2 reinforces the theory of stoichiometric requirement of the later in post-meiotic germ cells.

PPP1R42

Protein phosphatase 1 regulatory subunit 42 (PPP1R42), otherwise known as leucine-rich repeat protein (TLLR), was validated as PPP1CC2 interacting protein in mouse testis [223,224]. PPP1R42 binding to PPP1C is not solely dependent on the RVxF motif and it binds preferentially to PPP1CC2 when compared with PPP1CA [224]. PPP1R42 is associated with the spermatid cytoskeleton, being located at the manchette in early elongating spermatids and being later transported to the centrosome at the base of the flagellum, suggesting a possible role in the formation of the sperm tail. PPP1R42 interacts with proteins involved in protein stability, such as motor kinesin 1B (KIF1B) and β-tubulin [224]. Along with previous studies showing that PPP1CC2 is required for sperm maturation and that it is localized in developing spermatids, these facts support the theory that PPP1R42 links signaling molecules, including PPP1CC2, to the spermatid cytoskeleton in order to regulate important substrates involved in spermatid transformation [224]. Recently, it was demonstrated that PPP1R42 is localized to the basal body/centrosome of ciliated ARPE-19 cells, similar to its localization in elongating spermatids [225]. Also, PPP1R42 is a positive regulator of PPP1, a phosphatase known to regulate centrosome separation, which is illustrated by the reduction of PPP1 activity by inhibition of PPP1R42 expression, leading, in turn, to activation of NEK2, which is responsible for phosphorylation of centrosomal linker proteins, culminating in centrosome separation [225].

PPP1R11/ PPP1R7

PPP1R7 (phosphoprotein phosphatase 1 regulatory subunit 7, Sds22) was originally identified in yeast as a positive regulator of PPP1, required for mitotic metaphase/anaphase transition [226–228]. Furthermore, PPP1R7 is a PPP1C inhibitor as suggested by the demonstration of an inhibitory effect elicited by a synthetic polypeptide corresponding to the Sds22 sixth leucine-rich repeat (LRR) in cultured mammalian cells [229] and the lack of catalytic activity of the PPP1R7-PPP1CC2 complex in spermatozoa [230]. Likewise, PPP1R11 (phosphoprotein phosphatase 1 regulatory subunit 11, inhibitor 3, I3) is a potent heat-stable PP1 inhibitor and was identified in yeast two-hybrid studies designed to identify PIPs in human brain [231]. PPP1R11, PPP1R7 and PPP1CA were shown to form a trimeric complex in which PPP1CA is catalytically inactive [151,232]. Moreover, PPP1R11 is cleaved by caspase-3 and participates in the apoptotic response [233]. Recently, the formation of a complex between PPP1CC2, PPP1R11, PPP1R7, and actin in testis was demonstrated, in which PPP1CC2 appears to be catalytically inactive [234]. Furthermore, there is a reciprocal relationship between the levels of PPP1CC2 and PPP1R11. In the *Ppp1cc* knockout mice, PPP1R11 appears to be ubiquitinated and the protein levels are significantly reduced, which is overcome when transgenic PPP1CC2 is expressed. Cheng *et al* suggested that complex formation between

PPP1CC2 and PPP1R11 in testis might prevent proteolysis of the last and consequently, germ cell apoptosis.

14-3-3

14-3-3 (also known as YWHA) proteins comprise a family of highly conserved small acidic proteins, expressed in all eukaryotic cells and involved in the regulation of multiple cell signaling cascades [235,236]. Different 14-3-3 isoforms display a certain degree of tissue specificity [237]. It is well established that 14-3-3 is expressed in testis; however, the isoform specific expression of the seven 14-3-3 isoforms in different testicular cell types has not yet been fully characterized [238,239]. 14-3-3 family members and its binding partners are regulators of protein-protein interactions during spermatogenesis [240,241], with PPP1CC2 as one of its predominant interactors in testis [241]. Puri and colleagues proposed that 14-3-3, PGK-2 and PPP1CC2 might exist as a trimeric complex [242] and more recently they showed *in vivo* that PPP1CC2 and PGK-2 are present as a complex in testis and that PPP1CC2 bound to 14-3-3 is catalytically active [241]. Taking these evidences together with the fact that PGK-2 is hyperphosphorylated in *Ppp1cc* knockout mice testis, they suggested PGK-2 is a PPP1CC2 substrate and 14-3-3 serves as a scaffolding protein [241]. 14-3-3 zeta (YWHAZ) was also shown to interact with phosphorylated PPP1CC2 in spermatozoa from diverse species [243]. Phosphorylated PPP1CC2 and 14-3-3 both localize to the postacrosomal region of the head and principal piece of spermatozoa.

Other PIP potentially involved in spermatogenesis

We identified twelve PPP1CC interactors associated with mouse mutations causing male infertility due to impaired spermatogenesis (Table A.2). We retrieved PPP1CC interactors from the HIPPIE database [244]. HIPPIE is regularly updated by incorporating interaction data from major expert-curated experimental protein-protein interaction databases (such as BioGRID, HPRD, IntAct and MINT) using the web service PSICQUIC. The interaction search revealed 204 PPP1CC interactors. Then, proteins associated with defects in male fertility were obtained from the Jackson Laboratories mouse knockout database [245]. Tissue-specification was taken into consideration and the dataset was compared with published proteomes (testis, epididymis and spermatozoa) and tissue-expression databases (C-it database [246]; TiGER [247]; Very Gene database [248], HPA (Human Protein Atlas) [249]; and BioGPS [250]). Future studies on those interactors can increase the knowledge on PPP1CC2 function in spermatogenesis (Table A.2) and uncover new key players in the multifactorial regulation of this process.

Table A.2 - PPP1CC interacting proteins associated with mouse mutations causing male infertility due to impaired spermatogenesis. Protein overlaps with proteomic datasets included human testis, epididymis and spermatozoa proteomes. In gray are the proteins identified as highly specific to or strongly expressed in testis in at least one tissue-expression database.

PPP1CC interactor	Infertile KO mice – Phenotype	Overlap with proteomic datasets	Ref.
AKT1	abnormal spermatogenesis oligozoospermia		251
BRCA1	arrest of male meiosis abnormal spermatid morphology abnormal male germ cell apoptosis		252,253
CCND1	abnormal spermatogenesis		254
CDK1	abnormal male meiosis abnormal spermatocyte morphology abnormal spermatid morphology abnormal male germ cell apoptosis		255
CDK2	abnormal spermatogenesis abnormal spermiogenesis abnormal spermatocyte morphology abnormal spermatid morphology azoospermia abnormal male germ cell apoptosis		256,257
CTSL	abnormal spermatogenesis		258
ESR1	abnormal spermatogenesis oligozoospermia asthenozoospermia teratozoospermia detached sperm flagellum		259–261
HSPA2	arrest of spermatogenesis	Non-sperm located sperm-milieu epididymal and testicular protein	262
HSPA4	arrest of male meiosis abnormal spermatocyte morphology abnormal spermatid morphology oligozoospermia asthenozoospermia abnormal male germ cell apoptosis	Sperm located testicular and epididymal protein also detected in the epididymal fluid (sperm-milieu)	263
LMNA	arrest of male meiosis azoospermia	Sperm located epididymal protein also detected in the epididymal fluid (sperm-milieu)	264
PCNA	arrest of spermatogenesis		265
VDR	abnormal spermatogenesis oligozoospermia asthenozoospermia		266

2.3.5. Conclusion

Modern and non-invasive contraceptive methods for men are still not available. The currently available contraceptive options for men (condoms, vasectomy and withdrawal) are not ideal. Protein-protein interactions are a recent but promising class of drug targets. PPP1CC2-PIPs complexes are essential regulatory components in signaling cascades involved in spermatogenesis. An attractive approach to modulate PPP1 activity is to target specific interfaces between PPP1 and tissue/event-specific PIPs, disrupting their interaction [129,140]. One of these interfaces, which occur in PIPs, is the RVxF-motif, which binds to a site on PPP1 that is remote from the active site. Synthetic peptides that contain variants of the RVxF motif were reported to disrupt a subset of PIP–PPP1 complexes in vitro [163,267]. Additionally, PPP1CC2 has a unique 22 amino-acid C-

terminus that is thought to be important in the binding with its specific interactors, such as endophilin B1t and SPZ1 [143,144] that target the enzyme to a function essential for spermatogenesis. Currently two drugs (salubrinal and trichostatin A) are known to modulate PPP1 complexes [268]. Blocking PPP1CC2-PIP interactions in post-meiotic germ cells will prevent a correct sperm morphogenesis, which may represent a good contraceptive target (Figure A.7). For instance, TSSK1 and TSKS, testis-specific proteins, are post-meiotic in their expression patterns [219], which make them potential targets of reversible contraceptive intervention by preserving spermatogonia and spermatocytes.

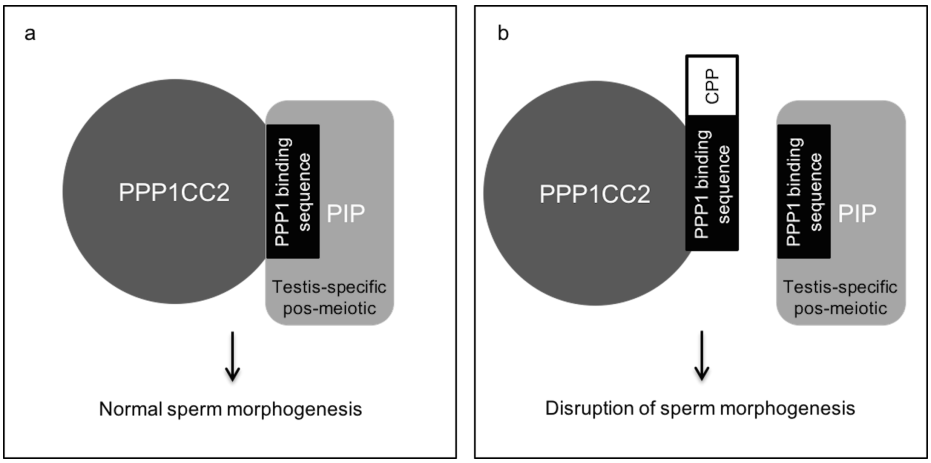

Figure A.7 - Schematic representation of the disruption of PPP1 complexes in post-meiotic germ cells. PPP1CC2 is essential for a correct spermatozoa morphogenesis. An attractive approach to modulate PPP1 is to target specific interfaces between PPP1 and tissue-specific PIPs, using peptides based on PPP1 interacting sequences. PIP, PPP1 Interacting Protein; CPP, Cell Penetrating Peptide sequence.

2.4. Phosphoprotein phosphatase 1 complexes in sperm motility

2.4.1. Sperm motility

Paoli and colleagues defined sperm motility as a propagation of transverse waves along the flagellum in a proximal-distal direction. This produces an impulse that pushes the spermatozoon through the female genital tract [269]. To be motile, human spermatozoa requires (i) a morphological complete flagellum (see section 1.3.1.), (ii) energy to power flagellar movement and (iii) well-orchestrated signaling pathways.

The regulation of the flagellar bending appears to reside in the control of the ATPase activity of axonemal dynein arms. Although the mechanism is not yet fully understood, sperm motility appears to be modulated by alterations on pH, ATP availability, calcium concentration and phosphorylation [30]. Most of the times the root cause of asthenozoospermia is not known and poor sperm motility remains predominantly a clinical sign of infertility, rather than a true diagnosis of the cause of infertility; however research on the mechanisms involved in regulating sperm motility is still sparse [270].

2.4.1.1. Activated and hyperactivated motility

The motility pattern differs between ejaculated spermatozoa and spermatozoa that are recovered from the site of fertilization [271,272]. The two forms of motility (activated and hyperactivated) are characterized by differences in the amplitude of flagellar beat and trajectory pattern. Activated motility generates symmetrical, low amplitude flagellar beats resulting in relatively straight and progressive trajectory in moderately non-viscous media such as seminal plasma [30,271]. Activated motility is acquired in the epididymis and is involved in the initial stages of sperm transport through the female reproductive tract [273]. During transit through the female tract, motility switches to a hyperactivated state, which coincides with the onset of capacitation. This is characterized by asymmetrical, high amplitude flagellar beats, which facilitates sperm progression in the oviduct, dissociation with the oviductal epithelium, through mucoid oviductal secretions and provides the motile thrust needed for zona pellucida penetration [274].

2.4.1.2. Energy: Oxidative phosphorylation *versus* glycolysis

One of the key requirements for spermatozoa motility is energy to fuel the movement. ATP is the fuel used for axonemal dynein ATPases within the flagellum [275]. Also, protein modifications, such as, phosphorylation depend on ATP. So, it is not surprising that sperm require exceptionally more ATP than other cells [276]. It has been shown that the ATP production and availability in human

spermatozoa, is a cooperation between oxidative phosphorylation in mitochondria and glycolysis in the flagellum [276,277].

2.4.2. Role of PPP1 in sperm motility acquisition in the epididymis

During sperm maturation in the epididymis a series of biochemical and morphogenic changes occur resulting in progressive motility [160]. Those include alterations in pH, intracellular concentration of Ca^{2+} and cyclic adenosine mono-phosphate (cAMP) leading to shifts in the proteins phosphorylation status are also essential [278]. PPP1CC2 is the only PPP1 isoform highly enriched in sperm present along the entire flagellum including the mid-piece [161]. A number of previous studies have shown that PPP1CC2 plays a key role in sperm motility. The inhibition of PPP1CC2 activity in caudal sperm is tightly linked to the onset of progressive motility, and to a significant increase in vigorous movement in already progressively motile sperm [160,279]. The PPP1 inhibitors, okadaic acid and calyculin A both initiate and stimulate motility of epididymal spermatozoa [160,279]. Additionally, these phosphatase inhibitors also promote hyperactivated sperm motility and acrosome reaction [280,281]. A decline in PPP1CC2 activity occurs during epididymal sperm maturation not due to a decline in amounts of the enzyme but due to lowering of its catalytic activity. PPP1CC2 is also involved in sperm tail morphogenesis [125]. The *Ppp1cc*-null mice had malformed sperm tails, missing mitochondrial sheaths and disorganized outer dense fibers on the sperm [127]. Recent studies observed that PPP1CC2 alone in the absence of PPP1CC1 in testis restored sperm morphogenesis and sperm function [208].

2.4.2.1. PPP1CC2 complexes in sperm motility

PPP1CC2 activity during sperm maturation has been suggested to be mainly regulated by its inhibitors – PPP1R2 (inhibitor 2, I2), PPP1R7 (sds22) and PPP1R11 (inhibitor 3, I3) – YWHA (14-3-3) and AKAPs (Figure A.8). However, the role of these and other complexes in sperm motility still needs to be elucidated.

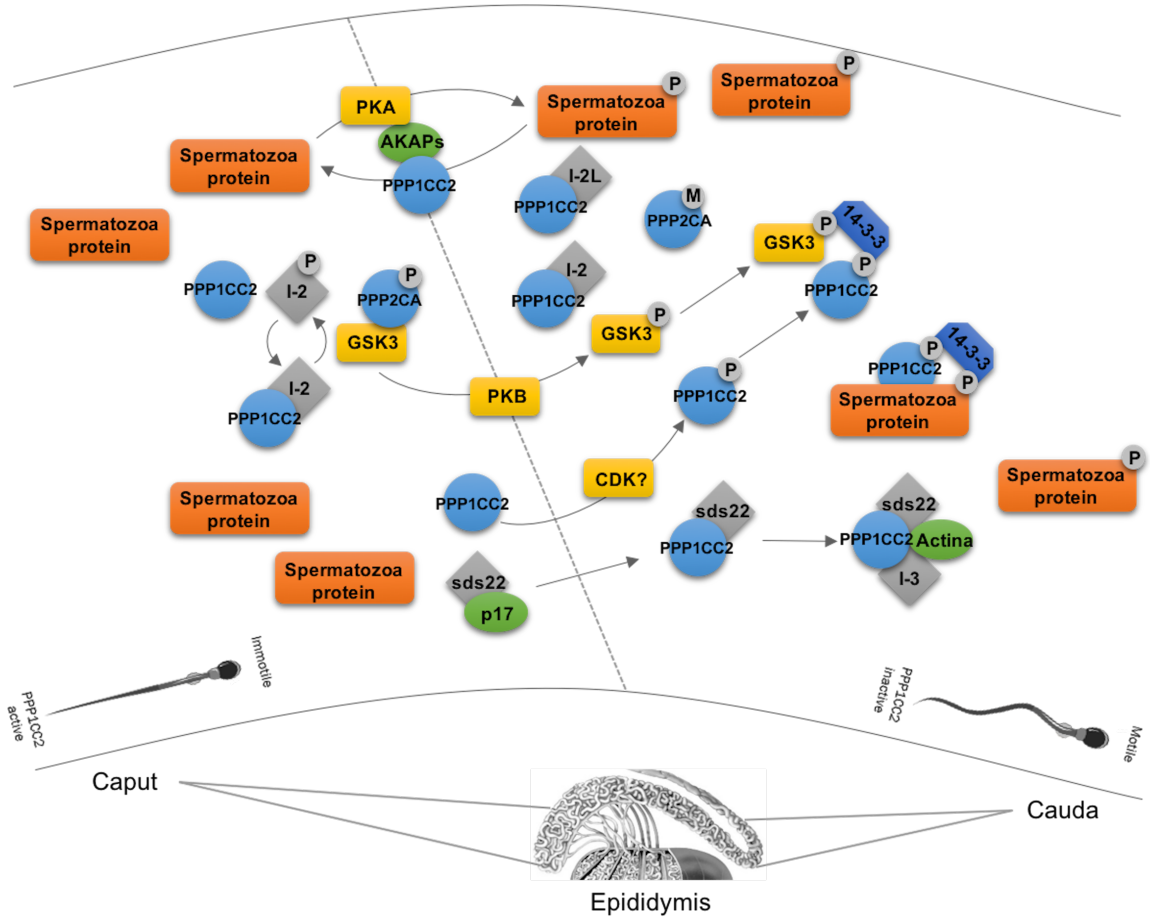

Figure A.8 - Schematic representation of the PPP1CC2 based regulation of sperm motility acquisition. AKAPs anchoring appear to modulate PPP1CC2 and PKA activities regulating phosphorylation events. In caput epididymis, PPP2CA is phosphorylated and consequently active, which in turn dephosphorylated GSK3 at Ser residues, rendering it active. GSK3 phosphorylates PPP1R2 (I2) at Thr73 which inhibits the interaction between PPP1R2 and PPP1CC2 resulting in active PPP1CC2. Sds22 (PPP1R7) is unable to inhibit PPP1CC2 since it is bound to p17. Active PPP1 results in protein dephosphorylation and consequently immotile spermatozoa. In cauda epididymis, PME1 activity decreases which increases PPP2CA methylation, resulting in inhibition of PPP2CA. Consequently, GSK3 serine phosphorylation increases leading to GSK3 inhibition. Also, Wnt binds to LRP6 receptor which promotes GSK3 inhibition. Calcium influx activates sAC, which produces cAMP activating Rap guanine nucleotide exchange factor (RAPGEFs), which activates PKB (AKT1) that phosphorylates GSK3 at serine residues inactivating it. GSK3 is inhibited, which leads to decrease Thr73 PPP1R2 phosphorylation. Consequently, PPP1R2 binds PPP1. Also, PPP1 is bound to PPPP1R2P3 (I2-L) that cannot be phosphorylated by GSK3. Also, a multimeric complex has been identified composed by PPP1CC2, sds22 (PPP1R7), actin and I3 (PPP1R11), where PPP1CC2 was inactive. Thus, PPP1 activity is inhibited and ser/thr phosphorylation of key residues increases leading to motile spermatozoa. PPP1CC22 activity may also be regulated by phosphorylation in a C-terminal threonine residue by a CDK, most likely CDK2. Phosphorylated GSK3 and phosphorylated PPP1CC2 are bound to YWHA (14-3-3) in caudal sperm. P, phosphorylated; M, methylated.

PPP1R2

PPP1R2 (I2) is capable of inhibiting the catalytic subunit of PPP1 leading to the production of a stable PPP1-PPP1R2 complex. GSK3 phosphorylates PPP1R2 in the PPP1-PPP1R2 complex, relieving the inhibition and producing active PPP1. Immotile bovine caput epididymal sperm contains 2-fold higher levels of protein phosphatase activity, identified as being PPP1CC2, and 6-fold higher GSK3 activity than do mature motile caudal sperm [160,161,279]. Thus, a model was proposed in which in the first segments of the epididymis (caput) the sperm is immotile due to the

activation of the PPP1R2/PPP1CC2 complex by GSK3, while in the last segment of the epididymis (cauda), PPP1R2P3 (PPP1R2 pseudogene 3) takes place and substitutes PPP1R2 as an irreversible inhibitor of PPP1CC2 triggering sperm motility [140]. Korrodi-Gregório *et al* demonstrated that PPP1R2P3 protein binds directly to PPP1CC and that this inhibitor cannot be phosphorylated by GSK3 since the key phosphosites are substituted to non-phosphorylated residues, T73P and S87R [202]. It is possible that PPP1R2P3 is somehow bound another protein that may keep it from binding to PPP1CC2 in immotile caput sperm, in a manner similar to what is suggest to occur with PPP1R7 (sds22) in caput sperm.

PPP1R11/ PPP1R7

PPP1R11/I3 is a potent heat-stable PPP1 inhibitor [231] and is a human homologue of the mouse t-complex expressed protein 5 (Tctex5), being genetically linked to the male infertility phenotypes of impaired sperm tail development and poor sperm motility [282]. In epididymal mouse spermatozoa Tctex5 is present in the head and principal piece of the tail [283]. These are also the locations where PPP1CC2 is expressed [284]. A yeast sds22 homologue, PPP1R7, was identified in sperm [285], and inhibits the PPP1 catalytic subunit in rat liver nuclei [229]. Consistently, a PPP1R7 homologue was also identified in rat testis in association with PPP1CC2 [286]. PPP1R7 was also identified in motile caudal spermatozoa as a regulator of PPP1CC2 catalytic activity [230]. In male germ cells PPP1CC2, PPP1R11, PPP1R7 and actin form a multimeric complex in which PPP1CC2 is inactive [234]. The stability of the complex depended on functional PPP1 interaction sites in PPP1R7 and PPP1R11, indicating that PPP1 mediates the interaction between these two proteins, forming a catalytically inactive complex in the germ cell [151]. The function of this complex in sperm motility, if any, still needs to be elucidated.

CDK2, GSK3 and 14-3-3

PPP1CC2, as well as other PPP1 isoforms, have at the C-terminus a consensus TPPR amino acid sequence containing a threonine residue (T311) that can be phosphorylated by cyclin-dependent kinases (CDKs) [287–289]. The proportion of phosphorylated PPP1CC2 in caudal sperm is higher than in caput epididymal sperm and is localized to the head equatorial region, implicated in sperm-egg binding, and in the principal piece of the tail [278]. In spermatozoa, phosphorylated PPP1CC22 is the only catalytically active form of the enzyme in caudal spermatozoa. Huang et al. revealed that that CDK2 is present in spermatozoa [278]. Interestingly, CDK2 knockout mice are viable but are sterile [257]. CDK2 regulation of PPP1CC2 may be achieved through binding of PPP1CC2 to the bridging molecule 14-3-3 (YWHA). 14-3-3 binds phosphorylated PPP1CC2 in spermatozoa [243]. Additionally, GSK3 was found to bind 14-3-3 [241,242]. Sperm 14-3-3 is present in the post-acrosomal region of the head and the principal piece, similar to PPP1CC2 [243]. As already stated, an increase in

GSK3 phosphorylation occur in parallel with motility stimulation in sperm [290]. Besides being infertile due to impaired sperm motility, the *Gsk3a* knockout mice revealed that PPP1CC2 activity was elevated in sperm [291]. Since, phosphorylation at the threonine residue is known to reduce PPP1 activity, Bhattacharjee and colleagues suggested that GSK3A might be responsible for PPP1CC2 phosphorylation in spermatozoa. Additionally, GSK3A may also be involved in regulating PPP1 inhibitors [291].

AKAPs

Compartmentalization of the cyclic AMP (cAMP)-dependent protein kinase (PKA) is mediated through association of its regulatory subunits with A-kinase anchoring proteins (AKAPs). To date, over 40 AKAPs have been identified, and in testis/sperm there are three AKAPs that have been related to PPP1CC2 (AKAP220, AKPA3 and AKAP4) [161]. Given that many AKAPs have been shown to be present in germ cells and localized to compartments related to motility where PPP1CC2 is also present they might be putatively involved in motility acquisition. AKAP220/AKAP11 binds PKA and PPP1, being a competitive inhibitor of PPP1 [292]. AKAP220 is present in human male germ cells and mature sperm and like RIIα, is located in the midpiece and is probably associated with cytoskeletal structures [293]. The midpiece associated AKAP220 could serve to anchor PKA and/or PPP1CC2, directly regulating the contractile machinery in the sperm axoneme. Furthermore, it has been shown that disruption of RII interaction with AKAPs, by membrane-permeable peptides, causes the arrest of sperm motility [294]. AKAP4/AKAP82 expression was only detected in testis and it was determined that transcription is initiated at 20-22 days after birth and the mRNA is present in spermatids but not in pachytene spermatocytes [295,296]. Targeted disruption of the *Akap4* gene causes absence of sperm motility together with a complete lack of fibrous sheath on the principal piece of mature mice sperm, causing male mice to be infertile [31]. Additionally, *Akap4* gene knockout mice exhibit a significant change in the activity and phosphorylation of PPP1CC2 [284]. AKAP3 is a testis-specific protein found only in the fibrous sheath and localized to the circumferential ribs of human sperm [297].

2.5. Amyloid precursor protein (APP) complexes in male fertility

Amyloid precursor protein (APP), a type I transmembrane glycoprotein consisting of a large extracellular domain, a single transmembrane domain, and a short cytoplasmic tail, is expressed ubiquitously and given its receptor-like and adhesive characteristics, may play important roles outside the nervous system Figure A.9. In fact, Fardilha *et al* have previously showed that APP is present in spermatozoa [298]. The APP superfamily includes APP and APP-like proteins (APLP) 1 and 2 that are codified in chromosome 21, chromosome 11 and chromosome 19, respectively. Alternative splicing of exons 7, 8 and 15 of the APP mRNA produces eight isoforms, ranging in size from 677-770 amino acids. Alternative splicing produces four APLP1 and two APLP2 protein isoforms. Although some isoforms may be cell type specific, APP and APLP2 are ubiquitously expressed. In contrast, APLP1 is expressed selectively in the nervous system [299]. The APP is synthesized on membrane-bound polysomes and matures as it is transported through the secretory pathway, becoming N- and O-glycosylated and tyrosyl-sulfated while it moves through the trans-Golgi network. Immature APP (being N-glycosylated only) may be cleaved in the endoplasmic reticulum (ER) or the cis-Golgi, but mature APP is rapidly degraded as it is transported to or from the cell surface via either a biosynthetic or endocytic pathway [300]. APP proteolytic processing originates alpha secreted APP (sAPP), a C-terminal domain (APP Intracellular Domain, AICD) and a non-toxic small peptide (p3). Alternative proteolytic routes originate beta sAPP, AICD and Abeta fragments [299]. The transmembrane structure of APP is consistent with a role as a receptor or a mediator of extracellular interactions. It has been suggested that APP may have CAM (Cell Adhesion Molecule)- and SAM (Substrate Adhesion Molecule)-like activities. Indeed, APP possesses several domains that promote binding to specific substrates, such as heparin and collagen, which implicate cell-surface APP in both cell-cell and cell-substrate adhesion [301]. Additionally, some studies indicate that full length APP can act as a cell surface G-protein coupled receptor (GPCR) and shows that APP binds heterotrimeric G proteins (Gαo) [302,303]. Recently, Deyts and colleagues discovered an interaction between APP intracellular domain and the heterotrimeric G-protein subunit Gαs [304].

Various lines of evidence implicate APP and APLP2 in fertility. APP was shown to be expressed in rat testis and localized in the acrosome region and growing tail of spermatids in the seminiferous tubules [305]. Knock-out mice, homozygotes to either APP(-/-) or APLP2 (-/-) were fertile, but mice with the deletion of both APP(-/-) and APLP2(-/-) were infertile (9 of 10 females and all males) [306]. Fardilha *et al* previously characterized the subcellular distribution of the APP superfamily members [298]. The presence of APP superfamily members along the entire length of the tail may be related to signaling events involved in sperm motility, whereas their presence in the head and

particularly in the equatorial region suggests their involvement in sperm-oocyte interaction [298]. Those results were consistent with the previous localization of APLP2 in mammalian sperm, but also prove the presence of APP itself in human sperm. APP and APLPs distribution only partially overlap, suggesting that besides a common role they might also have distinct functions in spermatozoa [298]. A human sperm transmembrane protein initially termed YWK-II (later shown to be an APLP2 homologue) was shown to be involved in fertilization [307,308]. The YWK-II gene was shown to be expressed in germ cells at various stages of differentiation and in the plasma membrane enveloping the acrosome of mature spermatozoa [308]. YWK-II/APLP2 antibodies agglutinate human and rat spermatozoa, and block the penetration of hamster eggs. Additionally the treatment of mice of both genders with YWK-II/APLP2 antibodies or a synthetic peptide results in reduction of zygote formation [309]. APLP2/YWK-II also exhibits properties of a receptor and its extracellular domain was shown to interact with Müllerian-inhibiting substance [310]. Müllerian-inhibiting substance increases the viability and longevity of human spermatozoa through binding the YWK-II component on the sperm membrane [310]. Huang and colleagues showed that YWK-II component binds to a GTP-binding protein (Gαo) and was phosphorylated by PKC and cdc2 kinase in the cytoplasmic domain. Thus, APLP2/YWK-II functions as a novel Gαo-protein-coupled receptor for Müllerian inhibiting substance in cell survival [307].

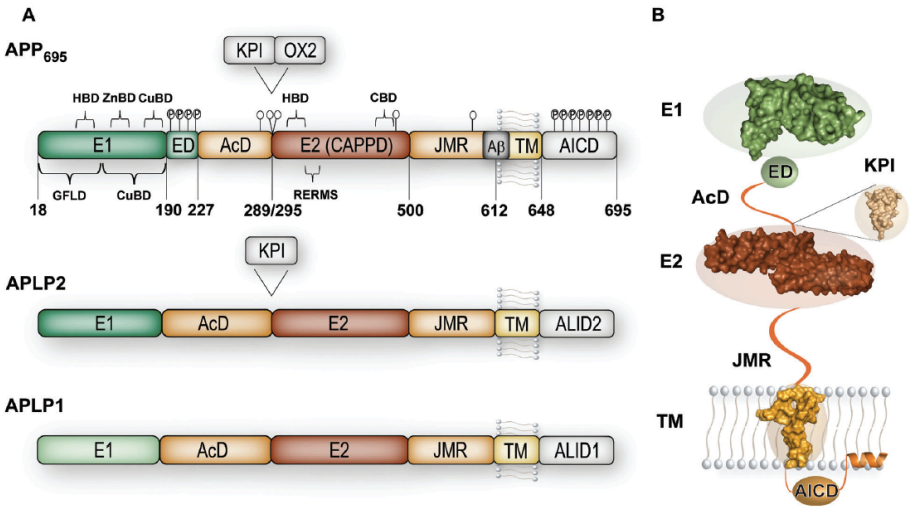

Figure A.9 - Overall structure and conservation of APP-family proteins. (A) Domain architecture, functional segments and conservation of APP-family proteins. APP and its mammalian homologues APLP1 and APLP2 share on overall a similar domain architecture including the E1-domain, the acidic region (AcD), the E2-domain (also called central APP domain, CAPPD), the juxtamembrane region (JMR), the transmembrane region (TM) and an intracellular domain [APP intracellular domain (AICD); APP-like intracellular domain (ALID1/ALID2)]. The Aβ-peptide and the extension domain (ED) are only present in APP, the KPI/OX2-insertion only in APP and APLP2 and the E1-domain is less conserved in APLP1 as indicated by its light green color. Additional functional units are indicated by brackets [heparin binding domain (HBD); copper binding domain (CuBD); zinc binding domain (ZnBD); collagen binding domain (CBD); growth factor like domain (GFLD)]. Phosphorylation and glycosylation sites are shown as P and empty circles, respectively. (B) The two folded domains E1 and E2 of APP as well as the transmembrane segment connecting the JMR with the AICD are shown as surface representation based on their respective crystal or NMR structures. The KPI-domain, only present in the longer splicing forms in between the AcD and the E2-domain, is likewise shown as surface representation and the surface-associated helix at the very C-terminus of APP is shown as idealized α-helix [311] .

References

1. Kerr, J. B. Functional cytology of the human testis. *Baillieres. Clin. Endocrinol. Metab.* 6, 235–50 (1992).
2. Kerr, J. B. Ultrastructure of the seminiferous epithelium and intertubular tissue of the human testis. *J. Electron Microsc. Tech.* 19, 215–40 (1991).
3. Clermont, Y. & Perey, B. Quantitative study of the cell population of the seminiferous tubules in immature rats. *Am. J. Anat.* 100, 241–67 (1957).
4. Orth, J. M., Gunsalus, G. L. & Lamperti, A. A. Evidence from Sertoli cell-depleted rats indicates that spermatid number in adults depends on numbers of Sertoli cells produced during perinatal development. *Endocrinology* 122, 787–94 (1988).
5. Johnson, L., Thompson, D. L. & Varner, D. D. Role of Sertoli cell number and function on regulation of spermatogenesis. *Anim. Reprod. Sci.* 105, 23–51 (2008).
6. Cheng, C. Y., Wong, E. W. P., Yan, H. H. N. & Mruk, D. D. Regulation of spermatogenesis in the microenvironment of the seminiferous epithelium: new insights and advances. *Mol. Cell. Endocrinol.* 315, 49–56 (2010).
7. Gould, S. F. & Bernstein, M. H. Fine structure of fetal human testis and epididymis. *Arch. Androl.* 2, 93–9 (1979).
8. Lejeune, H., Habert, R. & Saez, J. M. Origin, proliferation and differentiation of Leydig cells. *J. Mol. Endocrinol.* 20, 1–25 (1998).
9. Svechnikov, K., Landreh, L., Weisser, J., Izzo, G., Colón, E., Svechnikova, I. & Söder, O. Origin, development and regulation of human Leydig cells. *Horm. Res. pædiatrics* 73, 93–101 (2010).
10. Prince, F. P. Ultrastructural evidence of mature Leydig cells and Leydig cell regression in the neonatal human testis. *Anat. Rec.* 228, 405–17 (1990).
11. Benton, L., Shan, L. X. & Hardy, M. P. Differentiation of adult Leydig cells. *J. Steroid Biochem. Mol. Biol.* 53, 61–8 (1995).
12. Dacheux, J.-L. & Dacheux, F. New insights into epididymal function in relation to sperm maturation. *Reproduction* 147, R27–42 (2014).
13. Ferraretti, A. P. *et al.* Assisted reproductive technology in Europe, 2009: Results generated from European registers by ESHRE. *Hum. Reprod.* 28, 2318–2331 (2013).
14. Cooper, T. G. & Yeung, C. H. in *The Sperm Cell* (eds. De Jonge, C. & Barratt, C. L.) 72–107 (Cambridge University Press, 2006).
15. Cyr, D. G., Gregory, M., Dubé, E., Dufresne, J., Chan, P. T. K. & Hermo, L. Orchestration of occludins, claudins, catenins and cadherins as players involved in maintenance of the blood-epididymal barrier in animals and humans. *Asian J. Androl.* 9, 463–75 (2007).
16. Fardilha, M., Silva, J. V. & Conde, M. *Reprodução Humana Masculina: Princípios Fundamentais*. (ARC Publishing, 2015).
17. Cornwall, G. A. New insights into epididymal biology and function. *Hum. Reprod. Update* 15, 213–27
18. Aitken, R. J., Nixon, B., Lin, M., Koppers, A. J., Lee, Y. H. & Baker, M. A. Proteomic changes in mammalian spermatozoa during epididymal maturation. *Asian J. Androl.* 9, 554–64 (2007).
19. de Kretser, D. M., Loveland, K. L., Meinhardt, A., Simorangkir, D. & Wreford, N. Spermatogenesis. *Hum. Reprod.* 13 Suppl 1, 1–8 (1998).
20. Brewer, L., Corzett, M. & Balhorn, R. Condensation of DNA by spermatid basic nuclear proteins. *J. Biol. Chem.* 277, 38895–900 (2002).
21. Dadoune, J.-P. Expression of mammalian spermatozoal nucleoproteins. *Microsc. Res. Tech.* 61, 56–75 (2003).
22. Hammoud, S. S., Nix, D. A., Zhang, H., Purwar, J., Carrell, D. T. & Cairns, B. R. Distinctive chromatin in human sperm packages genes for embryo development. *Nature* 460, 473–8 (2009).
23. Oliva, R. Protamines and male infertility. *Hum. Reprod. Update* 12, 417–35
24. Ho, H.-C. & Suarez, S. S. Characterization of the intracellular calcium store at the base of the sperm flagellum that regulates hyperactivated motility. *Biol. Reprod.* 68, 1590–1596 (2003).
25. Oko, R. J. Developmental expression and possible role of perinuclear theca proteins in mammalian spermatozoa. *Reprod. Fertil. Dev.* 7, 777–97 (1995).

26. Moreno, R. D., Ramalho-Santos, J., Sutovsky, P., Chan, E. K. & Schatten, G. Vesicular traffic and golgi apparatus dynamics during mammalian spermatogenesis: implications for acrosome architecture. *Biol. Reprod.* 63, 89–98 (2000).
27. Yoshinaga, K. & Toshimori, K. Organization and modifications of sperm acrosomal molecules during spermatogenesis and epididymal maturation. *Microsc. Res. Tech.* 61, 39–45 (2003).
28. AfzeliusFZELIUS, B. Electron microscopy of the sperm tail; results obtained with a new fixative. *J. Biophys. Biochem. Cytol.* 5, 269–78 (1959).
29. Fawcett, D. W. The anatomy of the spermatozoon after 300 years. *Kaibogaku Zasshi.* 50, 326–7 (1975).
30. Turner, R. M. Moving to the beat: a review of mammalian sperm motility regulation. *Reprod. Fertil. Dev.* 18, 25–38 (2006).
31. Miki, K., Willis, W. D., Brown, P. R., Goulding, E. H., Fulcher, K. D. & Eddy, E. M. Targeted disruption of the Akap4 gene causes defects in sperm flagellum and motility. *Dev. Biol.* 248, 331–342 (2002).
32. Moore, H. D. M. in *Gametes: The Spermatozoon* (eds. Grudzinskas, J. G. & Yovich, J. L.) 140–157 (Cambridge University Press, 1995).
33. Owen, D. H. & Katz, D. F. A review of the physical and chemical properties of human semen and the formulation of a semen simulant. *J. Androl.* 26, 459–69
34. Coffey, D. in *Handbook of Andrology* (eds. Robaire, B., Pryor, J. L. & Trasler, J. M.) 21–4 (Allen Press Inc., 1995).
35. Poliakov, A., Spilman, M., Dokland, T., Amling, C. L. & Mobley, J. A. Structural heterogeneity and protein composition of exosome-like vesicles (prostasomes) in human semen. *Prostate* 69, 159–67 (2009).
36. Ronquist, G. & Brody, I. The prostasome: its secretion and function in man. *Biochim. Biophys. Acta* 822, 203–18 (1985).
37. Frenette, G., Lessard, C. & Sullivan, R. Selected proteins of 'prostasome-like particles' from epididymal cauda fluid are transferred to epididymal caput spermatozoa in bull. *Biol. Reprod.* 67, 308–13 (2002).
38. Arienti, G., Carlini, E., Nicolucci, A., Cosmi, E. V, Santi, F. & Palmerini, C. A. The motility of human spermatozoa as influenced by prostasomes at various pH levels. *Biol. Cell* 91, 51–4 (1999).
39. Fabiani, R., Johansson, L., Lundkvist, O. & Ronquist, G. Enhanced recruitment of motile spermatozoa by prostasome inclusion in swim-up medium. *Hum. Reprod.* 9, 1485–9 (1994).
40. Pawson, T. & Nash, P. Protein-protein interactions define specificity in signal transduction. *Genes and Development* 14, 1027–1047 (2000).
41. Olsen, J. V & Mann, M. Status of large-scale analysis of post-translational modifications by mass spectrometry. *Mol. Cell. Proteomics* 12, 3444–52 (2013).
42. Phizicky, E. M. & Fields, S. Protein-protein interactions: methods for detection and analysis. *Microbiol. Rev.* 59, 94–123 (1995).
43. Rao, V. S., Srinivas, K., Sujini, G. N. & Kumar, G. N. S. Protein-Protein Interaction Detection: Methods and Analysis. *Int. J. Proteomics* 2014, 1–12 (2014).
44. de Las Rivas, J. & Fontanillo, C. Protein-protein interactions essentials: Key concepts to building and analyzing interactome networks. *PLoS Comput. Biol.* 6, 1–8 (2010).
45. Bader, G. D., Betel, D. & Hogue, C. W. V. BIND: The Biomolecular Interaction Network Database. *Nucleic Acids Research* 31, 248–250 (2003).
46. Stark, C., Breitkreutz, B.-J., Reguly, T., Boucher, L., Breitkreutz, A. & Tyers, M. BioGRID: a general repository for interaction datasets. *Nucleic Acids Res.* 34, D535–D539 (2006).
47. Salwinski, L., Miller, C. S., Smith, A. J., Pettit, F. K., Bowie, J. U. & Eisenberg, D. The Database of Interacting Proteins: 2004 update. *Nucleic Acids Res.* 32, D449–D451 (2004).
48. Peri, S. *et al.* Human protein reference database as a discovery resource for proteomics. *Nucleic Acids Res.* 32, D497–D501 (2004).
49. Schaefer, M. H., Fontaine, J. F., Vinayagam, A., Porras, P., Wanker, E. E. & Andrade-Navarro, M. A. Hippie: Integrating protein interaction networks with experiment based quality scores. *PLoS One* 7, (2012).
50. Stelzl, U. *et al.* A human protein-protein interaction network: A resource for annotating the

proteome. *Cell* 122, 957–968 (2005).

51. Shannon, P., Markiel, A., Ozier, O., Baliga, N. S., Wang, J. T., Ramage, D., Amin, N., Schwikowski, B. & Ideker, T. Cytoscape: A software Environment for integrated models of biomolecular interaction networks. *Genome Res.* 13, 2498–2504 (2003).
52. Milroy, L.-G., Grossmann, T. N., Hennig, S., Brunsveld, L. & Ottmann, C. Modulators of Protein–Protein Interactions. *Chem. Rev.* 114, 4695–4748 (2014).
53. Nero, T. L., Morton, C. J., Holien, J. K., Wielens, J. & Parker, M. W. Oncogenic protein interfaces: small molecules, big challenges. *Nat. Rev. Cancer* 14, 248–62 (2014).
54. Wells, J. A. & McClendon, C. L. Reaching for high-hanging fruit in drug discovery at protein-protein interfaces. *Nature* 450, 1001–1009 (2007).
55. Jin, L., Wang, W. & Fang, G. Targeting protein-protein interaction by small molecules. *Annu. Rev. Pharmacol. Toxicol.* 54, 435–56 (2014).
56. Higueruelo, A. P., Jubb, H. & Blundell, T. L. Protein-protein interactions as druggable targets: Recent technological advances. *Curr. Opin. Pharmacol.* 13, 791–796 (2013).
57. Lukanowska, M., Howl, J. & Jones, S. Bioportides: Bioactive cell-penetrating peptides that modulate cellular dynamics. *Biotechnology Journal* 8, 918–930 (2013).
58. Howl, J., Matou-Nasri, S., West, D. C., Farquhar, M., Slaninová, J., Östenson, C. G., Zorko, M., Östlund, P., Kumar, S., Langel, Ü., McKeating, J. & Jones, S. Bioportide: An emergent concept of bioactive cell-penetrating peptides. *Cell. Mol. Life Sci.* 69, 2951–2966 (2012).
59. Futaki, S., Suzuki, T., Ohashi, W., Yagami, T., Tanaka, S., Ueda, K. & Sugiura, Y. Arginine-rich peptides. An abundant source of membrane-permeable peptides having potential as carriers for intracellular protein delivery. *J. Biol. Chem.* 276, 5836–5840 (2001).
60. Jones, S., Lukanowska, M., Suhorutsenko, J., Oxenham, S., Barratt, C., Publicover, S., Copolovici, D. M., Langel, Ü. & Howl, J. Intracellular translocation and differential accumulation of cell-penetrating peptides in bovine spermatozoa: evaluation of efficient delivery vectors that do not compromise human sperm motility. *Hum. Reprod.* 28, 1874–89 (2013).
61. Fields, S. & Song, O. A novel genetic system to detect protein-protein interactions. *Nature* 340, 245–246 (1989).
62. Stynen, B., Tournu, H., Tavernier, J. & Van Dijck, P. Diversity in Genetic In Vivo Methods for Protein-Protein Interaction Studies: from the Yeast Two-Hybrid System to the Mammalian Split-Luciferase System. *Microbiol. Mol. Biol. Rev.* 76, 331–382 (2012).
63. Bruckner, A., Polge, C., Lentze, N., Auerbach, D. & Schlattner, U. Yeast two-hybrid, a powerful tool for systems biology. *Int J Mol Sci* 10, 2763–2788 (2009).
64. Auerbach, D. & Stagljar, I. in *Proteomics and Protein–Protein Interactions: Biology, Chemistry, Bioinformatics, and Drug Design* (Springer, 2005).
65. Hirst, M., Ho, C., Sabourin, L., Rudnicki, M., Penn, L. & Sadowski, I. A two-hybrid system for transactivator bait proteins. *Proc. Natl. Acad. Sci.* 98, 8726–8731 (2001).
66. Joshi, P. B., Hirst, M., Malcolm, T., Parent, J., Mitchell, D., Lund, K. & Sadowski, I. Identification of protein interaction antagonists using the repressed transactivator two-hybrid system. *Biotechniques* 42, 635–44 (2007).
67. Serebriiskii, I., Khazak, V. & Golemis, E. A. A two-hybrid dual bait system to discriminate specificity of protein interactions. *J Biol Chem* 274, 17080–17087 (1999).
68. Serebriiskii, I. G., Mitina, O., Pugacheva, E. N., Benevolenskaya, E., Kotova, E., Toby, G. G., Khazak, V., Kaelin, W. G., Chernoff, J. & Golemis, E. A. Detection of peptides, proteins, and drugs that selectively interact with protein targets. *Genome Res* 12, 1785–1791 (2002).
69. Spektor, T. M. & Rice, J. C. Identification and characterization of posttranslational modification-specific binding proteins in vivo by mammalian tethered catalysis. *Proc Natl Acad Sci U S A* 106, 14808–14813 (2009).
70. Guo, D., Hazbun, T. R., Xu, X. J., Ng, S. L., Fields, S. & Kuo, M. H. A tethered catalysis, two-hybrid system to identify protein-protein interactions requiring post-translational modifications. *Nat Biotechnol* 22, 888–892 (2004).
71. Ehrhard, K. N., Jacoby, J. J., Fu, X. Y., Jahn, R. & Dohlman, H. G. Use of G-protein fusions to monitor integral membrane protein-protein interactions in yeast. *Nat Biotechnol* 18, 1075–1079 (2000).

72. Aronheim, A., Zandi, E., Hennemann, H., Elledge, S. J. & Karin, M. Isolation of an AP-1 repressor by a novel method for detecting protein-protein interactions. *Mol Cell Biol* 17, 3094–3102 (1997).
73. Schonhofer-Merl, S. & Torres-Ruiz, R. A. The Sos-recruitment system as a tool to analyze cellular localization of plant proteins: membrane localization of Arabidopsis thaliana PEPINO/PASTICCINO2. *Mol Genet Genomics* 283, 439–449 (2010).
74. Jaaro, H., Levy, Z. & Fainzilber, M. A genome wide screening approach for membrane-targeted proteins. *Mol Cell Proteomics* 4, 328–333 (2005).
75. Broder, Y. C., Katz, S. & Aronheim, A. The ras recruitment system, a novel approach to the study of protein-protein interactions. *Curr Biol* 8, 1121–1124 (1998).
76. Hubsman, M., Yudkovsky, G. & Aronheim, A. A novel approach for the identification of protein-protein interaction with integral membrane proteins. *Nucleic Acids Res* 29, E18 (2001).
77. Maroun, M. & Aronheim, A. A novel in vivo assay for the analysis of protein-protein interaction. *Nucleic Acids Res* 27, e4 (1999).
78. Johnsson, N. & Varshavsky, A. Split ubiquitin as a sensor of protein interactions in vivo. *Proc Natl Acad Sci U S A* 91, 10340–10344 (1994).
79. Fetchko, M. & Stagljar, I. Application of the split-ubiquitin membrane yeast two-hybrid system to investigate membrane protein interactions. *Methods* 32, 349–362 (2004).
80. Miller, J. P., Lo, R. S., Ben-Hur, A., Desmarais, C., Stagljar, I., Noble, W. S. & Fields, S. Large-scale identification of yeast integral membrane protein interactions. *Proc Natl Acad Sci U S A* 102, 12123–12128 (2005).
81. Reichel, C. & Johnsson, N. The split-ubiquitin sensor: measuring interactions and conformational alterations of proteins in vivo. *Methods Enzym.* 399, 757–776 (2005).
82. Urech, D. M., Lichtlen, P. & Barberis, A. Cell growth selection system to detect extracellular and transmembrane protein interactions. *Biochim Biophys Acta* 1622, 117–127 (2003).
83. Marsolier, M. C., Prioleau, M. N. & Sentenac, A. A RNA polymerase III-based two-hybrid system to study RNA polymerase II transcriptional regulators. *J Mol Biol* 268, 243–249 (1997).
84. Wilson, T. E., Fahrner, T. J., Johnston, M. & Milbrandt, J. Identification of the DNA binding site for NGFI-B by genetic selection in yeast. *Science (80-.).* 252, 1296–1300 (1991).
85. Feng, S. Y., Ota, K. & Ito, T. A yeast one-hybrid system to screen for methylated DNA-binding proteins. *Nucleic Acids Res* 38, e189 (2010).
86. Kim, J. Y., Park, O. G., Lee, J. W. & Lee, Y. C. One- plus two-hybrid system, a novel yeast genetic selection for specific missense mutations disrupting protein/protein interactions. *Mol Cell Proteomics* 6, 1727–1740 (2007).
87. Lefurgy, S. & Cornish, V. Finding Cinderella after the ball: A three-hybrid approach to drug target identification. *Chem Biol* 11, 151–153 (2004).
88. Hook, B., Bernstein, D., Zhang, B. & Wickens, M. RNA-protein interactions in the yeast three-hybrid system: affinity, sensitivity, and enhanced library screening. *RNA* 11, 227–233 (2005).
89. Eyckerman, S., Lemmens, I., Catteeuw, D., Verhee, A., Vandekerckhove, J., Lievens, S. & Tavernier, J. Reverse MAPPIT: screening for protein-protein interaction modifiers in mammalian cells. *Nat Methods* 2, 427–433 (2005).
90. Tavernier, J., Eyckerman, S., Lemmens, I., Van der Heyden, J., Vandekerckhove, J. & Van Ostade, X. MAPPIT: a cytokine receptor-based two-hybrid method in mammalian cells. *Clin Exp Allergy* 32, 1397–1404 (2002).
91. Roberts 3rd, G. G., Parrish, J. R., Mangiola, B. A. & Finley Jr., R. L. High-throughput yeast two-hybrid screening. *Methods Mol Biol* 812, 39–61 (2012).
92. Rezwan, M. & Auerbach, D. Yeast 'N'-hybrid systems for protein-protein and drug-protein interaction discovery. *Methods* 57, 423–429 (2012).
93. Hamdi, A. & Colas, P. Yeast two-hybrid methods and their applications in drug discovery. *Trends Pharmacol Sci* 33, 109–118 (2012).
94. Koegl, M. & Uetz, P. Improving yeast two-hybrid screening systems. *Br. Funct Genomic Proteomic* 6, 302–312 (2007).
95. Velasco-Garcia, R. & Vargas-Martinez, R. The study of protein-protein interactions in bacteria. *Can J Microbiol* 58, 1241–1257 (2012).
96. Venter, J. C. *et al.* The sequence of the human genome. *Science (80-.).* 291, 1304–1351 (2001).

97. Stumpf, M. P., Thorne, T., de Silva, E., Stewart, R., An, H. J., Lappe, M. & Wiuf, C. Estimating the size of the human interactome. *Proc Natl Acad Sci U S A* 105, 6959–6964 (2008).
98. Finley Jr., R. L. & Brent, R. Interaction mating reveals binary and ternary connections between Drosophila cell cycle regulators. *Proc Natl Acad Sci U S A* 91, 12980–12984 (1994).
99. Uetz, P. *et al.* A comprehensive analysis of protein-protein interactions in Saccharomyces cerevisiae. *Nature* 403, 623–627 (2000).
100. Ito, T., Chiba, T., Ozawa, R., Yoshida, M., Hattori, M. & Sakaki, Y. A comprehensive two-hybrid analysis to explore the yeast protein interactome. *Proc Natl Acad Sci U S A* 98, 4569–4574 (2001).
101. Giot, L. *et al.* A protein interaction map of Drosophila melanogaster. *Science (80-.).* 302, 1727–1736 (2003).
102. Rain, J. C., Selig, L., De Reuse, H., Battaglia, V., Reverdy, C., Simon, S., Lenzen, G., Petel, F., Wojcik, J., Schachter, V., Chemama, Y., Labigne, A. & Legrain, P. The protein-protein interaction map of Helicobacter pylori. *Nature* 409, 211–215 (2001).
103. Simonis, N. *et al.* Empirically controlled mapping of the Caenorhabditis elegans protein-protein interactome network. *Nat Methods* 6, 47–54 (2009).
104. Rual, J. F. *et al.* Towards a proteome-scale map of the human protein-protein interaction network. *Nature* 437, 1173–1178 (2005).
105. Futschik, M. E., Chaurasia, G. & Herzel, H. Comparison of human protein-protein interaction maps. *Bioinformatics* 23, 605–611 (2007).
106. Davy, A., Bello, P., Thierry-Mieg, N., Vaglio, P., Hitti, J., Doucette-Stamm, L., Thierry-Mieg, D., Reboul, J., Boulton, S., Walhout, A. J., Coux, O. & Vidal, M. A protein-protein interaction map of the Caenorhabditis elegans 26S proteasome. *EMBO Rep* 2, 821–828 (2001).
107. Colland, F., Jacq, X., Trouplin, V., Mougin, C., Groizeleau, C., Hamburger, A., Meil, A., Wojcik, J., Legrain, P. & Gauthier, J. M. Functional proteomics mapping of a human signaling pathway. *Genome Res* 14, 1324–1332 (2004).
108. Organization, W. H. *Antimicrobial resistance: global report on surveillance*. (World Health Organization, 2014).
109. Das, S. & Kalpana, G. V. Reverse two-hybrid screening to analyze protein-protein interaction of HIV-1 viral and cellular proteins. *Methods Mol Biol* 485, 271–293 (2009).
110. Parrish, J. R., Yu, J., Liu, G., Hines, J. A., Chan, J. E., Mangiola, B. A., Zhang, H., Pacifico, S., Fotouhi, F., DiRita, V. J., Ideker, T., Andrews, P. & Finley Jr., R. L. A proteome-wide protein interaction map for Campylobacter jejuni. *Genome Biol* 8, R130 (2007).
111. To, A., Bai, Y., Shen, A., Gong, H., Umamoto, S., Lu, S. & Liu, F. Yeast two hybrid analyses reveal novel binary interactions between human cytomegalovirus-encoded virion proteins. *PLoS One* 6, e17796 (2011).
112. Dyer, M. D., Neff, C., Dufford, M., Rivera, C. G., Shattuck, D., Bassaganya-Riera, J., Murali, T. M. & Sobral, B. W. The human-bacterial pathogen protein interaction networks of Bacillus anthracis, Francisella tularensis, and Yersinia pestis. *PLoS One* 5, e12089 (2010).
113. Li, H., Dou, W., Padikkala, E. & Mani, S. Reverse yeast two-hybrid system to identify mammalian nuclear receptor residues that interact with ligands and/or antagonists. *J Vis Exp* e51085 (2013). doi:10.3791/51085
114. Katsogiannou, M., Andrieu, C., Baylot, V., Baudot, A., Dusetti, N. J., Gayet, O., Finetti, P., Garrido, C., Birnbaum, D., Bertucci, F., Brun, C. & Rocchi, P. The functional landscape of Hsp27 reveals new cellular processes such as DNA repair and alternative splicing and proposes novel anticancer targets. *Mol Cell Proteomics* (2014). doi:10.1074/mcp.M114.041228
115. Cohen, P. T. W. Protein phosphatase 1--targeted in many directions. *J. Cell Sci.* 115, 241–256 (2002).
116. da Cruz e Silva, E. F., Fox, C. A., Ouimet, C. C., Gustafson, E., Watson, S. J. & Greengard, P. Differential expression of protein phosphatase 1 isoforms in mammalian brain. *J Neurosci* 15, 3375–3389 (1995).
117. Takizawa, N., Mizuno, Y., Ito, Y. & Kikuchi, K. Tissue distribution of isoforms of type-1 protein phosphatase PP1 in mouse tissues and its diabetic alterations. *J Biochem* 116, 411–415 (1994).
118. Shima, H., Hatano, Y., Chun, Y. S., Sugimura, T., Zhang, Z., Lee, E. Y. & Nagao, M. Identification of PP1 catalytic subunit isotypes PP1 gamma 1, PP1 delta and PP1 alpha in various rat tissues.

Biochem Biophys Res Commun 192, 1289–1296 (1993).

119. Fardilha, M., Ferreira, M., Pelech, S., Vieira, S., Rebelo, S., Korrodi-Gregorio, L., Sousa, M., Barros, A., Silva, V., da Cruz E Silva, O. a B. & da Cruz E Silva, E. F. 'OMICS' of Human Sperm: Profiling Protein Phosphatases. *OMICS* 17, 460–472 (2013).
120. Andreassen, P. R., Lacroix, F. B., Villa-Moruzzi, E. & Margolis, R. L. Differential subcellular localization of protein phosphatase-1 alpha, gamma1, and delta isoforms during both interphase and mitosis in mammalian cells. *J Cell Biol* 141, 1207–1215 (1998).
121. Trinkle-Mulcahy, L., Sleeman, J. E. & Lamond, A. I. Dynamic targeting of protein phosphatase 1 within the nuclei of living mammalian cells. *J Cell Sci* 114, 4219–4228 (2001).
122. Gregorio, L. K., Esteves, S. L. C., Fardilha, M., Korrodi-Gregório, L., Esteves, S. L. C., Fardilha, M., Korrodi-Gregorio, L., Esteves, S. L. C. & Fardilha, M. Protein phosphatase 1 catalytic isoforms: specificity toward interacting proteins. *Transl Res* 164, 366–391 (2014).
123. Ouimet, C. C., da Cruz e Silva, E. F. & Greengard, P. The alpha and gamma 1 isoforms of protein phosphatase 1 are highly and specifically concentrated in dendritic spines. *Proc Natl Acad Sci U S A* 92, 3396–3400 (1995).
124. Bordelon, J. R., Smith, Y., Nairn, A. C., Colbran, R. J., Greengard, P. & Muly, E. C. Differential localization of protein phosphatase-1alpha, beta and gamma1 isoforms in primate prefrontal cortex. *Cereb Cortex* 15, 1928–1937 (2005).
125. Chakrabarti, R., Kline, D., Lu, J., Orth, J., Pilder, S. & Vijayaraghavan, S. Analysis of Ppp1cc-null mice suggests a role for PP1gamma2 in sperm morphogenesis. *Biol. Reprod.* 76, 992–1001 (2007).
126. Sinha, N., Puri, P., Nairn, A. C. & Vijayaraghavan, S. Selective ablation of Ppp1cc gene in testicular germ cells causes oligo-teratozoospermia and infertility in mice. *Biol. Reprod.* 89, 128 (2013).
127. Varmuza, S., Jurisicova, A., Okano, K., Hudson, J., Boekelheide, K. & Shipp, E. B. Spermiogenesis is impaired in mice bearing a targeted mutation in the protein phosphatase 1cgamma gene. *Dev. Biol.* 205, 98–110 (1999).
128. Bollen, M., Peti, W., Ragusa, M. J. & Beullens, M. The extended PP1 toolkit: Designed to create specificity. *Trends in Biochemical Sciences* 35, 450–458 (2010).
129. Fardilha, M., Esteves, S. L. C., Korrodi-Gregório, L., da Cruz e Silva, O. A. B. & da Cruz e Silva, F. F. The physiological relevance of protein phosphatase 1 and its interacting proteins to health and disease. *Curr. Med. Chem.* 17, 3996–4017 (2010).
130. Veres, D. V, Gyurko, D. M., Thaler, B., Szalay, K. Z., Fazekas, D., Korcsmaros, T. & Csermely, P. ComPPI: a cellular compartment-specific database for protein-protein interaction network analysis. *Nucleic Acids Res* 43, D485–93 (2015).
131. Roy, J. & Cyert, M. S. Cracking the phosphatase code: docking interactions determine substrate specificity. *Sci Signal* 2, re9 (2009).
132. Meiselbach, H., Sticht, H. & Enz, R. Structural analysis of the protein phosphatase 1 docking motif: molecular description of binding specificities identifies interacting proteins. *Chem Biol* 13, 49–59 (2006).
133. Heroes, E., Lesage, B., Görnemann, J., Beullens, M., Van Meervelt, L. & Bollen, M. The PP1 binding code: A molecular-lego strategy that governs specificity. *FEBS Journal* 280, 584–595 (2013).
134. Hendrickx, A., Beullens, M., Ceulemans, H., Den Abt, T., Van Eynde, A., Nicolaescu, E., Lesage, B. & Bollen, M. Docking motif-guided mapping of the interactome of protein phosphatase-1. *Chem Biol* 16, 365–371 (2009).
135. Terrak, M., Kerff, F., Langsetmo, K., Tao, T. & Dominguez, R. Structural basis of protein phosphatase 1 regulation. *Nature* 429, 780–784 (2004).
136. Bennett, D., Lyulcheva, E., Alphey, L. & Hawcroft, G. Towards a comprehensive analysis of the protein phosphatase 1 interactome in Drosophila. *J Mol Biol* 364, 196–212 (2006).
137. Esteves, S. L., Korrodi-Gregorio, L., Cotrim, C. Z., van Kleeff, P. J., Domingues, S. C., da Cruz e Silva, O. A., Fardilha, M., da Cruz e Silva, E. F., da Cruz, E. S. O. A. E. F., Fardilha, M. & da Cruz, E. S. O. A. E. F. Protein Phosphatase 1gamma Isoforms Linked Interactions in the Brain. *J Mol Neurosci* 19, 179–197 (2013).
138. eEsteves, S. L., Domingues, S. C., da Cruz e Silva, O. A., Fardilha, M., da Cruz e Silva, E. F., Esteves, S. L., Domingues, S. C., da Cruz e Silva, O. A., Fardilha, M. & da Cruz e Silva, E. F.

Protein phosphatase 1alpha interacting proteins in the human brain. *Omics* 16, 3–17 (2012).

139. Santos, M., Rebelo, S., Van Kleeff, P. J., Kim, C. E., Dauer, W. T., Fardilha, M., da Cruz, E. S. O. A. & da Cruz, E. S. E. F. The nuclear envelope protein, LAP1B, is a novel protein phosphatase 1 substrate. *PLoS One* 8, e76788 (2013).
140. Fardilha, M., Esteves, S. L. C., Korrodi-Gregório, L., Vintém, A. P., Domingues, S. C., Rebelo, S., Morrice, N., Cohen, P. T. W., Da Cruz E Silva, O. A. B. & Da Cruz E Silva, E. F. Identification of the human testis protein phosphatase 1 interactome. in *Biochemical Pharmacology* 82, 1403–1415 (2011).
141. Korrodi-Gregorio, L. *et al.* TCTEX1D4, a novel protein phosphatase 1 interactor: connecting the phosphatase to the microtubule network. *Biol. Open* 2, 453–65 (2013).
142. Freitas, M. J., Korrodi-Gregorio, L., Morais-Santos, F., Cruz e Silva, E. & Fardilha, M. TCTEX1D4 interactome in human testis: unraveling the function of dynein light chain in spermatozoa. *Omics* 18, 242–253 (2014).
143. Hrabchak, C. & Varmuza, S. Identification of the spermatogenic zip protein Spz1 as a putative protein phosphatase-1 (PP1) regulatory protein that specifically binds the PP1c??2 splice variant in mouse testis. *J. Biol. Chem.* 279, 37079–37086 (2004).
144. Hrabchak, C., Henderson, H. & Varmuza, S. A testis specific isoform of endophilin B1, endophilin B1t, interacts specifically with protein phosphatase-1c??2 in mouse testis and is abnormally expressed in PP1c?? Null Mice. *Biochemistry* 46, 4635–4644 (2007).
145. Chen, C. Y., Lai, N. S., Yang, J. J., Huang, H. L., Hung, W. C., Li, C., Lin, T. H. & Huang, H. B. FLJ23654 encodes a heart protein phosphatase 1-binding protein (Hepp1). *Biochem Biophys Res Commun* 391, 698–702 (2010).
146. Skinner, J. A. & Saltiel, A. R. Cloning and identification of MYPT3: a prenylatable myosin targetting subunit of protein phosphatase 1. *Biochem J* 356, 257–267 (2001).
147. Ayllon, V., Cayla, X., Garcia, A., Roncal, F., Fernandez, R., Albar, J. P., Martinez, C. & Rebollo, A. Bcl-2 targets protein phosphatase 1 alpha to Bad. *J Immunol* 166, 7345–7352 (2001).
148. Llorian, M., Beullens, M., Andres, I., Ortiz, J. M. & Bollen, M. SIPP1, a novel pre-mRNA splicing factor and interactor of protein phosphatase-1. *Biochem J* 378, 229–238 (2004).
149. Gagnon, K. B., England, R., Diehl, L. & Delpire, E. Apoptosis-associated tyrosine kinase scaffolding of protein phosphatase 1 and SPAK reveals a novel pathway for Na-K-2C1 cotransporter regulation. *Am J Physiol Cell Physiol* 292, C1809–15 (2007).
150. Lee, K. Y., Bae, J. S., Yoon, S. & Hwang, D. S. Dephosphorylation of Orc2 by protein phosphatase 1 promotes the binding of the origin recognition complex to chromatin. *Biochem Biophys Res Commun* 448, 385–389 (2014).
151. Lesage, B., Beullens, M., Pedelini, L., Garcia-Gimeno, M. A., Waelkens, E., Sanz, P. & Bollen, M. A complex of catalytically inactive protein phosphatase-1 sandwiched between Sds22 and inhibitor-3. *Biochemistry* 46, 8909–19 (2007).
152. Kao, S. C., Chen, C. Y., Wang, S. L., Yang, J. J., Hung, W. C., Chen, Y. C., Lai, N. S., Liu, H. T., Huang, H. L., Chen, H. C., Lin, T. H. & Huang, H. B. Identification of phostensin, a PP1 F-actin cytoskeleton targeting subunit. *Biochem Biophys Res Commun* 356, 594–598 (2007).
153. Toledo, F. & Wahl, G. M. Regulating the p53 pathway: in vitro hypotheses, in vivo veritas. *Nat Rev Cancer* 6, 909–923 (2006).
154. Vassilev, L. T., Vu, B. T., Graves, B., Carvajal, D., Podlaski, F., Filipovic, Z., Kong, N., Kammlott, U., Lukacs, C., Klein, C., Fotouhi, N. & Liu, E. A. In vivo activation of the p53 pathway by small-molecule antagonists of MDM2. *Science (80-.).* 303, 844–848 (2004).
155. Lim, J., Hao, T., Shaw, C., Patel, A. J., Szabo, G., Rual, J. F., Fisk, C. J., Li, N., Smolyar, A., Hill, D. E., Barabasi, A. L., Vidal, M. & Zoghbi, H. Y. A protein-protein interaction network for human inherited ataxias and disorders of Purkinje cell degeneration. *Cell* 125, 801–814 (2006).
156. Li, J., Zhang, S., Gao, L., Chen, Y. & Xie, X. A cell-based high-throughput assay for the screening of small-molecule inhibitors of p53-MDM2 interaction. *J Biomol Screen* 16, 450–456 (2011).
157. Ruffner, H., Bauer, A. & Bouwmeester, T. Human protein-protein interaction networks and the value for drug discovery. *Drug Discov Today* 12, 709–716 (2007).
158. Boyce, M., Bryant, K. F., Jousse, C., Long, K., Harding, H. P., Scheuner, D., Kaufman, R. J., Ma, D., Coen, D. M., Ron, D. & Yuan, J. A selective inhibitor of eIF2alpha dephosphorylation protects cells

from ER stress. *Science (80-.).* 307, 935–939 (2005).

159. Brush, M. H., Guardiola, A., Connor, J. H., Yao, T. P. & Shenolikar, S. Deactylase inhibitors disrupt cellular complexes containing protein phosphatases and deacetylases. *J Biol Chem* 279, 7685–7691 (2004).
160. Vijayaraghavan, S., Stephens, D. T., Trautman, K., Smith, G. D., Khatra, B., da Cruz e Silva, E. F. & Greengard, P. Sperm motility development in the epididymis is associated with decreased glycogen synthase kinase-3 and protein phosphatase 1 activity. *Biol. Reprod.* 54, 709–718 (1996).
161. Fardilha, M., Esteves, S. L. C., Korrodi-Gregório, L., Pelech, S., da Cruz e Silva, O. A. B. & da Cruz e Silva, E. Protein phosphatase 1 complexes modulate sperm motility and present novel targets for male infertility. *Molecular Human Reproduction* 17, 466–477 (2011).
162. Valkov, E., Sharpe, T., Marsh, M., Greive, S. & Hyvonen, M. Targeting protein-protein interactions and fragment-based drug discovery. *Top Curr Chem* 317, 145–179 (2012).
163. Chatterjee, J., Beullens, M., Sukackaite, R., Qian, J., Lesage, B., Hart, D. J., Bollen, M. & Köhn, M. Development of a peptide that selectively activates protein phosphatase-1 in living cells. *Angew. Chemie - Int. Ed.* 51, 10054–10059 (2012).
164. Roosen-Runge, E. C. & Holstein, A. F. The human rete testis. *Cell Tissue Res.* 189, (1978).
165. HELLER, C. H. & CLERMONT, Y. KINETICS OF THE GERMINAL EPITHELIUM IN MAN. *Recent Prog. Horm. Res.* 20, 545–75 (1964).
166. Misell, L. M., Holochwost, D., Boban, D., Santi, N., Shefi, S., Hellerstein, M. K. & Turek, P. J. A stable isotope-mass spectrometric method for measuring human spermatogenesis kinetics in vivo. *J. Urol.* 175, 242–6; discussion 246 (2006).
167. Clermont, Y. Kinetics of spermatogenesis in mammals: seminiferous epithelium cycle and spermatogonial renewal. *Physiol. Rev.* 52, 198–236 (1972).
168. Clermont, Y. The cycle of the seminiferous epithelium in man. *Am. J. Anat.* 112, 35–51 (1963).
169. Schulze, C. Morphological characteristics of the spermatogonial stem cells in man. *Cell Tissue Res.* 198, 191–9 (1979).
170. LEBLOND, C. P. & CLERMONT, Y. Spermiogenesis of rat, mouse, hamster and guinea pig as revealed by the periodic acid-fuchsin sulfurous acid technique. *Am. J. Anat.* 90, 167–215 (1952).
171. Payne, A. H., Wong, K. L. & Vega, M. M. Differential effects of single and repeated administrations of gonadotropins on luteinizing hormone receptors and testosterone synthesis in two populations of Leydig cells. *J. Biol. Chem.* 255, 7118–22 (1980).
172. Cohen, P. The origins of protein phosphorylation. *Nat. Cell Biol.* 4, E127–30 (2002).
173. Liu, D., Matzuk, M. M., Sung, W. K., Guo, Q., Wang, P. & Wolgemuth, D. J. Cyclin A1 is required for meiosis in the male mouse. *Nat Genet* 20, 377–380 (1998).
174. Chen, M. S., Hurov, J., White, L. S., Woodford-Thomas, T. & Piwnica-Worms, H. Absence of apparent phenotype in mice lacking Cdc25C protein phosphatase. *Mol. Cell. Biol.* 21, 3853–3861 (2001).
175. Besset, V., Rhee, K. & Wolgemuth, D. J. The cellular distribution and kinase activity of the Cdk family member Pctaire1 in the adult mouse brain and testis suggest functions in differentiation. *Cell Growth Differ.* 10, 173–181 (1999).
176. Rhee, K. & Wolgemuth, D. J. Cdk family genes are expressed not only in dividing but also in terminally differentiated mouse germ cells, suggesting their possible function during both cell division and differentiation. *Dev Dyn* 204, 406–420 (1995).
177. Mikolcevic, P., Sigl, R., Rauch, V., Hess, M. W., Pfaller, K., Barisic, M., Pelliniemi, L. J., Boesl, M. & Geley, S. Cyclin-dependent kinase 16/PCTAIRE kinase 1 is activated by cyclin Y and is essential for spermatogenesis. *Mol. Cell. Biol.* 32, 868–879 (2012).
178. Kimmins, S., Crosio, C., Kotaja, N., Hirayama, J., Monaco, L., Hoog, C., van Duin, M., Gossen, J. A. & Sassone-Corsi, P. Differential functions of the Aurora-B and Aurora-C kinases in mammalian spermatogenesis. *Mol Endocrinol* 21, 726–739 (2007).
179. Tseng, T. C., Chen, S. H., Hsu, Y. P. & Tang, T. K. Protein kinase profile of sperm and eggs: cloning and characterization of two novel testis-specific protein kinases (AIE1, AIE2) related to yeast and fly chromosome segregation regulators. *DNA Cell Biol* 17, 823–833 (1998).
180. Yuan, W., Leisner, T. M., McFadden, A. W., Clark, S., Hiller, S., Maeda, N., O'Brien, D. A. & Parise, L. V. CIB1 is essential for mouse spermatogenesis. *Mol. Cell. Biol.* 26, 8507–8514 (2006).

181. Almog, T. & Naor, Z. The role of Mitogen activated protein kinase (MAPK) in sperm functions. *Mol Cell Endocrinol* 314, 239–243 (2010).
182. Iwanaga, A., Wang, G., Gantulga, D., Sato, T., Baljinnyam, T., Shimizu, K., Takumi, K., Hayashi, M., Akashi, T., Fuse, H., Sugihara, K., Asano, M. & Yoshioka, K. Ablation of the scaffold protein JLP causes reduced fertility in male mice. *Transgenic Res.* 17, 1045–1058 (2008).
183. Burton, K. A. & McKnight, G. S. PKA, germ cells, and fertility. *Physiology* 22, 40–46 (2007).
184. Skalhegg, B. S., Huang, Y., Su, T., Idzerda, R. L., McKnight, G. S. & Burton, K. A. Mutation of the Calpha subunit of PKA leads to growth retardation and sperm dysfunction. *Mol. Endocrinol.* 16, 630–639 (2002).
185. Nolan, M. A., Babcock, D. F., Wennemuth, G., Brown, W., Burton, K. A. & McKnight, G. S. Sperm-specific protein kinase A catalytic subunit Calpha2 orchestrates cAMP signaling for male fertility. *Proc Natl Acad Sci U S A* 101, 13483–13488 (2004).
186. Moorhead, G. B. G., Trinkle-Mulcahy, L. & Ulke-Lemée, A. Emerging roles of nuclear protein phosphatases. *Nat. Rev. Mol. Cell Biol.* 8, 234–44 (2007).
187. Tonks, N. K. Protein tyrosine phosphatases--from housekeeping enzymes to master regulators of signal transduction. *FEBS J.* 280, 346–78 (2013).
188. Barford, D., Das, A. K. & Egloff, M. P. The structure and mechanism of protein phosphatases: insights into catalysis and regulation. *Annu. Rev. Biophys. Biomol. Struct.* 27, 133–64 (1998).
189. Berndt, N., Campbell, D. G., Caudwell, F. B., Cohen, P., da Cruz e Silva, E. F., da Cruz e Silva, O. B. & Cohen, P. T. Isolation and sequence analysis of a cDNA clone encoding a type-1 protein phosphatase catalytic subunit: homology with protein phosphatase 2A. *FEBS Lett.* 223, 340–6 (1987).
190. Cohen, P. T. Novel protein serine/threonine phosphatases: variety is the spice of life. *Trends Biochem. Sci.* 22, 245–51 (1997).
191. da Cruz e Silva, O. B. & Cohen, P. T. W. A second catalytic subunit of type-2A protein phosphatase from rabbit skeletal muscle. *FEBS Lett.* 226, 176–178 (1987).
192. da Cruz e Silva, O. B., Alemany, S., Campbell, D. G. & Cohen, P. T. Isolation and sequence analysis of a cDNA clone encoding the entire catalytic subunit of a type-2A protein phosphatase. *FEBS Lett.* 221, 415–22 (1987).
193. da Cruz e Silva, O. B., da Cruz e Silva, E. F. & Cohen, P. T. Identification of a novel protein phosphatase catalytic subunit by cDNA cloning. *FEBS Lett.* 242, 106–10 (1988).
194. Honkanen, R. E. & Golden, T. Regulators of serine/threonine protein phosphatases at the dawn of a clinical era? *Curr. Med. Chem.* 9, 2055–75 (2002).
195. Cohen, P. The regulation of protein function by multisite phosphorylation--a 25 year update. *Trends Biochem. Sci.* 25, 596–601 (2000).
196. Ceulemans, H. & Bollen, M. Functional diversity of protein phosphatase-1, a cellular economizer and reset button. *Physiol. Rev.* 84, 1–39 (2004).
197. Virshup, D. M. & Shenolikar, S. From Promiscuity to Precision: Protein Phosphatases Get a Makeover. *Molecular Cell* 33, 537–545 (2009).
198. Boens, S., Szekér, K., Van Eynde, A. & Bollen, M. Interactor-guided dephosphorylation by protein phosphatase-1. *Methods Mol. Biol.* 1053, 271–81 (2013).
199. Bollen, M. Combinatorial control of protein phosphatase-1. *Trends Biochem. Sci.* 26, 426–31 (2001).
200. Durfee, T., Becherer, K., Chen, P. L., Yeh, S. H., Yang, Y., Kilburn, A. E., Lee, W. H. & Elledge, S. J. The retinoblastoma protein associates with the protein phosphatase type 1 catalytic subunit. *Genes Dev.* 7, 555–69 (1993).
201. Connor, J. H., Weiser, D. C., Li, S., Hallenbeck, J. M. & Shenolikar, S. Growth arrest and DNA damage-inducible protein GADD34 assembles a novel signaling complex containing protein phosphatase 1 and inhibitor 1. *Mol. Cell. Biol.* 21, 6841–50 (2001).
202. Korrodi-gregório, L., Ferreira, M., Vintém, A. P., Wu, W., Muller, T., Marcus, K., Vijayaraghavan, S., Brautigan, D. L., Odete, A. B., Fardilha, M. & Edgar, F. Identification and characterization of two distinct PPP1R2 isoforms in human spermatozoa. (2013). doi:10.1186/1471-2121-14-15
203. De Munter, S., Köhn, M. & Bollen, M. Challenges and opportunities in the development of protein phosphatase-directed therapeutics. *ACS Chem. Biol.* 8, 36–45 (2013).
204. Tsaytler, P., Harding, H. P., Ron, D. & Bertolotti, A. Selective inhibition of a regulatory subunit of

protein phosphatase 1 restores proteostasis. *Science* 332, 91–4 (2011).

205. Oppedisano-Wells, L. & Varmuza, S. Protein phosphatase 1cgamma is required in germ cells in murine testis. *Mol. Reprod. Dev.* 65, 157–66 (2003).
206. Forgione, N., Vogl, A. W. & Varmuza, S. Loss of protein phosphatase 1c{gamma} (PPP1CC) leads to impaired spermatogenesis associated with defects in chromatin condensation and acrosome development: an ultrastructural analysis. *Reproduction* 139, 1021–9 (2010).
207. Soler, D. C., Kadunganattil, S., Ramdas, S., Myers, K., Roca, J., Slaughter, T., Pilder, S. H. & Vijayaraghavan, S. Expression of transgenic PPP1CC2 in the testis of Ppp1cc-null mice rescues spermatid viability and spermiation but does not restore normal sperm tail ultrastructure, sperm motility, or fertility. *Biol. Reprod.* 81, 343–52 (2009).
208. Sinha, N., Pilder, S. & Vijayaraghavan, S. Significant Expression Levels of Transgenic PPP1CC2 in Testis and Sperm Are Required to Overcome the Male Infertility Phenotype of Ppp1cc Null Mice. *PLoS One* 7, (2012).
209. Hsu, S. H., Shyu, H. W., Hsieh-Li, H. M. & Li, H. Spz1, a novel bHLH-Zip protein, is specifically expressed in testis. *Mech Dev* 100, 177–187 (2001).
210. Sha, J. H., Zhou, Z. M., Li, J. M., Lin, M., Zhu, H., Zhu, H., Zhou, Y. D., Wang, L. L., Wang, Y. Q. & Zhou, K. Y. Expression of a novel bHLH-Zip gene in human testis. *Asian J Androl* 5, 83–88 (2003).
211. Hsu, S. H., Hsieh-Li, H. M. & Li, H. Dysfunctional spermatogenesis in transgenic mice overexpressing bHLH-Zip transcription factor, Spz1. *Exp. Cell Res.* 294, 185–198 (2004).
212. Pierrat, B., Simonen, M., Cueto, M., Mestan, J., Ferrigno, P. & Heim, J. SH3GLB, a new endophilin-related protein family featuring an SH3 domain. *Genomics* 71, 222–234 (2001).
213. MacLeod, G. & Varmuza, S. Tandem affinity purification in transgenic mouse embryonic stem cells identifies DDOST as a novel PPP1CC2 interacting protein. *Biochemistry* 51, 9678–9688 (2012).
214. Roboti, P. & High, S. The oligosaccharyltransferase subunits OST48, DAD1 and KCP2 function as ubiquitous and selective modulators of mammalian N-glycosylation. *J Cell Sci* 125, 3474–3484 (2012).
215. Yamagata, T., Tsuru, T., Momoi, M. Y., Suwa, K., Nozaki, Y., Mukasa, T., Ohashi, H., Fukushima, Y. & Momoi, T. Genome organization of human 48-kDa oligosaccharyltransferase (DDOST). *Genomics* 45, 535–540 (1997).
216. Luk, J. M., Mok, B. W., Shum, C. K., Yeung, W. S., Tam, P. C., Tse, J. Y., Chow, J. F., Woo, J., Kam, K. & Lee, K. F. Identification of novel genes expressed during spermatogenesis in stage-synchronized rat testes by differential display. *Biochem Biophys Res Commun* 307, 782–790 (2003).
217. Nixon, B., Mitchell, L. A., Anderson, A. L., Mclaughlin, E. A., O'bryan, M. K. & Aitken, R. J. Proteomic and functional analysis of human sperm detergent resistant membranes. *J. Cell. Physiol.* 226, 2651–2665 (2011).
218. Xu, B., Hao, Z., Jha, K. N., Zhang, Z., Urekar, C., Digilio, L., Pulido, S., Strauss 3rd, J. F., Flickinger, C. J. & Herr, J. C. Targeted deletion of Tssk1 and 2 causes male infertility due to haploinsufficiency. *Dev Biol* 319, 211–222 (2008).
219. MacLeod, G., Shang, P., Booth, G. T., Mastropaolo, L. A., Manafpoursakha, N., Vogl, A. W. & Varmuza, S. PPP1CC2 can form a kinase/phosphatase complex with the testis-specific proteins TSSK1 and TSKS in the mouse testis. *Reproduction* 147, 1–12 (2014).
220. Shang, P., Baarends, W. M., Hoogerbrugge, J., Ooms, M. P., van Cappellen, W. A., de Jong, A. A., Dohle, G. R., van Eenennaam, H., Gossen, J. A. & Grootegoed, J. A. Functional transformation of the chromatoid body in mouse spermatids requires testis-specific serine/threonine kinases. *J Cell Sci* 123, 331–339 (2010).
221. Li, Y., Sosnik, J., Brassard, L., Reese, M., Spiridonov, N. A., Bates, T. C., Johnson, G. R., Anguita, J., Visconti, P. E. & Salicioni, A. M. Expression and localization of five members of the testis-specific serine kinase (Tssk) family in mouse and human sperm and testis. *Mol Hum Reprod* 17, 42–56 (2011).
222. Xu, B., Hao, Z., Jha, K. N., Digilio, L., Urekar, C., Kim, Y. H., Pulido, S., Flickinger, C. J. & Herr, J. C. Validation of a testis specific serine/threonine kinase [TSSK] family and the substrate of TSSK1 & 2, TSKS, as contraceptive targets. *Soc Reprod Fertil Suppl* 63, 87–101 (2007).
223. Wang, R. & Sperry, A. O. Identification of a novel Leucine-rich repeat protein and candidate PP1 regulatory subunit expressed in developing spermatids. *BMC Cell Biol* 9, 9 (2008).

224. Wang, R., Kaul, A. & Sperry, A. O. TLRR (lrrc67) interacts with PP1 and is associated with a cytoskeletal complex in the testis. *Biol. Cell* 102, 173–189 (2010).
225. DeVaul, N., Wang, R. & Sperry, A. O. PPP1R42, a PP1 binding protein, regulates centrosome dynamics in ARPE-19 cells. *Biol Cell* 105, 359–371 (2013).
226. Ohkura, H. & Yanagida, M. S. pombe gene sds22+ essential for a midmitotic transition encodes a leucine-rich repeat protein that positively modulates protein phosphatase-1. *Cell* 64, 149–157 (1991).
227. Renouf, S., Beullens, M., Wera, S., Van Eynde, A., Sikela, J., Stalmans, W. & Bollen, M. Molecular cloning of a human polypeptide related to yeast sds22, a regulator of protein phosphatase-1. *FEBS Lett* 375, 75–78 (1995).
228. Ceulemans, H., Van Eynde, A., Perez-Callejon, E., Beullens, M., Stalmans, W. & Bollen, M. Structure and splice products of the human gene encoding sds22, a putative mitotic regulator of protein phosphatase-1. *Eur J Biochem* 262, 36–42 (1999).
229. Dinischiotu, A., Beullens, M., Stalmans, W. & Bollen, M. Identification of sds22 as an inhibitory subunit of protein phosphatase-1 in rat liver nuclei. *FEBS Lett.* 402, 141–4 (1997).
230. Huang, Z., Khatra, B., Bollen, M., Carr, D. W. & Vijayaraghavan, S. Sperm PP1gamma2 is regulated by a homologue of the yeast protein phosphatase binding protein sds22. *Biol. Reprod.* 67, 1936–1942 (2002).
231. Zhang, J., Zhang, L., Zhao, S. & Lee, E. Y. Identification and characterization of the human HCG V gene product as a novel inhibitor of protein phosphatase-1. *Biochemistry* 37, 16728–34 (1998).
232. Pedelini, L., Marquina, M., Arino, J., Casamayor, A., Sanz, L., Bollen, M., Sanz, P. & Garcia-Gimeno, M. A. YPI1 and SDS22 proteins regulate the nuclear localization and function of yeast type 1 phosphatase Glc7. *J Biol Chem* 282, 3282–3292 (2007).
233. Huang, H. S. & Lee, E. Y. Protein phosphatase-1 inhibitor-3 is an in vivo target of caspase-3 and participates in the apoptotic response. *J Biol Chem* 283, 18135–18146 (2008).
234. Cheng, L., Pilder, S., Nairn, A. C., Ramdas, S. & Vijayaraghavan, S. PP1??2 and PPP1R11 are parts of a multimeric complex in developing testicular germ cells in which their steady state levels are reciprocally related. *PLoS One* 4, (2009).
235. Aitken, A., Collinge, D. B., van Heusden, B. P., Isobe, T., Roseboom, P. H., Rosenfeld, G. & Soll, J. 14-3-3 proteins: a highly conserved, widespread family of eukaryotic proteins. *Trends Biochem Sci* 17, 498–501 (1992).
236. Tzivion, G. & Avruch, J. 14-3-3 proteins: active cofactors in cellular regulation by serine/threonine phosphorylation. *J Biol Chem* 277, 3061–3064 (2002).
237. Perego, L. & Berruti, G. Molecular cloning and tissue-specific expression of the mouse homologue of the rat brain 14-3-3 theta protein: characterization of its cellular and developmental pattern of expression in the male germ line. *Mol Reprod Dev* 47, 370–379 (1997).
238. Chaudhary, J. & Skinner, M. K. Characterization of a novel transcript of 14-3-3 theta in Sertoli cells. *J Androl* 21, 730–738 (2000).
239. Berruti, G. A novel rap1/B-Raf/14-3-3 theta protein complex is formed in vivo during the morphogenetic differentiation of postmeiotic male germ cells. *Exp Cell Res* 257, 172–179 (2000).
240. Sun, S., Wong, E. W., Li, M. W., Lee, W. M. & Cheng, C. Y. 14-3-3 and its binding partners are regulators of protein-protein interactions during spermatogenesis. *J Endocrinol* 202, 327–336 (2009).
241. Puri, P., Acker-Palmer, A., Stahler, R., Chen, Y., Kline, D. & Vijayaraghavan, S. Identification of testis 14–3-3 binding proteins by tandem affinity purification. *Spermatogenesis* 1, 354–365 (2011).
242. Puri, P., Myers, K., Kline, D. & Vijayaraghavan, S. Proteomic analysis of bovine sperm YWHA binding partners identify proteins involved in signaling and metabolism. *Biol. Reprod.* 79, 1183–1191 (2008).
243. Huang, Z., Myers, K., Khatra, B. & Vijayaraghavan, S. Protein 14-3-3zeta binds to protein phosphatase PP1gamma2 in bovine epididymal spermatozoa. *Biol. Reprod.* 71, 177–84 (2004).
244. Schaefer, M. H., Lopes, T. J., Mah, N., Shoemaker, J. E., Matsuoka, Y., Fontaine, J. F., Louis-Jeune, C., Eisfeld, A. J., Neumann, G., Perez-Iratxeta, C., Kawaoka, Y., Kitano, H. & Andrade-Navarro, M. A. Adding protein context to the human protein-protein interaction network to reveal meaningful interactions. *PLoS Comput Biol* 9, e1002860 (2013).
245. Bult, C. J., Kadin, J. A., Richardson, J. E., Blake, J. A. & Eppig, J. T. The mouse genome database: Enhancements and updates. *Nucleic Acids Res.* 38, D586–92 (2009).

246. Gellert, P., Jenniches, K., Braun, T. & Uchida, S. C-It: A knowledge database for tissue-enriched genes. *Bioinformatics* 26, 2328–2333 (2010).
247. Liu, X., Yu, X., Zack, D. J., Zhu, H. & Qian, J. TiGER: a database for tissue-specific gene expression and regulation. *BMC Bioinformatics* 9, 271 (2008).
248. Yang, X., Ye, Y., Wang, G., Huang, H., Yu, D. & Liang, S. VeryGene: linking tissue-specific genes to diseases, drugs, and beyond for knowledge discovery. *Physiol. Genomics* 43, 457–460 (2011).
249. Uhlen, M., Oksvold, P., Fagerberg, L., Lundberg, E., Jonasson, K., Forsberg, M., Zwahlen, M., Kampf, C., Wester, K., Hober, S., Wernerus, H., Bjorling, L. & Ponten, F. Towards a knowledge-based Human Protein Atlas. *Nat Biotechnol* 28, 1248–1250 (2010).
250. Wu, C., Orozco, C., Boyer, J., Leglise, M., Goodale, J., Batalov, S., Hodge, C. L., Haase, J., Janes, J., Huss, J. W. & Su, A. I. BioGPS: an extensible and customizable portal for querying and organizing gene annotation resources. *Genome Biol.* 10, R130 (2009).
251. Chen, W. S., Xu, P. Z., Gottlob, K., Chen, M. L., Sokol, K., Shiyanova, T., Roninson, I., Weng, W., Suzuki, R., Tobe, K., Kadowaki, T. & Hay, N. Growth retardation and increased apoptosis in mice with homozygous disruption of the Akt1 gene. *Genes Dev* 15, 2203–2208 (2001).
252. Ludwig, T., Fisher, P., Ganesan, S. & Efstratiadis, A. Tumorigenesis in mice carrying a truncating Brca1 mutation. *Genes Dev* 15, 1188–1193 (2001).
253. Xu, X., Aprelikova, O., Moens, P., Deng, C. X. & Furth, P. A. Impaired meiotic DNA-damage repair and lack of crossing-over during spermatogenesis in BRCA1 full-length isoform deficient mice. *Development* 130, 2001–2012 (2003).
254. Zhang, Q., Sakamoto, K., Liu, C., Triplett, A. A., Lin, W. C., Rui, H. & Wagner, K. U. Cyclin D3 compensates for the loss of cyclin D1 during ErbB2-induced mammary tumor initiation and progression. *Cancer Res* 71, 7513–7524 (2011).
255. Satyanarayana, A., Berthet, C., Lopez-Molina, J., Coppola, V., Tessarollo, L. & Kaldis, P. Genetic substitution of Cdk1 by Cdk2 leads to embryonic lethality and loss of meiotic function of Cdk2. *Development* 135, 3389–3400 (2008).
256. Berthet, C., Aleem, E., Coppola, V., Tessarollo, L. & Kaldis, P. Cdk2 knockout mice are viable. *Curr Biol* 13, 1775–1785 (2003).
257. Ortega, S., Prieto, I., Odajima, J., Martín, A., Dubus, P., Sotillo, R., Barbero, J. L., Malumbres, M. & Barbacid, M. Cyclin-dependent kinase 2 is essential for meiosis but not for mitotic cell division in mice. *Nat. Genet.* 35, 25–31 (2003).
258. Wright, W. W., Smith, L., Kerr, C. & Charron, M. Mice that express enzymatically inactive cathepsin L exhibit abnormal spermatogenesis. *Biol Reprod* 68, 680–687 (2003).
259. Eddy, E. M., Washburn, T. F., Bunch, D. O., Goulding, E. H., Gladen, B. C., Lubahn, D. B. & Korach, K. S. Targeted disruption of the estrogen receptor gene in male mice causes alteration of spermatogenesis and infertility. *Endocrinology* 137, 4796–4805 (1996).
260. Lubahn, D. B., Moyer, J. S., Golding, T. S., Couse, J. F., Korach, K. S. & Smithies, O. Alteration of reproductive function but not prenatal sexual development after insertional disruption of the mouse estrogen receptor gene. *Proc Natl Acad Sci U S A* 90, 11162–11166 (1993).
261. Chen, M., Hsu, I., Wolfe, A., Radovick, S., Huang, K., Yu, S., Chang, C., Messing, E. M. & Yeh, S. Defects of prostate development and reproductive system in the estrogen receptor-alpha null male mice. *Endocrinology* 150, 251–259 (2009).
262. Dix, D. J., Allen, J. W., Collins, B. W., Mori, C., Nakamura, N., Poorman-Allen, P., Goulding, E. H. & Eddy, E. M. Targeted gene disruption of Hsp70-2 results in failed meiosis, germ cell apoptosis, and male infertility. *Proc Natl Acad Sci U S A* 93, 3264–3268 (1996).
263. Held, T., Barakat, A. Z., Mohamed, B. A., Paprotta, I., Meinhardt, A., Engel, W. & Adham, I. M. Heat-shock protein HSPA4 is required for progression of spermatogenesis. *Reproduction* 142, 133–144 (2011).
264. Alsheimer, M., Liebe, B., Sewell, L., Stewart, C. L., Scherthan, H. & Benavente, R. Disruption of spermatogenesis in mice lacking A-type lamins. *J Cell Sci* 117, 1173–1178 (2004).
265. Roa, S., Avdievich, E., Peled, J. U., Maccarthy, T., Werling, U., Kuang, F. L., Kan, R., Zhao, C., Bergman, A., Cohen, P. E., Edelmann, W. & Scharff, M. D. Ubiquitylated PCNA plays a role in somatic hypermutation and class-switch recombination and is required for meiotic progression. *Proc Natl Acad Sci U S A* 105, 16248–16253 (2008).

266. Kinuta, K., Tanaka, H., Moriwake, T., Aya, K., Kato, S. & Seino, Y. Vitamin D is an important factor in estrogen biosynthesis of both female and male gonads. *Endocrinology* 141, 1317–1324 (2000).
267. Kepp, O., Galluzzi, L., Giordanetto, F., Tesniere, A., Vitale, I., Martins, I., Schlemmer, F., Adjemian, S., Zitvogel, L. & Kroemer, G. Disruption of the PP1/GADD34 complex induces calreticulin exposure. *Cell Cycle* 8, 3971–3977 (2009).
268. Tsaytler, P. & Bertolotti, A. Exploiting the selectivity of protein phosphatase 1 for pharmacological intervention. *FEBS Journal* 280, 766–770 (2013).
269. Paoli, D., Gallo, M., Rizzo, F., Baldi, E., Francavilla, S., Lenzi, A., Lombardo, F. & Gandini, L. Mitochondrial membrane potential profile and its correlation with increasing sperm motility. *Fertil. Steril.* 95, 2315–9 (2011).
270. Turner, R. M. Tales from the tail: what do we really know about sperm motility? *J. Androl.* 24, 790–803 (2003).
271. KATZ, D. F. Movement Characteristics of Hamster Spermatozoa Within the Oviduct. *Biol. Reprod.* 22, 759–764 (1980).
272. Chevrier, C. & Dacheux, J. L. Analysis of the flagellar bending waves of ejaculated ram sperm. *Cell Motil. Cytoskeleton* 8, 261–73 (1987).
273. Gaddum-Rosse, P. Some observations on sperm transport through the uterotubal junction of the rat. *Am. J. Anat.* 160, 333–41 (1981).
274. Suarez, S. S. & Ho, H. C. Hyperactivation of mammalian sperm. *Cell Mol Biol* 49, 351–356 (2003).
275. Piomboni, P., Focarelli, R., Stendardi, A., Ferramosca, A. & Zara, V. The role of mitochondria in energy production for human sperm motility. *Int. J. Androl.* 35, 109–124 (2012).
276. Miki, K. Energy metabolism and sperm function. *Soc. Reprod. Fertil. Suppl.* 65, 309–325 (2007).
277. du Plessis, S., Agarwal, A., Mohanty, G. & van der Linde, M. Oxidative phosphorylation versus glycolysis: what fuel do spermatozoa use? *Asian J. Androl.* 17, 230 (2015).
278. Huang, Z. & Vijayaraghavan, S. Increased Phosphorylation of a Distinct Subcellular Pool of Protein Phosphatase, PP1 2, During Epididymal Sperm Maturation. *Biol. Reprod.* 70, 439–447 (2004).
279. Smith, G. D., Wolf, D. P., Trautman, K. C., da Cruz e Silva, E. F., Greengard, P. & Vijayaraghavan, S. Primate sperm contain protein phosphatase 1, a biochemical mediator of motility. *Biol. Reprod.* 54, 719–727 (1996).
280. Si, Y. Hyperactivation of hamster sperm motility by temperature-dependent tyrosine phosphorylation of an 80-kDa protein. *Biol. Reprod.* 61, 247–52 (1999).
281. Si, Y. & Okuno, M. Role of tyrosine phosphorylation of flagellar proteins in hamster sperm hyperactivation. *Biol. Reprod.* 61, 240–6 (1999).
282. Pilder, S. H., Olds-Clarke, P., Phillips, D. M. & Silver, L. M. Hybrid sterility-6: a mouse t complex locus controlling sperm flagellar assembly and movement. *Dev. Biol.* 159, 631–42 (1993).
283. Pilder, S. H., Lu, J., Han, Y., Hui, L., Samant, S. A., Olugbemiga, O. O., Meyers, K. W., Cheng, L. & Vijayaraghavan, S. The molecular basis of 'curlicue': a sperm motility abnormality linked to the sterility of t haplotype homozygous male mice. *Soc. Reprod. Fertil. Suppl.* 63, 123–33 (2007).
284. Huang, Z., Somanath, P. R., Chakrabarti, R., Eddy, E. M. & Vijayaraghavan, S. Changes in intracellular distribution and activity of protein phosphatase PP1gamma2 and its regulating proteins in spermatozoa lacking AKAP4. *Biol. Reprod.* 72, 384–392 (2005).
285. Mishra, S., Somanath, P. R., Huang, Z. & Vijayaraghavan, S. Binding and inactivation of the germ cell-specific protein phosphatase PP1gamma2 by sds22 during epididymal sperm maturation. *Biol. Reprod.* 69, 1572–9 (2003).
286. Chun, Y. S., Park, J. W., Kim, G. T., Shima, H., Nagao, M., Kim, M. S. & Chung, M. H. A sds22 homolog that is associated with the testis-specific serine/threonine protein phosphatase 1gamma2 in rat testis. *Biochem. Biophys. Res. Commun.* 273, 972–6 (2000).
287. Brautigan, D. L. Flicking the switches: phosphorylation of serine/threonine protein phosphatases. *Semin. Cancer Biol.* 6, 211–7 (1995).
288. Kwon, Y. G., Lee, S. Y., Choi, Y., Greengard, P. & Nairn, a C. Cell cycle-dependent phosphorylation of mammalian protein phosphatase 1 by cdc2 kinase. *Proc. Natl. Acad. Sci. U. S. A.* 94, 2168–2173 (1997).
289. Liu, C. W., Wang, R. H., Dohadwala, M., Schönthal, A. H., Villa-Moruzzi, E. & Berndt, N.

Inhibitory phosphorylation of PP1alpha catalytic subunit during the G(1)/S transition. *J. Biol. Chem.* 274, 29470–5 (1999).

290. Somanath, P. R., Jack, S. L. & Vijayaraghavan, S. Changes in sperm glycogen synthase kinase-3 serine phosphorylation and activity accompany motility initiation and stimulation. *J. Androl.* 25, 605–17
291. Bhattacharjee, R., Goswami, S., Dudiki, T., Popkie, A. P., Phiel, C. J., Kline, D. & Vijayaraghavan, S. Targeted disruption of glycogen synthase kinase 3A (GSK3A) in mice affects sperm motility resulting in male infertility. *Biol. Reprod.* 92, 65 (2015).
292. Schillace, R. V, Voltz, J. W., Sim, A. T., Shenolikar, S. & Scott, J. D. Multiple interactions within the AKAP220 signaling complex contribute to protein phosphatase 1 regulation. *J. Biol. Chem.* 276, 12128–34 (2001).
293. Reinton, N., Collas, P., Haugen, T. B., Skâlhegg, B. S., Hansson, V., Jahnsen, T. & Taskén, K. Localization of a novel human A-kinase-anchoring protein, hAKAP220, during spermatogenesis. *Dev. Biol.* 223, 194–204 (2000).
294. Vijayaraghavan, S., Goueli, S. A., Davey, M. P. & Carr, D. W. Protein kinase A-anchoring inhibitor peptides arrest mammalian sperm motility. *J. Biol. Chem.* 272, 4747–52 (1997).
295. Carrera, A., Gerton, G. L. & Moss, S. B. The major fibrous sheath polypeptide of mouse sperm: structural and functional similarities to the A-kinase anchoring proteins. *Dev. Biol.* 165, 272–84 (1994).
296. Fulcher, K. D., Mori, C., Welch, J. E., O'Brien, D. A., Klapper, D. G. & Eddy, E. M. Characterization of Fsc1 cDNA for a mouse sperm fibrous sheath component. *Biol. Reprod.* 52, 41–9 (1995).
297. Brown, P. R., Miki, K., Harper, D. B. & Eddy, E. M. A-kinase anchoring protein 4 binding proteins in the fibrous sheath of the sperm flagellum. *Biol. Reprod.* 68, 2241–8 (2003).
298. Fardilha, M., Vieira, S. I., Barros, A., Sousa, Már., Da Cruz e Silva, O. A. B. & Da Cruz e Silva, E. F. Differential Distribution of Alzheimer's Amyloid Precursor Protein Family Variants in Human Sperm. *Ann. N. Y. Acad. Sci.* 1096, 196–206 (2007).
299. Thinakaran, G. & Koo, E. H. Amyloid precursor protein trafficking, processing, and function. *J Biol Chem* 283, 29615–29619 (2008).
300. De Strooper, B., Umans, L., Van Leuven, F. & Van Den Berghe, H. Study of the synthesis and secretion of normal and artificial mutants of murine amyloid precursor protein (APP): cleavage of APP occurs in a late compartment of the default secretion pathway. *J Cell Biol* 121, 295–304 (1993).
301. Multhaup, G. Identification and regulation of the high affinity binding site of the Alzheimer's disease amyloid protein precursor (APP) to glycosaminoglycans. *Biochimie* 76, 304–311 (1994).
302. Okamoto, T., Takeda, S., Murayama, Y., Ogata, E. & Nishimoto, I. Ligand-dependent G protein coupling function of amyloid transmembrane precursor. *J Biol Chem* 270, 4205–4208 (1995).
303. Brouillet, E., Trembleau, A., Galanaud, D., Volovitch, M., Bouillot, C., Valenza, C., Prochiantz, A. & Allinquant, B. The amyloid precursor protein interacts with Go heterotrimeric protein within a cell compartment specialized in signal transduction. *J Neurosci* 19, 1717–1727 (1999).
304. Deyts, C., Vetrivel, K. S., Das, S., Shepherd, Y. M., Dupre, D. J., Thinakaran, G. & Parent, A. T. Novel GalphaS-protein signaling associated with membrane-tethered amyloid precursor protein intracellular domain. *J Neurosci* 32, 1714–1729 (2012).
305. Shoji, M., Kawarabayashi, T., Harigaya, Y., Yamaguchi, H., Hirai, S., Kamimura, T. & Sugiyama, T. Alzheimer amyloid beta-protein precursor in sperm development. *Am J Pathol* 137, 1027–1032 (1990).
306. von Koch, C. S., Zheng, H., Chen, H., Trumbauer, M., Thinakaran, G., van der Ploeg, L. H. T., Price, D. L. & Sisodia, S. S. Generation of APLP2 KO Mice and Early Postnatal Lethality in APLP2/APP Double KO Mice. *Neurobiol. Aging* 18, 661–669 (1997).
307. Huang, P., Miao, S., Fan, H., Sheng, Q., Yan, Y., Wang, L. & Koide, S. S. Expression and characterization of the human YWK-II gene, encoding a sperm membrane protein related to the Alzheimer βA4-amyloid precursor protein. *Mol. Hum. Reprod.* 6, 1069–1078 (2000).
308. Zhuang, D., Qiao, Y., Zhang, X., Miao, S., Koide, S. S. & Wang, L. YWK-II protein/APLP2 in mouse gametes: potential role in fertilization. *Mol Reprod Dev* 73, 61–67 (2006).
309. Yan, Y. C., Bai, Y., Wang, L. F., Miao, S. Y. & Koide, S. S. Characterization of cDNA encoding a

human sperm membrane protein related to A4 amyloid protein. *Proc Natl Acad Sci U S A.* 87, 2405–2408 (1990).

310. Tian, X. Y., Sha, Y. S., Zhang, S. M., Chen, Y. B., Miao, S. Y., Wang, L. F. & Koide, S. S. Extracellular domain of YWK-II, a human sperm transmembrane protein, interacts with rat Mullerian-inhibiting substance. *Reproduction* 121, 873–880 (2001).

311. Coburger, I., Hoefgen, S. & Than, M. E. The structural biology of the amyloid precursor protein APP - a complex puzzle reveals its multi-domain architecture. *Biol. Chem.* 395, 485–98 (2014).

Aims

The present work aimed primarily to identify, characterize and modulate non-hormonal targets for male contraception, selectively expressed in testis and sperm, in order to specifically inhibit/disrupt a process essential to reproduction, such as, post-meiotic events in spermatogenesis, sperm maturation in the epididymis or sperm function (**Aim 1**).

Moreover, many questions regarding the etiology of male infertility remain unanswered with idiopathic infertility as the most common type of male infertility. Thus, we intended to determine the association between semen parameters and age, and the expression and activity of signaling proteins in order to establish a biomarker "fingerprint" to assess male fertility based on molecular parameters (**Aim 2**).

To that end the following aims were proposed:

Aim 1. Identification, characterization and modulation of protein complexes in human testis and spermatozoa as potential targets for pharmacological intervention in male fertility

1.1. Construction and analysis of a testis/sperm-enriched interaction network: unraveling the PPP1CC2 interactome (**Chapter 3.1.**) – *Submitted to Biology of Reproduction*

1.2. Modulation of PPP1CC2/AKAP4 and PPP1CC2-specific interactions in spermatozoa using cell-penetrating peptides as a drug intracellular delivery system (**Chapter 3.2.**) – *In the process to file a patent application*

1.3. Characterization of SARP2, a PPP1 interacting protein, in testis and spermatozoa (**Chapter 3.3.**) – *Published in Reproduction, Fertility and Development*

1.4. Construction of APP interaction network in human testis: sentinel proteins for male reproduction (**Chapter 3.4.**) – *Published in BMC Bioinformatics*

Aim 2. Identification of signaling proteins as targets for diagnostic intervention in male fertility

2.1. Profiling signaling proteins in human spermatozoa: biomarker identification for sperm quality evaluation (**Chapter 4.1.**) – *Published in Fertility and Sterility*

2.2. Unraveling the association between age and signaling proteins in human spermatozoa (**Chapter 4.2.**) – *To be submitted to Fertility and Sterility*

B. RESULTS

3. Identification, characterization and modulation of protein complexes in human testis and spermatozoa as potential targets for pharmacological intervention in male fertility

3.1. Construction and analysis of a human testis/sperm-enriched interaction network: unraveling the PPP1CC2 interactome

Joana Vieira Silva[1], Sooyeon Yoon[2], Pieter-Jan De Bock[3,4], Alexander V. Goltsev[2], Kris Gevaert[3,4], José Fernando F. Mendes[2], Margarida Fardilha[1]

[1] Laboratory of Signal Transduction, Department of Medical Sciences, Institute of Biomedicine – iBiMED, University of Aveiro, 3810-193 Aveiro, Portugal.

[2] Physics Department, I3N, University of Aveiro, 3810-193 Aveiro, Portugal

[3] Department of Medical Protein Research, VIB, B-9000 Ghent, Belgium

[4] Department of Biochemistry, Ghent University, B-9000 Ghent, Belgium

Corresponding author: Margarida Fardilha, Departamento de Ciências Médicas, Universidade de Aveiro, Campus Universitário de Santiago, Agra do Crasto – Edifício 30, 3810-193 Aveiro, Portugal. T: +351-918143947. E: mfardilha@ua.pt

Silva JV, Yoon S, De Bock PJ, Goltesev AV, Gevaert K, Mendes JF, Fardilha M. Construction and analysis of a human testis/sperm-enriched interaction network: unraveling the PPP1CC2 interactome. Submitted to Biology of Reproduction.

3.1.1. Abstract

Phosphoprotein phosphatase 1 catalytic subunit gamma 2 (PPP1CC2), a *PPP1CC* tissue-specific alternative splice restricted to testicular germ cells and spermatozoa, is essential for spermatogenesis and spermatozoa motility. The key to understand PPP1CC2 regulation lies on the characterization of its interacting partners. This study aimed to integrate tissue-specific protein expression and protein-protein interaction data in order to identify key PPP1CC2 complexes for male reproductive functions and potential targets for male contraception. We construct a testis/sperm-enriched protein interaction network using the breath-first searching algorithm and analyzed the topological properties and biological context of the network. A total of 1,778 proteins and 32,187 interactions between them were identified in the testis/sperm-enriched network. The network analysis revealed the members of functional modules that interact more tightly with each other. In the network, PPP1CC was located in the fourth maximum core part (k=41) and had 106 direct interactors. Sixteen PPP1CC interactors were involved in spermatogenesis-related categories. Also, PPP1CC had 50 direct interactors, highly interconnected and many of them part of the network maximum core (k=44), associated with motility-related annotations, including several previously uncharacterized interactors, such as, LMNA, JAK2 and RIPK3. One of the most intriguing interactors was A-kinase anchor protein 4 (AKAP4), a testis-specific protein related to infertility phenotypes and involved in all major motility-related annotations. We demonstrated for the first time the interaction between PPP1CC2 and AKAP4 in human spermatozoa and the potential of the complex as contraceptive target.

3.1.2. Introduction

Some proteins are known to be expressed in a tissue-specific manner and therefore, the signal transduction cascades in which they are involved are diverse, reflecting the specific biological roles of each individual tissue [1]. Expression of the phosphoprotein phosphatase 1 catalytic subunit gamma 2 (PPP1CC2), a PPP1 isoform, is restricted to testicular germ cells and spermatozoa. PPP1, an evolutionarily conserved phospho Ser/Thr-protein phosphatase, catalyzes the majority of eukaryotic protein dephosphorylation reactions in a highly regulated and selective manner [2]. Three genes, *PPP1CA*, *PPP1CB* and *PPP1CC*, encode four PPP1 isoforms, PPP1CA, PPP1CB, PPP1CC1, and PPP1CC2, which show a high degree of sequence similarity (~90%) [3]. The *PPP1CC* transcript undergoes tissue-specific splicing, giving rise to an ubiquitously expressed isoform, PPP1CC1 and a testis-enriched and sperm-specific isoform, PPP1CC2 [4]. PPP1CC2 has an unique 22 amino acid C-terminus, which is highly identical in mammals and plays a role in binding to specific regulatory subunits [5]. Targeted disruption of the mouse *Ppp1cc* gene results in male infertility due to aberrant spermiogenesis [6]. However, this deficiency causes no obvious

abnormality in other tissues. Additionally, the production of normal spermatozoa can take place in the complete absence of PPP1CC1 [7]. Inhibition of PPP1 in spermatozoa by treatment with inhibitors results in initiation and stimulation of motility [8,9]. These results indicate that PPP1CC2 functions in the regulation of mammalian spermatogenesis and sperm motility [10,11]. Over the past two decades it has become apparent that PPP1's functional versatility is achieved by its ability to interact with multiple targeting and regulatory subunits known as PPP1 interacting proteins or PIPs [2,10–12]. PIPs generally fall into one of four categories: substrates, inhibitors, subcellular targeting subunits or substrate specifying subunits. PIPs show an exceptional diversity in brain and testis [13] and tissue-restricted expression of PIPs accounts for the specificity of PPP1 activity [3,13]. Another aspect of the regulation of the PPP1 activity lies in the selectivity of some PIPs. Most PIPs appear to interact with all PPP1 isoforms however, an increasing number seems to preferentially interact with a specific PPP1 isoform [3] and this may be caused by differences at the C-termini of the PPP1 isoforms. For instance, Repo-man and Neurabin-1 preferentially bind to PPP1CC1 [14,15]. Some PIPs are fully isoform specific; e.g., SPZ1 and a testis-specific Endophilin B1 isoform (SH3GLB1), which only interacts with PPP1CC2 [16,17]. MYPT1 (PPP1R12A) on the other hand selectively interacts with a specific region of the PPP1CB C-terminus [18]. It is noteworthy that the study of PPP1 isoform-specific functions has some major hindrances: first, most studies do not specify the isoform used and second there is a lack of isoform-specific antibodies and inhibitors. Also, when reconstructing the PPP1 interactome, the time-point at which the proteins are expressed, the tissue, cell type and intracellular compartment where the proteins are localized, and the methods used to validate the interaction all need to be taken into account. Furthermore, the initial job of identifying PPP1 interactors is a main challenge as the interactions between PPP1 isoforms and their interactors are typically transitory and weak [19].

In this study, we aimed to use a tissue-specific network-based approach [20] to characterize the human testis and spermatozoa interactome in order to identify new, yet poorly explored candidates involved in PPP1CC2 regulation of male fertility.

3.1.3. Material and Methods

Identification of PPP1CC interacting proteins

The HIPPIE database [21] was used for retrieving human protein-protein interaction (PPI) data (released May 09, 2014 and downloaded March 23, 2015). This database is regularly updated by incorporating interaction data from major expert-curated experimental PPI databases (such as Bell09, BioGRID, HPRD, IntAct and MINT). In addition, PPP1CC2 interacting proteins from other sources were included. First, the PubMed database was searched for proteins with published literature showing the preferential binding to PPP1CC2 and/or tissue, cellular, subcellular

localization that matches PPP1CC2. Second, the PubMed database was also used to search for PPP1CC2 substrates [22,23]. Finally, Yeast Two-Hybrid (Y2H) data from our laboratory [5] was also considered and proteins that only interacted with PPP1CC2 C-terminus were included.

Identification of proteins highly enriched or specifically expressed in testis

From the C-it database [24], testis-specific proteins were searched with the keywords, 'testis-enriched' for 'Human'. The limitation factors for the literature information were 5 for PubMed and 3 for MeSH terms. The proteins with a SymAtals z-score higher than |1.96| were selected. In the UniGene database [25] the tissue-specific proteins were searched using 'testis restricted' in 'Homo sapiens' as keywords. The TiGER [26] and the Very Gene [27] databases were also searched for 'Testis' in 'Tissue View' category. In HPA (Human Protein Atlas) [1] the protein list was obtained within the "Tissue enriched" category. In the BioGPS portal the keywords, 'testis, spermatogonia, spermatid, spermatozoa' in 'Human' were used. Using the plugin 'Gene expression/activity chart', proteins highly expressed in testis-related categories were selected. If the expression level was less than the mean value or the data were not shown, the corresponding proteins were removed from the list. In addition, proteins that had high correlation levels of expression ($\geq$0.9) with testis-specific proteins were investigated.

Development of testis-enriched/specific PPI network and network properties analysis

In order to construct a testis/sperm-enriched PPI network, the testis-enriched/specific proteins and their direct interactions were collected from the HIPPIE database, the literature search, and the Y2H experimental data from our laboratory. Their direct interacting partners were selected regardless of their tissue specificity. Then, the inner connections between those proteins were captured. The isolated interactions from the major cluster of the network were kept. However, the amount of isolated clusters was negligibly small to analyze the network's properties and the biological functionality of the whole network. To figure out the functional relations among the testis-enriched/specific proteins, specifically PPP1CC's role in male fertility, the topological properties of the network, such as connectivity, betweenness centrality, clustering coefficient, modularity, and k-core of the network were analyzed. For searching the notable biological functions of PPP1CC, subnetworks related to spermatogenesis and sperm motility were extracted from the main testis/sperm-enriched PPI network. First, the proteins associated with spermatogenesis and sperm motility annotations and their first connected neighbors were selected. Also, the inner connections between them were kept. For each group, we checked how PPP1CC and its directly interacting partners correlate to the specific biological functions.

Bioinformatic analyses: gene ontology, pathways and involvement in diseases

The data were analyzed using the Database for Annotation, Visualization and Integrated Discovery (DAVID) v6.7 [28]. The UniProt identifiers of all proteins were entered into the DAVID functional annotation program. The overall set of human protein-coding genes was used as background in DAVID. The AmiGO Term Enrichment tool was used to annotate the proteins in broader gene ontology terms whenever necessary. Protein identities associated with defects in male fertility were obtained from the Jackson Laboratories mouse knockout database [29]. The OMIM [25] and the UniProt databases were also queried with the term 'male infertility' and the associated genes or proteins were downloaded. The full-length codifying sequence of AKAP4 was retrieved from NCBI with the purpose of performing a PPP1 binding motif search using ScanProsite [30].

Ethical approval

This study was approved by the Ethics and Internal Review Board of the Hospital Infante D. Pedro E.P.E. (Aveiro, Portugal) and was conducted in accordance with the ethical standards of the Helsinki Declaration. All donors signed informed consent allowing the samples to be used for scientific purposes.

Sperm extracts

Ejaculated semen samples were obtained from healthy donors by masturbation into a sterile container. Basic semen analysis was performed by qualified technicians according to World Health Organization (WHO) guidelines [31]. After semen liquefaction, sperm cells were washed three times in phosphate buffered saline (PBS) by centrifugation (600 g for 5 min at 4°C). For immunocytochemistry assays, washed sperm cells were placed onto a glass coverslip and dried at room temperature. For Western blot and immunoprecipitation assays, sperm cells were lysed in 1X RIPA buffer (0.5M Tris-HCl, pH 7.4, 1.5M NaCl, 2.5% deoxycholic acid, 10% NP-40, 10mM EDTA) (Millipore Iberica S.A.U., Madrid, Spain) supplemented with protease (10 mM benzamidine, 1.5 μM aprotinin, 5 μM pepstatin A, 2 μM leupeptin, 1 mM PMSF) and phosphatase (1 mM sodium fluoride, 2.5 mM sodium pyrophosphate, 50 mM beta-glycerophosphate, 1 mM sodium orthovanadate) inhibitors, and centrifuged at 16000 g for 20 min at 4ºC. The supernatant was used for the subsequent steps (sperm soluble extract). The pellet (sperm insoluble extract) was ressuspended in 1% SDS (sperm insoluble extract).

Antibodies

The anti-PPP1CC2 antibody was raised in rabbit against the specific PPP1CC2 C-terminal peptide (VGSGLNPSIQKASNYRNNTVLY) and has been described previously [32]. Mouse anti-AKAP4 (ab56551) used for the immunofluorescence studies was obtained from Abcam (Cambridge, UK). Rabbit anti-AKAP4 (ab123415) used for the Western blot and immunoprecipitation studies was obtained from Abcam (Cambridge, UK). The infrared IRDye labelled anti-rabbit secondary

antibody for the Western blot analyses was obtained from LI-COR Biosciences (Lincoln, NE, USA) and the fluorescently labeled secondary antibodies (Texas Red-X goat anti-rabbit IgG and Alexa Fluor 488 goat anti-mouse IgG) for the immunocytochemistry studies were obtained from Life Technologies (Carlsbad, CA)).

Immunoprecipitation

RIPA supernatant sperm extracts were pre-cleared using Dynabeads Protein G (Life Technologies S.A., Madrid, Spain). A direct immunoprecipitation approach was performed using 1 μg of homemade rabbit anti-PPP1CC2 or rabbit anti-AKAP4 (ab123415, Abcam, Cambridge, UK), pre-incubated with Dynabeads Protein G during 1 h at 4ºC with rotation. After incubation, pre-cleared sperm extracts were applied to the antibody-Dynabeads complex and incubated overnight with rotation at 4ºC. After washing three times with PBS in 3% BSA for 10 min with rotation at 4ºC, the beads were re-suspended in 1% SDS.

Western blotting

Extracts were resolved by 12% SDS–polyacrylamide gel electrophoresis (PAGE). Proteins were subsequently electrotransferred onto nitrocellulose membranes. Nonspecific protein-binding sites on the membrane were blocked with 5% nonfat dry milk in Tris-buffered saline (TBS: 25 mM Tris-HCl, pH 7.4, 150 mM NaCl). The blots were then washed twice for 15 min each with TBST (TBS containing 0.1% Tween 20) and then incubated with primary antibodies for 2h at room temperature. After the wash, the blots were incubated with the appropriate secondary antibody for 1 h at room temperature. Blots were washed with TBST three times 15 min each. Blots were immunodetected using the Odyssey Infrared Imaging System (LI-COR Biosciences, US).

Membrane overlay

Immunoprecipitation extracts loaded onto SDS-PAGE gel and subsequently transferred to a nitrocellulose membrane were then overlaid with purified PPP1CC2 protein, prepared as described previously [33]. After washing to remove excess protein, bound PPP1CC2 was detected by incubating the membrane with a homemade rabbit anti-PPP1CC2 antibody, raised against a isoform-specific C-terminal peptide [8]. Immunoreactive bands were revealed by incubation with an Infrared IRDye-labeled anti-rabbit specific followed by Odyssey Infrared Imaging System (LI-COR Biosciences, US) detection.

Mass spectrometry

After immunoprecipitation, SDS in the samples was removed using HIPPR detergent removal spin columns (Pierce). Next, the samples were boiled for 5 min and put on ice for another 5 min. The

proteins were then digested overnight by trypsin (Promega) at 37°C. The peptide mixtures were acidified with formic acid to stop the digestion.

LC-MS/MS analysis was performed using an Ultimate 3000 HPLC system (Dionex) in-line connected to an LTQ Orbitrap XL mass spectrometer (ThermoScientific). The peptides were first trapped on a pre-column (in-house, 100 µm internal diameter (I.D.) x 20 mm, 5 µm beads C18 Reprosil-HD, Dr. Maisch) after which they were loaded onto an analytical column (in-house, 75 µm I.D. x 150 mm, 3 µm beads C18 Reprosil-HD, Dr. Maisch). The peptides were separated using a linear gradient over 30 min from 2% solvent A (0.05% formic acid, 2% acetonitrile) to 55% solvent B (0.05% formic acid, 80% acetonitrile) at a flow rate of 300 nl/min. The mass spectrometer was operated in data-dependent acquisition mode during which the six most intense ions were selected for fragmentation with a dynamic exclusion of 60 s. Mascot Distiller (version 2.3.2, Matrix Science) was used to generate Mascot Generic Files (MGFs) as previously described [34]. The Mascot search algorithm (version 2.3, Matrix Science) was used to search these peak lists against the human subsection of the Swiss-Prot database (version 2013_06, 20,257 entries). Trypsin/P was set as the protease used, allowing for one missed cleavage. Mass tolerances were set to 10 ppm and 0.5 Da for the precursor and fragment ions respectively. Protein N-terminal acetylation, methionine oxidation and N-pyroglutamate were set as variable modifications. Only peptide spectrum matches that ranked first and scored above the identity threshold set at the 99% confidence level were withheld. The raw data files have been submitted to the ProteomeXchange database (PXD002888).

Immunocytochemistry of human spermatozoa

Washed spermatozoa were placed onto a glass coverslip and dried at room temperature in a six well plate containing one coverslip per well. To each well, 4% paraformaldehyde in PBS was added and wells were incubated for 10 min. Subsequently, spermatozoa were washed twice. For permeabilization, methanol at -20 C was added for 2 min and specimens were then washed twice before being blocked for 30 min with 3% BSA in PBS and then incubated with primary antibodies [homemade rabbit anti-PPP1CC2 (previously described in [35]), and mouse anti-AKAP4 (ab56551, Abcam, Cambridge, UK)] for 1 h at room temperature. After three washes, the fluorescently labeled secondary antibodies [Texas Red-X goat anti-rabbit IgG (Life Technologies, Carlsbad, CA) and Alexa Fluor 488 goat anti-mouse IgG (Life Technologies, Carlsbad, CA)] were added and the coverslips were incubated for 30 min at room temperature. Finally, samples were washed and the coverslips mounted on microscope glass slides with one drop of antifading reagent containing DAPI for nucleic acid staining (Vectashield; Vector Laboratories). Negative controls were processed in parallel by adding PBS instead of the first antibodies. Fluorescence images were

obtained using an Imager.Z1 (Zeiss), Axio-Cam HRm camera (Zeiss) and AxioVision software (Zeiss).

3.1.4. Results

Identification of highly enriched or specific testis proteins

We identified a total of 1,919 unique proteins highly specific or strongly expressed in testis. Of all proteins, 610 proteins (31.8% of the total 1,919 highly testis-specific proteins) were identified in at least two databases and were further considered as strongly expressed in testis (Supplementary Table D.1). The criteria used in the tissue-expression databases were set for maximum stringency to identify tissue-specific proteins with a high confidence level. The GO term enrichment analysis of the testis-enriched proteins revealed that the most significant biological process categories were all reproduction-related, such as sexual reproduction (p=3.71E-156), spermatogenesis (p=5.36E-147) and fertilization (p=4.33E-44) (Supplementary Table D.2), which support our approach. Concerning the cellular component, the top 3 significant categories were sperm part (p=6.02E-54), motile cilium (p=1.47E-43) and acrosomal vesicle (p=1.65E-39) (Supplementary Table D.2).

Identification of PPP1CC interacting proteins

In this study, PPP1CC2 (testis-enriched and sperm-specific isoform) and PPP1CC (whenever the tissue-specific alternative splicing product was not specified) were considered. We identified 313 PPP1CC/PPP1CC2 interactors from different sources (Supplementary Table D.3). From the PPI databases 252 PPP1CC interactors were identified. Thirty-two proteins were identified as PPP1CC2 interactors using a literature search (Table B.1). From those, SPZ1, ACE, TSSK1B, AKAP4, HSPA2 and FADS2 were associated with infertility phenotypes in gene knockout mice. A total of 37 proteins were identified as candidate PPP1CC2 substrates in testis (Table B.1). From those, 5 had been previously associated with infertility phenotypes in gene knockout mice (HMGA1, HSPA4, SYCP2, YBX2 and HSPA2). In the Y2H screens, 36 proteins (corresponding to 45% of all PPP1CC isoforms identified) were obtained exclusively from the Y2H screen in which the PPP1CC2 C-terminus was used as bait, meaning that they might represent specific binders of the PPP1CC2 isoform (Table B.1). Of the 313 direct PPP1CC interactors identified from several sources (PPI databases, literature search, substrates and Y2H), 10 interactors were identified as highly specific to or strongly expressed in the testis in at least two database (AKAP4, PGK2, TSKS, TSSK1B, YBX2, SPZ1, NEK2, C9orf50, GLB1L and PPP1R2P9).

Table B.1 – PPP1CC2 regulatory subunits/substrates identified by literature searching and Y2H screen. The PIPs shown were chosen taking into consideration if PPP1CC isoforms were distinguished and if there was substantial work that showed preferential binding to PPP1CC2 giving the cellular and sub-cellular context. *indicate an infertility phenotype in knockout mice; + represent proteins with testis-specific alternative splicing isoforms.

Candidate PPP1CC2 substrates identified in testis by MacLeod *et al*. 2014 and Henderson *et al*. 2010 (gray)		**PPP1CC2 interactors identified in a Y2H using PPP1CC2's C-terminus as bait and a human testis library (Fardilha *et al*. 2010)**		**Specific regulatory subunits of PPP1CC2 isoform identified by a literature searching**		
Uniprot ID	**Gene Name**	**Uniprot ID**	**Gene name**	**Uniprot ID**	**Gene name**	**Reference**
Q9UKV3	ACIN1	O14727	APAF1	Q7Z4L9	PPP1R42	[57,58]
Q9NYF8	BCLAF1	Q9UBL3	ASH2L	Q9Y371	SH3GLB1 +	[17]
Q7Z7K6	CENPV	Q86VG3	C11orf74	P39656	DDOST	[59]
P55884	EIF3B	Q5SZB4	C9orf50	Q15435	PPP1R7	[60,61]
Q6UN15	FIP1L1	Q6PJW8	CNST	O60927	PPP1R11	[61]
P17096	HMGA1 *	Q92905	COPS5	Q9UJT2	TSKS	[41]
P34932	HSPA4 *	P07711	CTSL	P63104	YWHAZ +	[62]
Q6PKG0	LARP1	Q7L576	CYFP1	Q9BXG8	SPZ1 *	[16]
Q4G0J3	LARP7	Q9NYF0	DACT1	Q5JR98	TCTEX1D4	[63]
O95819	MAP4K4	Q9NR20	DYRK4	P41236	PPP1R2	[64]
Q15154	PCM1	Q9H0I2	ENKD1	Q6NXS1	PPP1R2P3	[64]
Q13442	PDAP1	Q6UWU2	GLB1L	O14990	PPP1R2P9	[65]
O75475	PSIP1	O43708	GSTZ1	Q96I34	PPP1R16A	[66]
P15151	PVR	O60674	JAK2	O00299	CLIC1	[67]
Q86X27	RALGPS2	Q6B0I6	KDM4D	Q9Y696	CLIC4	[67]
Q9UKM9	RALY	Q9NPI7	KRCC1	Q9NZA1	CLIC5	[67]
P49792	RANBP2	O95819	MAP4K4	P17252	PRKCA	[68]
Q9H7N4	SCAF1	O60551	NMT2	Q12972	PPP1R8 +	[45]
O75533	SF3B1	Q9UHY1	NRBP1	P51955	NEK2 +	[45]
Q86XK3	SFR1	Q7Z5V6	PPP1R32	Q8N9B4	ANKRD42 +	[35,69]
Q8IYB3	SRRM1	Q8TAP8	PPP1R35	P12821	ACE * +	[62]
Q9UQ35	SRRM2	Q12972	PPP1R8	P07205	PGK2	[62]
Q9BX26	SYCP2 *	Q96S59	RANBP9	P11021	HSPA5	[62]
O60343	TBC1D4	Q6ZMZ0	RNF19B	Q9BXA7	TSSK1B *	[41]
Q9Y2W1	THRAP3	P23921	RRM1	Q9UKA4	AKAP11	[11]
Q07157	TJP1	Q9NRG7	SDR39U1	Q5JQC9	AKAP4 *	[70]
Q9UKE5	TNIK	O43556	SGCE	O75969	HSPA2 *	[22]
Q14669	TRIP12	Q9H0A9	SPATC1L	P54652	UQCRC2	[41]
Q9Y2T7	YBX2 *	Q5JR98	TCTEX1D4	P22695	FADS2 *	[41]
P09488	GSTM1	Q5VZQ5	TEX36	O95864	SCCPDH	[41]
P63261	ACTG1	Q9BXJ8	TMEM120A	Q8NBX0	ATP5C1	[41]
P60709	ACTB	Q9HBL0	TNS1	P36542		
P55795	HNRNPH2	Q92547	TOPB1			
Q9NY65	TUBA8 T	Q13595	TRA2A			
P54652	HSPA2 *	Q3B726	TWISTNB			
P11021	HSPA5	Q8IW00	VSTM4			
P07437	TUBB					

PPI networks

Among 610 testis-enriched/specific proteins only 316 proteins have interactions in the PPI databases. The remaining 294 testis-enriched/specific proteins have no PPI information; therefore, they were excluded for generating the testis-enriched network. With 316 testis-enriched/specific proteins, we capture their directly interacting neighbors (1,462 non-testis-enriched proteins included) and their inner connections between the proteins. The total number of proteins in the testis/spermatozoa-specific PPI network is *N*=1,778 and the total number of interactions between

them is L=32,187. The averaged connectivity, number of neighbors of a node in the network, is $<q>$=36.2 with the power-law connectivity distribution, $P(q) \sim q^{-\gamma}$, where γ is the degree exponent [44]. We find that the average shortest path length between two nodes is l =2.63 and the longest distance between two nodes is 6. Thus, the testis-enriched/specific network has a sparse structure with hubs and small-world properties. The mean clustering coefficient is C=0.19. The clustering coefficient characterizes how nearest neighboring nodes of a node are connected to each other. If all of them are tightly connected to each other, then they form a clique and the clustering coefficient is 1. For a sparse random uncorrelated network of finite size N, this coefficient is close to zero [44]. Note that the value C=0.19 is about ten times larger than the clustering coefficient expected for a sparse random uncorrelated network (in the latter case $C = <q>/N \sim 0.02$). Therefore, the testis-enriched network has a complex motifs structure, which may play a functional role, and contains numerous hubs, i.e. highly connected proteins. According to the degree-degree correlation analysis, which aims to reveal correlations between connectivities of nearest neighbors, the Pearson coefficient of the network is small and negative, r=-0.04 (note that r=0 in uncorrelated networks [44].) This result shows that the degree correlations in the testis/spermatozoa-specific PPI network are very weak and disassortative. The disassortativity means that weakly connected nodes prefer to have strongly connected neighbors, on average. The topological properties of the testis-enriched/specific network are shown in Supplementary Table D.4.

The k-core is the network subgraph in which all nodes have degree at least k [36,37]. The k-core is obtained by recursively removing nodes with connectivity lower than k. Among the 316 testis-strongly expressed proteins in the network, only 19% of them remain after 10-core decomposition (Supplementary Table D.4 B). In the maximum k-core subgraph in which each node has at least k=44 connectivity, only RPL10L and HSPA1L remained in the core part (Supplementary Table D.4 B). The most significant cellular compartment annotations among the proteins in the highest k-core were intracellular non-membrane-bounded organelle (60.4%; p=3.5E-38) and cytosol (56.2% of the proteins; p=6.0E-60), more specifically the cytosolic ribosome (29.7%, p=3.2E-88). Also, 37.5% shared the same biological process (translation, p=7.2E-67). Among the proteins strongly expressed in testis, PBK, TUBA3C, and PIAS2 are located in high k-cores with k=42, 36, and 36, respectively (Supplementary Table D.4 B). PPP1CC is located in the fourth maximum core part (k=41). PPP1CC in this network has 106 nearest neighbors (Figure B.1). Among those, 27.4% (29 proteins) are involved in cell cycle (p=4.50E-13) and 22.6% (24 proteins) in regulation of programmed cell death (p=9.50E-09). Nineteen PPP1CC interactors from the network were associated with male infertility phenotypes knockout mice (LMNA, ESR1, TP53, PGK2, CDK4, CDK2, AKT1, HSPA4, BRCA1, CDKN2A, TRIM28, LBR, AKAP4, RIF1, SIAH1, AURKB, RANBP9, YBX2 and IKBKG, Supplementary Table D.5).

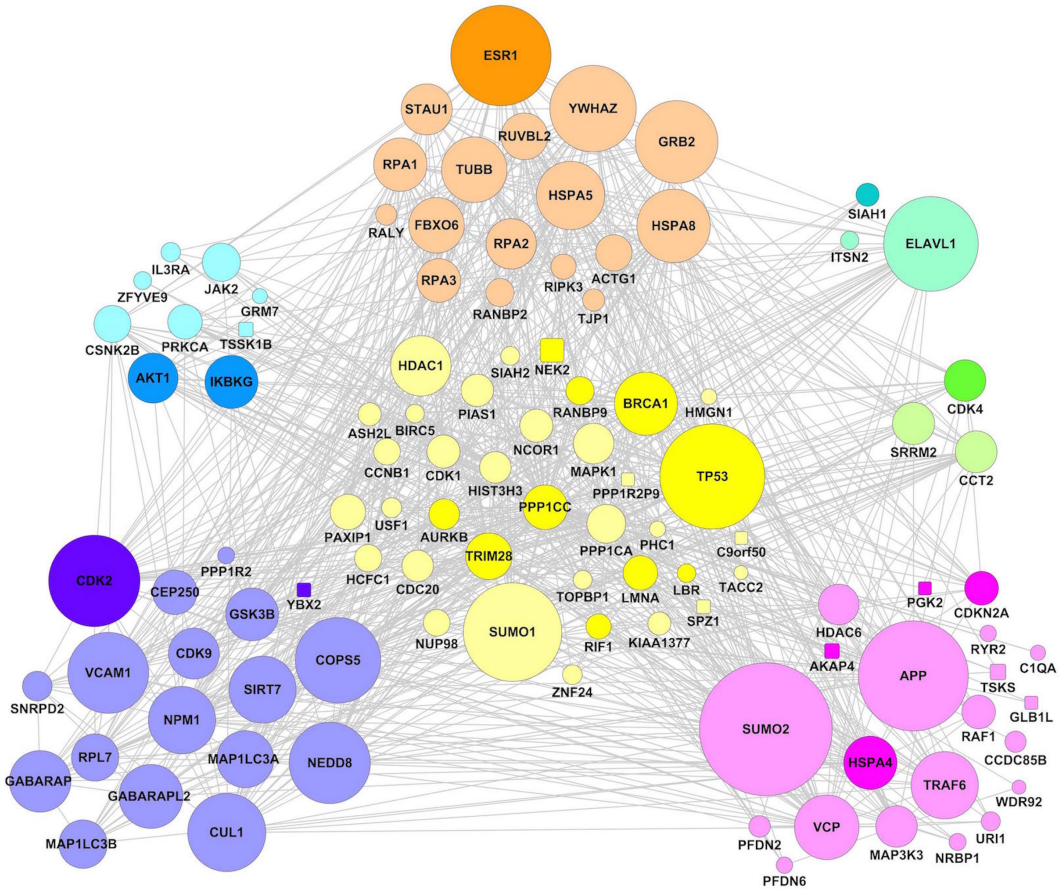

Figure B.1 – PPP1CC interactors in the testis/sperm-enriched network. Node sizes represent relative degree of the nodes and other interactions of the nodes are not expressed for simplicity's sake. Square nodes represent testis-enriched/specific proteins; Darker node color represents infertility related proteins; Node color according the modularity: module 1, light-cyan; module 2, violet; module 3, pink; module 4, orange; module 5, yellow; module 6, light-green; module 7, aquamarine.

We identified community structures in the network without taking into account overlapping by use of a modularity matrix following the method in reference [38] (Supplementary Table D.4 B). Seven modules were identified in the network, which have 19.3% (module 1), 5% (module 2), 12.7% (module 3), 13.3% (module 4), 25.3% (module 5), 7.7% (module 6) and 35.7% (module 7) of testis-enriched/specific proteins. PPP1CC was located in module 5 in this network and our analysis showed that module 5 included the highest percentage of proteins with a similar functional role. In Supplementary Table D.6 lists listed the top 10 most statistically significant categories for both biological process and cellular component in each module. Modules 2 and 5 included a higher percentage of proteins with a similar functional role. Module 5 included 320 proteins of which 52.8% are involved in regulation of transcription (p = 1.3E-54) and 38.4% are localized at the nuclear lumen (p = 2.1E-57). From the KEGG analyses, the most significant pathway associated with module 5 is cell cycle (8.5%, p = 6.9E-19). Among the 272 proteins in module 2, 28.8% were

involved in translation, more specifically in translational elongation (p = 1.7E-98). KEGG analysis corroborated these results and indicated that 22.7% proteins in module 2 were associated with ribosomes (p=4.6E-83). Module 1 included 223 proteins of which 22.0% were involved in protein kinase cascade (p=2.4E-32). Pathway analysis revealed that the most significant pathway was the JAK-STAT signaling (22.0%; p=4.6E-38). The most prominent biological process detected in module 6 (80 proteins) was RNA processing (20%, p=1.0E-10), more specifically RNA splicing (18.8%; p=2.4E-10).

Fifty-nine genes associated with the term "male infertility" were extracted from OMIM database and 18 (AR, CFTR, ACR, FSHR, CATSPER1, PIWIL1, FKBP6, PRND, FKBP4, CLCN2, TEX11, ZBTB16, PRM1, SEPT12, PICK1, SPAG6, AURKC and DAZL) overlapped with proteins from the network. Proteins associated with "male infertility" were also searched in UniProtKB and 45 records were obtained from which 32 (AR, CFTR, ACR, FSHR, CATSPER1, PIWIL1, FKBP6, PRND, FKBP4, CLCN2, TEX11, ZBTB16, PRM1, SEPT12, PICK1, SPAG6, AURKC, DAZL, DAZ1, DAZ4, DZIP3, PUM2, SYCP3, CREM, DDX4, DNAI1, HSFY1, INSL3, NEK2, RXFP2, TAF7L and TSSK2) were part of the testis/sperm-enriched network.

PPP1CC in spermatogenesis and motility

We selected the proteins annotated with GO terms related to spermatogenesis (Supplementary Table D.7 A) and associated with abnormal spermatogenesis phenotypes. Then, extracted PPP1CC interactors annotated in those categories from the testis/sperm-enriched network (Figure B.2). In this subnetwork, we had 16 direct connections to PPP1CC.

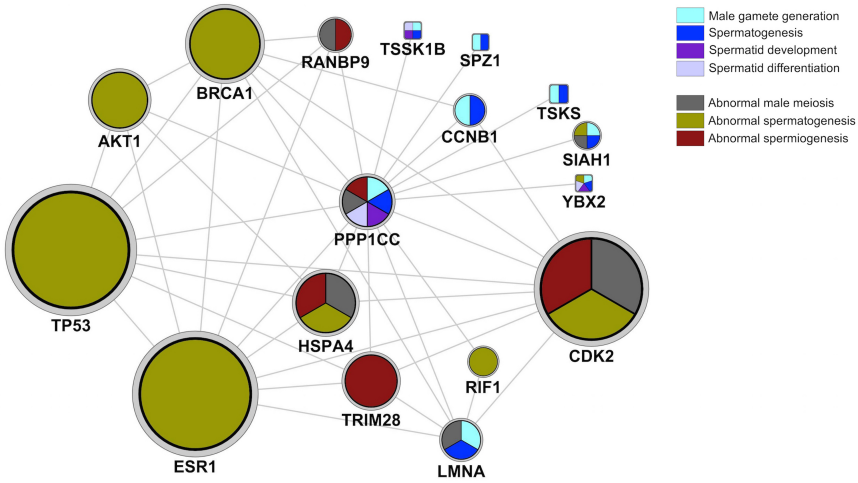

Figure B.2 – PPP1CC-based sub-network for spermatogenesis extracted from the testis/sperm-enriched network. PPP1CC and its interactors associated with spermatogenesis-related annotations were extracted from the network. Square nodes represent testis-enriched proteins; Node colors represent spermatogenesis-related annotations. Node size according to the degree in the network.

A PPP1CC-based subnetwork for sperm motility was also constructed. The PPP1CC interactors associated with motility annotations (Supplementary Table D.7 B) were extracted from the testis/sperm-enriched network (Figure B.3). In this subnetwork, PPP1CC had 50 direct connections.

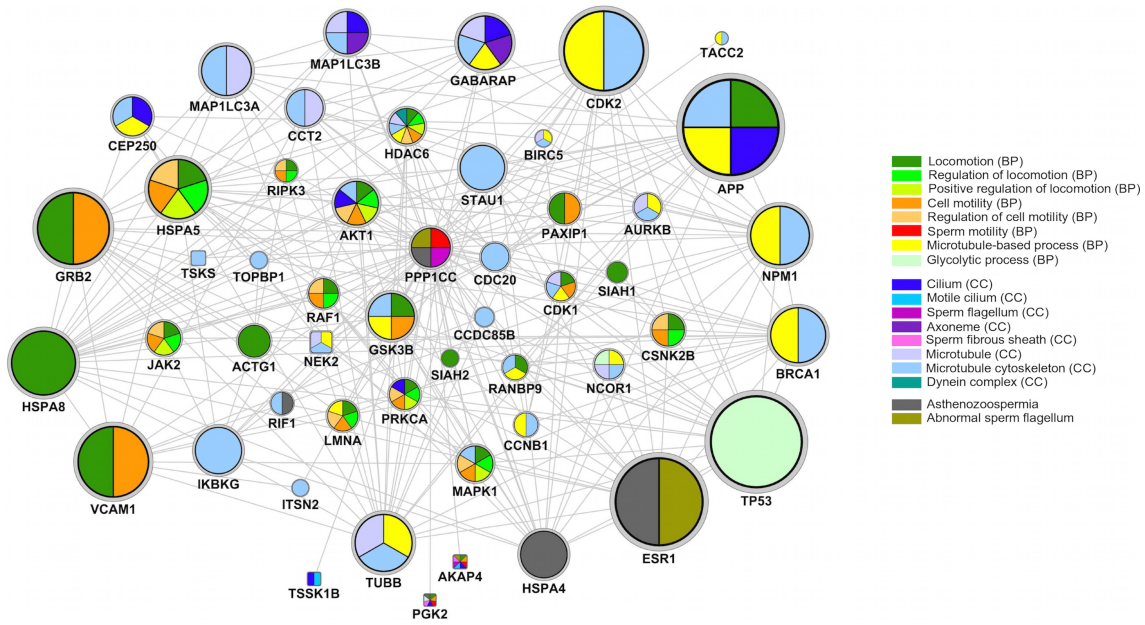

Figure B.3 – PPP1CC-based sub-network for sperm motility extracted from the testis/sperm-enriched network. PPP1CC and its interactors associated with motility-related annotations were extracted from the network. Square nodes represent testis-enriched proteins; Node colors represent motility-related annotations. Node size according to the degree in the network.

PPP1CC2 and AKAP4 interaction in human spermatozoa

To demonstrate the interaction of PPP1CC2 and AKAP4 in human spermatozoa we performed a co-immunoprecipitation using an isoform-specific anti-PPP1CC2 antibody from three independent normozoospermic human ejaculated sperm samples followed by mass spectrometry analysis (Figure B.4 A). Using the Orbitrap XL mass spectrometer 6 peptides were identified that matched PPP1CC (Table B.2). Mass spectrometry data of the same immunoprecipitates showed that AKAP4 was also present. Fourteen peptides were identified that matched AKAP4 (Table B.2). Additionally, several previously well-characterized PPP1 interacting proteins, such as 14-3-3 (YWHAQ), were also identified. This is the first report of AKAP4 recovery from multiple PPP1CC2 immunoprecipitates of human sperm extracts. Endogenous PPP1CC2 was also shown to coimmunoprecipitate with endogenous AKAP4 in normozoospermic human spermatozoa by Western blot (Figure B.4 B right panel). However, the signal was weak. This was expected since AKAP4 is present in the insoluble fraction of the spermatozoa and is very resistant to extraction (Figure B.4 B left panel). Additionally, we also showed that the amount of AKAP4 in

asthenozoospermic samples (AZ) was reduced compared with normozoospermic samples (NZ) (Figure B.4 B, left panel). To further confirm the interaction between PPP1CC2 and AKAP4, endogenous immunoprecipitated AKAP4 from human spermatozoa was also found to directly interact with PPP1CC2 by blot overlay (Figure B.4 C). In addition, and particularly relevant to PIPs, the canonical PPP1 binding motif RVxF was detected by bioinformatics analysis, comprising a region within amino acids 40-44 of human AKAP4 protein, ^{40}FCIVK^{44}. We also examined the localization of those proteins in human spermatozoa. Double immunolabeling experiments demonstrated co-localization of PPP1CC2 and AKAP4 in the human sperm flagellum (Figure B.4 C). A co-localization in the flagellum was detected in 97% of the cells (100 cells in each independent experiment were scored), which supports the role of these proteins in motility.

Table B.2 – Peptides identified by Orbitrap XL mass spectrometry for AKAP4 and PPP1CC, after immunoprecipitation of human spermatozoa samples with rabbit anti-PPP1CC2 antibody.

Sequence	Modified sequence	Start	End	Score	Id threshold
AKAP4 (Accession Q5JQC9)					
VGDTEGEYHR	NH2-VGDTEGEYHR-COOH	140	149	75	31
				44	31
NTNNNQSPSAPPAKPPSTQR	NH2-NTNNNQSPSAPPAKPPSTQR-COOH	184	203	65	34
				86	34
LSSLVIQMAHK	NH2-LSSLVIQM<Mox>AHK-COOH	224	234	40	34
NLHNITGVLMTDSDFVSAVK	NH2-NLHNITGVLM<Mox>TDSDFVSAVK-COOH	389	408	54	34
QNATDIMEAMLK	NH2-QNATDIM<Mox>EAM<Mox>LK-COOH	417	428	53	33
RLVSALIGEEK	NH2-RLVSALIGEEK-COOH	429	439	54	32
LVSALIGEEK	NH2-LVSALIGEEK-COOH	430		76	34
SQSLSYASLK	NH2-SQSLSYASLK-COOH	443	452	49	34
NQSLEFSTMK	NH2-NQSLEFSTM<Mox>K-COOH	462	471	64	32
VGEHILK	NH2-VGEHILK-COOH	496	502	42	31
LIQYHLTQQTK	NH2-LIQYHLTQQTK-COOH	551	561	77	33
MDMSNIVLMLIQK	NH2-M<Mox>DM<Mox>SNIVLM<Mox>LIQK-COOH	624	636	75	34
YSNDGAALAELEEQAASANKPNFR	NH2-YSNDGAALAELEEQAASANKPNFR-COOH	714	737	59	32
ERQPDEAVGK	NH2-ERQPDEAVGK-COOH	831	840	64	34
PPP1CC (Accession P36873)					
ADLDKLNIDSIIQR	Ace-ADLDKLNIDSIIQR-COOH	2	15	100	33
NVQLQENEIR	NH2-NVQLQENEIR-COOH	27	36	71	35
EIFLSQPILLELEAPLK	NH2-EIFLSQPILLELEAPLK-COOH	44	60	116	25
IKYPENFFLLR	NH2-IKYPENFFLLR-COOH	112	122	34	31
YPENFFLLR	NH2-YPENFFLLR-COOH	114		55	34
AHQVVEDGYEFFAK	NH2-AHQVVEDGYEFFAK-COOH	247	260	68	33

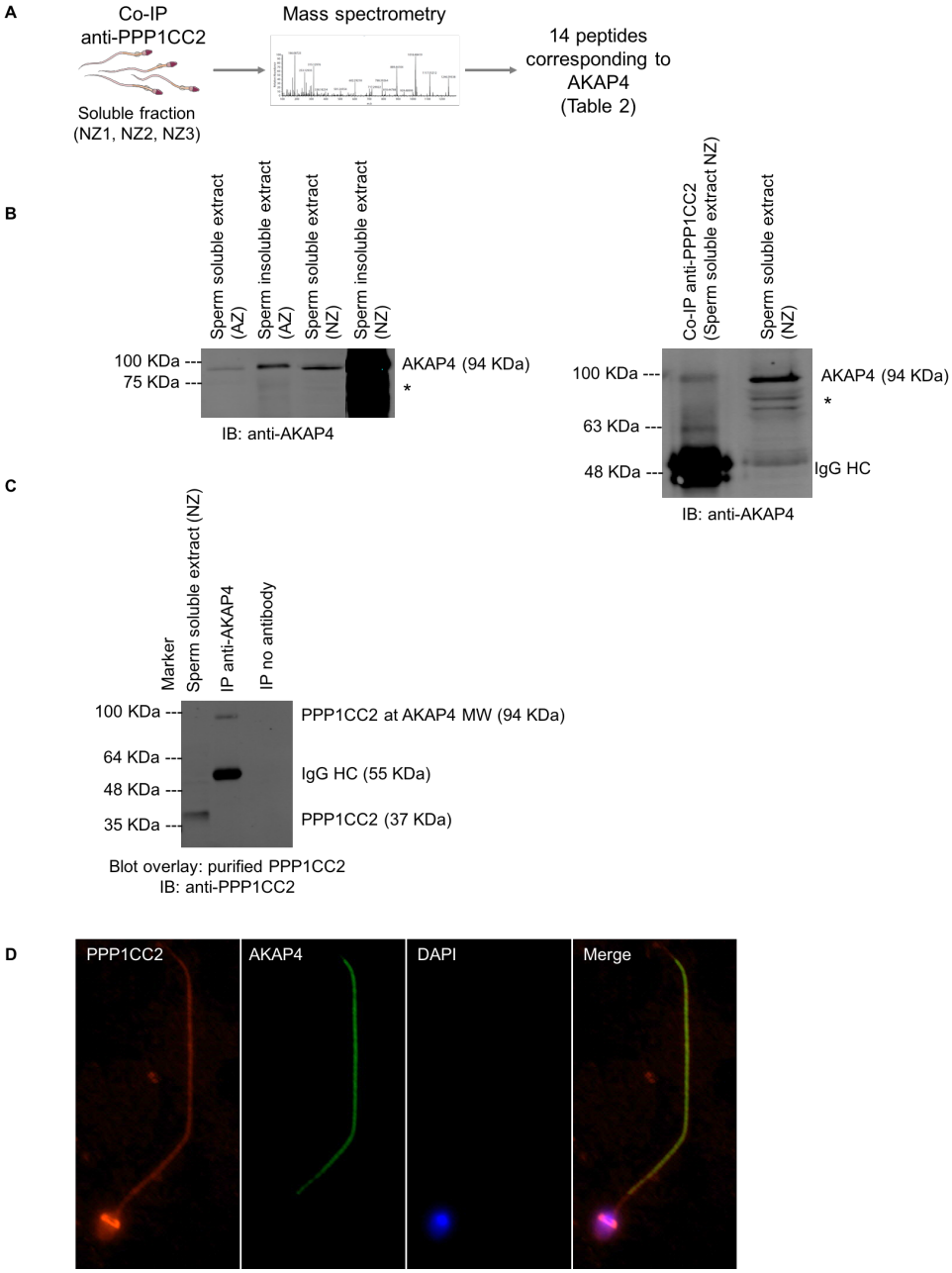

Figure B.4 – PPP1CC2 and AKAP4 interact in human spermatozoa. (A) Co-immunoprecipitation, using an isoform-specific anti-PPP1CC2 antibody from ejaculated normozoospermic (NZ) sperm samples, followed by mass spectrometry analysis identified 14 peptides that matched AKAP4 (see Table 2). (B) Left panel - Western blot analysis of AKAP4 expression in both soluble and insoluble fractions of ejaculated asthenozoospermic (AZ) and NZ sperm samples; Sperm preparations corresponding to 5x106 cells were loaded in the lanes. Right panel – Soluble sperm extract was co-immunoprecipitated with anti-PPP1CC2 antibody and immunoblotted with anti-AKAP4 antibody. Sperm soluble extract preparation corresponding to 10x106 cells was also loaded. (C) Human sperm soluble extract was immunoprecipitated with anti-AKAP4 antibody or no primary antibody (No Ab) in control and extracts were run on SDS-PAGE gels. Prior to immunoblot with anti-PPP1CC2 antibody the membrane was overlaid with recombinant PPP1CC2. Image is representative from three independent experiments. Sperm soluble extract preparation corresponding to 5x106 cells was also loaded. (D) Co-localization of PPP1CC2 and AKAP4 in human spermatozoa was demonstrated by dual fluorescence staining (PPP1CC2 with Texas Red staining and AKAP4 with FITC staining). Double labeling of human spermatozoa revealed co-localization of PPP1CC2 and AKAP4 over the flagellum. Nucleus was stained with DAPI. Negative controls with the secondary antibodies alone were performed and presented no reactivity (data not shown). Images are representative from three independent experiments. Co-IP, co-immunoprecipitation; IP, immunoprecipitation; IB, immunoblot; HC, heavy chain; NZ, normozoospermic; AZ, asthenozoospermic. Note that anti-AKAP4 antibody has a reported unspecific band at approximately 72 KDa (*).

3.1.5. Discussion

In this study, we characterized the interactome of PPP1CC2 in human testis and spermatozoa using a tissue-specific network-based approach. This methodology led to the identification of functional relationships between proteins associated with male reproductive functions and new candidates, currently poorly explored, such as AKAP4, that might be involved in PPP1CC2-based regulation of male fertility.

Tissue-specific gene expression results in the presence or absence of certain protein complexes leading to functional implications. Of the 313 direct PPP1CC/PPP1CC2 interactors identified from several sources (PPI databases, literature search, substrates and Y2H), 10 were identified as highly specific to or strongly expressed in the testis in at least two databases (AKAP4, PGK2, TSKS, TSSK1B, YBX2, SPZ1, NEK2, C9orf50, GLB1L and PPP1R2P9). A PubMed search revealed that 7 of those PPP1CC interactors had been previously studied in the context of male fertility, strengthening our approach. AKAP4, a testis-specific protein transcribed only in the postmeiotic phase of spermatogenesis, is the major fibrous sheath protein of the principle piece of sperm flagellum involved in motility regulation [39]. PGK2 is a glycolytic enzyme that is not required for the completion of spermatogenesis, but is essential for sperm motility [40]. TSKS mediates the interaction between PPP1CC2 and TSSK1B and has been proposed to play a critical role in the completion of spermatogenesis [41]. YBX2 was proposed as a PPP1CC2 substrate in testis [23] and its depletion leads to spermatogenic arrest due to incomplete nuclear condensation in spermatids [42]. SPZ1 was identified as a specific binding partner of PPP1CC2 isoform in testis [16]. NEK2 has been shown to be involved in chromosome condensation during the first meiotic division [43–45].

Functional relationships can be neglected when considering only tissue-specific proteins [46]. We addressed this challenge by integrating tissue-specific proteins with their interacting proteins to construct a testis/sperm-enriched network. By generating such a network, we can effectively represent the diversity of tissue-specific protein functions. However, this study presents limitations since the knowledge of protein tissue distribution is still quite limited and the databases do not take into consideration tissue-specific alternative splicing products from a single gene, which is particularly relevant in the testis [47]. From the PPI data, including the HIPPIE database, Y2H data and literature search results, we selected the 616 testis-enriched proteins direct interactions and then captured inner connections between these proteins. A total of 1,778 proteins and 32,187 interactions between them were identified in the testis/sperm-enriched network. In the testis/sperm-enriched network PPP1CC had 106 nearest neighbors (Figure B.1).

Since *k*-cores represent the densest parts of networks, they play an important role in the structure and dynamics of complex network systems. It can provide insights into the members of functional

modules interacting more tightly with each other, since most interacting proteins in protein complexes share similar functions [48]. Most testis-specific proteins are located at the periphery of the network. In the maximum *k*-core subgraph in which each node has at least *k*=44 connectivity, only RPL10L and HSPA1L remained in the core part (Supplementary Table D.4 B). HSPA1L is a testis-specific heat shock protein chaperone present in the human sperm surface, suggested to be involved in binding to the zona-pellucida [49]. RPL10L, previously reported to be expressed exclusively in the testis [50], is a ribosomal protein involved in spermatogenesis.

Community is another important feature of network structure. Nodes in a community are more highly inter-connected to each other than to nodes out of the community and are usually involved in the same function, for instance, the communities in PPI networks are identified as functional modules [51]. We identified community structures in the network without taking into account overlapping by use of a modularity matrix following the method in reference [38] (Supplementary Table D.4 B). Seven modules were identified in the testis/sperm-enriched network. PPP1 interactors in each module are represented in Figure B.1. Changes that occur during spermatogenesis require transcription, translation and post-translational modifications of numerous ubiquitous and germ cell-specific products, and those processes appear to be regulated by the highly interconnected proteins in modules 5, 2 and 1, respectively. Additionally, alternative splicing regulation has been particularly relevant in testis and module 6 reflects the relevance of this process in the testis/sperm-enriched network [47].

Two decades ago, scientists started paying attention not only to the role of PPP1CC2 in spermatogenesis, but also to a prominent role of PPP1CC2 in the regulation of sperm motility [5,6,9,11]. We explored the biological functionalities of proteins in the PPI network based on GO term search and phenotype analysis and constructed PPP1CC-centric spermatogenesis and sperm motility subnetworks (Figure B.2 and Figure B.3). In the PPP1CC-centric spermatogenesis subnetwork, we had 16 direct connections to PPP1CC (Figure B.2). From those, only SPZ1, TSKS, TSSK1B, YBX2 and YWHAZ were already described in the literature as potentially involved in spermatogenesis (for review see [10]). Future studies on the other spermatogenesis-associated interactors presented in Figure B.2 can increase the knowledge on PPP1CC2 function in spermatogenesis and uncover new key players in the multifactorial regulation of this process. For instance the subnetwork showed that, TSSK1B, YBX2, HSPA4, TRIM28, RANBP9 and CDK2 were specifically involved in spermiogenesis (Figure B.2). Interestingly, targeted disruption of mouse *Ppp1cc* gene results in male infertility due to aberrant spermiogenesis.

In the PPP1CC-centric motility subnetwork, PPP1CC had 50 direct connections. As shown in Figure B.3, motility-related PPP1CC interactors were highly interconnected and many of them

were in the core part (k=44) of the testis/sperm-enriched network (Supplementary Table D.4 C). The large number of PPP1CC interactors involved in motility-associated categories emphasizes the role of this protein in regulating this function. We identified several previously uncharacterized interactors, such as, LMNA, JAK2, RIPK3, PGK2, CSNK2B, CDK1 and RAF1, as players in this process (Figure B.3). One of the most intriguing interactors resulting from the analysis of the PPP1CC-centric motility subnetwork was AKAP4: (1) testis/sperm-specific protein, (2) involved in all major motility-related annotations and (3) related to a motility-related infertility phenotype. The *Akap4* knockout mice revealed that AKAP4 is not involved in spermatogenesis, but sperm failed to show progressive motility [39]. Miki and colleagues concluded that effective sperm motility is lost in the absence of AKAP4 because signal transduction enzymes fail to become associated with the fibrous sheath. In fact, The *Akap4* gene knockout mice present a significant increase in the activity and decrease in phosphorylation of PPP1CC2 in spermatozoa [52]. Here we show for the first time, the interaction between AKAP4 and PPP1CC2 in human spermatozoa and their co-localization in the sperm flagellum (Figure B.4). We speculate that AKAP4 may recruit PPP1CC2 to the fibrous sheath regulating the catalytic activity of PPP1CC22 by modulating its ability to interact with other proteins. Additionally, AKAP4 was previously shown to suffer changes in its phosphorylation status during the spermatozoa epididymal maturation [53] which may be, in turn, regulated by PPP1CC2. AKAP220/AKAP11 was previously described as a direct interactor and a competitive inhibitor PPP1 [54].

Blocking motility-related PPP1CC2-PIP interactions, such as PPP1CC2/AKAP4, during the epididymal transit will potentially generate active PPP1 that efficiently dephosphorylates a subset of substrates, preventing motility acquisition, which represents good contraceptive targets. An attractive approach to modulate PPP1 activity is to target specific interfaces between PPP1 and tissue/event-specific PIPs, disrupting their interaction. One of these interfaces, which occur in AKAP4, is the RVxF-motif, which binds to a domain on PPP1 that is remote from the active site. Synthetic peptides that contain variants of the RVxF motif were reported to disrupt a subset of PIP–PPP1 complexes *in vitro* [55,56].

3.1.6. References

1. Uhlén, M. *et al.* Tissue-based map of the human proteome. (2015). doi:10.1126/science.1260419
2. Fardilha, M., Esteves, S. L. C., Korrodi-Gregório, L., da Cruz e Silva, O. A. B. & da Cruz e Silva, F. F. The physiological relevance of protein phosphatase 1 and its interacting proteins to health and disease. *Curr. Med. Chem.* 17, 3996–4017 (2010).
3. Korrodi-Gregório, L., Esteves, S. L. C. & Fardilha, M. Protein phosphatase 1 catalytic isoforms: specificity toward interacting proteins. *Transl. Res.* 164, 366–91 (2014).
4. Fardilha, M., Ferreira, M., Pelech, S., Vieira, S., Rebelo, S., Korrodi-Gregorio, L., Sousa, M., Barros, A., Silva, V., da Cruz E Silva, O. a B. & da Cruz E Silva, E. F. 'OMICS' of Human Sperm: Profiling Protein Phosphatases. *OMICS* 17, 460–472 (2013).
5. Fardilha, M., Esteves, S. L. C., Korrodi-Gregório, L., Vintém, A. P., Domingues, S. C., Rebelo, S., Morrice, N., Cohen, P. T. W., Da Cruz E Silva, O. A. B. & Da Cruz E Silva, E. F. Identification of the human testis protein phosphatase 1 interactome. in *Biochemical Pharmacology* 82, 1403–1415 (2011).
6. Varmuza, S., Jurisicova, A., Okano, K., Hudson, J., Boekelheide, K. & Shipp, E. B. Spermiogenesis is impaired in mice bearing a targeted mutation in the protein phosphatase 1cgamma gene. *Dev. Biol.* 205, 98–110 (1999).
7. Sinha, N., Pilder, S. & Vijayaraghavan, S. Significant Expression Levels of Transgenic PPP1CC2 in Testis and Sperm Are Required to Overcome the Male Infertility Phenotype of Ppp1cc Null Mice. *PLoS One* 7, (2012).
8. Vijayaraghavan, S., Stephens, D. T., Trautman, K., Smith, G. D., Khatra, B., da Cruz e Silva, E. F. & Greengard, P. Sperm motility development in the epididymis is associated with decreased glycogen synthase kinase-3 and protein phosphatase 1 activity. *Biol. Reprod.* 54, 709–718 (1996).
9. Smith, G. D., Wolf, D. P., Trautman, K. C., da Cruz e Silva, E. F., Greengard, P. & Vijayaraghavan, S. Primate sperm contain protein phosphatase 1, a biochemical mediator of motility. *Biol. Reprod.* 54, 719–727 (1996).
10. Silva, J. V, Freitas, M. J. & Fardilha, M. Phosphoprotein phosphatase 1 complexes in spermatogenesis. *Curr. Mol. Pharmacol.* 7, 136–46 (2014).
11. Fardilha, M., Esteves, S. L. C., Korrodi-Gregório, L., Pelech, S., da Cruz e Silva, O. A. B. & da Cruz e Silva, E. Protein phosphatase 1 complexes modulate sperm motility and present novel targets for male infertility. *Molecular Human Reproduction* 17, 466–477 (2011).
12. Heroes, E., Lesage, B., Görnemann, J., Beullens, M., Van Meervelt, L. & Bollen, M. The PP1 binding code: A molecular-lego strategy that governs specificity. *FEBS Journal* 280, 584–595 (2013).
13. Virshup, D. M. & Shenolikar, S. From Promiscuity to Precision: Protein Phosphatases Get a Makeover. *Molecular Cell* 33, 537–545 (2009).
14. Trinkle-Mulcahy, L., Andersen, J., Yun, W. L., Moorhead, G., Mann, M. & Lamond, A. I. Repo-Man recruits PP1?? to chromatin and is essential for cell viability. *J. Cell Biol.* 172, 679–692 (2006).
15. Terry-Lorenzo, R. T., Carmody, L. C., Voltz, J. W., Connor, J. H., Li, S., Donelson Smith, F., Milgram, S. L., Colbran, R. J. & Shenolikar, S. The neuronal actin-binding proteins, neurabin I and neurabin II, recruit specific isoforms of protein phosphatase-1 catalytic subunits. *J. Biol. Chem.* 277, 27716–27724 (2002).
16. Hrabchak, C. & Varmuza, S. Identification of the spermatogenic zip protein Spz1 as a putative protein phosphatase-1 (PP1) regulatory protein that specifically binds the PP1c??2 splice variant in mouse testis. *J. Biol. Chem.* 279, 37079–37086 (2004).
17. Hrabchak, C., Henderson, H. & Varmuza, S. A testis specific isoform of endophilin B1, endophilin B1t, interacts specifically with protein phosphatase-1c??2 in mouse testis and is abnormally expressed in PP1c?? Null Mice. *Biochemistry* 46, 4635–4644 (2007).
18. Terrak, M., Kerff, F., Langsetmo, K., Tao, T. & Dominguez, R. Structural basis of protein phosphatase 1 regulation. *Nature* 429, 780–784 (2004).
19. Cohen, P. T. W. Protein phosphatase 1--targeted in many directions. *J. Cell Sci.* 115, 241–256 (2002).
20. Prassas, I., Chrystoja, C. C., Makawita, S. & Diamandis, E. P. Bioinformatic identification of proteins with tissue-specific expression for biomarker discovery. *BMC Med.* 10, 39 (2012).

21. Schaefer, M. H., Fontaine, J. F., Vinayagam, A., Porras, P., Wanker, E. E. & Andrade-Navarro, M. A. Hippie: Integrating protein interaction networks with experiment based quality scores. *PLoS One* 7, (2012).
22. Henderson, H., Macleod, G., Hrabchak, C. & Varmuza, S. New candidate targets of protein phosphatase-1c-gamma-2 in mouse testis revealed by a differential phosphoproteome analysis. *Int. J. Androl.* 34, 339–351 (2011).
23. MacLeod, G., Taylor, P., Mastropaolo, L. & Varmuza, S. Comparative phosphoproteomic analysis of the mouse testis reveals changes in phosphopeptide abundance in response to Ppp1cc deletion. *EuPA Open Proteomics* 2, 1–16 (2014).
24. Gellert, P., Jenniches, K., Braun, T. & Uchida, S. C-It: A knowledge database for tissue-enriched genes. *Bioinformatics* 26, 2328–2333 (2010).
25. Wheeler, D. L., Church, D. M., Federhen, S., Lash, A. E., Madden, T. L., Pontius, J. U., Schuler, G. D., Schriml, L. M., Sequeira, E., Tatusova, T. A. & Wagner, L. Database resources of the national center for biotechnology. *Nucleic Acids Research* 31, 28–33 (2003).
26. Liu, X., Yu, X., Zack, D. J., Zhu, H. & Qian, J. TiGER: a database for tissue-specific gene expression and regulation. *BMC Bioinformatics* 9, 271 (2008).
27. Yang, X., Ye, Y., Wang, G., Huang, H., Yu, D. & Liang, S. VeryGene: linking tissue-specific genes to diseases, drugs, and beyond for knowledge discovery. *Physiol. Genomics* 43, 457–460 (2011).
28. Dennis, G., Sherman, B. T., Hosack, D. A., Yang, J., Gao, W., Lane, H. C. & Lempicki, R. A. DAVID: Database for Annotation, Visualization, and Integrated Discovery. *Genome Biol.* 4, P3 (2003).
29. Bult, C. J., Kadin, J. A., Richardson, J. E., Blake, J. A. & Eppig, J. T. The mouse genome database: Enhancements and updates. *Nucleic Acids Res.* 38, D586–92 (2009).
30. Sigrist, C. J. A., De Castro, E., Cerutti, L., Cuche, B. A., Hulo, N., Bridge, A., Bougueleret, L. & Xenarios, I. New and continuing developments at PROSITE. *Nucleic Acids Res.* 41, (2013).
31. Edition, F. Examination and processing of human semen. *World Health* Edition, F, 286 (2010).
32. da Cruz e Silva, E. F., Fox, C. A., Ouimet, C. C., Gustafson, E., Watson, S. J. & Greengard, P. Differential expression of protein phosphatase 1 isoforms in mammalian brain. *J Neurosci* 15, 3375–3389 (1995).
33. Watanabe, T., da Cruz e Silva, E. F., Huang, H. B., Starkova, N., Kwon, Y. G., Horiuchi, A., Greengard, P. & Nairn, A. C. Preparation and characterization of recombinant protein phosphatase 1. *Methods Enzym.* 366, 321–338 (2003).
34. Ghesquière, B., Colaert, N., Helsens, K., Dejager, L., Vanhaute, C., Verleysen, K., Kas, K., Timmerman, E., Goethals, M., Libert, C., Vandekerckhove, J. & Gevaert, K. In vitro and in vivo protein-bound tyrosine nitration characterized by diagonal chromatography. *Mol. Cell. Proteomics* 8, 2642–2652 (2009).
35. Silva, J. V., Korrodi-Gregório, L., Luers, G., Cardoso, M. J., Patrício, A., Maia, N., da Cruz E Silva, E. F. & Fardilha, M. Characterisation of several ankyrin repeat protein variant 2, a phosphoprotein phosphatase 1-interacting protein, in testis and spermatozoa. *Reprod. Fertil. Dev.* (2015). doi:10.1071/RD14303
36. Dorogovtsev, S. N. Lectures on Complex Networks. *University of Aveiro* (2010). doi:10.1093/acprof:oso/9780199548927.001.0001
37. Chalupa, J., Leath, P. L. & Reich, G. R. Bootstrap percolation on a Bethe lattice. *Journal of Physics C: Solid State Physics* 12, L31–L35 (2001).
38. Newman, M. E. J. Modularity and community structure in networks. *Proc. Natl. Acad. Sci. U. S. A.* 103, 8577–8582 (2006).
39. Miki, K., Willis, W. D., Brown, P. R., Goulding, E. H., Fulcher, K. D. & Eddy, E. M. Targeted disruption of the Akap4 gene causes defects in sperm flagellum and motility. *Dev. Biol.* 248, 331–342 (2002).
40. Danshina, P. V, Geyer, C. B., Dai, Q., Goulding, E. H., Willis, W. D., Kitto, G. B., McCarrey, J. R., Eddy, E. M. & O'Brien, D. A. Phosphoglycerate kinase 2 (PGK2) is essential for sperm function and male fertility in mice. *Biol. Reprod.* 82, 136–145 (2010).
41. MacLeod, G., Shang, P., Booth, G. T., Mastropaolo, L. A., Manafpoursakha, N., Vogl, A. W. & Varmuza, S. PPP1CC2 can form a kinase/phosphatase complex with the testis-specific proteins

TSSK1 and TSKS in the mouse testis. *Reproduction* 147, 1–12 (2014).

42. Yang, J., Morales, C. R., Medvedev, S., Schultz, R. M. & Hecht, N. B. In the absence of the mouse DNA/RNA-binding protein MSY2, messenger RNA instability leads to spermatogenic arrest. *Biol. Reprod.* 76, 48–54 (2007).
43. Di Agostino, S., Rossi, P., Geremia, R. & Sette, C. The MAPK pathway triggers activation of Nek2 during chromosome condensation in mouse spermatocytes. *Development* 129, 1715–1727 (2002).
44. Di Agostino, S., Fedele, M., Chieffi, P., Fusco, A., Rossi, P., Geremia, R. & Sette, C. Phosphorylation of high-mobility group protein A2 by Nek2 kinase during the first meiotic division in mouse spermatocytes. *Mol. Biol. Cell* 15, 1224–1232 (2004).
45. Fardilha, M., Wu, W., Sá, R., Fidalgo, S., Sousa, C., Mota, C., Da Cruz E Silva, O. A. B. & Da Cruz E Silva, E. F. Alternatively spliced protein variants as potential therapeutic targets for male infertility and contraception. in *Annals of the New York Academy of Sciences* 1030, 468–478 (2004).
46. Bossi, A. & Lehner, B. Tissue specificity and the human protein interaction network. *Mol. Syst. Biol.* 5, 260 (2009).
47. Elliott, D. J. & Grellscheid, S. N. Alternative RNA splicing regulation in the testis. *Reproduction* 132, 811–819 (2006).
48. Gavin, A.-C. *et al.* Functional organization of the yeast proteome by systematic analysis of protein complexes. *Nature* 415, 141–147 (2002).
49. Naaby-Hansen, S. & Herr, J. C. Heat shock proteins on the human sperm surface. *J. Reprod. Immunol.* 84, 32–40 (2010).
50. Uechi, T., Maeda, N., Tanaka, T. & Kenmochi, N. Functional second genes generated by retrotransposition of the X-linked ribosomal protein genes. *Nucleic Acids Research* 30, 5369–5375 (2002).
51. Jonsson, P. F., Cavanna, T., Zicha, D. & Bates, P. A. Cluster analysis of networks generated through homology: automatic identification of important protein communities involved in cancer metastasis. *BMC Bioinformatics* 7, 2 (2006).
52. Huang, Z., Somanath, P. R., Chakrabarti, R., Eddy, E. M. & Vijayaraghavan, S. Changes in intracellular distribution and activity of protein phosphatase PP1gamma2 and its regulating proteins in spermatozoa lacking AKAP4. *Biol. Reprod.* 72, 384–392 (2005).
53. Baker, M. A., Hetherington, L., Weinberg, A., Naumovski, N., Velkov, T., Pelzing, M., Dolman, S., Condina, M. R. & Aitken, R. J. Analysis of phosphopeptide changes as spermatozoa acquire functional competence in the epididymis demonstrates changes in the post-translational modification of Izumo1. *J. Proteome Res.* 11, 5252–64 (2012).
54. Schillace, R. V, Voltz, J. W., Sim, A. T., Shenolikar, S. & Scott, J. D. Multiple interactions within the AKAP220 signaling complex contribute to protein phosphatase 1 regulation. *J. Biol. Chem.* 276, 12128–34 (2001).
55. Chatterjee, J., Beullens, M., Sukackaite, R., Qian, J., Lesage, B., Hart, D. J., Bollen, M. & Köhn, M. Development of a peptide that selectively activates protein phosphatase-1 in living cells. *Angew. Chemie - Int. Ed.* 51, 10054–10059 (2012).
56. Tappan, E. & Chamberlin, A. R. Activation of Protein Phosphatase 1 by a Small Molecule Designed to Bind to the Enzyme's Regulatory Site. *Chem. Biol.* 15, 167–174 (2008).
57. Wang, R., Kaul, A. & Sperry, A. O. TLRR (lrrc67) interacts with PP1 and is associated with a cytoskeletal complex in the testis. *Biol. Cell* 102, 173–189 (2010).
58. Wang, G. *et al.* In-depth proteomic analysis of the human sperm reveals complex protein compositions. *J. Proteomics* 79, 114–122 (2013).
59. MacLeod, G. & Varmuza, S. Tandem affinity purification in transgenic mouse embryonic stem cells identifies DDOST as a novel PPP1CC2 interacting protein. *Biochemistry* 51, 9678–9688 (2012).
60. Huang, Z., Khatra, B., Bollen, M., Carr, D. W. & Vijayaraghavan, S. Sperm PP1gamma2 is regulated by a homologue of the yeast protein phosphatase binding protein sds22. *Biol. Reprod.* 67, 1936–1942 (2002).
61. Cheng, L., Pilder, S., Nairn, A. C., Ramdas, S. & Vijayaraghavan, S. PP1??2 and PPP1R11 are parts of a multimeric complex in developing testicular germ cells in which their steady state levels are reciprocally related. *PLoS One* 4, (2009).
62. Puri, P., Myers, K., Kline, D. & Vijayaraghavan, S. Proteomic analysis of bovine sperm YWHA

binding partners identify proteins involved in signaling and metabolism. *Biol. Reprod.* 79, 1183–1191 (2008).

63. Korrodi-Gregório, L., Vieira, S. I., Esteves, S. L. C., Silva, J. V, Freitas, M. J., Brauns, A.-K., Luers, G., Abrantes, J., Esteves, P. J., da Cruz E Silva, O. a B., Fardilha, M. & da Cruz E Silva, E. F. TCTEX1D4, a novel protein phosphatase 1 interactor: connecting the phosphatase to the microtubule network. *Biol. Open* 2, 453–65 (2013).
64. Korrodi-gregório, L., Ferreira, M., Vintém, A. P., Wu, W., Muller, T., Marcus, K., Vijayaraghavan, S., Brautigan, D. L., Odete, A. B., Fardilha, M. & Edgar, F. Identification and characterization of two distinct PPP1R2 isoforms in human spermatozoa. (2013). doi:10.1186/1471-2121-14-15
65. Korrodi-Gregório, L., Abrantes, J., Muller, T., Melo-Ferreira, J., Marcus, K., da Cruz E Silva, O. A., Fardilha, M. & Esteves, P. J. Not so pseudo: the evolutionary history of protein phosphatase 1 regulatory subunit 2 and related pseudogenes. *BMC Evol. Biol.* 13, 242 (2013).
66. Ruan, Y., Cheng, M., Ou, Y., Oko, R. & Van Der Hoorn, F. A. Ornithine decarboxylase antizyme Oaz3 modulates protein phosphatase activity. *J. Biol. Chem.* 286, 29417–29427 (2011).
67. Myers, K., Somanath, P. R., Berryman, M. & Vijayaraghavan, S. Identification of chloride intracellular channel proteins in spermatozoa. *FEBS Lett.* 566, 136–140 (2004).
68. Rotman, T., Etkovitz, N., Spiegel, A., Rubinstein, S. & Breitbart, H. Protein kinase A and protein kinase C(alpha)/PPP1CC2 play opposing roles in the regulation of phosphatidylinositol 3-kinase activation in bovine sperm. *Reproduction* 140, 43–56 (2010).
69. Browne, G. J., Fardilha, M., Oxenham, S. K., Wu, W., Helps, N. R., da Cruz E Silva, O. A. B., Cohen, P. T. W. & da Cruz E Silva, E. F. SARP, a new alternatively spliced protein phosphatase 1 and DNA interacting protein. *Biochem. J.* 402, 187–196 (2007).
70. Huang, Z. & Vijayaraghavan, S. Increased Phosphorylation of a Distinct Subcellular Pool of Protein Phosphatase, PP1 2, During Epididymal Sperm Maturation. *Biol. Reprod.* 70, 439–447 (2004).

3.2. Modulation of PPP1CC2/AKAP4 and PPP1CC2-specific interactions in spermatozoa using cell-penetrating peptides as a drug intracellular delivery system

Joana Vieira Silva[1], Sarah Jones[2], Maria João Freitas[1], John Howl[2] and Margarida Fardilha[1]

[1] Laboratory of Signal Transduction, Department of Medical Sciences, Institute of Biomedicine – iBiMED, University of Aveiro, 3810-193 Aveiro, Portugal.

[2] Molecular Pharmacology Group, University of Wolverhampton, Wolverhampton, UK.

Corresponding author: Margarida Fardilha, Departamento de Ciências Médicas, Universidade de Aveiro, Campus Universitário de Santiago, Agra do Crasto – Edifício 30, 3810-193 Aveiro, Portugal. T: +351-918143947. E: mfardilha@ua.pt

In the process to file a patent application

3.2.1. Abstract

The large number of unintended pregnancies worldwide highlights the need for new contraceptive methods. Still, modern and non-invasive contraceptives for men are not available. The mechanism of spermatozoa motility acquisition is a perfect target for a new male contraceptive since it affects only the post-testicular sperm maturation. Phosphoprotein phosphatase 1 catalytic subunit gamma 2 (PPP1CC2), a PPP1 isoform restricted to testicular germ cells and spermatozoa, is essential for sperm motility acquisition. In an effort to understand PPP1CC2 regulation in male germ cells, we have devoted efforts to characterize its interacting partners (PPP1 Interacting Proteins, PIPs). Protein-protein interactions (PPIs) are a promising class of drug targets. Cell penetrating peptides (CPPs) represent a widely recognized intracellular delivery system to target PPIs. In the present study, we designed peptide sequences capable of selectively disrupting PPP1-PIPs complexes as a strategy to modulate sperm motility. These endogenous sequences were covalently coupled to inert CPPs as sychnologically-organized bioportide constructs in order to affect intracellular delivery and potentially modulate PPP1 function. Herein, we demonstrate for the first time the potential of CPPs to deliver peptide sequences that target unique PPIs in spermatozoa. Specifically, a bioportide that mimics the unique 22 amino acid C-terminus of PPP1CC2, potentially compromising isoform-specific interactions, inhibited sperm motility. Additionally, a peptide sequence that mimics the interaction interface between PPP1CC2 and a sperm-specific PPI - AKAP4 - was also successfully delivered to sperm cells with an impact upon sperm motility.

3.2.2. Introduction

Despite currently available contraceptives, the world's population has risen to an alarming level, and overpopulation continues to be a significant contributor to environmental degradation and human suffering worldwide. It is estimated that half of all conceptions are unintended [1,2]. The contraceptive shortfall results in over 20% of pregnancies ending in abortion [3,4]. Furthermore, undesired pregnancies result in children who suffer from poverty and negligence. These statistics illustrates the urgent need to develop new male contraceptive methods to overcome uncontrolled fertility. Condom and vasectomy have been the main methods of male contraception and he development of new male contraceptives has focused upon hormonal modulation [5,6]. However the severe side effects have been an obstacle to this technology [7]. The mechanism of sperm motility is a perfect target for a new male contraceptive, since it allows normal hormone and spermatozoa production and affects only the post-testicular sperm maturation. The spermatozoon is a specialized cell virtually incapable of genetic expression. Any functional alteration (e.g. motility aquisition) in these cells depends on processes such as protein post-translational modifications (e.g. phosphorylation), or mechanisms based on the disruption/formation of protein complexes.

Phosphoprotein phosphatase 1 (PPP1) is a major serine/threonine phosphatase in eukaryotic cells [8,9]. PPP1CC2 is a testis-enriched and sperm specific-isoform, distributed along the entire flagellum [10,11,12]. The observation that PPP1C had a two-fold higher activity in immotile bovine caput epididymal sperm compared to mature motile caudal sperm is consistent with it being directly involved in sperm motility [10,11]. Moreover, inhibition of PPP1CC2 activity by okadaic acid or calyculin A induced and stimulated motility in caput and caudal sperm, respectively [10,11].

Regulation of PPP1 catalytic activity is mediated via binding to specific regulatory subunits, the PPP1 interacting proteins (PIPs) [13–18]. We previously characterized testis/sperm-enriched/specific PIPs by integrating tissue-specific protein-expression, PPI data and constructing a testis/sperm-specific network. We analyzed several topological properties of the network and specified the biological and physiological properties that allowed the identification of sperm-specific PPP1CC2 complexes potentially involved in sperm motility. Previously uncharacterized PIPs, such as A kinase anchor protein 4 (AKAP4, also called fibrous sheath component 1 or AKAP 82) were identified. AKAP4 is the major fibrous sheath protein of the principle piece of sperm flagellum. Absent or weak AKAP4-labelling seems to be associated with absent or weak sperm motility [19]. Additionally, AKAP4 and AKAP3 gene deletions were found in men with dysplasia of the fibrous sheath, which causes severe asthenozoospermia (reduced motility) or total immotility [20–22]. The male mice lacking AKAP4 were infertile, the motility of their sperm was poor, the principal piece of the flagellum was reduced in diameter, the fibrous sheath was incompletely developed, and other proteins usually found in the principal piece region of the flagellum were either absent or reduced in amount [23]. The *Akap4* gene knockout mice also presented a significant change in the activity and phosphorylation status of PPP1CC2 [24]. Besides reporting AKAP4 as a PPP1CC2 interactor in spermatozoa (see section 3.1.), we also described the presence of a canonical PPP1 binding motif RVxF in AKAP4. The interfaces between PPP1 and PIPs represent an excellent target for pharmacological intervention. Regarding PPP1, only a few *in vitro* studies used synthetic peptides (based on the RVxF motif) to disrupt the PPP1-PIP complex [25] and currently only two drugs (salubrinal e trichostatin A) modulate PPP1 complexes (for review see [8]). However, modulation of human spermatozoa physiology by synthetic peptides or small molecules that disrupt PPP1 complexes was never accomplished. The therapeutic targeting of PPIs with selective inhibitors is a widely recognized strategy [26]. However, the cellular bilayered lipid membrane is an obstacle for the development of therapeutic agents against intracellular targets. Cell penetrating peptides (CPPs) represent a very promising intracellular delivery system to target PPIs [27]. CPPs can efficiently traverse the lipid membrane and deliver a wide range of therapeutic moieties, including small drugs, more bulky proteins and oligonucleotides [28]. It was recently demonstrated that CPPs are able of translocate into the sperm cell without affecting its viability and motility [27].

The main goal of this study was to design and synthesize peptides capable of selectively disrupting PPP1-PIPs complexes. These endogenous sequences and structural analogues were coupled to inert CPPs in order to affect significant intracellular delivery and so modulate PPP1 function.

3.2.3. Methods

Microwave-assisted solid phase peptide synthesis

Peptide sequences derived from (a) the 22 amino acid C-terminus of the human PPP1CC2 (^{303}KPNATRPVTPPRVASGLNPSIQKASNYRNNTVLY^{336}) [PPP1CC2-CT], (b) the region including the PPP1 binding motif (^{40}KVICF^{44}) of the human AKAP4 (^{33}GQQDQDRKVICFVDVSTLNV^{52}) [AKAP4-BM] and (c) a mutated homologue (^{33}GQQDQDRAAAAAVDVSTLNV^{52}) [AKAP4-BM M] were synthesized using microwave-assisted solid-phase peptide synthesis. These endogenous sequences were coupled to a CPP – penetratin (RQIKIWFQNRRMKWKK) (Table B.3).

Microwave-assisted solid phase peptide synthesis was performed using a Discover SPS Microwave Peptide Synthsizer (CEM Microwave Technology Ltd, Buckingham, UK) with fibre optic temperature control. Peptides were synthesized (0.1 mmol scale) using Rink amide MBHA resins pre-loaded with the first amino acid (AnaSpec, Inc., Cambridge Bioscience Ltd, Cambridge, UK) and employed an N-α-Fmoc protection strategy with HCTU activation. Deprotection with 7 ml of 20 % piperidine was performed for 3 min at 50 W/75 °C A majority of AA coupling reactions were accomplished with a 4-fold molar excess of Fmoc-protected AA with HCTU and diisopropylethylamine (DIPEA), molar ratio of 1:1:2 (AA/HCTU/DIPEA), in 4 ml for 10 min at 25 W/75 °C. Arg coupling was performed in two stages: 30 min 0 W/~25 °C followed by 5 min at 17 W/75 °C. To reduce racemization of Cys and His, coupling conditions were 5 min at 0 W/~25 °C followed by 6 min at 17 W/50 °C with the hindered base collidine (TMP) at a molar ratio of 1:1:2 (AA/HCTU/TMP; [29]). Aspartimide formation was reduced by the substitution of piperidine for 5 % piperazine and 0.1 M 1-hydroxybenztriazole hydrate (HOBt) in the deprotection solution. Fluorescent peptides, to be used in cell imaging and quantitative uptake analyses, were synthesized by amino-terminal acylation with 6-carboxy-tetramethylrhodamine (TAMRA) (Novabiochem, Beeston, UK) as previously described [30]. Peptides were purified by semi-preparative scale high-performance liquid chromatography, and the predicted masses of all peptides were confirmed by matrix-assisted laser desorption ionization (MALDI) time of flight mass spectrometry. Sequences, abbreviations and masses of all peptides used in this study are shown in Table B.3.

Table B.3 – Peptide sequences, abbreviations and molecular masses. To enable both quantitative and qualitative uptake analysis, peptides were extended with TAMRA. Peptide masses (M+ H+) were confirmed by MALDI time of flight mass spectrometry. Underlined, penetratin (CPP); Bold, PPP1 binding motif (pattern: [RK]-X(0,1)-[VI]-{P}-[FW]). [1]The last amino acid of PPP1CC2 C-terminus (glutamic acid) was excluded due to its negative charge.

Peptide designation	Abbreviation	Peptide sequence	Mass (g/mol)
PPP1CC2 C-terminal [1]	PPP1CC2-CT	*NH_2-* RQIKIWFQNRRMKWKKKPNATRPVTPPRVASGLNPSI QKASNYRNNTVLY-*H*	5953,0124
AKAP4 binding motif	AKAP4-BM	*H-* KKWKMRRNQFWIKIQRVNLTSVAV**FCIVK**RDQDQQG *-NH_2*	4448,3148
AKAP4 binding motif mutant	AKAP4-BM M	*H-* KKWKMRRNQFWIKIQRVNLTSVAV**AAAAA**RDQDQQ G-*NH_2*	4212,9217

Semen samples

This study was approved by the Ethics and Internal Review Board of the Hospital Infante D. Pedro E.P.E. (Aveiro, Portugal) and was conducted in accordance with the ethical standards of the Helsinki Declaration. Human semen samples were obtained from a randomized group of donors, by masturbation to a sterile container. All donors signed informed consent allowing the samples to be used for scientific purposes. Basic semen analysis was performed according to World Health Organization (WHO) guidelines. Fresh semen from Holstein Frisian bulls was obtained from LusoGenes, LDA (Aveiro, Portugal). Semen was collected by artificial vagina and assessed by a certified veterinarian. Human and bovine spermatozoa were isolated and washed from seminal plasma by centrifugation (800 g for 5 min, 3 times) using ALLGrade Wash medium (LifeGlobal, Brussels, Belgium). Spermatozoa pellets were resuspended in medium to a final concentration of $20x10^6$ cells/0.5 mL and incubated at 37 °C with 5 % CO_2 until the appropriated treatments were added.

Microscopy evaluation of the intracellular accumulation of the peptides

Isolated bovine and human spermatozoa ($40x10^6$ cells) were resuspended and incubated with 10 μM TAMRA-labeled peptides for 1 h at 37 °C in a humidified atmosphere of 5 % CO_2. Cells were then washed three times (800 g for 5 min) in ALLGrade Wash medium (LigeGlobal, Brussels, Belgium). To confirm if the fluorescently labeled peptides were not merely surface associated, we divided the sperm cell population in two and used a trypsin incubation to remove any surface associated peptides. In summary, half of the cells were set aside ($20x10^6$ cells) and fixed in 4 % paraformaldehyde (PFA) for 20 min. The other half was incubated with 1 % (wt/vol) trypsin at 37 °C, collected by centrifugation at 3000 g, washed in ALLGrade Wash medium (LigeGlobal, Brussels, Belgium) and resuspended in 4 % PFA 20 min. Fixed cells from each preparation were spread into coverslips and allowed to air dry. After mounting, slides were assessed by fluorescence microscopy (Imager.Z1, Axio-Cam HRm camera and AxioVision software, Zeiss, Jena, Germany).

Quantitative analyses of the peptides translocation

Translocation efficacy of CPP-mediated intracellular delivery of the peptides sequences was determined by quantitative uptake analysis of fluorescently labeled moieties and based upon the method previously described by Holm et al. [31]. Isolated bovine and human spermatozoa were incubated with 10 μM TAMRA-labeled peptides for 1 h at 37 °C in a humidified atmosphere of 5 % CO_2. Cells were then washed four times with PBS, detached with 1 % (w/v) trypsin at 37 °C, collected by centrifugation at 3000 g and lysed in 300 μl 0.1 M NaOH for 2 h on ice. 250 μl of each sample cell lysate were transferred to a black 96-well plate, and analyzed using an Infinite® 200 PRO (Tecan, Switzerland) (λAbs 544 nm/λEm 590 nm).

Cell viability assays

Bovine spermatozoa viability was evaluated using the trypan blue viability test according to manufacturer's guidelines. Human spermatozoa viability was measured using the CellTiter 96® AQueous Non-Radioactive Cell Proliferation Assay (Promega, Madison, USA) according to manufacturer's guidelines. The reduction of tetrazolium compounds has previously been used as a reliable and rigorous assessment of spermatozoa viability [32].

Motility assays

Media were prepared and peptides (PPP1CC2-CT, PPP1CC2-CT TAMRA, AKAP4 and AKAP4 M) were added to individual volumes. Bovine and human sperm cells were added to the media to give a total volume of 500 μl. Approximately, $20x10^6$ sperm cells per treatment/well were used. Control samples included sperm cells in media. The influence on sperm motility parameters was assessed using the Sperm Class Analyzer CASA System (Microptic S L, Barcelona, Spain) with SCA® v5.4 software. Samples and controls (2 μl) were loaded into individual chambers of Leja Standrat Count 8 chamber slide 20 μm depth (Leja Products B. V., The Netherlands) which were pre-heated at 37 °C. This temperature was maintained while at least 1000 sperm cells/per measurement were evaluated. Each peptide was tested on samples from 3 individual donors and all the conditions were performed in triplicate.

3.2.4. Results

Therefore, CPPs were used to deliver PPI disruptor peptide sequences into sperm cells aiming at affecting their motility. A peptide sequence that mimics the unique 22 amino acid C-terminus of PPP1CC2 (PPP1CC2-CT) and is conserved in both bovine and human was used to compromise the isoform-specific interactions between PPP1CC2 and its interactors. The AKAP4-BM peptide mimics the PPP1 binding motif RVxF in AKAP4 (^{40}KVICF^{44}), which is also conserved in both species, and was used to disrupt PPP1CC2-AKAP4 complexes. A peptide with a mutation in the

PPP1 binding motif of AKAP4 (AKAP4-BM M) was used as a control of the AKAP4-BM. A negative control (samples without any treatment) was used in all the experiments.

Peptides translocate into bovine and human spermatozoa

Fluorescent microscopy clearly revealed the intracellular accumulation of the peptides within bovine and human spermatozoa (Figure B.5). Quantitative uptake analyses also demonstrated a range of translocation efficacies amongst those peptides tested (Figure B.5, Supplementary Table D.8). To confirm that the fluorescently labeled peptides were not merely surface associated, peptide-treated spermatozoa were firstly incubated with high concentrations of exogenous trypsin that rapidly degrades polycationic peptides as previously described [33]. The microscopy analyses showed that the PPP1CC2-CT and AKAP4 BM peptides internalized very efficiently in both human and bovine spermatozoa, while the AKAP4 BM M peptide internalized less efficiently giving rise to a reduced florescent signal (Figure B.5). Quantitative comparison of the uptake efficacies (Figure B.5) was in accordance with the microscopic observations. The PPP1CC2-CT and AKAP4 BM peptides revealed higher cellular uptake, when compared to the AKAP4 BM M peptide, probably reflecting specific binding of PPP1CC2-CT and AKAP4 BM peptides after membrane translocation . The uptake of the peptides differed between species, with human spermatozoa revealing higher uptake of all the peptides when compared with bovine cells.

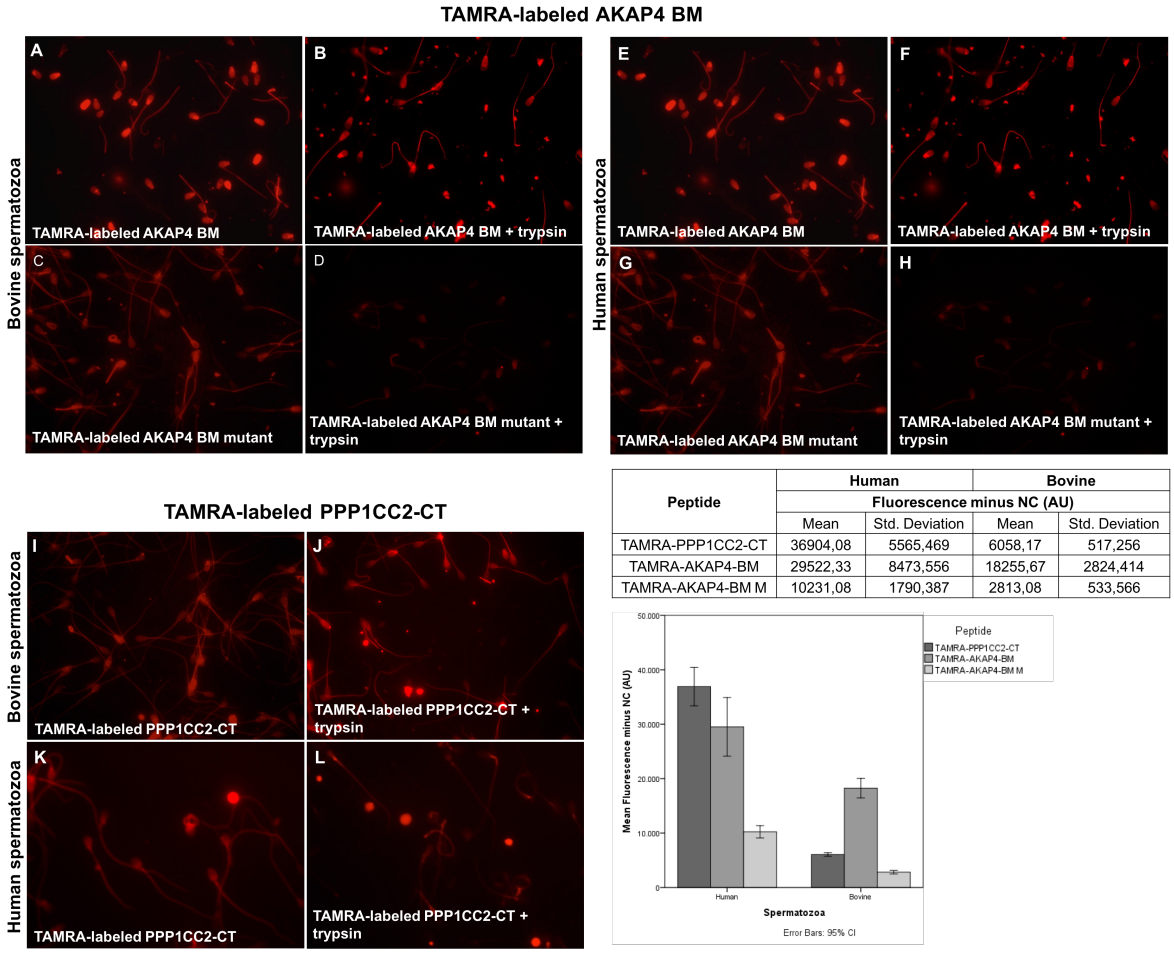

Peptide	Human		Bovine	
	Fluorescence minus NC (AU)			
	Mean	Std. Deviation	Mean	Std. Deviation
TAMRA-PPP1CC2-CT	36904,08	5565,469	6058,17	517,256
TAMRA-AKAP4-BM	29522,33	8473,556	18255,67	2824,414
TAMRA-AKAP4-BM M	10231,08	1790,387	2813,08	533,566

Figure B.5 – Intracellular accumulation of the TAMRA-labeled peptides. Upper panel and lower panel (left): To establish that the detected fluorescence was not attributed to surface-associated peptide, isolated sperm cells were incubated for 1h with 10 µM TAMRA-labeled peptide and subsequently treated with 1% (w/v) trypsin. Negative controls without the TAMRA-labeled peptides were performed and presented no reactivity (data not shown). Images are representative from three independent experiments. Lower panel (right): Quantitative analysis of peptide translocation into bovine and human spermatozoa. Bovine and human spermatozoa were incubated with TAMRA-labeled bioportides (10 µM) for 1 h at 37°C. Data are expressed as fluorescence (minus negative control). Three independent experiments were performed in quadruplicate. Error bars 95% CI.

Impact of the protein-protein interaction disruptor peptides on sperm motility

Bovine and human spermatozoa were exposed to different extracellular peptide concentrations (10 and 20 µM) and motility parameters were assessed at 1 and 2 h. For reference, negative controls were performed in the absence of peptides (Supplementary Table D.9 - D.15).

The percentage of viable spermatozoa was not significantly changed after treatment with peptides, except by the 2h incubation with the AKAP4-BM peptide where a slight decrease was observed (Figure B.7, Supplementary Table D-12).

PPP1CC2-CT peptide

Exposure of bovine spermatozoa to 10 µM PPP1CC2-CT induced a decrease in both fast (mean decrease at 1h of 55,9 ± 19,4%; at 2h 53,9 ± 19,9%; compared with negative control) and slow (mean decrease at 1h of 49,9 ± 41%; at 2h 17,4 ± 57%; compared with negative control) progressive motility. Incubation of bovine spermatozoa with 20 µM PPP1CC2-CT induced similar effects: decrease in both fast (mean decrease at 1h of 64,2 ± 8,3%; at 2h 44,6 ± 9,7%; compared with negative control) and slow (mean decrease at 1h of 31,4 ± 35%; compared with negative control) progressive motility. In contrast, immotile spermatozoa increased with both 10 µM (mean increase at 1h of 72,5 ± 33,6%; at 2h 128,3 ± 85,3%; compared with negative control) and 20 µM PPP1CC2-CT (mean increase at 1h of 86,2 ± 72,3%; at 2h 79,1 ± 37,0%; compared with negative control). No significant alterations were observed in non-progressive motility (Figure B.6, Supplementary Table D-11).

Both PPP1CC2-CT and TAMRA-PPP1CC2-CT induced a similar effect on sperm motility parameters (Figure B.6; Supplementary Table D-11), revealing that the fluorescent labelling did not affect significantly peptides action.

There were no significant differences between the concentrations tested (10 and 20 µM) for any motility parameter, suggesting that there was no concentration-dependent effect of the PPP1CC2-CT peptides for the concentrations tested.

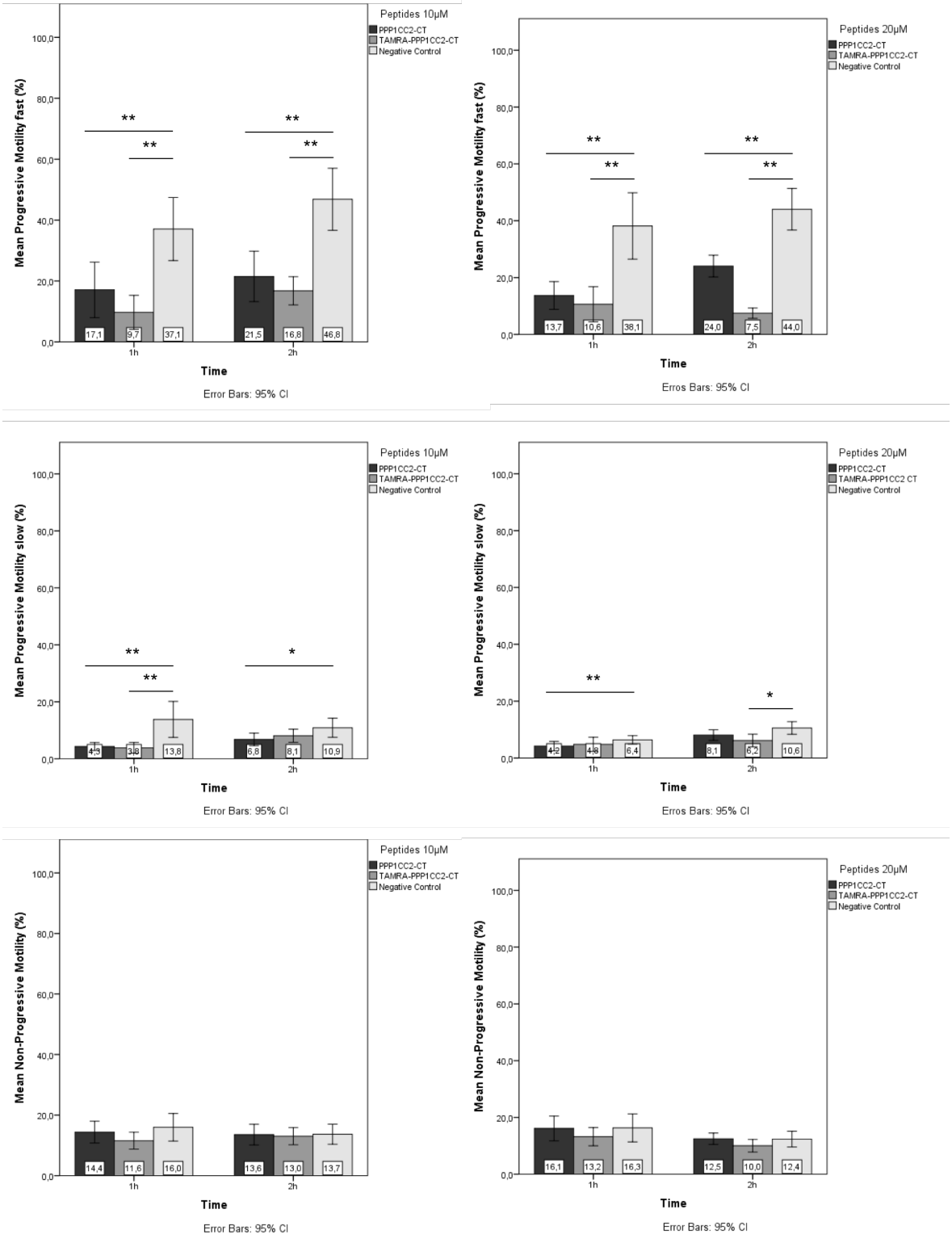

Figure B.6 – Impact of the PPP1CC2-CT peptides (PPP1CC2-CT and TAMRA-PPP1CC2-CT) treatment in bovine spermatozoa motility and viability parameters: (A) fast progressive motility; (B) slow progressive motility; (C) non-progressive motility; (D) immotile spermatozoa; and (E) viability. Graph bars represent the mean values of three independent experiments performed in triplicate. Error bars 95% CI. Statistically significant findings are indicated with a (*). * P<0.05; ** P<0.01.

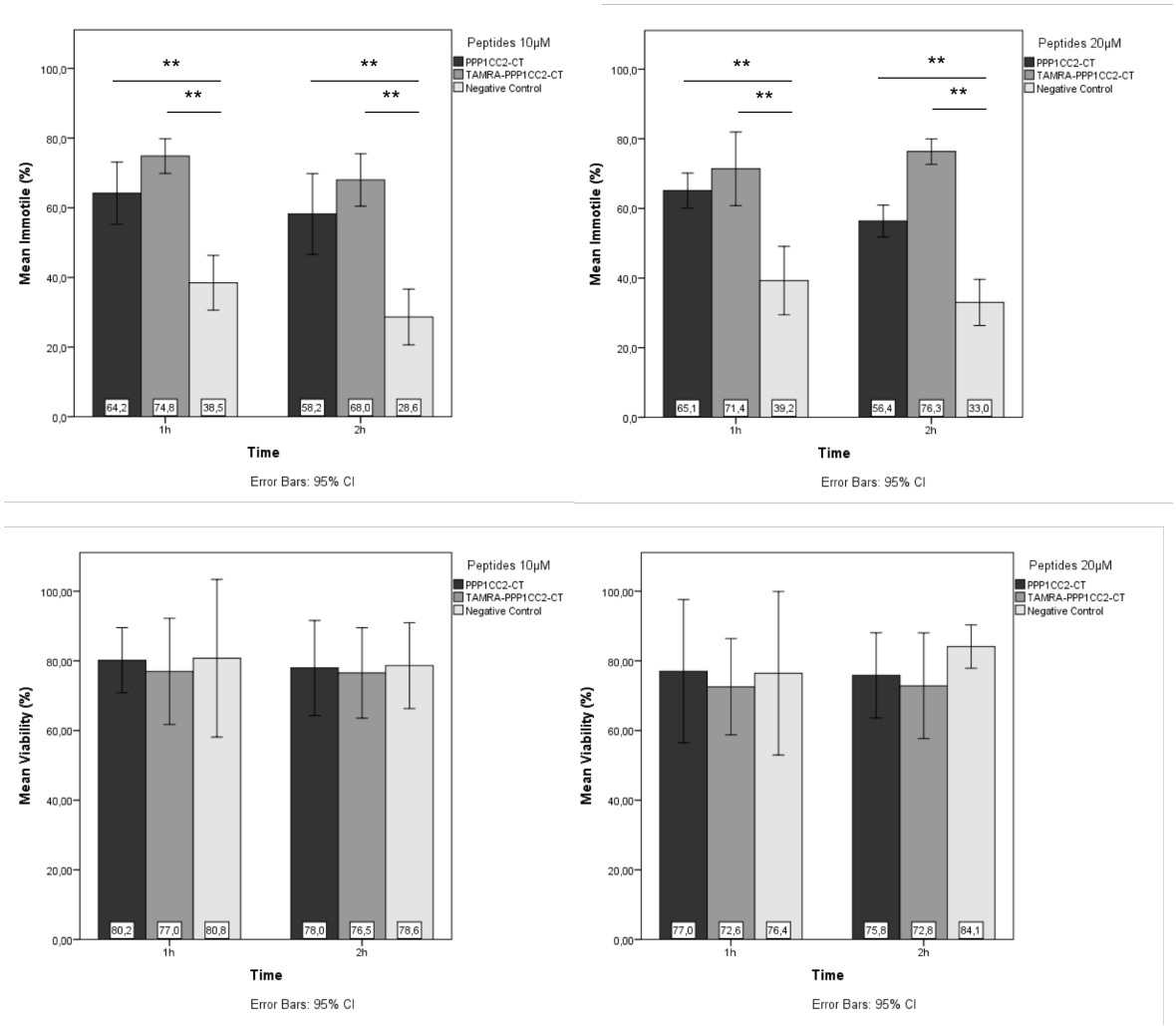

Figure B.6 – (continuation) Impact of the PPP1CC2-CT peptides (PPP1CC2-CT and TAMRA-PPP1CC2-CT) treatment in bovine spermatozoa motility and viability parameters: (A) fast progressive motility; (B) slow progressive motility; (C) non-progressive motility; (D) immotile spermatozoa; and (E) viability. Graph bars represent the mean values of three independent experiments performed in triplicate. Error bars 95% CI. Statistically significant findings are indicated with a (*). * P<0.05; ** P<0.01.

Exposure of human spermatozoa to 10 µM PPP1CC2-CT did not induced any significant alterations in the motility parameters (data not shown). Exposure 20 µM PPP1CC2-CT induced a decrease in fast progressive motility at 2h (mean decrease of 34,5 ± 12,3%; compared with negative control) (Supplementary Table D-14).

AKAP4-BM peptide

Exposure of bovine spermatozoa to 10 µM AKAP4-BM induced a decrease in both fast (mean decrease at 1h of 41,9 ± 20,0%; at 2h 43,9 ± 15,3%; compared with AKAP4-BM M; mean decrease at 1h of 49,8 ± 22,5%; at 2h 50,5 ± 9,7%; compared with negative control) and slow (mean

decrease at 2h 21,6 ± 64,4%; compared with AKAP4-BM M; mean decrease at 2h 42,4 ± 20,4%; compared with negative control) progressive motility. Incubation with 20 µM AKAP4-BM induced a decrease in both fast (mean decrease at 1h of 95,0 ± 6,5%; at 2h 98,4 ± 2,6%; compared with AKAP4-BM M; mean decrease at 1h of 95,7 ± 5,4%; at 2h 98,6 ± 2,9%; compared with negative control) and slow (mean decrease at 1h of 95,7 ± 4,7%; at 2h 94,1 ± 4,9%; compared with AKAP4-BM M; mean decrease at 1h of 95,3 ± 4,8%; at 2h 94,2 ± 4,8%; compared with negative control) progressive motility. In addition, exposure to 20 µM AKAP4-BM peptide led to a significant decrease in non-progressive motility (mean decrease at 1h of 63,1 ± 8,3%; at 2h 63,0 ± 7,5%; compared with AKAP4-BM M; mean decrease at 1h of 50,0 ± 10,9%; at 2h 59,4 ± 13,2%; compared with negative control). In contrast, immotile spermatozoa increased with both 10 µM (mean decrease at 1h of 49,9 ± 33,2%; at 2h 73,5 ± 43,3%; compared with AKAP4-BM M; mean decrease at 1h of 90,0 ± 51,4%; at 2h 91,8 ± 25,4%; compared with negative control) and 20 µM AKAP4-BM (mean decrease at 1h of 155,7 ± 46,1%; at 2h 123,2 ± 38,1%; compared with AKAP4-BM M; mean decrease at 1h of 91,8 ± 25,4%; at 2h 183,7 ± 88,4%; compared with negative control) (Figure B.7, Supplementary Table D-12). Application of the mutated AKAP4-BM did not lead to significant differences in motility parameters in bovine spermatozoa (compared with negative control), with two exceptions (fast progressive motility at 1h with 20 µM incubation and the percentage of immotile spermatozoa with 10 µM incubation at 1h) (Figure B.7, Supplementary Table D-12).

Upon exposure to the AKAP4-BM peptide, at both 1h and 2h, the progressive (fast and slow) and the non-progressive motility were higher at a lower peptide concentration (10 µM) compared with the higher concentration (20 µM), while the percentage of immotile spermatozoa was higher with 20 µM peptide incubation, suggesting a concentration-dependent effect for the concentrations tested.

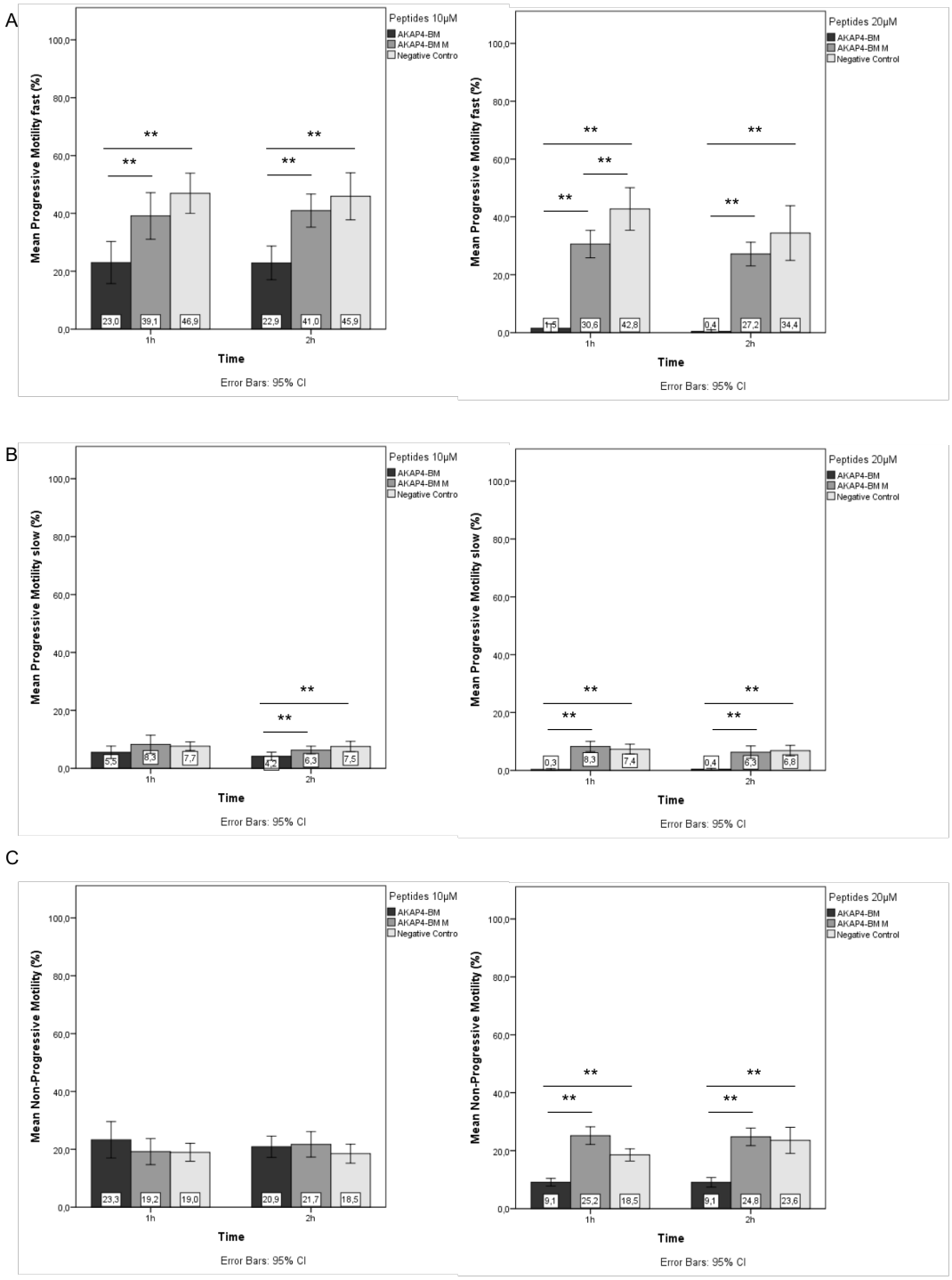

Figure B.7 – Impact of the AKAP4-BM peptides (AKAP4-BM and AKAP4-BM M) treatment in bovine spermatozoa motility and viability parameters: (A) fast progressive motility; (B) slow progressive motility; (C) non-progressive motility; (D) immotile spermatozoa; and (E) viability. Graph bars represent the mean values of three independent experiments performed in triplicate. Error bars 95% CI. Statistically significant findings are indicated with a (*). * P<0.05; ** P<0.01.

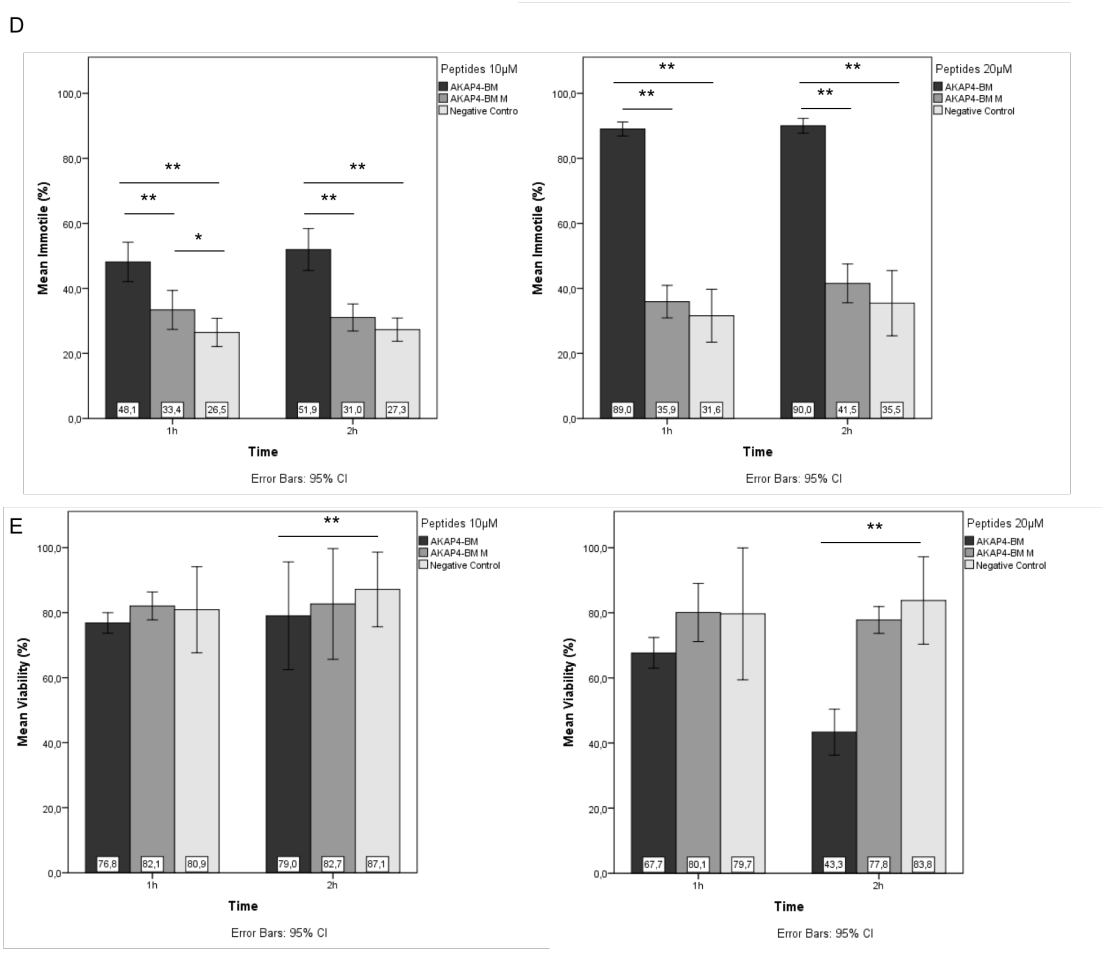

Figure B.7 – (continuation) Impact of the AKAP4-BM peptides (AKAP4-BM and AKAP4-BM M) treatment in bovine spermatozoa motility and viability parameters: (A) fast progressive motility; (B) slow progressive motility; (C) non-progressive motility; (D) immotile spermatozoa; and (E) viability. Graph bars represent the mean values of three independent experiments performed in triplicate. Error bars 95% CI. Statistically significant findings are indicated with a (*). * P<0.05; ** P<0.01.

Exposure of human spermatozoa to 20 µM AKAP4-BM induced significant alterations in the motility parameters (Figure B.8, Supplementary Table D-15). A decrease in both fast (mean decrease at 1h of 87,0 ± 4,3%; at 2h 82,7 ± 20,7%; compared with AKAP4-BM M; mean decrease at 1h of 49,8 ± 22,5%; at 2h 50,5 ± 9,7%; compared with negative control) and slow (mean decrease at 1h 85,1 ± 5,2%; at 2h 82,3 ± 11,5%; compared with AKAP4-BM M; mean decrease at 1h 87,6 ± 5,2%; at 2h 85,7 ± 8,7%; compared with negative control) progressive motility was observed. In addition, a significant decrease in non-progressive motility (mean decrease at 1h of 43,4 ± 24,8%; at 2h 50,6 ± 21,0%; compared with AKAP4-BM M; mean decrease at 1h 31,0 ± 26,9%; at 2h 58,6 ± 16,1%; compared with negative control) was also observed. In contrast, immotile spermatozoa increased (mean decrease at 1h of 47,3 ± 19,2%; at 2h 41,9 ± 14,7%; compared with AKAP4-BM M; mean decrease at 1h of 63,0 ± 27,8%; at 2h 74,5 ± 28,3%;

compared with negative control). Application of the mutated AKAP4-BM did not lead to significant differences in motility parameters in human spermatozoa (compared with negative control), with one exception (fast progressive motility at 2h with 20 µM incubation).

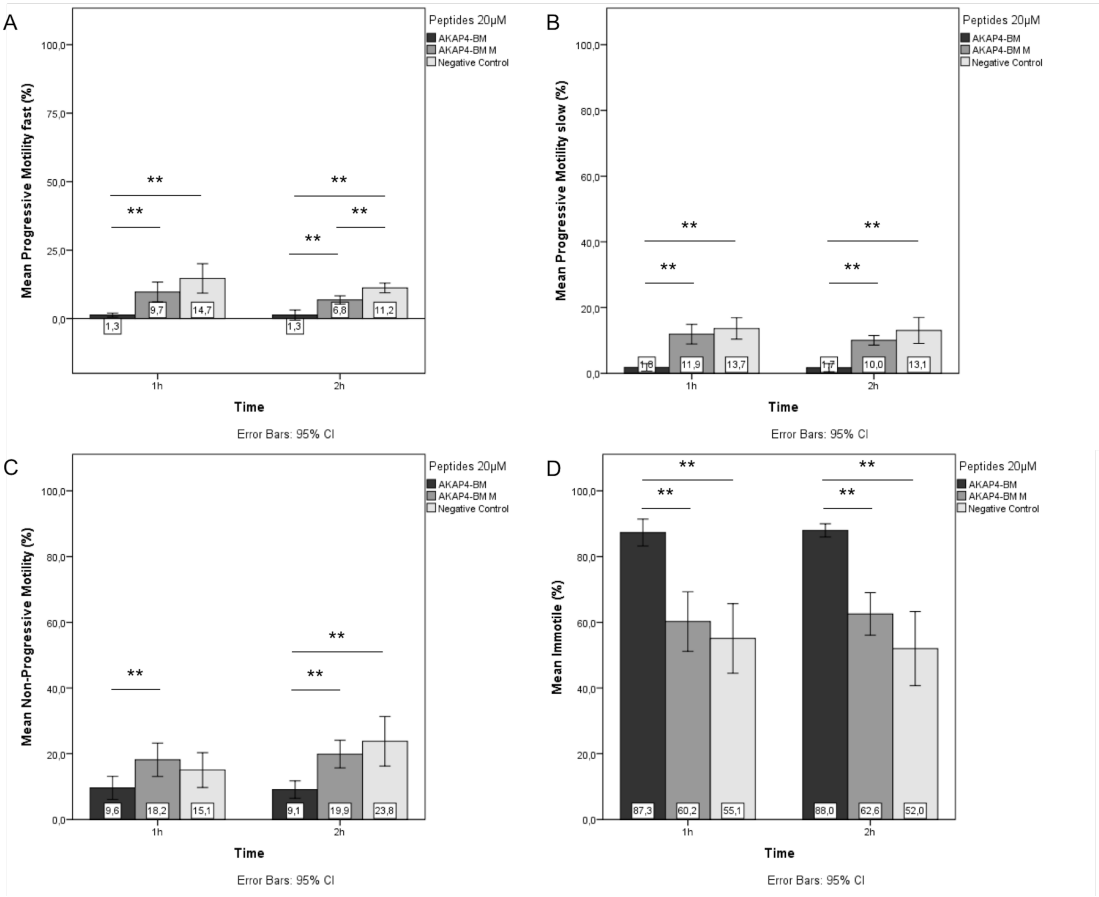

Figure B.8 – Impact of the AKAP4-BM peptides (AKAP4-BM and AKAP4-BM M) treatment in human spermatozoa motility parameters: (A) fast progressive motility; (B) slow progressive motility; (C) non-progressive motility; and (D) immotile spermatozoa; Graph bars represent the mean values of three independent experiments performed in triplicate. Error bars 95% CI. Statistically significant findings are indicated with a (*). * P<0.05; ** P<0.01.

3.2.5. Discussion

One strategy to improve intracellular drug delivery is to employ CPPs to overcome the permeability barrier represented by a lipid bilayer. These cationic and/or amphipathic peptides are a class of transport vectors, usually less than 30 amino acids in length, which possess the ability to rapidly translocate into mammalian cells. CPPs have the ability to carry along various cargo molecules, including oligonucleotides, peptides, proteins, plasmids, liposomes, and nanoparticles, which do not readily diffuse into the cytoplasm. The cargo may be reversibly or irreversibly linked to the CPP [34,35]. Jones et al have shown previously that CPPs enter mammalian spermatozoa rapidly, with a half-time between 1 and 3 min, dependent on the CPP [27]. The 16-amino acid long

peptide penetratin was used in this study to deliver PPI disruptor peptide sequences in sperm cells. Penetratin was chosen for its very efficient translocation into spermatozoa flagellum [27]. The intracellular accumulation of fluorescence-labeled peptides was verified and quantified and it was established that the detected fluorescence was not attributed to surface-associated CPP (Figure B.5). Further studies using a range of peptide concentrations should be performed in order to adjust the external concentrations of different peptides to achieve approximately the same uptake.

Exposure of bovine and human spermatozoa to the PPI disruptor peptide sequences induced significant alterations in motility parameters without altering the cell viability. Here we showed that a peptide that mimics the unique 22 amino acid C-terminus of PPP1CC2 coupled with a CPP was able to penetrate the sperm cell and led to a statistically significant effect on sperm motility (Figure B.6). In bovine spermatozoa, upon treatment with the PPP1CC2-CT peptide, the percentage of progressive motile spermatozoa decreased significantly. In turn, the percentage of immotile spermatozoa increased significantly. The percentage of non-progressive spermatozoa was not affected significantly after peptide treatment (Figure B.6). In human spermatozoa, exposure to PPP1CC2-CT peptide induced a decrease in fast progressive motility. We hypothesize that the PPP1CC2-CT peptide, which mimics the unique 22 amino acid C-terminus of PPP1CC2, competes with isoform-specific interactions potentially involved in the targeting/inhibition of this phosphatase, affecting its action and, consequently, spermatozoa motility. Endophilin B1t, a testis enriched isoform of the somatic endophilin B1a, and the spermatogenic zip protein (Spz1) represent two PPP1CC2 isoform-specific interactors previously identified [36,37]. Both endophilin B1t and Spz1 do not interact with other PPP1C isoforms or with a truncated PPP1CC2 mutant lacking the unique C-terminus. Endophilin B1t and Spz1 were previously shown to specifically inhibit PPP1CC2 isoform activity towards phosphorylase *a* [36,37]. As stated previously, PPP1 inhibition is essential for sperm motility. Further studies comparing the PPP1CC2 interactome in spermatozoa with and without incubation with the competition peptide will allow the identification of other isoform-specific interactors.

In this study we also demonstrated that a peptide that mimics the interaction interface between PPP1CC2 and AKAP4 (AKAP4-BM peptide) based on the RVxF motif was also successfully delivered to sperm cells and led to a statistically significant effect on sperm motility (Figure B.7 and Figure B.8). Upon treatment of bovine spermatozoa with the AKAP4-BM peptide, the percentage of progressive and non-progressive motile spermatozoa decreased significantly. In turn, the percentage of immotile spermatozoa increased significantly. Exposure of human spermatozoa to the AKAP4-BM peptide also induced a significant decrease in both progressive and non-progressive motility and an increase in immotile spermatozoa. Exposure to the mutated AKAP4-BM did not lead to significant differences in motility parameters in both bovine and human

spermatozoa (compared with negative control), with one exception in human sperm cells (fast progressive motility at 2h with 20 μM incubation).

Several findings suggest that the AKAP/PRKA/PPP1 complex is essential for regulation of sperm motility. In somatic cells, members of the AKAP family scaffold both kinases and phosphatases to a single place within the cell. In testis/sperm there are three AKAPs that have been directly related to PPP1CC2 (AKPA220, AKAP3 and AKAP4) and many more show a similar localization. AKAP220 binds PRKA and PPP1, being a competitive inhibitor of PPP1 [38, 39]. Brown et al. reported that AKAP4 anchors AKAP3 and two novel spermatogenetic cells-specific proteins, Fibrous sheath interacting proteins 1 and 2 (FSIP1 and FSIP2) (Figure B.9) [40, 41]. Compartmentalization of proteins to the flagellum via AKAPs is believed to ensure that the appropriate proteins find themselves in the right place at the right time to facilitate normal flagellar function. In support of this, mice containing a targeted mutation of the AKAP4 gene had a reduction in or a total loss of several proteins (in addition to PRKA) from the flagellum [23]. We have previously reported for the first time that AKAP4 interacts with PPP1CC2 in ejaculated spermatozoa (see chapter 3.1.). If AKAP4 is a scaffold for localizing and grouping functionally important proteins in addition to PRKA, its interaction with PPP1CC2 suggests a key role for AKAP4 in organizing the phosphorylation/dephosphorylation pathways that are required for the regulation of spermatozoa motility (Figure B.9). Huang and colleagues reported a significant decrease in PPP1CC2 phosphorylation and increase in its activity in spermatozoa lacking AKAP4. This suggests that AKAP4 is required to regulate the phosphorylation level, and consequently the activity, of PPP1CC2 in spermatozoa. Since PPP1CC2 inhibition is required for sperm motility, and AKAP4 is necessary for PPP1CC2 activity inhibition, it is reasonable to assume that the loss of PPP1CC2-AKAP4 interaction due to the competitive peptide is associated with immotile spermatozoa. Further studies are needed to determine the alterations on PPP1 activity and phosphorylation status upon exposure to the competition AKAP4 BM peptide. Additionally, competition assays will be used to conclusively determine that the effect of the AKAP4-BM peptide is due to AKAP4-PPP1CC2 interaction interference.

Given that AKAP4 undergoes several phosphorylation changes during the epididymal transit [42], it is plausible that PPP1CC2 may potentially be involved in regulating AKAP4 phosphorylation state. During the early stages of epididymal transit, AKAP4 is phosphorylated on the binding site for the regulatory subunits (PRKA1/RI and PRKA2/RII) of PRKA and, PRKA2A (RIIα) itself is also phosphorylated exclusively in caput/corpus-derived bovine spermatozoa. Baker and colleagues hypothesize that the two “negative” charges may have a repulsive role preventing the interaction from occurring contributing to maintaining the spermatozoa in a quiescent state in the early stages of the epididymal journey (Figure B.9) [42]. In fact, disruption of the anchoring of the RII subunit of

PRKA to AKAPs, by membrane-permeable peptides, resulted in an arrest of bovine sperm motility [43, 44].

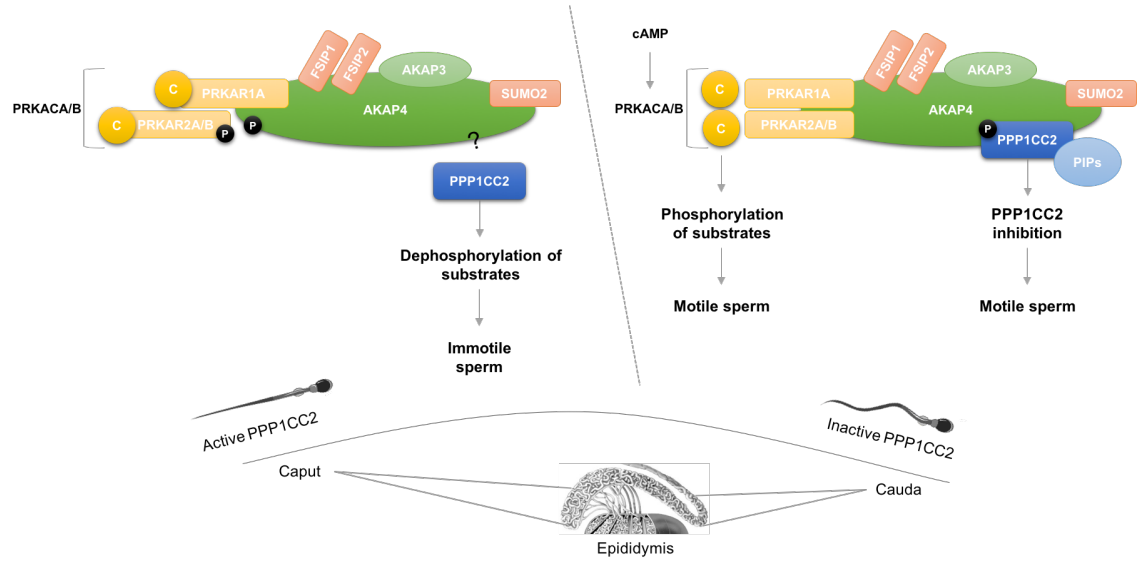

Figure B.9 – Putative roles of AKAP4 complexes in spermatozoa motility acquisition. In caput epididymis, PPP1CC2 is free and active resulting in the dephosphorylation of residues in key sperm proteins and therefore leading to immotile spermatozoa. In cauda epididymis, PPP1CC2 is bound to inhibitors (e.g. PPP1R2, PPP1R2P3, PPP1R7 and PPP1R11) and phosphorylated in a C-terminal threonine residue by a CDK. Thus, phosphorylation (by ser/thr protein kinases, such as, PRKACA) increases, leading to motile spermatozoa. The absence of AKAP4 leads to a significant decrease in PPP1CC2 phosphorylation and increase in its activity. Further studies are needed to establish if AKAP4/PPP1CC2 interaction occurs in the early stages of the epididymal transit or if AKAP4 recruits PPP1CC2 during the epididymal transit in order to allow PPP1CC2 phosphorylation and inhibition and, consequently, sperm motility acquisition. AKAP4 interactome also includes the regulatory subunits of PRKACA (also known as PKA) - PRKAR1A (also known as RIα) and PRKAR2A (also known as RIIα), PRKAR2B (RIIβ), AKAP3, SUMO2, FSIP1 and FSIP2. PIPs, PPP1 interacting proteins.

Further studies to test additional concentrations and incubation times in human spermatozoa are needed in order to clarify the impact of the peptides in spermatozoa. Additional studies are also needed to confirm the alterations on PPP1 activity by using phosphatase assays and of global protein serine/threonine phosphorylation status upon exposure to the PPI disruption peptides. The assessment of phosphatase activity and global phosphorylation levels will help to understand the changes produced by the peptides at the cellular level and that have a profound impact on motility.

3.2.6. References

1. Henshaw, S. K. Unintended pregnancy in the United States. *Fam. Plann. Perspect.* 30, 24–29, 46
2. Singh, S., Sedgh, G. & Hussain, R. Unintended Pregnancy: Worldwide Levels, Trends, and Outcomes. *Stud. Fam. Plann.* 41, 241–250 (2010).
3. Finer, L. B. & Henshaw, S. K. Abortion incidence and services in the United States in 2000. *Perspect. Sex. Reprod. Health* 35, 6–15
4. Jones, R. K., Darroch, J. E. & Henshaw, S. K. Contraceptive use among U.S. women having abortions in 2000-2001. *Perspect. Sex. Reprod. Health* 34, 294–303
5. Kogan, P. & Wald, M. Male Contraception. *Urol. Clin. North Am.* 41, 145–161 (2014).
6. Chao, J., Page, S. T. & Anderson, R. A. Male contraception. *Best Pract. Res. Clin. Obstet. Gynaecol.* 28, 845–857 (2014).
7. Nya-Ngatchou, J.-J. & Amory, J. K. New approaches to male non-hormonal contraception. *Contraception* 87, 296–299 (2013).
8. Fardilha, M., Esteves, S. L. C., Korrodi-Gregório, L., da Cruz e Silva, O. A. B. & da Cruz e Silva, F. F. The physiological relevance of protein phosphatase 1 and its interacting proteins to health and disease. *Curr. Med. Chem.* 17, 3996–4017 (2010).
9. Sinha, N., Pilder, S. & Vijayaraghavan, S. Significant Expression Levels of Transgenic PPP1CC2 in Testis and Sperm Are Required to Overcome the Male Infertility Phenotype of Ppp1cc Null Mice. *PLoS One* 7, (2012).
10. Vijayaraghavan, S., Stephens, D. T., Trautman, K., Smith, G. D., Khatra, B., da Cruz e Silva, E. F. & Greengard, P. Sperm motility development in the epididymis is associated with decreased glycogen synthase kinase-3 and protein phosphatase 1 activity. *Biol. Reprod.* 54, 709–718 (1996).
11. Smith, G. D., Wolf, D. P., Trautman, K. C., da Cruz e Silva, E. F., Greengard, P. & Vijayaraghavan, S. Primate sperm contain protein phosphatase 1, a biochemical mediator of motility. *Biol. Reprod.* 54, 719–727 (1996).
12. Fardilha, M., Ferreira, M., Pelech, S., Vieira, S., Rebelo, S., Korrodi-Gregorio, L., Sousa, M., Barros, A., Silva, V., da Cruz E Silva, O. a B. & da Cruz E Silva, E. F. 'OMICS' of Human Sperm: Profiling Protein Phosphatases. *OMICS* 17, 460–472 (2013).
13. Silva, J. V., Korrodi-Gregório, L., Luers, G., Cardoso, M. J., Patrício, A., Maia, N., da Cruz E Silva, E. F. & Fardilha, M. Characterisation of several ankyrin repeat protein variant 2, a phosphoprotein phosphatase 1-interacting protein, in testis and spermatozoa. *Reprod. Fertil. Dev.* (2015). doi:10.1071/RD14303
14. Browne, G. J., Fardilha, M., Oxenham, S. K., Wu, W., Helps, N. R., da Cruz E Silva, O. A. B., Cohen, P. T. W. & da Cruz E Silva, E. F. SARP, a new alternatively spliced protein phosphatase 1 and DNA interacting protein. *Biochem. J.* 402, 187–196 (2007).
15. Silva, J. V, Freitas, M. J. & Fardilha, M. Phosphoprotein phosphatase 1 complexes in spermatogenesis. *Curr. Mol. Pharmacol.* 7, 136–46 (2014).
16. Fardilha, M., Esteves, S. L. C., Korrodi-Gregório, L., Vintém, A. P., Domingues, S. C., Rebelo, S., Morrice, N., Cohen, P. T. W., Da Cruz E Silva, O. A. B. & Da Cruz E Silva, E. F. Identification of the human testis protein phosphatase 1 interactome. in *Biochemical Pharmacology* 82, 1403–1415 (2011).
17. Korrodi-Gregório, L., Vieira, S. I., Esteves, S. L. C., Silva, J. V, Freitas, M. J., Brauns, A.-K., Luers, G., Abrantes, J., Esteves, P. J., da Cruz E Silva, O. a B., Fardilha, M. & da Cruz E Silva, E. F. TCTEX1D4, a novel protein phosphatase 1 interactor: connecting the phosphatase to the microtubule network. *Biol. Open* 2, 453–65 (2013).
18. Korrodi-gregório, L., Ferreira, M., Vintém, A. P., Wu, W., Muller, T., Marcus, K., Vijayaraghavan, S., Brautigan, D. L., Odete, A. B., Fardilha, M. & Edgar, F. Identification and characterization of two distinct PPP1R2 isoforms in human spermatozoa. (2013). doi:10.1186/1471-2121-14-15
19. Moretti, E., Scapigliati, G., Pascarelli, N. A., Baccetti, B. & Collodel, G. Localization of AKAP4 and tubulin proteins in sperm with reduced motility. *Asian J. Androl.* 9, 641–9 (2007).
20. Turner, R. M., Musse, M. P., Mandal, A., Klotz, K., Jayes, F. C., Herr, J. C., Gerton, G. L., Moss, S. B. & Chemes, H. E. Molecular genetic analysis of two human sperm fibrous sheath proteins, AKAP4 and AKAP3, in men with dysplasia of the fibrous sheath. *J. Androl.* 22, 302–15

21. Matzuk, M. M. & Lamb, D. J. The biology of infertility: research advances and clinical challenges. *Nat. Med.* 14, 1197–213 (2008).
22. Baccetti, B., Collodel, G., Gambera, L., Moretti, E., Serafini, F. & Piomboni, P. Fluorescence in situ hybridization and molecular studies in infertile men with dysplasia of the fibrous sheath. *Fertil. Steril.* 84, 123–9 (2005).
23. Miki, K., Willis, W. D., Brown, P. R., Goulding, E. H., Fulcher, K. D. & Eddy, E. M. Targeted disruption of the Akap4 gene causes defects in sperm flagellum and motility. *Dev. Biol.* 248, 331–342 (2002).
24. Huang, Z., Somanath, P. R., Chakrabarti, R., Eddy, E. M. & Vijayaraghavan, S. Changes in intracellular distribution and activity of protein phosphatase PP1gamma2 and its regulating proteins in spermatozoa lacking AKAP4. *Biol. Reprod.* 72, 384–392 (2005).
25. Chatterjee, J., Beullens, M., Sukackaite, R., Qian, J., Lesage, B., Hart, D. J., Bollen, M. & Köhn, M. Development of a peptide that selectively activates protein phosphatase-1 in living cells. *Angew. Chemie - Int. Ed.* 51, 10054–10059 (2012).
26. Arkin, M. R., Tang, Y. & Wells, J. A. Small-Molecule Inhibitors of Protein-Protein Interactions: Progressing toward the Reality. *Chem. Biol.* (2014). doi:10.1016/j.chembiol.2014.09.001
27. Jones, S., Lukanowska, M., Suhorutsenko, J., Oxenham, S., Barratt, C., Publicover, S., Copolovici, D. M., Langel, Ü. & Howl, J. Intracellular translocation and differential accumulation of cell-penetrating peptides in bovine spermatozoa: evaluation of efficient delivery vectors that do not compromise human sperm motility. *Hum. Reprod.* 28, 1874–89 (2013).
28. Svensen, N., Walton, J. G. A. & Bradley, M. Peptides for cell-selective drug delivery. *Trends in Pharmacological Sciences* 33, 186–192 (2012).
29. Palasek, S. A., Cox, Z. J. & Collins, J. M. Limiting racemization and aspartimide formation in microwave-enhanced Fmoc solid phase peptide synthesis. *J. Pept. Sci.* 13, 143–8 (2007).
30. Jones, S., Martel, C., Belzacq-Casagrande, A. S., Brenner, C. & Howl, J. Mitoparan and target-selective chimeric analogues: Membrane translocation and intracellular redistribution induces mitochondrial apoptosis. *Biochim. Biophys. Acta - Mol. Cell Res.* 1783, 849–863 (2008).
31. Holm, T., Johansson, H., Lundberg, P., Pooga, M., Lindgren, M. & Langel, U. Studying the uptake of cell-penetrating peptides. *Nat. Protoc.* 1, 1001–5 (2006).
32. Iqbal, M., Aleem, M., Ijaz, A., Rehman, H. & Yousaf, M. S. Assessment of buffalo semen with MTT reduction assay. *Rev. Vet.* 21, 826–831 (2010).
33. Ho, H.-C., Granish, K. A. & Suarez, S. S. Hyperactivated motility of bull sperm is triggered at the axoneme by Ca2+ and not cAMP. *Dev. Biol.* 250, 208–17 (2002).
34. Howl, J., Matou-Nasri, S., West, D. C., Farquhar, M., Slaninová, J., Östenson, C. G., Zorko, M., Östlund, P., Kumar, S., Langel, Ü., McKeating, J. & Jones, S. Bioportide: An emergent concept of bioactive cell-penetrating peptides. *Cell. Mol. Life Sci.* 69, 2951–2966 (2012).
35. Howl, J. & Jones, S. Insights into the molecular mechanisms of action of bioportides: a strategy to target protein-protein interactions. *Expert Rev. Mol. Med.* 17, e1 (2015).
36. Hrabchak, C. & Varmuza, S. Identification of the spermatogenic zip protein Spz1 as a putative protein phosphatase-1 (PP1) regulatory protein that specifically binds the PP1c??2 splice variant in mouse testis. *J. Biol. Chem.* 279, 37079–37086 (2004).
37. Hrabchak, C., Henderson, H. & Varmuza, S. A testis specific isoform of endophilin B1, endophilin B1t, interacts specifically with protein phosphatase-1c??2 in mouse testis and is abnormally expressed in PP1c?? Null Mice. *Biochemistry* 46, 4635–4644 (2007).
38. Schillace, R. V, Voltz, J. W., Sim, A. T., Shenolikar, S. & Scott, J. D. Multiple interactions within the AKAP220 signaling complex contribute to protein phosphatase 1 regulation. *J. Biol. Chem.* 276, 12128–34 (2001).
39. Reinton, N., Collas, P., Haugen, T. B., Skâlhegg, B. S., Hansson, V., Jahnsen, T. & Taskén, K. Localization of a novel human A-kinase-anchoring protein, hAKAP220, during spermatogenesis. *Dev. Biol.* 223, 194–204 (2000).
40. Brown, P. R., Miki, K., Harper, D. B. & Eddy, E. M. A-kinase anchoring protein 4 binding proteins in the fibrous sheath of the sperm flagellum. *Biol. Reprod.* 68, 2241–8 (2003).
41. Carrera, A., Gerton, G. L. & Moss, S. B. The major fibrous sheath polypeptide of mouse sperm: structural and functional similarities to the A-kinase anchoring proteins. *Dev. Biol.* 165, 272–84

(1994).

42. Baker, M. A., Hetherington, L., Weinberg, A., Naumovski, N., Velkov, T., Pelzing, M., Dolman, S., Condina, M. R. & Aitken, R. J. Analysis of phosphopeptide changes as spermatozoa acquire functional competence in the epididymis demonstrates changes in the post-translational modification of Izumo1. *J. Proteome Res.* 11, 5252–64 (2012).
43. Vijayaraghavan, S., Goueli, S. A., Davey, M. P. & Carr, D. W. Protein kinase A-anchoring inhibitor peptides arrest mammalian sperm motility. *J. Biol. Chem.* 272, 4747–52 (1997).
44. Burton, K. A., Treash-Osio, B., Muller, C. H., Dunphy, E. L. & McKnight, G. S. Deletion of type IIalpha regulatory subunit delocalizes protein kinase A in mouse sperm without affecting motility or fertilization. *J. Biol. Chem.* 274, 24131–6 (1999).

3.3. Characterization of several ankyrin repeat protein variant 2, a phosphoprotein phosphatase 1-interacting protein, in testis and spermatozoa

Joana Vieira Silva[1], Luís Korrodi-Gregório[1], Georg Luers[2], Maria João Cardoso[1], António Patrício[3], Nuno Maia[3], Edgar F. da Cruz e Silva[1†] and Margarida Fardilha[1]

[1] Laboratory of Signal Transduction, Department of Medical Sciences, Institute of Biomedicine – iBiMED, University of Aveiro, 3810-193 Aveiro, Portugal.

[2] Institute for Anatomy and Experimental Morphology, Center for Experimental Medicine, University Hamburg-Eppendorf, D-20246 Hamburg, Germany

[3] Hospital Infante D. Pedro E.P.E., 3810-193 Aveiro, Portugal

[†] deceased on 2nd of March, 2010

Corresponding author: Margarida Fardilha, Departamento de Ciências Médicas, Universidade de Aveiro, Campus Universitário de Santiago, Agra do Crasto – Edifício 30, 3810-193 Aveiro, Portugal. T: +351-918143947. E: mfardilha@ua.pt

Silva JV, Korrodi-Gregório L, Luers G, Cardoso MJ, Patrício A, Maia N, da Cruz E Silva EF, Fardilha M. Characterisation of several ankyrin repeat protein variant 2, a phosphoprotein phosphatase 1-interacting protein, in testis and spermatozoa. Reproduction, Fertility and Development. 2015; 7. doi: 10.1071/RD14303.

3.3.1. Abstract

Phosphoprotein phosphatase 1 (PPP1) catalytic subunit gamma 2 (PPP1CC2), a PPP1 isoform, is largely restricted to testicular germ cells and spermatozoa. The key to understanding PPP1 regulation in male germ cells lies in the identification and characterization of its interacting partners. This study was undertaken to determine the expression patterns of the several ankyrin repeat protein variant 2 (SARP2), a PPP1-interacting protein, in testis and spermatozoa. SARP2 was found to be highly expressed in testis and spermatozoa, and its interaction with human spermatozoa endogenous PPP1CC2 was confirmed by immunoprecipitation. Expression analysis by RT-qPCR revealed that SARP2 and PPP1CC2 mRNA levels were significantly higher in the spermatocyte fraction. However, microscopy revealed that SARP2 protein was only present in the nucleus of elongating and mature spermatids and in spermatozoa. In spermatozoa, SARP2 was prominently expressed in the connecting piece and flagellum, as well as, to a lesser extent, in the acrosome. A yeast two-hybrid approach was used to detect SARP2-interacting proteins and a relevant interaction with a novel sperm associated antigen 9 (SPAG9) variant, a testis and spermatozoa-specific c-Jun N-terminal kinase-binding protein, was validated in human spermatozoa. Given the expression pattern of SARP2 and its association with PPP1CC2 and SPAG9, it may play a role in spermiogenesis and sperm function, namely in sperm motility and the acrosome reaction.

3.3.2. Introduction

Spermatozoa are devoid of any major transcriptional and translational activity; thus, post-translational modifications and mechanisms based on disruption or formation of protein complexes are central in regulating sperm function [1–4]. Phosphoprotein phosphatase 1 (PPP1), a major Ser/Thr protein phosphatase, catalyses most of the eukaryotic protein dephosphorylation events in a highly regulated and selective manner [5–7]. The predominant PPP1 catalytic subunit in both testicular germ cells and spermatozoa is PPP1 catalytic subunit gamma 2 (PPP1CC2), one of the four highly conserved PPP1 isoforms (along with PPP1CA, PPP1CB and PPP1CC1; [2,8,9]). The PPP1CC1 and PPP1CC2 isoforms are alternatively spliced products from the single PPP1CC gene. These polypeptides differ at their C-termini, in which PPP1CC2 has a unique 22-amino acid extension. Targeted disruption of the mouse Ppp1cc gene results in male infertility due to aberrant spermiogenesis [10,11]. However, this deficiency causes no obvious abnormality in other tissues, probably due to compensatory expression of PPP1CA and PPP1CB. Recent data show that mice fertility is restored upon expression of transgenic PPP1CC2 alone and that sufficient levels of expression are required to achieve this outcome [12,13]. In addition, inhibition of PPP1CC2 in spermatozoa using PPP1 inhibitors results in the initiation and stimulation of motility [3,14,15]. These

results indicate that PPP1CC2 has a crucial role in the regulation of mammalian spermatogenesis and sperm motility.

Over the past two decades, it has become apparent that PPP1 versatility is achieved by its ability to interact with multiple targeting and regulatory subunits known as PPP1-interacting proteins (PIPs) [5,16,17]. PIPs are ubiquitously expressed and show exceptional diversity in brain, testis and white blood cells [2,7,8,17]. Several PIPs have been characterized in somatic cells and considerable progress has been made in defining how they regulate PPP1 [18]. However, understanding of PPP1 regulation, specifically the testis and sperm-enriched isoform (PPP1CC2), in male germ cells is limited [8]. The key to understanding the roles of PPP1 is identifying and characterizing its regulatory subunits.

Several ankyrin repeat protein variant 2 (SARP2) was first identified in a yeast two-hybrid (YTH) screen using PPP1CC1 as bait [8]. SARP2 (National Center for Biotechnology Information (NCBI) EF041819.1) is an alternatively spliced transcript variant of the ANKRD42 gene [19]. In addition to a consensus RVxF PPP1 binding motif (354KVHF357), SARP2 possess another PPP1- docking motif that consists of eight ankyrin repeats (AnkCap) [19]. The RVxF motif lies partially within the first ankyrin repeat, in contrast with other proteins; for example, in myosin phosphatase target subunit 1 (MYPT1) the PPP1-binding motif precedes the ankyrin repeats. In addition, SARP was shown to inhibit PPP1 catalytic activity when phosphorylase was used as a substrate [19].

In the present study we characterized the expression patterns of the SARP2 isoform in testis and spermatozoa and established how it is related to PPP1CC2. In addition, we identified a new sperm-associated antigen 9 (SPAG9) variant that interacts with SARP2 in the testis and spermatozoa.

3.3.3. Materials and Methods

Unless stated otherwise, all reagents were purchased from Sigma-Aldrich Química (Sintra, Portugal).

Human testicular biopsies

Testicular biopsies for immunofluorescence microscopy were obtained from three individual patients presenting at the Department of Andrology, University Hospital Hamburg-Eppendorf. Informed consent was obtained and the study was conducted in accordance with the Helsinki Declaration. Tissues were taken for diagnostic purposes and their histology was extrapolated from examinations of parallel biopsies from the same testis as part of the routine diagnostic work-up. Only samples presenting normal spermatogenesis on histological analysis were used. Testicular biopsies for western blot analysis and immunoelectron microscopy were collected in vivo, after Ethics Committee approval was obtained, from a brain-dead 35-year-old man at the Centro Hospitalar de Coimbra (Coimbra, Portugal) during a procedure to collect organs for transplantation.

Different regions of both testes were collected and the biopsies were diagnosed as 'normal' based on histopathological analysis. Testicular biopsies for research purposes are covered by the legislation of the Portuguese Constitution (decreto-lei no. 274/99; 22 July 1999). Human testis extracts for western blot analysis were prepared by homogenization using 1% sodium dodecyl sulfate (SDS).

Human sperm samples

Ejaculated sperm samples were obtained from eight donors by masturbation into an appropriate sterile container. All donors signed informed consent allowing the samples to be used for scientific purposes, and all human samples were used in accordance with the appropriate Ethics and Internal Review Board guidelines. A copy of the written consent is available for review. Basic semen analysis (concentration, motility and morphology) was performed by experienced technicians according to the World Health Organization guidelines (World Health Organization 2013) and only normal sperm samples were used. For all procedures, spermatozoa were washed three times in 1x phosphate-buffered saline (PBS). For immunoprecipitation, spermatozoa were lysed in 1x radioimmunoprecipitation buffer (RIPA) buffer (Millipore Iberica, Madrid, Spain) supplemented with protease inhibitors (10 mM benzamidine, 1.5 mM aprotinin, 5 mM pepstatin A, 2 mM leupeptin, 1mM phenylmethylsulphonyl fluoride) and phosphatase inhibitors (1mMsodium fluoride, 2.5 mM sodium pyrophosphate, 50mM b-glycerophosphate, 1mM sodium orthovanadate), sonicated three times for 10 s and centrifuged at 16 000g for 20 min at 4°C. The supernatant was collected and used in the subsequent steps. For western blot analysis, extracts were resuspended in1% SDS. For immunocytochemistry, washed spermatozoa were placed directly on coverslips. For the colocalisation studies with an acrosome marker, spermatozoa were subjected to a swim-up procedure, as described previously [20].

Animals

C57/Bl6 mice were used for the isolation of testicular germ cells and BALB/c mice were used for immunohistochemistry studies. Housing of mice was approved by the responsible government commission and all animals were kept under standard conditions at the animal facility of the University Hospital Hamburg-Eppendorf under a 12-h light–dark. Male mice, 6–10 weeks of age, were used.

Antibodies

The anti-PPP1CC2 antibody was raised in rabbit against the specific PPP1CC2 C-terminal peptide (VGSGLNPSIQKASNYRNNTVLY) and has been described previously [15]. Anti-SARP2 antibody was raised in rabbits against the specific SARP2 C-terminal peptide (DSASCESNKEKRRVK) and was affinity purified (Figure B.10 a). Anti-SPAG9 antibody was obtained from Sigma-Aldrich, the

infrared IRDye labelled anti-rabbit secondary antibody was obtained from LI-COR Biosciences (Lincoln, NE, USA) and the secondary antibodies for the immunofluorescence studies were obtained from Molecular Probes, (Eugene, OR, USA).

Expression analysis in isolated testicular germ cells

Cell populations were isolated from mouse testis using an established protocol based on unit gravity sedimentation that isolates germ cell populations from a heterogeneous suspension of mouse testis [21]. The three fractions were microscopically evaluated as spermatocytes (Spc), round spermatids (rSpd) and elongated spermatids (eSpd), based on their predominance. Total RNA from isolated cells was prepared using the RNeasy Plus Universal Midi Kit (Qiagen, Hilden, Germany). The RNA concentration was determined spectrophotometrically (NanoDrop 1000 Spectrophotometer; Thermo Scientific, Bremen, Germany). For synthesis of cDNA, a reverse transcription reaction was performed using 1 µg RNA and a Transcriptor First Strand cDNA Synthesis Kit (Roche, Mannheim, Germany). Expression levels of distinct mRNAs were determined by RT-qPCR using the LightCycler 480 SYBR Green I Master (Roche) and the following cycle conditions: initial denaturation at 95°C for 15 min, followed by 45 cycles of denaturation (94°C, 15 s), annealing (58°C, 30 s) and polymerization (72°C, 30 s). Thereafter, a melting curve was generated over the range 55–95°C with 30 s/1°C rampage. Polymerase chain reaction (PCR) analysis was performed on 96-well plates using the Light Cycler 480 Real-Time PCR System (Roche). The combination of Gapdh and Hprt was identified as the optimal reference genes for the testis and all expression levels were calculated as relative values using the mean expression of both reference genes. All samples were run in triplicate and mean values were used to calculate expression levels of the different genes. Relative gene expression was quantified using the $2^{-\Delta\Delta CT}$ method [22]. The cDNA obtained from the cell suspension of whole testis was used as control sample for RT-qPCR reactions. Genes already established as markers for each step of spermatogenesis were analysed to ensure minimal contamination from other spermatogenic cells. The primers used are listed in Supplementary Table D-16 and D.17, and were made to span exon–exon junctions (intron splice sites) in order to avoid genomic DNA amplification.

Immunoprecipitation

RIPA supernatant sperm extracts were precleared using Dynabeads Protein G (Life Technologies, Madrid, Spain). Using a direct immunoprecipitation approach, 1 µg rabbit anti-PPP1CC2 or anti-SPAG9 was pre-incubated with Dynabeads Protein G for 1 h at 4°C with rotation. After incubation, sperm precleared extracts were applied to the antibody–dynabeads complex and incubated overnight with rotation at 4°C. After washing three times with 1xPBS for 10 min with rotation at 4°C, the beads were resuspended in the appropriate buffer. For gel loading, beads were

resuspended in 1% SDS and boiled for 5min. For overlay assays, beads were resuspended in 0.1M glycine-HCl (pH 2.5).

Western blotting

Extracts were mass normalised using the bicinchoninic acid (BCA) assay (Fisher Scientific, Loures, Portugal). Extracts were resolved by 10% SDS–polyacrylamide gel electrophoresis (PAGE). Proteins were subsequently electrotransferred onto nitrocellulose membranes and immunodetected with appropriate antibodies using the Odyssey Infrared Imaging System (LI-COR Biosciences).

Immunofluorescence of human testis

For fluorescence microscopy of cryosections, human testis biopsies and testes of BALB/c mice were fixed with 4% paraformaldehyde and 0.1M HEPES, pH 7.4, and subsequently immersed in 30% sucrose solution for approximately 4 h. Tissues were frozen in isopentane at -30°C and stored at -80°C until further analysis. Cryosections (10–14 mm) were cut on a Microm HM500 O cryostate (Microm, Walldorf, Germany). Non-specific binding sites were blocked with 3% bovine serum albumin (BSA) and incubated with primary antibodies (rabbit anti-PPP1CC2, 1:500; and rabbit anti-SARP2, 1:100) for 2 h at room temperature and then incubated with a fluorochrome conjugated rabbit secondary antibody (Alexa Fluor 594 Goat Anti-Rabbit IgG) for 1 h. Negative controls were processed in parallel by adding Tris-buffered saline Tween-20 (TBST) instead of the primary antibodies. Nuclei were stained with 40, 60-diamidino-2-phenylindole (DAPI; 1:200; Vectashield; Vector Laboratories, Burlingame, CA, USA) for 5 min at room temperature and washed twice with TBST for 5 min. Finally, samples were inspected under a fluorescence microscope (Axio Vision Rel 4.8 series; Zeiss, Jena, Germany).

Immunoelectron microscopy of human testis

After collection, human testicular biopsies were immediately immersed in fixative (4% depolymerised paraformaldehyde, 0.05% glutaraldehyde in 0.1M cacodylate buffer, pH 7.4, and 2% sucrose). Fixed samples were embedded into LRWhite resin (Sigma-Aldrich, Seelze, Germany) after dehydration in a graded series of ethanol (medium grade). LR White-filled gelatin capsules were polymerised at 50°C for 3 days. After preparation of semithin sections (1 mm) and observation under a light microscope, blocks were trimmed for areas with defined stages of seminiferous tubules. Ultrathin sections (80nm) were cut on a Leica microtome (VT1000S), collected on 100-mesh nickel grids and thereafter coated on the back with a 1% formvar film (support film). The sections were incubated with glycine solution (0.05M glycine in TBST, pH 7.4) for 15min to disable free aldehyde groups. Subsequently, sections were incubated in blocking

solution (1% BSA in TBST, pH 7.4) for 30 min at room temperature. Sections were incubated overnight at room temperature with anti-SARP2 antibody in a wet chamber. The sections were then washed and incubated for 90min at room temperature with a protein A–gold solution (1:50; 12 nm colloidal gold particles). Negative controls were processed in parallel by addition of TBST instead of the primary antibodies. The grids were rinsed on droplets of washing solution (0.1% BSA in TBST, pH 7.4) three times for 10 min and subsequently contrasted with uranyl acetate for 2 min and lead citrate for 45 s. Sections were examined using a LEO 906 electron microscope (LEO, Oberkochen, Germany).

Immunocytochemistry of human spermatozoa

An aliquot (25 µL) of washed spermatozoa was placed onto a glass coverslip precoated with 100 µg/mL 1 poly-L-ornithine and dried room temperature in a six-well plate containing one coverslip per well. To each well, 4% paraformaldehyde in 1xPBS was added and left to stand for 10min. Subsequently, spermatozoa were washed twice with 1xPBS for 10 min. For permeabilisation, a 1:1 methanol:acetone solution was added for 2min and specimens were then washed twice with 1xPBS for 10 min before being blocked for 1 h with 3% BSA in 1xPBS and then incubated with primary antibodies (rabbit anti-PPP1CC2, 1:1000; and rabbit anti-SARP2, 1:250) for 2 h at room temperature. After three washes with PBS, the fluorescent-labelled secondary antibody (goat anti-rabbit Texas-Red; 1:300; Molecular Probes) was added and the coverslips were incubated for 2 h at room temperature. Finally, samples were washed three times with 1xPBS and the coverslips mounted on microscope glass slides with one drop of antifading reagent containing DAPI for nucleic acid staining (Vectashield; Vector Laboratories). Fluorescence assessment of the acrosomal state was determined with fluorescein isothiocyanate-labelled Pisum sativum agglutinin (PSA-FITC), as described previously [23]. Briefly, 1106 motile spermatozoa were incubated in capacitating medium (37°C, 5% CO2) for 2 h. To induce the acrosome reaction, capacitated spermatozoa were incubated with progesterone (3 mM), for 30 min. Then, the sperm samples were applied to the coverslip and left to dry. Fixation and permeabilisation was performed with 95% ethanol for 30 min. The fixed sperm smear was placed in PSA-FITC for 1 h. The following procedure was the same as described in the 'Immunocytochemistry of human spermatozoa' section. Images were acquired using an epifluorescence microscope (IX81; Olympus Portugal – Opto-Digital Tecnologias, Lisboa, Portugal) and digital camera equipped with appropriate software (Olympus Portugal – Opto-Digital Tecnologias, Lisboa, Portugal).

YTH screening of the human testis library

The cDNA of the C-terminus of SARP2 (EDSASCESNKEKRRVKKKVSS) was subcloned into SalI/SmaI-digested pAS2–1, which adds a galactosidase (GAL4)-binding domain (GAL4BD)

peptide to the N-terminal part of the protein. The product, pAS-SARP2 C-terminal (bait), was inserted in Saccharomyces cerevisiae Y187 strain to confirm the expression of GAL4BD-SARP2 C-terminal recombinant protein and to test for self-activation of reporter genes, which was negative (data not shown). The yeast AH109 strain was transformed with a human testis cDNA library, inserted into a pACT2 vector (prey), which adds a GAL4 activation domain (GAL4AD) peptide to the N-terminal part of the proteins. For library screening, transformed Y187 and AH109 yeast strains were mated and half the mating mixture was plated onto high-stringency medium (quadruple dropout medium: supplemented dropout (s.d.)/–Ade/–His/–Leu/–Trp) and the other half onto low-stringency medium (triple dropout medium: s.d./–His/–Leu/–Trp) and plates were then incubated at 30°C until colonies appeared (maximum 2 weeks). Colonies obtained on the low-stringency plates were replica plated onto high-stringency medium. Finally, all high-stringency growing colonies were plated onto selective medium containing X-a-Galactosidase (X-a-Gal) and incubated at 30°C until blue colonies appeared (maximum 2 weeks) to check for MDS1/EVI1-like gene 1 (MEL-1) expression (indicated by the appearance of a blue colour). All YTH reagents were purchased from Clontech (Enzifarma, Portugal).

Recovery of plasmids from yeast and sequence analysis

Yeast plasmid was recovered by the boiling method and used to transform Escherichia coli XL1-Blue strain. The plasmid DNAs were extracted from three isolated colonies of each transformation and digested to identify bait and prey plasmids. Recovered prey plasmids were analysed by DNA sequencing, using an automated DNA sequencer (Applied Biosystems, Carlsbad, CA, USA). A GAL4-AD primer (TACCACTACAATGGATG) was used to amplify the library cDNAs. The DNA sequences obtained were compared against the GenBank database, using the BLAST algorithm to identify the corresponding proteins.

Membrane overlay

A single Rosetta (DE3; Novagen, Madison, WI, USA) colony transformed with recombinant His-tagged SARP2 (amino acids 331–847) was selected and grown overnight in 3 mL Luria–Bertani and ampicillin medium at 37°C. Aliquots (0.5 mL) were transferred to 50 mL Luria–Bertani and ampicillin until A600 reached 0.6. Expression was induced with 1mMisopropyl β-D-thiogalactoside at 37°C for 3 h with shaking. Cells were recovered by centrifugation (12 000g, 1 min, 4°C), resuspended in 0.5 mL of 1% SDS and increasing protein quantities of the bacterial extracts were loaded onto 12% gels for SDS-PAGE and subsequently transferred to nitrocellulose membranes that were then overlaid with SPAG9 immunoprecipitate. After washing with PBS to remove excess protein, bound SPAG9 was detected by incubating the membrane with a rabbit anti-SPAG9 antibody. Immunoreactive bands were revealed by incubation with an infrared goat anti-

rabbit IgG labeled with IRDye followed by detection using the Odyssey Infrared Imaging System (LI-COR Biosciences).

3.3.4. Results

SARP2 tissue expression and interaction with PPP1CC2 in human spermatozoa

A tissue screen with an isoform-specific antibody (Figure B.10 a) recognising the C-terminus of SARP2 was performed on several tissues (Figure B.10 b). SARP2 was found to be highly expressed in human spermatozoa. SARP2 was also expressed in human and mouse testis, but at lower levels than in human spermatozoa. The predicted molecular mass for SARP2 was 94.3 kDa (849 amino acids). Previously, it was shown that an antibody recognizing both isoforms (SARP1 and SARP2) revealed a different immunoreactive profile [19]. This could mean that the expression levels observed previously in liver, heart, lung, intestine and cortex were primarily SARP1 [19]. Given that SARP2 is highly expressed in human spermatozoa, RIPA-soluble extracts and insoluble fractions of human sperm lysates were resolved by SDS-PAGE and immunoblotted (Figure B.10 c). The results showed that SARP2 was present in both fractions, but was more abundant in the insoluble fraction. To prove the interaction between SARP2 and PPP1CC2 in sperm cells, endogenous PPP1CC2 immunoprecipitated from human spermatozoa was found to coimmunoprecipitate with endogenous SARP2 isoform (Figure B.10 d).

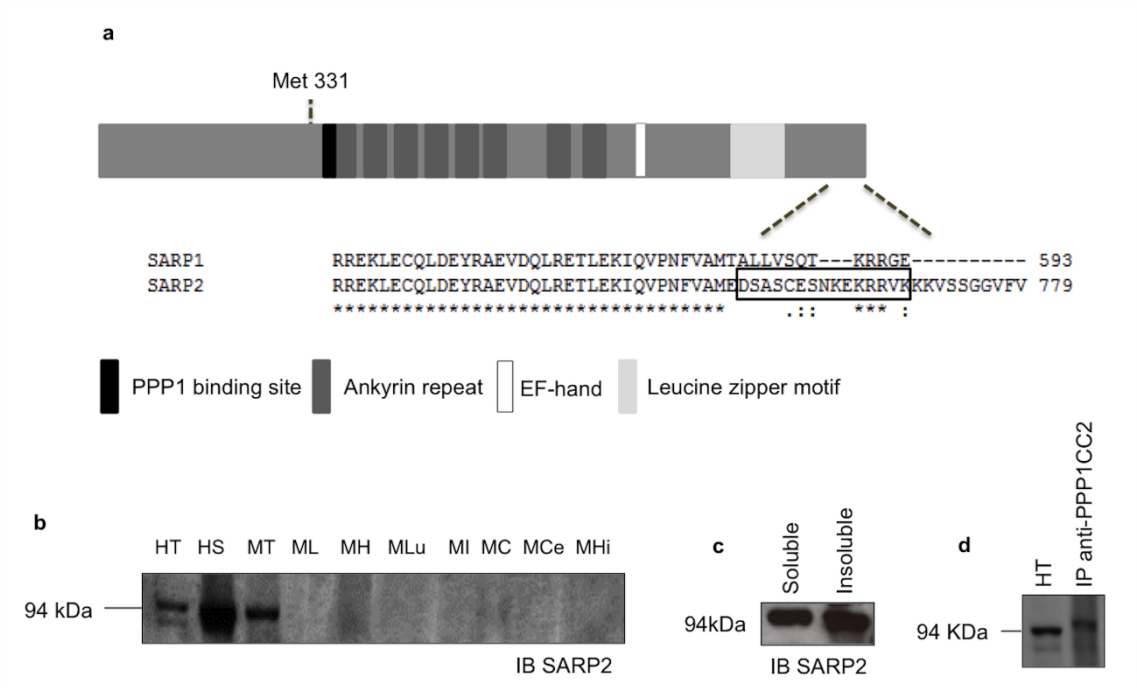

Figure B.10 - Several ankyrin repeat protein variant 2 (SARP2) is enriched in the testis and spermatozoa and binds to phosphoprotein phosphatase 1 (PPP1) catalytic subunit gamma 2 (PPP1CC2) in human spermatozoa. (a) Schematic representation of SARP2 (National Center for Biotechnology Information (NCBI) EF041819.1), an alternatively spliced transcript variant of the ANKRD42 gene (NCBI GeneID: 338699). SARP2 possesses a PPP1-binding motif, eight

ankyrin repeats, a putative EF hand and a putative leucine zipper domain. Homology analysis of the C-termini of SARP isoforms was performed using a CLUSTALW2 (EMBL-EBI, Wellcome Trust Genome Campus, Hinxton, Cambridgeshire, UK) multiple sequence alignment. The black box in the C-terminal indicates the peptide used to generate SARP2 antisera in rabbit. (b) The SARP2 protein expression profile was analysed in extracts of human testis and spermatozoa and other mouse tissues (50 mg) by western blot using SARP2 isoform-specific antibody. The molecular mass of SARP2 (90 kDa) on sodium dodecyl sulfate–polyacrylamide gel electrophoresis (SDSPAGE) is consistent with it possessing the same N-terminal sequence as SARP3 (NCBI: DQ508934). (c) The presence of SARP2 in the RIPA supernatant (soluble fraction) and pellet (insoluble fraction) of sperm lysates was analysed using anti-SARP2 antibody: 50 mg of both fractions were subjected to SDS-PAGE. (d) PPP1CC2 was immunoprecipitated (IP) from human sperm extract using anti-PPP1CC2 antibody and SARP2 was detected with the corresponding antibody. As a control, 50 mg human testis extract was also loaded. HT, human testis; HS, human spermatozoa; IB, immunoblot; MT, mouse testis; ML, mouse liver; MH, mouse heart; MLu, mouse lung; MI, mouse intestine; MC, mouse cortex; MCe, mouse cerebellum; MHi, mouse hippocampus; aa, amino acid.

Expression profiling of SARP2 and PPP1C isoforms in isolated cell fractions of mouse testis

Because of the localisation of SARP2 and PPP1CC2 in mammalian testis, we investigated the mRNA expression of different SARP and PPP1C isoforms during spermatogenesis by RT pPCR using whole testis sample as control. Analyses of the DCT values show that the PPP1CC2 isoform is by far the most abundant isoform in all fractions with 5-, 15-, 40- and 200-fold higher expression than SARP2 and the PPP1CB, PPP1CC1 and PPP1CA isoforms, respectively. We obtained the highest relative gene expression values for all genes at the spermatocyte stage with exception of Ppp1ca gene, in which the expression levels were higher at the round spermatids fraction (1.6-fold). Expression of Ppp1c mRNA was detected in all testicular fractions. Higher relative Ppp1cb and Ppp1cc expression was observed in spermatocytes (2.4- and 1.9-fold, respectively; Figure B.11). In terms of the PPP1CC isoforms, the relative mRNA expression of PPP1CC2 was greater than that of PPP1CC1 (1.6-and 1.1-fold, respectively). The relative expression of PPP1CC1 was not altered during spermatogenesis. Furthermore, although Ppp1cb was strongly expressed in the spermatocyte fraction (2.4- fold), reduced levels were seen in spermatid fractions. Thus, of all the genes analysed, Ppp1cb was the one that underwent the greatest decline in the late stages of spermatogenesis (Figure B.11). Regarding the Ankrd42 gene, the primer that recognises all SARP isoforms exhibited a similar profile compared with the primer specific for the SARP2 isoform. This reinforces our protein expression data, which showed SARP2 as the only isoform present. In addition, the relative expression of SARP2 decreased 0.3-fold in elongated spermatids, similar to what was obtained for the sperm-specific PPP1CC2 isoform (Figure B.11).

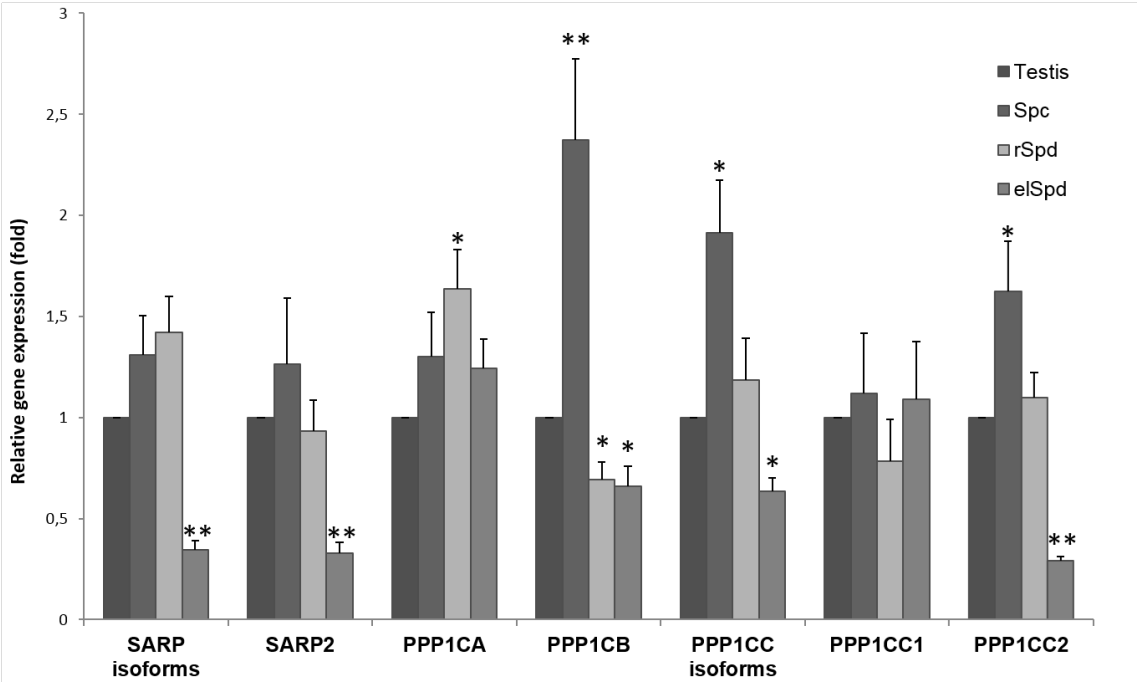

Figure B.11 - Relative gene expression of several ankyrin repeat protein (SARP) and phosphoprotein phosphatase 1 (PPP1) catalytic subunit (PPP1C) isoforms. Relative expression values for the isolated cell fractions were calculated by the ΔΔCT method. *Altered mRNA expression (1.5-fold) compared with control (testis). **Altered mRNA expression (twofold) compared with control (testis). All altered expression values highlighted are significant ($p<0.01$). P-values were calculated based on Student's t-test of the replicate $2(^{-\Delta\Delta CT})$ values for each gene in the control group and treatment groups. Spc, spermatocyte; rSpd, round spermatid; elSpd, elongated spermatid.

Localisation of SARP2 in the testis

Immunofluorescence studies showed that during the course of spermatid differentiation, SARP2 immunoreactivity was first observed in the nucleus of late elongating spermatids (Figure B.12). This localisation of SARP2 was consistent in human and mouse testis. Round spermatids and less mature germ cells showed no specific staining (Figure B.12). Direct evidence of localisation was provided at the ultrastructural level by electron microscopy (Figure B.12 d–f). Electron microscopic studies on human testis also confirmed the association of SARP2 with the nucleus of haploid germ cells, more specifically in elongated and mature spermatids. Round spermatids and more immature germ cells showed no staining (Figure B.12 d–f).

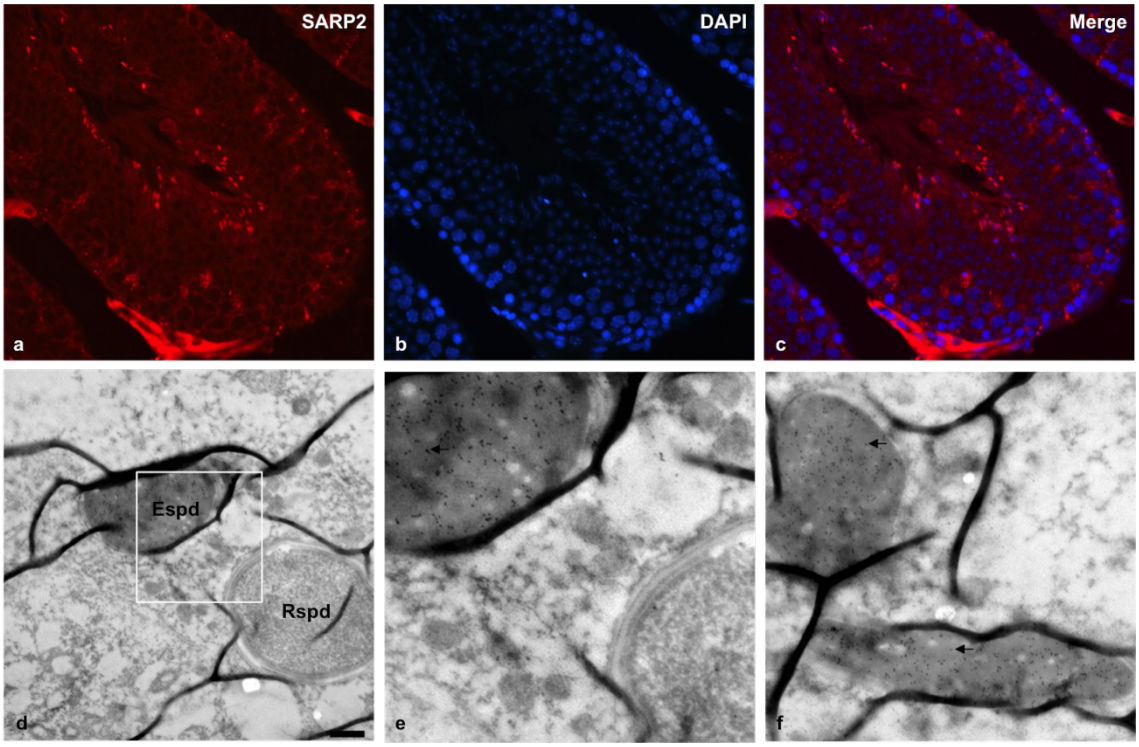

Figure B.12 - Several ankyrin repeat protein variant 2 (SARP2) localisation in the testis. (a–c) Immunofluorescence of SARP2 in mouse testis. Strong immunostaining was observed in elongated spermatids. Identical fluorescence staining patterns were observed in human testis (data not shown). 40, 60-Diamidino-2-phenylindole (DAPI; blue) was used to stain nuclei. Representative images are shown from three independent experiments. (d–f) Electron micrographs of immunoreactivity for SARP2 in human testis. In elongated spermatids (Espd) SARP2 shows significant staining in the nucleus, whereas round spermatids (Rspd) shows no labelling. (e) Higher magnification view of the region indicated by the box in (d). Arrows indicate gold particles indicating positive staining. Representative images are shown from two independent experiments. Scale bar = 500 nm.

Localisation of SARP2 in human spermatozoa

Given the presence of SARP2 in late-stage germ cells, we further analysed the subcellular localisation of this protein in mature human ejaculated spermatozoa. Four human sperm samples were evaluated and a total of 1600 cells was assessed. As seen in Figure B.13 c, SARP2 immunoreactivity was predominantly detected in the connecting piece (54.69%) and in the entire length of the flagellum (100%). In addition, in approximately 33.75% of spermatozoa, staining also appeared in the acrosome (Figure B.13 f). To confirm acrosomal localisation, spermatozoa were capacitated and the acrosome reaction was induced. PSA-FITC was used as an acrosome marker, which means that the acrosome reaction was assessed by disappearance of the labelling. Before the acrosome reaction, the colocalisation pattern between PSA-FITC and SARP2 supported acrosomal localisation of the protein (Figure B.13 e–h). After the acrosome reaction, both SARP2 and PSA staining disappeared, further confirming SARP2 as an intra-acrosomal protein (Figure B.13 i–l). The staining was specific because there was no fluorescence observed in the negative controls, when the primary antibodies were omitted (data not shown).

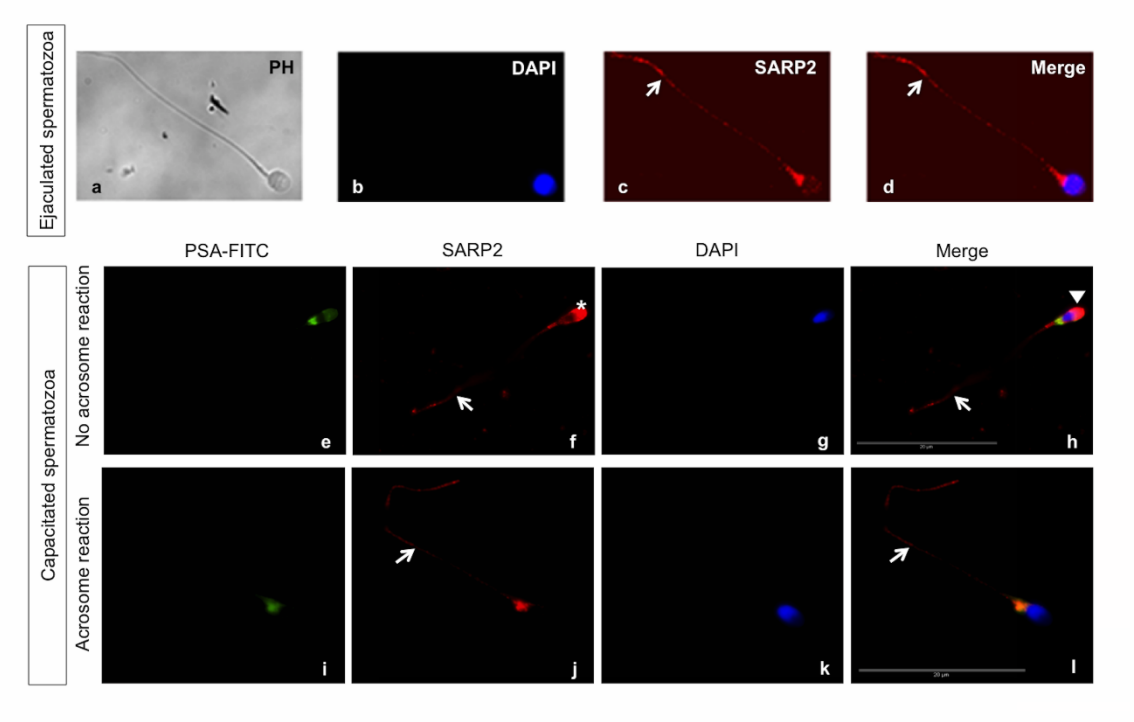

Figure B.13 - Subcellular localisation of several ankyrin repeat protein variant 2 (SARP2) in human spermatozoa. (a–d) Human ejaculated spermatozoa stained with anti-SARP2 antibody and detected using a Texas Red secondary antibody. Representative images are shown from four independent experiments. (e–l) Subcellular localisation of SARP2 in human capacitated spermatozoa stained with: (f, j) anti-SARP2 antibody and detected using a Texas Red secondary antibody before (f) and after (j) the acrosome reaction; (e, i) fluorescein isothiocyanate-labelled Pisum sativum agglutinin (PSAFITC) before (e) and after (i) the acrosome reaction. Arrowheads indicate colocalisation of SARP2 and PSA. Asterisks represent the acrosomal localisation of SARP2 before the acrosome reaction. Arrows indicate staining of SARP2 in the flagellum. Representative images are shown from two independent experiments. Nuclei were stained with 40,60-diamidino-2-phenylindole (DAPI; blue).

SPAG9, a SARP2-interacting protein

To identify proteins capable of interacting with SARP2, an YTH screen was performed with the SARP2 C-terminal as bait. From the 1.1×10^6 clones screened, 513 positives were obtained. The results suggest that SARP2 interacts with several proteins implicated in processes crucial to reproduction, such as cell differentiation, cell motility and cell adhesion. One of the positive clones (clone 71) identified from the human testis library contained a cDNA found to encode the c-Jun-N-terminal kinase (JNK)-interacting protein 4 (also known SPAG9). Sequencing of the clone determined that it corresponds to a new variant of SPAG9, now termed SPAG9 variant 5 and submitted to the NCBI (KJ624756; Figure B.14). Alternative splicing of the SPAG9 gene results in multiple transcript variants. In the GenBank database there are four SPAG9 variants (NM_001130528.2, NM_001130527.2, NM_003971.5 and NM_001251971.1). SPAG9 variant 5 seems to be complete and differs from the rest of the database variants due to the extension of exon 6, which originates a stop codon, giving rise to a shorter isoform (Figure B.14 a). This new isoform encodes a 275-amino acid protein that is missing the coiled coil domains, the leucine zipper motif

and the transmembrane domain described for SPAG9, but possesses the conserved JNK-binding domain (JBD; Figure B.14 b) [24]. Binding of SPAG9 to SARP2 was demonstrated by blot overlay. His6-SARP2 (331–847) expression was induced in bacteria. After SDS-PAGE resolution, samples were transferred onto a nitrocellulose membrane that was incubated successively with recombinant SPAG9 immunoprecipitate, rabbit anti-SPAG9 antibody, anti-rabbit infrared secondary antibodies and developed using the Odyssey infrared-imaging system. Immunoreactive bands of the expected molecular weights were observed, corresponding to the expressed SARP2. Increased quantities of His6-SARP2 resulted in a proportionate increase SPAG9 binding, thus demonstrating its specific interaction with SARP2 (Figure B.14 c). The existence of SARP2–SPAG9 complexes in vivo was shown by co-immunoprecipitation of the latter from human spermatozoa (Figure B.14 d). In addition, and particularly relevant to PIPs, the canonical PPP1 binding motif RVxF was detected in SPAG9 by bioinformatics analysis, 102KFIEF106. Usually, the flanked N- and C-terminus regions of the RVxF motif have four or five basic (KR) and acidic (DE) amino acids, respectively. In this case, the flanked C-terminal region of the RVxF motif is enriched in acidic residues (four of seven residues).

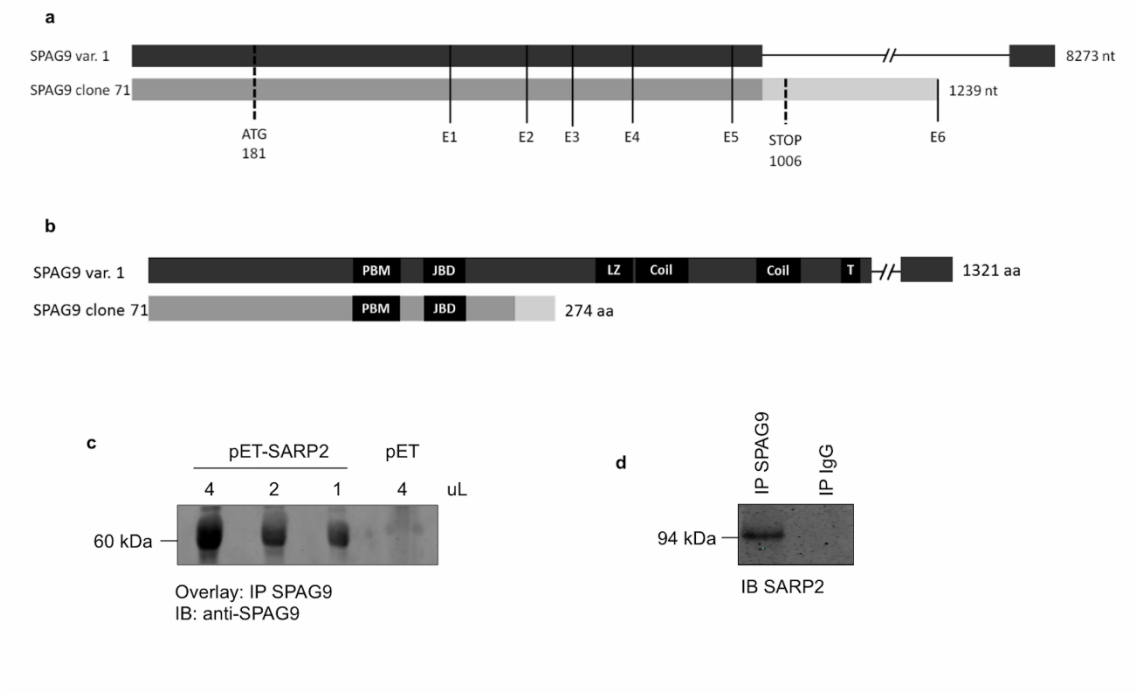

Figure B.14 - Interaction between several ankyrin repeat protein variant 2 (SARP2) and sperm-associated antigen 9 (SPAG9). (a) Schematic illustration of SPAG9 variant 5 encoded by clone 71 and SPAG9 variant 1, previously described in the databases (NCBI, National Center for Biotechnology Information, U.S. National Library of Medicine, USA). SPAG9 transcript variant 1 (NM_001130528.2, NP_001124000.1) represents the longest transcript (8273 bp). The new SPAG9 variant 5 differs in its C-terminus from the other SPAG9 variants described in GenBank (light grey). The end of each exon is indicated. SPAG9 variant 5 coding DNA sequence (CDS) comprises nucleotides (nt) 181–1006, which encode 275 amino acids. (b) Schematic comparison of the protein domain structures of SPAG9 variant 1 and the new SPAG9 variant 5. (c) SARP2 was expressed in bacteria and the membranes overlaid with SPAG9 immunoprecipitate (performed under non-denaturing conditions). Binding was detected with SPAG9 antibody. Lanes 1–3, 4, 2 and 1 mL

bacterial lysate expressing SARP2, respectively; lane 4, 4 mL soluble bacterial lysate expressing pET vector alone. Molecular weights of the proteins are given in kDa. (d) SPAG9 was immunoprecipitated from human sperm extract using SPAG9 antibody and SARP2 was detected with an isoform-specific antibody. aa, amino acids; PBM, phosphoprotein phosphatase 1 binding motif; JBD, c-Jun N-terminal kinase-binding domain; LZ, leucine zipper motif; Coil, extended coiled-coildomain; T, transmembrane domain; IB, immunoblotting; IP,immunoprecipitation;E, exon.

3.3.5. Discussion

The SARP2 interaction was originally identified in an YTH screen of a human testis cDNA library using the PPP1CC isoform as bait [19]. In the present study we show that SARP2 is highly expressed and interacts with PPP1CC2 in human spermatozoa (Figure B.10 b, d). The present study revealed that SARP2 exhibits tissue, cell type and spermatogenic stage enrichment. We showed that SARP2 is more abundant in testis and spermatozoa (Figure B.10 b) and that within the testis SARP2 protein localizes in post-meiotic haploid spermatids, specifically in mid-late stages of elongating spermatids (Figure B.12). The absence of the SARP2 protein in spermatogonia and spermatocytes suggests that SARP2 is translated post-meiotically in humans and mice. Using RT-PCR, we found that both PPP1CC2 and SARP2 are highly transcribed in spermatocytes and round spermatids and that expression falls markedly in elongated spermatids, in which protein abundance is high (Figure B.11 and Figure B.12). The changes that occur during spermiogenesis require the transcription, translation and post-translational modification of numerous constitutive and germ cell-specific gene products during the early steps of spermiogenesis [25,26]. The comparison between RNA and protein expression in the testis is not as simple as in other tissues. Increasing evidence shows that mRNAs are transcribed in early stage germ cells, when the genome is more accessible, and stored to be translated in later stages of spermatogenesis, when the haploid genome repacking makes transcription virtually absent [27]. Therefore, the presence of SARP2 protein in late germ cells (elongating spermatids) does not imply that its mRNA will be increased in these cells. Moreover, it has already been shown that the human spermatozoon is enriched in nucleosomes, histone 3 Lys27 trimethylated (H3K27 me3), H3K4 me2 and H3K4 me3 in regulatory regions of genes with specific functions. Whereas H3K27 me3 tags sperm developmental regulators, H3K4 me2 tags genes relevant to spermatogenesis. The ANKRD42 promoter is enriched in H3K4 me2 and not H3K27 me3, suggesting a role for this gene in spermatogenesis. High enrichment of SARP2 in the nucleus of elongating spermatids (Figure B.12) is consistent with the putative nuclear localisation signal at the N-terminus. In addition to SARP2 expression, the interaction with PPP1CC2 strengthens the idea that it may participate in spermatid development. Furthermore, the peak in PPP1CC2 protein levels in the testis overlaps that of SARP2 [28] in the spermatogenic phase, when PPP1CC2 is essential [10]. In spermatozoa, SARP2 is predominantly localised in the flagellum (Figure B.13), which is similar to PPP1CC2 [9]. The fact that both primary antibodies (anti-PPP1CC2 and anti-SARP2) were raised in rabbits did not allow visualisation of both proteins in the

same preparation. Localisation studies also showed that, to a lesser extent, SARP2 is located in the acrosome (Figure B.13). Nevertheless, the most consistent localisation pattern for SARP2 is the sperm tail, which, together with the interaction with PPP1CC2, may suggest involvement of SARP2 in sperm motility. In further support of this, SARP2 was predominantly expressed in the sperm insoluble fraction, which is consistent with SARP2 being tightly attached to the axoneme with a possible role in sperm motility. Moreover, SARP2 possesses an EF hand-type Ca^{2+}-binding motif and it is well established that Ca^{2+} is pivotal in controlling sperm function [29]. However, we tested binding to Ca^{2+} using ^{45}Ca-binding assay and Ruthenium red staining and no positive binding was obtained (data not shown). Additional studies are required to determine the biological significance of the interaction between SARP2 and PPP1CC2 in testis and spermatozoa. The known actions of SARP2 include the capacity to bind DNA and the ability to inhibit PPP1 catalytic activity [19]. Given that a high level of PPP1C2 catalytic activity suppresses sperm motility [15], further studies are needed to identify the role of this complex in the acquisition of sperm motility. In addition, because a bioinformatics search revealed that SARP2 can be phosphorylated at multiple residues, one can also deduce that SARP2 can be a substrate for PPP1.

To identify proteins capable of interacting with SARP2, an YTH screen was performed with SARP2 C-terminal as bait. One of the 513 positive clones identified from a human testis cDNA library was found to encode a novel SPAG9 variant, a JIP associated with the mitogen-activated protein kinase signalling cascade (Figure B.14). The newly identified SPAG9 variant has lost the extended coiled-coil domains and transmembrane domain, which were previously shown to be essential for dimerisation and proper localisation [24]. The JBD of SPAG9, which is also present in the novel SPAG9 variant, was shown to be involved in JNK interaction (Figure B.14). SPAG9 interacts with higher binding affinity with JNK2 and JNK3 than JNK1 [24]. SPAG9 has been described as a testis-specific protein, transcribed postmeiotically in human and non-human primates [30], that is not only restricted to the acrosome, but also undergoes relocation to the equatorial region in a stage-specific manner during acrosome reaction [24]. In the present study we showed that SARP2 is also located in the acrosome. Studies have shown that anti-SPAG9 antibodies inhibit the binding of human spermatozoa to intact human oocytes, as well as to matched hemizona, indicating that SPAG9 may have a role in sperm–egg interactions [24,31]. Recent studies revealed the location of SPAG9 protein in the flagella of human spermatozoa [32], which is similar to the localisation of SARP2 in the present study and previously described for PPP1CC2 [9]. Because SARP2, SPAG9 and PPP1CC2 colocalise in human spermatozoa, it is reasonable to deduce that the three proteins can be associated and can function as a tri-complex. In addition to the consensus RVxF PPP1 binding motif, SARP2 possesses another PPP1- docking motif, which consists of eight ankyrin repeats (Ank-Cap). The AnkCap motif is involved in substrate selection [33], meaning that

SARP2 can act to prevent or promote the dephosphorylation of substrates by occupying or providing docking sites for substrates (Figure B.15). A bioinformatics search revealed that SPAG9 could be phosphorylated at multiple residues. So, future studies should investigate whether SPAG9 is a PPP1CC2 binding partner and whether it is a substrate for PPP1. In addition, the potential interaction between the testis and spermatozoa-specific proteins SPAG9 and PPP1CC2 may be indirect and mediated by a common interactor, such as SARP2 [34].

In the present study, we have shown conclusively that the SARP2 isoform is highly enriched in testis and spermatozoa. The localisation of SARP2 in late germ cells and in spermatozoa, and its interaction with PPP1CC2 and SPAG9, lays the basis for future studies in spermiogenesis, acrosome reaction and sperm motility. We speculate that the actions of SARP2 can directly affect the catalytic activity of PPP1CC2, or rather regulate PPP1CC2 by modulating its ability to interact with other proteins, namely SPAG9 and JNK, which, in turn, may be involved in the regulation of PPP1CC2 function (Figure B.15).

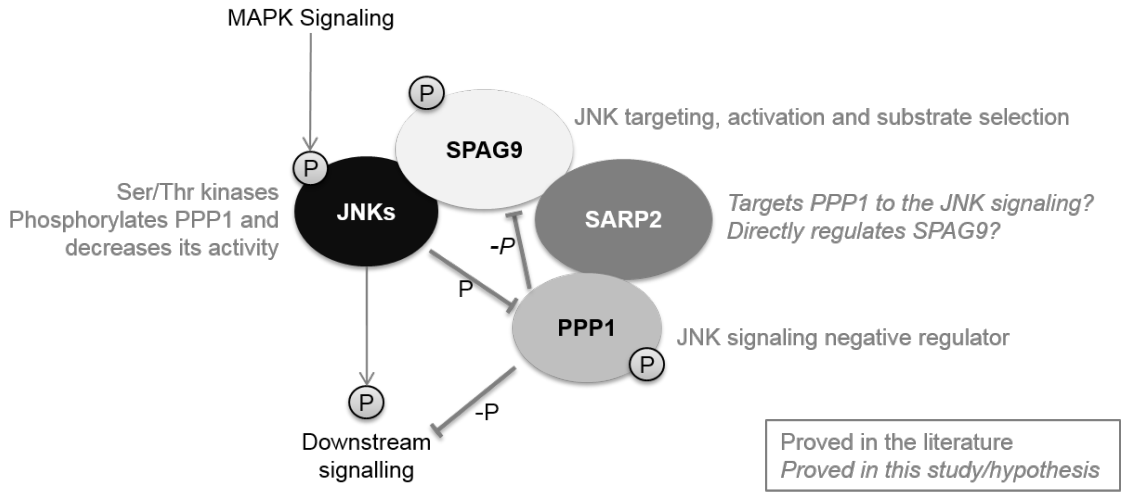

Figure B.15 - Schematic representation of potential relationships between several ankyrin repeat protein variant 2 (SARP2), phosphoprotein phosphatase 1 (PPP1) catalytic subunit gamma 2 (PPP1CC2) and sperm-associated antigen 9 (SPAG9). SPAG9 protein is a c-Jun N-terminal kinase (JNK)-interacting protein (JIP) exclusively expressed in the testis. The JNK modules are regulated by several different scaffold proteins (JIPs), which target the JNK to different subcellular localisations and play roles in kinase activation and/or substrate selection. Effects that are consistent with the model or may be predicted on the basis of studies on other cell types or denote speculation and indicated in red. MAPK, mitogen-activated protein kinase.

3.3.6. References

1. Naz, R. K. & Rajesh, P. B. Role of tyrosine phosphorylation in sperm capacitation / acrosome reaction. *Reprod. Biol. Endocrinol.* 2, 75 (2004).
2. Fardilha, M., Esteves, S. L. C., Korrodi-Gregório, L., Pelech, S., da Cruz e Silva, O. A. B. & da Cruz e Silva, E. Protein phosphatase 1 complexes modulate sperm motility and present novel targets for male infertility. *Molecular Human Reproduction* 17, 466–477 (2011).
3. Korrodi-gregório, L., Ferreira, M., Vintém, A. P., Wu, W., Muller, T., Marcus, K., Vijayaraghavan, S., Brautigan, D. L., Odete, A. B., Fardilha, M. & Edgar, F. Identification and characterization of two distinct PPP1R2 isoforms in human spermatozoa. (2013). doi:10.1186/1471-2121-14-15
4. Korrodi-Gregório, L., Vieira, S. I., Esteves, S. L. C., Silva, J. V, Freitas, M. J., Brauns, A.-K., Luers, G., Abrantes, J., Esteves, P. J., da Cruz E Silva, O. a B., Fardilha, M. & da Cruz E Silva, E. F. TCTEX1D4, a novel protein phosphatase 1 interactor: connecting the phosphatase to the microtubule network. *Biol. Open* 2, 453–65 (2013).
5. Cohen, P. T. W. Protein phosphatase 1--targeted in many directions. *J. Cell Sci.* 115, 241–256 (2002).
6. Ceulemans, H. & Bollen, M. Functional diversity of protein phosphatase-1, a cellular economizer and reset button. *Physiol. Rev.* 84, 1–39 (2004).
7. Fardilha, M., Esteves, S. L. C., Korrodi-Gregório, L., da Cruz e Silva, O. A. B. & da Cruz e Silva, F. F. The physiological relevance of protein phosphatase 1 and its interacting proteins to health and disease. *Curr. Med. Chem.* 17, 3996–4017 (2010).
8. Fardilha, M., Esteves, S. L. C., Korrodi-Gregório, L., Vintém, A. P., Domingues, S. C., Rebelo, S., Morrice, N., Cohen, P. T. W., Da Cruz E Silva, O. A. B. & Da Cruz E Silva, E. F. Identification of the human testis protein phosphatase 1 interactome. in *Biochemical Pharmacology* 82, 1403–1415 (2011).
9. Fardilha, M., Ferreira, M., Pelech, S., Vieira, S., Rebelo, S., Korrodi-Gregorio, L., Sousa, M., Barros, A., Silva, V., da Cruz E Silva, O. a B. & da Cruz E Silva, E. F. 'OMICS' of Human Sperm: Profiling Protein Phosphatases. *OMICS* 17, 460–472 (2013).
10. Varmuza, S., Jurisicova, A., Okano, K., Hudson, J., Boekelheide, K. & Shipp, E. B. Spermiogenesis is impaired in mice bearing a targeted mutation in the protein phosphatase 1cgamma gene. *Dev. Biol.* 205, 98–110 (1999).
11. Forgione, N., Vogl, A. W. & Varmuza, S. Loss of protein phosphatase 1c{gamma} (PPP1CC) leads to impaired spermatogenesis associated with defects in chromatin condensation and acrosome development: an ultrastructural analysis. *Reproduction* 139, 1021–9 (2010).
12. Soler, D. C., Kadunganattil, S., Ramdas, S., Myers, K., Roca, J., Slaughter, T., Pilder, S. H. & Vijayaraghavan, S. Expression of transgenic PPP1CC2 in the testis of Ppp1cc-null mice rescues spermatid viability and spermiation but does not restore normal sperm tail ultrastructure, sperm motility, or fertility. *Biol. Reprod.* 81, 343–52 (2009).
13. Sinha, N., Pilder, S. & Vijayaraghavan, S. Significant Expression Levels of Transgenic PPP1CC2 in Testis and Sperm Are Required to Overcome the Male Infertility Phenotype of Ppp1cc Null Mice. *PLoS One* 7, (2012).
14. Smith, G. D., Wolf, D. P., Trautman, K. C., da Cruz e Silva, E. F., Greengard, P. & Vijayaraghavan, S. Primate sperm contain protein phosphatase 1, a biochemical mediator of motility. *Biol. Reprod.* 54, 719–727 (1996).
15. Vijayaraghavan, S., Stephens, D. T., Trautman, K., Smith, G. D., Khatra, B., da Cruz e Silva, E. F. & Greengard, P. Sperm motility development in the epididymis is associated with decreased glycogen synthase kinase-3 and protein phosphatase 1 activity. *Biol. Reprod.* 54, 709–718 (1996).
16. Virshup, D. M. & Shenolikar, S. From Promiscuity to Precision: Protein Phosphatases Get a Makeover. *Molecular Cell* 33, 537–545 (2009).
17. Heroes, E., Lesage, B., Görnemann, J., Beullens, M., Van Meervelt, L. & Bollen, M. The PP1 binding code: A molecular-lego strategy that governs specificity. *FEBS Journal* 280, 584–595 (2013).
18. Bollen, M., Peti, W., Ragusa, M. J. & Beullens, M. The extended PP1 toolkit: Designed to create specificity. *Trends in Biochemical Sciences* 35, 450–458 (2010).
19. Browne, G. J., Fardilha, M., Oxenham, S. K., Wu, W., Helps, N. R., da Cruz E Silva, O. A. B.,

Cohen, P. T. W. & da Cruz E Silva, E. F. SARP, a new alternatively spliced protein phosphatase 1 and DNA interacting protein. *Biochem. J.* 402, 187–196 (2007).

20. De Jonge, C. J. & Barratt, C. L. R. Methods for the assessment of sperm capacitation and acrosome reaction excluding the sperm penetration assay. *Methods Mol. Biol.* 927, 113–8 (2013).
21. Dastig, S., Nenicu, A., Otte, D. M., Zimmer, A., Seitz, J., Baumgart-Vogt, E. & Lüers, G. H. Germ cells of male mice express genes for peroxisomal metabolic pathways implicated in the regulation of spermatogenesis and the protection against oxidative stress. *Histochem. Cell Biol.* 136, 413–25 (2011).
22. Livak, K. J. & Schmittgen, T. D. Analysis of relative gene expression data using real-time quantitative PCR and the 2(-Delta Delta C(T)) Method. *Methods* 25, 402–8 (2001).
23. Cross, N. L., Morales, P., Overstreet, J. W. & Hanson, F. W. Two simple methods for detecting acrosome-reacted human sperm. *Gamete Res.* 15, 213–226 (1986).
24. JAGADISH, N., RANA, R., SELVI, R., MISHRA, D., GARG, M., YADAV, S., HERR, J. C., OKUMURA, K., HASEGAWA, A., KOYAMA, K. & SURI, A. Characterization of a novel human sperm-associated antigen 9 (SPAG9) having structural homology with c-Jun N-terminal kinase-interacting protein. *Biochem. J.* 389, 73–82 (2005).
25. Eddy, E. M. Male Germ Cell Gene Expression. *Recent Prog. Horm. Res.* 57, 103–128 (2002).
26. Dadoune, J.-P., Siffroi, J.-P. & Alfonsi, M.-F. Transcription in haploid male germ cells. *Int. Rev. Cytol.* 237, 1–56 (2004).
27. Ivell, R., Danner, S. & Fritsch, M. Post-meiotic gene products as targets for male contraception. *Mol. Cell. Endocrinol.* 216, 65–74 (2004).
28. Chakrabarti, R., Kline, D., Lu, J., Orth, J., Pilder, S. & Vijayaraghavan, S. Analysis of Ppp1cc-null mice suggests a role for PP1gamma2 in sperm morphogenesis. *Biol. Reprod.* 76, 992–1001 (2007).
29. Publicover, S. J. Ca2+ signalling in the control of motility and guidance in mammalian sperm. *Front. Biosci.* Volume, 5623 (2008).
30. Shankar, S., Mohapatra, B. & Suri, A. Cloning of a Novel Human Testis mRNA Specifically Expressed in Testicular Haploid Germ Cells, Having Unique Palindromic Sequences and Encoding a Leucine Zipper Dimerization Motif. *Biochem. Biophys. Res. Commun.* 243, 561–565 (1998).
31. JAGADISH, N., RANA, R., MISHRA, D., GARG, M., SELVI, R. & SURI, A. Characterization of immune response in mice to plasmid DNA encoding human sperm associated antigen 9 (SPAG9). *Vaccine* 24, 3695–3703 (2006).
32. Wang, Y., Chen, J., Yu, Z., Xu, X. & Gui, Y. [Expression and location of SPAG9 in human ejaculated spermatozoa]. *Zhonghua Nan Ke Xue* 15, 771–4 (2009).
33. Terrak, M., Kerff, F., Langsetmo, K., Tao, T. & Dominguez, R. Structural basis of protein phosphatase 1 regulation. *Nature* 429, 780–784 (2004).
34. MacLeod, G., Shang, P., Booth, G. T., Mastropaolo, L. A., Manafpoursakha, N., Vogl, A. W. & Varmuza, S. PPP1CC2 can form a kinase/phosphatase complex with the testis-specific proteins TSSK1 and TSKS in the mouse testis. *Reproduction* 147, 1–12 (2014).

3.4. Construction of APP interaction network in human testis: sentinel proteins for male

Joana Vieira Silva[1], Sooyeon Yoon[2], Sara Domingues[3], Sofia Guimarães[3], Alexander V. Goltsev[2], Edgar Figueiredo da Cruz e Silva1[+], José Fernando F. Mendes[2], Odete Abreu Beirão da Cruz e Silva[3], Margarida Fardilha[1]

[1] Laboratory of Signal Transduction, Department of Medical Sciences, Institute of Biomedicine – iBiMED, University of Aveiro, 3810-193 Aveiro, Portugal.

[2] Physics Department, I3N, University of Aveiro, 3810-193 Aveiro, Portugal

[3] Laboratory of Neurosciences, Centre for Cell Biology, Health Sciences Department and Biology Department, University of Aveiro, 3810-193 Aveiro, Portugal

[+] Deceased on 2nd March 2010

Corresponding author: Margarida Fardilha, Departamento de Ciências Médicas, Universidade de Aveiro, Campus Universitário de Santiago, Agra do Crasto – Edifício 30, 3810-193 Aveiro, Portugal. T: +351-918143947. E: mfardilha@ua.pt

Silva JV, Yoon S, Domingues S, Guimarães S, Goltsev AV, da Cruz E Silva EF, Mendes JF, da Cruz E Silva OA, Fardilha M. Amyloid precursor protein interaction network in human testis: sentinel proteins for male reproduction. BMC Bioinformatics. 2015; 16:12. doi: 10.1186/s12859-014-0432-9.

3.4.1. Abstract

Amyloid precursor protein (APP) is widely recognized for playing a central role in Alzheimer's disease pathogenesis. Although APP is expressed in several tissues outside the human central nervous system, the functions of APP and its family members in other tissues are still poorly understood. APP is involved in several biological functions, which might be potentially important for male fertility, such as cell adhesion, cell motility, signaling, and apoptosis. Furthermore, APP superfamily members are known to be associated with fertility. Knowledge on the protein networks of APP in human testis and spermatozoa will shed light on the function of APP in the male reproductive system. We performed a Yeast Two-Hybrid screen and a database search to study the interaction network of APP in human testis and sperm. To gain insights into the role of APP superfamily members in fertility, the study was extended to APP-like protein 2 (APLP2). We analyzed several topological properties of the APP interaction network and the biological and physiological properties of the proteins in the APP interaction network were also specified by gene ontologyand pathways analyses. We classified significant features related to the human male reproduction for the APP interacting proteins and identified modules of proteins with similar functional roles, which may show cooperative behavior for male fertility. The present work provides the first report on the APP interactome in human testis. Our approach allowed the identification of novel interactions and recognition of key APP interacting proteins for male reproduction, particularly in sperm-oocyte interaction.

3.4.2. Introduction

Amyloid precursor protein (APP) is known as a pathological hallmark of Alzheimer's disease (AD). Nevertheless, APP, a type I transmembrane glycoprotein consisting of a large extracellular domain, a single transmembrane domain, and a short cytoplasmic tail, is expressed ubiquitously and given its receptor-like and adhesive characteristics may play important roles outside the nervous system. In fact, we have previously showed that APP is present in spermatozoa [1]. The APP superfamily includes APP and APP-like proteins (APLP) 1 and 2. Alternative splicing of the APP mRNA produces eight isoforms, ranging in size from 677-770 amino acids [2]. Alternative splicing produces four APLP1 and two APLP2 protein isoforms. Although some isoforms may be cell type specific, APP and APLP2 are ubiquitously expressed. In contrast, APLP1 is expressed selectively in the nervous system [3]. Only APP, but not APLP1 and 2, contains a sequence encoding the beta-amyloid domain. The transmembranar structure of APP is consistent with a role of APP as a receptor or a mediator of extracellular interactions. It has been suggested that APP may have CAM (Cell Adhesion Molecule) and SAM (Substrate Adhesion Molecule) like activities [4].

Various lines of evidence implicate APP and APLP2 in fertility. APP was shown to be expressed in rat testis and localized in the acrosome region and growing tail of spermatids in the seminiferous tubules [5]. Knock-out mice, homozygotes to either APP(-/-) or APLP2(-/-) were fertile, but mice with the deletion of both APP(-/-) and APLP2(-/-) were infertile (9 of 10 females and all males) [6]. We previously characterized the subcellular distribution of the APP superfamily members in spermatozoa using a variety of antibodies that either recognizes APP-specific epitopes or the epitopes shared with other APP family members [1]. The presence of APP superfamily members along the entire length of the tail may be related to signaling events involved in sperm motility, whereas their presence in the head and particularly in the equatorial region suggests their involvement in sperm-oocyte interaction [1]. These results not only were consistent with the previous localization of APLP2 in mammalian sperm, but also prove the presence of APP itself in human sperm. APP and APLPs distribution only partially overlap suggesting that, besides a common role, they might also have distinct functions in spermatozoa. A human sperm transmembrane protein initially termed YWK-II (later shown to be an APLP2 homologue) was shown to be involved in fertilization [7,8]. The YWK-II gene was shown to be expressed in germ cells at various stages of differentiation and in the plasma membrane enveloping the acrosome of mature spermatozoa [7].

The discovery of tissue-specific interacting proteins can lead to the identification of pathways for the APP family members associated with testis and sperm functions. Hence, we performed a Yeast Two-Hybrid (YTH) screen of a human testis cDNA library using APP as bait. A comprehensive bioinformatic analysis was also performed using the APP interacting proteins identified in the YTH in addition to the proteins selected from public protein-protein interactions (PPI) databases (DB) and published APP interactome data [9] associated with testis/sperm. APLP2 interacting partners were also included. Additionally, protein interaction maps were constructed allowing the visualization of PPI data as a connectivity graph and the data was subjected to a statistical analysis based on the complex network theory. The advantage of this approach is that it allows the study not only of the local properties of proteins in the network, but also their global structural characteristics in the entire network of PPI. We reveal that proteins with similar biological functions are tightly connected to each other and form dense groups (modules or *k*-cores) in the networks. Also, the function, cellular distribution and pathways were analyzed and significant features were classified.

3.4.3. Methods

Human testis library screening by Yeast Two-Hybrid

The APP cDNA was directionally subcloned into EcoRI/BamHI digested pAS2-1 (GAL4 binding domain expression vector) to produce pAS-APP. This expression vector was first used to confirm the expression of the resulting fusion proteins (GAL4-APP) in yeast strain AH109. For library

screening, the yeast strain AH109 transformed with pAS-APP, was mated with yeast strain Y187 expressing the human testis cDNA library in the pACT-2 vector (Gal4 activation domain expression vector). Half the mating mixture was plated onto high stringency medium (quadruple dropout medium (QDO): SD/-Ade/-His/-Leu/-Trp) and the other half onto low stringency medium (triple dropout medium (TDO): SD/-His/- Leu/-Trp), and the plates were incubated at 30ºC. Colonies obtained in the low stringency plates were replica plated onto high stringency medium. Finally, all high stringency surviving colonies were plated onto selective medium containing X-α-Gal and incubated at 30ºC to check for MEL-1 expression (indicated by the appearance of a blue colour) [10]. All the YTH reagents were purchased from Enzifarma, Clontech, Portugal. All other nonspecified reagents were purchased from Sigma-Aldrich, Portugal. This study did not require ethics approval since the material used was purchased for Enzifarma, Clontech, Portugal (human testis cDNA library which contained cDNAs already inserted in pACT-2 vector.

Recovery of plasmids from yeast and sequence analysis

Yeast plasmid DNA was recovered and used to transform E. coli XL1-Blue. Plasmid DNA was obtained from each resulting bacterial colony and digested with the restriction enzyme HindIII (NEB, Ipswich, USA) to identify the corresponding library plasmids. DNA sequence analysis was performed using an Automated DNA Sequencer (Applied Biosystems, Carlsbad, USA) using the GAL4-AD primer - TACCACTACAATGGATG (Enzifarma, Clontech, Portugal). The DNA sequences obtained were compared to the GenBank DB, using the BLAST algorithm, to identify the corresponding encoded proteins.

Data mining of APP and APLP2 interacting proteins from public DB and published interactome

Several data sources were used to human protein-protein interaction data retrieval. First, we collected all interaction data of human proteins from: APID [11], BioGRID [12], DIP [13], HPRD [14], InnateDB [15], Intact [16], MINT [17], Reactome [18], TopFind, and STRING [19]. The interaction search was restricted to Homo sapiens (Human, 9606) protein pairs. Then, only the interactions defined as "association (MI:0941)" under the interaction type categories (http://www.ebi.ac.uk/ontology-lookup/browse.do?ontName=MI) and "experimental interaction detection (MI:0045)" from STRING were extracted. Next, we unified protein names based on the Uniprot ID and gene symbols in order to prevent abundant interactions caused by the different notations for the same gene between DBs. We removed proteins which have unreviewed, no gene symbols or Uniprot IDs, and removed (obsolete) genes from the Uniprot database up to the date of our data-mining and their interactors from our PPI list. We also included the interacting proteins from the published

APP interactome [9] and the YTH experiment (37 proteins). Finally, 248,714 interactions between 15,189 proteins were obtained in total.

Identification of testis/sperm specific proteins in public DBs and publish human proteomes

From the large PPI data obtained in the previous data-mining, we narrowed down the candidate proteins into the testis/sperm enriched proteins. We first used three distinct data sources to select the proteins associated with the testis: UniProt [20], UniGene [21] and the Human Protein Reference Database (HPRD) [14]. From UniGene expressed sequence tags (ESTs) from Homo sapiens were used as source of gene expression data. Among our previous interaction data set, we chose all proteins associated with the keywords ‘‘testis’’ and/or “sperm” in the description of tissue-specificity. Then, we kept the interactions, if both proteins in a pair of interaction were associated to testis/sperm. We got totally 155,457 interactions among 12,884 proteins in this procedure.

Second, tissue-expression DBs (C-It, TiGER, UniGene, BioGPS, VeryGene and HPA) were used in order to identify the interactors characterized as highly specific or strongly expressed in testis/sperm. The C-it DB was queried with the keywords, 'testis-enriched' for 'Human'. The limitation factors for the literature information were 5 for PubMed and 3 for MeSH terms. Proteins with a SymAtals z-score higher than |1.96| were chosen. The TiGER and the Very Gene database were also searched for 'Testis' in 'Tissue View' category. In HPA (Human Protein Atlas), proteins listed within the fields of high or medium HPA evidence and annotated protein expression based on IHC staining patterns in normal male reproductive tissues were selected. Also, the BioGPS was used to find testis/sperm restricted proteins with the keywords, 'testis, sperm, epididymis, spermatid, spermatogonia, spermatozoa, spermatocyte' in 'Human'. Using the plugin 'Gene expression/activity chart', the proteins with highly/strongly expressed in testis were selected. If the expression level was less than mean value or the data were not shown, those proteins were removed from the list. Also the proteins with high correlation level of expression ($\geq$0.9) with testis-specific proteins, such as ACRV1, AKAP4, BRDT, PGK2, TSGA10, and TSPY8 were selected. From this search, 1,949 testis/sperm enriched proteins were obtained.

Development of protein-protein network and network properties analysis

From testis/sperm enriched proteins, APP/APLP2 interactors were selected. Functional relationships can be neglected when considering only tissue-enriched/specific proteins. This challenge was addressed by integrating tissue-enriched/specific APP/APLP2 interactors with its interacting proteins regardless whether they were enriched or not. Using the breath-first searching (BFS) algorithm, direct connectors with APP and the interactions between those proteins were kept. The same procedure was applied to APLP2. Since APLP2 is the nearest neighbor of APP, we combined two sub-networks and analyzed several network properties. We extended this local

network to the second order neighbors of APP in order to see the wide relations around APP and APLP2. All YTH data were included in this process. Finally, 1,803 interactions between 457 proteins were obtained for the local APP/APLP2 network and 17,188 interactions between 2,733 proteins for the extended APP/APLP2 network.

Bioinformatic analyses: gene ontology, pathways and involvement in diseases

The interactome was analyzed using the Database for Annotation, Visualization and Integrated Discovery (DAVID) v6.7 [22]. The UniProt [20] identifiers (UniProt_ID) for the proteins were entered into the DAVID functional annotation program. Overall, the proteins were analyzed for gene ontologies and pathways using the Homo sapiens genome-wide genes with at least one annotation in the analyzing categories as background. Proteins associated with defects in male fertility, or a functional or morphological defect in the epididymis, testis, or sperm were obtained from the Jackson Laboratories mouse knockout database (http://www.informatics.jax.org/). To obtain a list of the genes that have a male infertility phenotype, we also queried the OMIM [23], Phenopedia [24] and the Uniprot database [20] with the term "male infertility", and then downloaded the associated genes.

3.4.4. Results

In this study, we characterized the testis/spermatozoa interactome of APP using a network-based approach (Figure B.16).

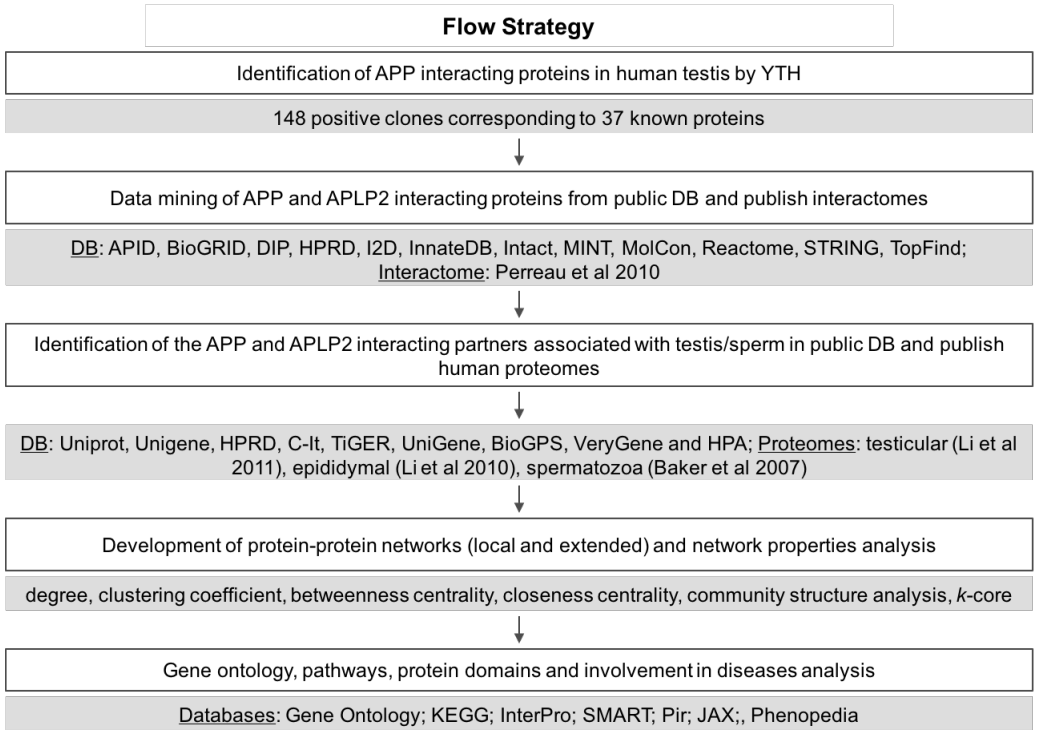

Figure B.16 - Experimental methodology.

Identification of APP interacting proteins in human testis by Yeast Two-Hybrid screening

Nowadays the YTH methodology is a very robust technique to identify PPI [10,25,26]. The method that we use has been highly improved and overcomes the initial problems of the YTH, e.g. the appearance of false positive or false negative interactions [27], since, for instance, we use four reporter genes with different strength promoters [10,25,26].

In order to identify APP interacting proteins expressed in human testis, an YTH screen of a human testis cDNA library was carried out using full-length human APP. The screen yielded 147 positive clones from a total of $3x10^8$ clones screened. After partial or complete sequence analysis (depending on the length of the positive clone's cDNAs), in silico searches of the GenBank DB allowed their identification and classification into three separate groups. Table B.4 corresponds to library inserts encoding known proteins identified as putative APP interactors. The second and third groups correspond to clones putatively encoding novel APP interacting proteins with homology to genomic sequences and lists positives where the GenBank sequence similarity did not correspond to an annotated gene and false positive hits, respectively. Table B.4 lists only 1 positive encoding a previously identified APP interacting protein (RANBP9) (Figure B.17). 77 clones encoded 36 known proteins that were not previously associated with APP (Figure B.17). Only the clones in Table B.4 were included in the network and further functional analyses.

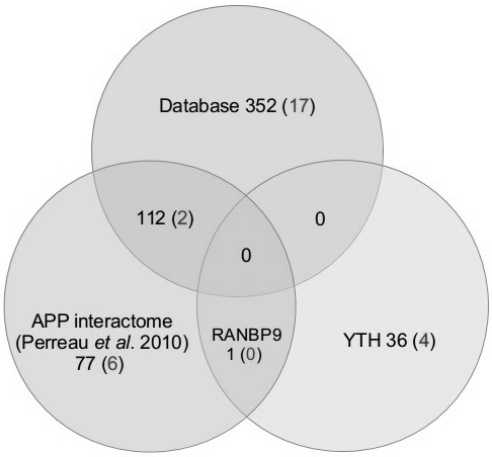

Figure B.17 - Diagram for the number of proteins interacting with APP from each dataset. The numbers indicate testis/sperm-annotated proteins interacting with APP from the different data sources; the numbers within parentheses represent the proteins enriched in testis and sperm. Self-connection for APP was neglected.

Table B.4 - Human testis cDNA library inserts encoding known proteins identified as putative APP interactors.

	GenBank acession	Uniprot ID	Gene symbol	Protein name	Chr	No. of clones
1	NM_022735	Q9H3P7	ACBD3	Golgi esidente protein GCP60	1	1
2	NM_007247	Q9UMZ2	SYNRG	Synergin gamma	17	2
3	NM_007348	P18850	ATF6	Cyclic AMP-dependent transcription factor ATF-6 alpha	1	5
4	NM_018844	Q9UHQ4	BCAP29	B-cell receptor-associated protein 29	7	1

	GenBank acession	Uniprot ID	Gene symbol	Protein name	Chr	No. of clones
5	BC002461	Q12982	BNIP2	BCL2/adenovirus E1B 19 kDa protein-interacting protein 2	15	1
6	NM_020531	Q9HDC9	APMAP	Adipocyte plasma membrane-associated protein	20	2
7	NM_001745	P49069	CAMLG	Calcium signal-modulating cyclophilin ligand	5	4
8	NM_019052	Q8TD31	CCHCR1	Coiled-coil alpha-helical rod protein 1	6	1
9	NM_004356	P60033	CD81	CD81 antigen	11	5
10	NM_002414	P14209	CD99	CD99 antigen	X/Y	7
11	NM_000747	P11230	CHRNB1	Acetylcholine receptor subunit beta	17	2
12	NM_030782	Q96KA5	CLPTM1L	Cleft lip and palate transmembrane protein 1-like protein	5	1
13	NM_006837	Q92905	COPS5	COP9 signalosome complex subunit 5	8	3
14	NM_006368	O43889	CREB3	Cyclic AMP-responsive element-binding protein 3	9	1
15	NM_021227.3	Q9NRP0	OSTC	Oligosaccharyltransferase complex subunit OSTC	4	3
16	NM_004413	P16444	DPEP1	Dipeptidase 1	16	5
17	NM_024293	Q8NC44	FAM134A	Protein FAM134A	2	1
18	NM_020937	Q8IYD8	FANCM	Fanconi anemia group M protein	14	2
19	NM_000146	P02792	FTL	Ferritin light chain	19	1
20	NM_002510	Q14956	GPNMB	Transmembrane glycoprotein NMB	7	1
21	NM_002213	P18084	ITGB5	Integrin beta-5	3	1
22	NM_018559	Q8IXQ4	KIAA1704	Uncharacterized protein KIAA1704	13	2
23	NM_024874	Q8IZA0	KIAA0319L	KIAA0319-like, transcript variant 1		1
24	NM_014400	O95274	LYPD3	Ly6/PLAUR domain-containing protein 3	19	1
25	NM_005493	Q96S59	RANBP9	Ran-binding protein 9	6	4
26	NM_002951	P04844	RPN2	Dolichyl-diphosphooligosaccharide--protein glycosyltransferase subunit 2	20	1
27	NM_005086	Q14714	SSPN	Sarcospan	12	3
28	NM_004206	Q9BRL7	SEC22C	Vesicle-trafficking protein SEC22c	3	9
29	NM_003164	Q13190	STX5	Syntaxin-5	11	1
30	NM_003487	Q92804	TAF15	TATA-binding protein-associated factor 2N	17	1
31	NM_016495	Q9P0N9	TBC1D7	TBC1 domain family member 7	6	1
32	NM_182559	Q86WS5	TMPRSS12	Transmembrane protease serine 12	12	1
33	NM_003270	O43657	TSPAN6	Tetraspanin-6	X	3
34	NP_001001790	Q8N4H5	TOMM5	Mitochondrial import receptor subunit TOM5 homolog	9	1
35	NM_001242313.1	P0C7N4	TMEM191B	Transmembrane protein 191B		1
36	NM_001207052.1	A6NGB0	TMEM191C	Transmembrane protein 191C		
37	NR_003377	A8MUH7	PDZK1P1	Putative PDZ domain-containing protein 1P	1	1

Analysis of the YTH screen revealed that the most abundant interaction was detected with SEC22C (9 out of the 147 positive clones). This protein is involved in vesicle transport between the ER and the Golgi complex.

The 37 proteins identified as APP interactors were classified into broad functional categories according to Gene Ontology annotation using the DAVID bioinformatics resource (Supplementary Table D.18). Regarding the biological process, the categories with the largest number of proteins were related to intracellular transport (20.6%) and protein localization (20.6%). From the proteins involved in transport, 5 were linked with vesicle-mediated transport (SYNRG, BCAP29, SEC22C,

FTL and STX5). Also, 5 proteins (CD99, LYPD3, GPNMB, ITGB5 and SSPN) were associated with cell adhesion. CD81, CREB3 and FANCM were annotated as being involved in reproduction. The majority of APP interactors identified in the YTH (67.6%) are intrinsic to membrane and 7 are specifically at the plasma membrane (Supplementary Table D.18). Analysis of human proteomes (testis, epididymis, and spermatozoa) allowed the classification of DPEP1 and TMPRSS12 as testicular proteins; ITGB5 and COPS5 as sperm-located testicular proteins also detected in epididymal fluid; and FTL as a non-sperm located epididymal fluid protein (Supplementary Table D.19). CD81, CD99, COPS5 and FAM134 were identified as testis/sperm-enriched in tissue-expression DBs [28–31]. Also, TMPRSS12 was reported in the Unigene as a testicular/spermatozoa restricted protein. To determine which proteins are known to be important for normal male reproductive function, the dataset was screened against the Jackson Laboratory mutant mouse DB [23] and Phenopedia [24]. From the APP interactors identified in the YTH screen, 3 were connected with reproductive phenotypes in gene knockout models (RANBP9, CREB3 and FANCM). From the comparison with the disease genes listed in Phenopedia no results were obtained.

Identification of literature curated interactions

In order to identify the potentially relevant interactors of APP and APLP2 to male fertility, human PPI were collected from currently available public DBs, including APID [11], BioGRID [12], DIP [13], HPRD [14], InnateDB [15], Intact [16], MINT [17], Reactome [18], TopFind, and STRING [19]. Only the interactions between both proteins associated with the terms “testis” and “sperm” in Unigene [21], HPRD [14] and Uniprot [20] were selected. Then, the interactors characterized as highly specific to or strongly expressed in testis/sperm were identified from tissue-expression DBs (C-It [28], TiGER [29], UniGene [21], BioGPS [32], VeryGene [30] and HPA [31]). (See Methods and Supplementary Table D.20). Besides the DBs, the tissue expression data was also retrieved from the published proteomes of reproductive tissues [33–36]. This analysis allowed the classification of the APP direct interactors into distinct but overlapped localizations. First, we focused on local interactions of APP/APLP2, that is, the first direct interactors of APP/APLP2 and interactions between them. We identified 455 proteins connected to APP (Methods) including the partners identified by YTH (Figure B.18 a). All the proteins in the YTH data were newly found as interactors of APP except RANBP9, which was previously published as an APP interactor [9]. The absence of protein overlapping may be due to the fact that the YTH was performed using a library from human testis and the previous APP interactors were mainly identified in neuronal tissues. Indeed, published data indicate that 4% of the mammalian genome (more than 2,300 genes) encodes genes specifically expressed in the male germ line during or after the completion of spermatogenesis. Regarding APLP2, we identified 6 proteins (including APP) as its interactors from the DBs which were highly specific to or strongly expressed in testis. In total, 1,803 interactions were identified between 457 proteins including APP

and APLP2. Only one protein (BRCA1) among the nearest neighbors of APLP2 was not directly connected to APP which may reflect an isoform-specific role for APLP2.

Second, we extended the local interaction network of APP/APLP2 into the second nearest neighborhoods since the local network of APP could limit an overview of the pathways in which this protein may be involved in testis and spermatozoa. In this network, we had 2,733 proteins and17,188 interactions between them (Methods).

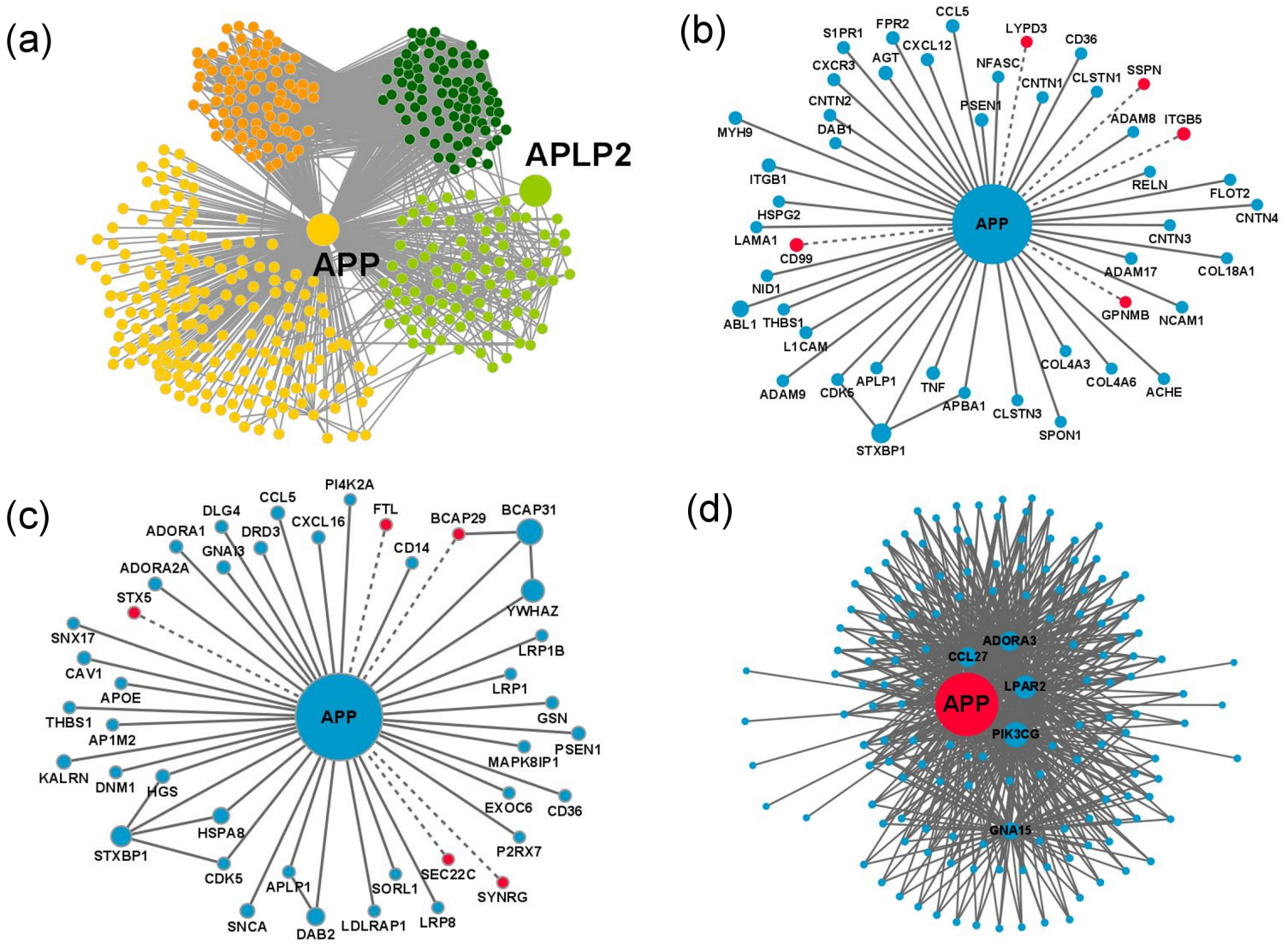
(a)
APLP2
APP
(b)
APP
CCL5
S1PR1
FPR2
CXCL12
LYPD3
CD36
CXCR3
AGT
NFASC
CNTN1
CLSTN1
SSPN
CNTN2
PSEN1
ADAM8
ITGB5
MYH9
DAB1
ITGB1
RELN
FLOT2
CNTN4
HSPG2
LAMA1
CNTN3
CD99
ADAM17
COL18A1
NID1
GPNMB
NCAM1
ABL1
THBS1
L1CAM
COL4A3
COL4A6
ACHE
ADAM9
CDK5
APLP1
TNF
APBA1
CLSTN3
SPON1
STXBP1
(c)
APP
PI4K2A
CCL5
DLG4
FTL
BCAP29
BCAP31
ADORA1
CXCL16
DRD3
CD14
GNAI3
ADORA2A
YWHAZ
STX5
SNX17
LRP1B
CAV1
LRP1
APOE
GSN
THBS1
PSEN1
AP1M2
MAPK8IP1
KALRN
DNM1
HGS
EXOC6
CD36
HSPA8
P2RX7
STXBP1
CDK5
SEC22C
APLP1
SORL1
SYNRG
SNCA
DAB2
LDLRAP1
LRP8
(d)
APP
ADORA3
CCL27
LPAR2
PIK3CG
GNA15

Figure B.18 - APP protein-protein interaction networks. (a) Local APP/APLP2 network. Proteins with light orange (M1) and dark orange (M4) are mostly involved in G-protein coupled receptor protein signaling pathway (Biological Process; BP) and located at the plasma membrane (Cellular Component; CC). Proteins with light green (M2) and dark green (M3) are mostly involved in regulation of apoptosis (BP) and located at the cell surface (CC). (b) Subnetwork of APP interactors involved in cell adhesion (BP) extracted from the extended APP/APLP2 protein-protein interaction network. (c) Subnetwork of APP interactors involved in vesicle-mediated transport (BP) extracted from the extended network. Red colored nodes represent the proteins from the YTH screen. Blue colored nodes indicate interactors extracted from the DBs. Node size represents relative degree of the nodes and the other interactions of nodes are neglected for the sake of simplicity. Dashed lines represent the interactions revealed by the YTH screening in human testis and solid lines are interactions from DBs. (d) Subnetwork of APP interactors involved in G-protein-coupled singnal pathways.

Topological analysis of APP/APLP2 PPI network

The overall structural properties for the local and extended APP/APLP2 network showed mostly linear relationship between degree [the number of nearest neighbors (connectivity) of a certain node] and betweenness centrality [fraction of shortest paths between all other nodes that pass through a certain node (Supporting Text)]. In our APP/APLP2 local network, proteins with high connectivity also revealed high centrality which can be a significant indication of the relevant proteins in a biological network.

Local APP/APLP2 interaction network

In the testis/sperm related APP/APLP2 network (Figure B.18 a), most proteins were densely connected to each other. Average degree of this network was <q> = 3.95 and global clustering coefficient was C = 0.51. The clustering coefficient reflects how neighbors of a node are connected to each other (Supporting Text). It is known that proteins with high connectivity (hubs) in PPI networks potentially have functional importance in biological systems and are likely to be critical proteins [37]. The key proteins for disease are known to have low clustering coefficients in addition to high connectivities [38]. In order to characterize the APP network topology, the clustering coefficients of each protein were calculated. Betweenness centrality and closeness centrality of each protein in the APP/APLP2 network were also measured to find the relevant proteins involved in pathways (Supporting Text). In biological networks, e.g. signaling pathways and genetic interactions, the dysfunction of the proteins with high centrality may be crucial for the other biological functions due to missing of signal transference. In yeast, the proteins with high betweenness centrality, but small number of degrees were found to be important links between well connected modules [39]. Proteins with high centrality rank in our network were represented in Supplementary Table D.21. The top rated interactors included a calcium/phospholipid-binding protein which promotes membrane fusion and is involved in exocytosis (ANXA1, annexin A1). PIK3CG (phosphatidylinositol 4,5-bisphosphate 3-kinase catalytic subunit gamma isoform), PLCB3 (1-phosphatidylinositol 4,5-bisphosphate phosphodiesterase beta-3), LPAR2 (lysophosphatidic acid receptor 2), RLN3 (relaxin-3 receptor 2) and ADORA3 (protein ADORA,

isoform 3) also composed the top rated proteins and were all related with the G-protein coupled receptor signaling pathway.

The proteins identified as APP/APLP2 interactors were classified into functional categories according to Gene Ontology annotation using the DAVID program [22]. Regarding the biological process, the results revealed that the categories with the largest number of proteins were related to cell surface receptor linked signal transduction (43.0%; p value = 7.0E-60) and G-protein coupled receptor protein signaling pathway (33.3%; p value = 7.5E-58). 50.8% of the proteins were located at the plasma membrane (p value = 2.4E-26) and 23.2% in the extracellular region (p value = 1.7E-6). 13.0% were associated with vesicles (p value = 1.8E-11). These vesicle related proteins may participate in specialized vesicle activity in the testis, such as acrosome formation. Additionally, 13.9% are annotated as part of a cell projection (e.g. a flagellum) (p value = 1.0E-12).

Metabolic pathways were analyzed using the KEGG PATHWAY [40], which indicated that the top 4 significant categories were: Neuroactive ligand-receptor interaction (16.3%; p value = 2.5E-34); Chemokine signaling pathway (10.4%; p value = 1.3E-18); Calcium signaling pathway (8.6%; p value = 1.8E-13); and Progesterone-mediated oocyte maturation (5.5%; p value = 2.2E-11).

In order to find the core and peripheral part of the local APP/APLP2 network, k-core analysis was performed. k-core is a subgraph of a graph in which all vertices have at least k-degree (Supporting Text). The core of this network has a connectivity, k = 11, between them. 75.0% of the proteins within this core shared the same biological process GO category (G-protein coupled receptor protein signaling pathway; p value = 6.6E-15) and 50.0% share the same subcellular localization (plasma membrane; p value = 6.9E-4).

Four modules were identified by community detection analysis (Supporting Text). The nodes in a community are more tightly connected to each other than to nodes out of the community and may perform a common function. Our analysis shows that, in the local APP/APLP2 network, 206 proteins are included in module 1 (light orange in Figure B.18 a). Among them, 19.7 % were involved in the regulation of apoptosis (p value = 1.5E-12) and the most significant represented cellular localization was the cell surface (16.3%, p value = 2.3E-17. The most prominent biological process detected in module 2 (which comprised 84 proteins in total, dark green in Figure B.18 a) was G-protein coupled receptor protein signaling pathway (76.2 %; p value = 6.6E-52) and 71.4 % of the proteins in module 2 shared the same localization (plasma membrane; p value = 5.6E-15). Module 3 included 85 proteins (light green in the Figure B.18 a), which were mainly involved in G-protein coupled receptor protein signaling pathway (94.0%; p value = 5.0E-80) and localized at the plasma membrane (76.2%, p value = 2.5E-18). Similarly to module 1, the most significant category in module 4 (which comprised 82 proteins in total, dark orange in Figure B.18 a) was

regulation of apoptosis (39.0%, p value = 4.8E-19). Modules 2 and 3 also share a common biological function and cellular component. In the local APP/APLP2 network, the core part of the network, that is, the proteins with the highest k-core (k=11) which includes APP, shared the same biological function (G-protein coupled receptor protein signaling pathway). The core part was included mostly in module 2, which was also associated with the same function. Therefore, this result showed that APP might be involved in G-protein coupled receptor protein signaling pathway in human testis/sperm. In addition, APP has high possibility that it is associated with regulation of apoptosis according to the results that the most interaction partners surrounding APP share the same function within modular structure.

Extended APP/APLP2 network

The local APP network only allows us to study relationships between APP and its nearest neighboring proteins. In order to study relationships with other proteins, we extended the network to the second nearest neighbors of APP. Topological properties of the extended networks are analyzed in Supplementary Table D.22. From *k*-core analysis, a densely connected group with high k (= 17)-core was found (186 proteins). The proteins in the core were involved in cell cycle (41.1%; p value = 6.4E-46). Also, the majority of proteins were found in the cytosol (49.2%; p value = 1.0E-41) and the nucleoplasm (40.0%, p value = 2.0E-38).

Based on the community structure analysis, APP is located in module 2. The most significant biological processes associated with this module were proteolysis (19.3%; p value = 6.6E-9) and cell adhesion (15.9%; p value = 1.3E-9). Additionally, the majority of proteins were located at the plasma membrane (42.0%; p value = 1.3E-6) and at the extracellular region (32.4%; p value = 5.4E-12). Table B.5 represents the gene ontology analysis for the modules of the extended network in which at least 40% of proteins shared a biological function.

Table B.5 - Enriched GO categories for each module of the extended network. Only modules with at least 40.0% of the proteins sharing a biological function are represented. M, modularity.

M	Most significant Biological Process			Most significant Cellular Component		
	GO term	p value	%	GO term	p value	%
4	cell cycle	2.7E-82	60.2	cytosol	4.3E-41	48.8
	regulation of ubiquitin-protein ligase activity during mitotic cell cycle	1.3E-130	41.0	proteasome complex	1.9E-67	25.3
5	DNA metabolic process	1.2E-88	45.0	nuclear lumen	2.1E-56	48.6
				nucleoplasm	8.7E-66	44.1
7	microtubule-based process	3.8E-40	40.0	microtubule cytoskeleton	6.1E-68	70.8
				centrosome	3.8E-70	58.4
10	cell cycle	6.6E-20	47.2	chromosomal part	1.2E-19	39.6
				chromosome, centromeric region	7.9E-26	35.8
11	G-protein coupled receptor protein signaling pathway	9.5E-141	63.1	plasma membrane	4.3E-45	65.1
12	modification-dependent protein catabolic process	1.7E-16	40.4	endoplasmic reticulum	4.2E-9	32.7

Specific topological features of proteins from YTH

Based on the extended network structure analyses, COPS5 has a large number of connections (q=152) and also a relatively high betweenness centrality (b=0.046) among our 37 YTH proteins, contrasting with a low clustering coefficient (C=0.014). COPS5 is sperm-located testicular protein [41]. CD81 (q=27, b=0.005, C=0.029), CD99 (q=13, b=0.001, C=0.064) and IGTB5 (q=10, b=0.0003, C=0.089) also revealed prominent topological properties (Supplementary Table D.22).

Topological role of APP and APLP2 in the network

Previous data has shown that the absence of both APP and APLP2 lead to the abnormal developments of sexual organs, the reduction of synaptic vesicles, and even postnatal lethality in mice [6]. On the other hand, the absence of either APP or APLP2 does not affect viability and fertility. Based on these, one can imagine that these two proteins should co-exist for the mammalian life maintenance. Here, we focus on the role of APP and APLP2 for the human male fertility. Based on experimental results of gene knock-outs in mice [6], one can assume that APP and APLP2 are simultaneously involved in important pathways. Some proteins or protein complexes cannot accomplish biological functions in the absence of APP/APLP2, because this blocks the functional routes between the proteins. In order to find a conformity of the functional property within a structural property, we checked the local triangle structure between APP, APLP2, and the common interactors (CDK1, DAB2, JUN, and PIK3CA). Among the interactors of APLP2, only BRCA1 is not connected to APP. These common interactors of APP and APLP2 form a small modular structure. Therefore, one can guess the proteins in this module possibly share a biological function in testis.

3.4.5. Discussion

Biomolecular networks are now frameworks that facilitate many discoveries in molecular biology. The theoretical advances in network science in parallel with high throughput efforts to map biological networks, offer an excellent opportunity to apply the principles of theoretical physics to the molecular biomedicine field.

The APP network in testis/sperm was built first using an YTH screen and then expanded by incorporating literature curated interactions. Since protein profiles of the different tissues are critical to understand the unique characteristics of the various human cell types, in this study, we took into account the tissue expression of the interactors in the network. From the YTH screen, we reported the identification of 36 novel APP interacting proteins in human testis/sperm. Only 1 positive encoded a previously identified APP interacting protein (RANBP9). This may be explained by the fact of testis being a very peculiar organ which possesses specific patterns of

transcription and expresses novel protein isoforms [37]. APLP2 interacting partners were also included in this study.

To determine which PPI in our APP/APLP2 network were biologically more relevant for male reproduction, we performed network structure analyses and bioinformatic analyses. Based on the community/modularity analysis of the PPI network along with gene ontology analysis, we confirmed that proteins involved in similar functions are group together and form modules. The biological process GO category more significantly represented in the APP/APLP2 local network in human testis/sperm was cell surface receptor linked signal transduction with 43.0% of the proteins annotated in this class. These proteins may indicate how the male germ cells interact with the outside world. Among those proteins, 33.3% carry the GO functional tag for G-protein coupled receptor protein signaling pathway. Some studies indicate that full length APP can function as a cell surface GPCR and show that APP binds heterotrimeric G proteins (Gαo) [42,43]. Recently, Deyts and colleagues discovered an interaction between APP intracellular domain and the heterotrimeric G-protein subunit Gαs [44]. G protein-coupled receptors signalling pathways have been proposed to control several processes essential for sperm function and fertilization, namely in sperm capacitation and acrosome reaction [45–48]. APLP2/YWK-II also exhibits properties of a receptor and its extracellular domain was shown to interact with Müllerian-inhibiting substance [47]. Müllerian-inhibiting substance increases the viability and longevity of human spermatozoa through binding the APLP2/YWK-II component on the sperm membrane [48]. Huang and colleagues showed that APLP2/YWK-II component binds to a GTP-binding protein (Gαo).

The most abundant interaction detected in the YTH was with SEC22C. This protein is involved in vesicle transport between the ER and the Golgi complex [49]. Vesicular membrane trafficking is an essential process during acrosome biogenesis [50]. Also, SEC22C may control the APP traffic through the secretory pathway. Besides SEC22C, other four YTH clones (BCAP29, FTL, STX5, and SYNRG) are involved in vesicle-mediated transport (Figure B.18 c). This GO term includes the regulation of the acrosomal vesicle exocytosis, an essential process for fertilization, which begins with the fusion of the outer acrosomal membrane with the sperm plasma membrane and ends with the exocytosis of the acrosomal contents into the oocyte.

The cellular component category most enriched in the GO term analysis of the APP/APLP local network was the plasma membrane. Fertilization is achieved through gamete interactions, specifically cell adhesion and then membrane fusion of the gamete plasma membranes. The occurrence of 50.8% of proteins in the plasma membrane may suggest their involvement in sperm-egg interaction. Additionally, 10.2% of APP interactors are involved in cell adhesion (Figure B.18 b). Of these, CD99, GPNMB, ITGB5, LYPD3, and SSPN were identified in the YTH screen

performed using a testis library. The APP yeast mating efficiency in the YTH was much higher than usual (50%, when compared to a normal 5%), which may be related to APP cell adhesion properties. This strengthens previous results suggesting APP to be involved in cell-to-cell contact, a very important process in gamete fusion. Recent approaches to identify candidate proteins involved in sperm-egg interaction have been characterizing the sperm proteome and analyzing specific subpopulations of interest, for instance, glycoslylated proteins and integrins. Additionally, proteins with motifs or belonging to families of interest like transmembrane domains and the tetrasparin family should also be considered. Interestingly, some of the YTH positive clones are included in those categories. APP interacts with ITGB5, identified in the YTH screen, and ITGB1 [51], both belonging to the integrin beta chain family. Integrins on eggs became of interest with the discovery of an integrin ligand-like domain in ADAM2, a sperm antigen essential for sperm-egg interaction.TSPAN6 and CD81 belong to the tetraspanin family. The discovery that the knockout of CD9, a member of the tetraspanin family, in mouse leads to healthy, but subfertile females due to defective sperm-egg interaction revolutionized the fertility field. CD81 is 45% identical to CD9 and Cd81 knockout mouse also presents defects in female fertility. Cd9-/-/Cd81-/- female mice are completely infertile. We found that, in local network, APP, TSPAN6, ITGB1, ITGB5, GPNMB, LYPD3, SSPN, CD81 and CD99 were in the same module (module 1). However, in extended network, APP, TSPAN6, GPNMB, LYPD3, SSPN, and ITGB5 were in module 2, whereas ITGB1, CD81, CD9 and CD99 were well connected in module 9 in which 20.3% of the proteins share the biological function – cell adhesion (Figure B.18 b). We also identified tissue-specific APP interacting proteins which can lead to the identification of pathways for the APP family members associated with testis and sperm functions. TMPRSS12, a transmembrane serine protease, was identified in the YTH screen and was reported in the Unigene as testicular/spermatozoa restricted. TMPRSS12 belongs to the same module from network community as APP. Since this protein is connected to APP only, it cannot have any route to the main network without APP. Sperm-surface proteases were already shown to be required for fertilization [52]. There is also evidence for the participation of serine proteolytic activities during spermatogenesis and sperm maturation [53]. However, most of the specific proteases that are involved in these processes are unknown. The exact localization of TMPRSS12 at sperm membrane has to be determined.

The present work provided the first report on APP interactome in human testis. We identified several novel APP interactions in human testis and incorporated YTH data and PPI databases to construct the PPI network of APP in human testis and spermatozoa. The protein interaction network allowed the recognition of proteins complexes and modules crucial for several biological functions, such as cell adhesion.

3.4.6. References

1. Fardilha M, Vieira SI, Barros A, Sousa Már, Da Cruz e Silva OAB, Da Cruz e Silva EF. Differential Distribution of Alzheimer's Amyloid Precursor Protein Family Variants in Human Sperm. *Ann N Y Acad Sci*. 2007;1096(1):196-206. doi:10.1196/annals.1397.086.
2. Tanzi R, Gaston S, Bush A, et al. Genetic heterogeneity of gene defects responsible for familial Alzheimer disease. *Genetica*. 1993;91(1-3):255-263.
3. Thinakaran G, Koo EH. Amyloid precursor protein trafficking, processing, and function. *J Biol Chem*. 2008;283(44):29615-29619.
4. Multhaup G. Identification and regulation of the high affinity binding site of the Alzheimer's disease amyloid protein precursor (APP) to glycosaminoglycans. *Biochimie*. 1994;76(3-4):304-311.
5. Shoji M, Kawarabayashi T, Harigaya Y, et al. Alzheimer amyloid beta-protein precursor in sperm development. *Am J Pathol*. 1990;137(5):1027-1032.
6. von Koch CS, Zheng H, Chen H, et al. Generation of APLP2 KO Mice and Early Postnatal Lethality in APLP2/APP Double KO Mice. *Neurobiol Aging*. 1997;18(6):661-669. doi:10.1016/s0197-4580(97)00151-6.
7. Zhuang D, Qiao Y, Zhang X, Miao S, Koide SS, Wang L. YWK-II protein/APLP2 in mouse gametes: potential role in fertilization. *Mol Reprod Dev*. 2006;73(1):61-67.
8. Huang P, Miao S, Fan H, et al. Expression and characterization of the human YWK-II gene, encoding a sperm membrane protein related to the Alzheimer βA4-amyloid precursor protein. *Mol Hum Reprod*. 2000;6(12):1069-1078. doi:10.1093/molehr/6.12.1069.
9. Perreau VM, Orchard S, Adlard PA, et al. A domain level interaction network of amyloid precursor protein and Aβ of Alzheimer's disease. *PROTEOMICS – Clin Appl*. 2010;4(10-11):851. doi:10.1002/prca.201090068.
10. Fardilha M, Esteves SLC, Korrodi-Gregório L, et al. Identification of the human testis protein phosphatase 1 interactome. In: *Biochemical Pharmacology*.Vol 82.; 2011:1403-1415. doi:10.1016/j.bcp.2011.02.018.
11. Prieto C, De Las Rivas J. APID: Agile Protein Interaction DataAnalyzer. *Nucleic Acids Res*. 2006;34(Web Server issue):W298-W302. doi:10.1093/nar/gkl128.
12. Chatr-Aryamontri A, Breitkreutz BJ, Heinicke S, et al. The BioGRID interaction database: 2013 update. *Nucleic Acids Res*. 2013;30(Database issue):30. doi:10.1093/nar/gks1158.
13. Xenarios I, Salwinski L, Duan XJ, Higney P, Kim SM, Eisenberg D. DIP, the Database of Interacting Proteins: a research tool for studying cellular networks of protein interactions. *Nucleic Acids Res*. 2002;30(1):303-305.
14. Keshava Prasad TS, Goel R, Kandasamy K, et al. Human Protein Reference Database--2009 update. *Nucleic Acids Res*. 2009;37(Database issue):D767-D772. doi:10.1093/nar/gkn892.
15. Lynn DJ, Winsor GL, Chan C, et al. InnateDB: facilitating systems-level analyses of the mammalian innate immune response. *Mol Syst Biol*. 2008;4:218. doi:10.1038/msb.2008.55.
16. Kerrien S, Aranda B, Breuza L, et al. The IntAct molecular interaction database in 2012. *Nucleic Acids Res*. 2012;40(D1):D841-D846. doi:10.1093/nar/gkr1088.
17. Licata L, Briganti L, Peluso D, et al. MINT, the molecular interaction database: 2012 update. *Nucleic Acids Res*. 2011;40(Database issue):D857-D861. doi:10.1093/nar/gkr930.
18. Matthews L, Gopinath G, Gillespie M, et al. Reactome knowledgebase of human biological pathways and processes. *Nucleic Acids Res*. 2009;37(Database issue):D619-D622. doi:10.1093/nar/gkn863.
19. Snel B, Lehmann G, Bork P, Huynen MA. STRING: a web-server to retrieve and display the repeatedly occurring neighbourhood of a gene. *Nucleic Acids Res*. 2000;28(18):3442-3444.
20. Consortium TU. Update on activities at the Universal Protein Resource (UniProt) in 2013. *Nucleic Acids Res*. 2013;41(D1):D43-D47. doi:10.1093/nar/gks1068.
21. Wheeler DL, Church DM, Federhen S, et al. Database resources of the national center for biotechnology. *Nucleic Acids Res*. 2003;31(1):28-33. doi:10.1093/nar/gkg033.
22. Dennis G, Sherman BT, Hosack DA, et al. DAVID: Database for Annotation, Visualization, and Integrated Discovery. *Genome Biol*. 2003;4(5):P3. doi:10.1186/gb-2003-4-9-r60.
23. Eppig JT, Blake JA, Bult CJ, Kadin JA, Richardson JE. The Mouse Genome Database (MGD): comprehensive resource for genetics and genomics of the laboratory mouse. *Nucleic Acids Res*.

2012;40(Database issue):D881-D886. doi:10.1093/nar/gkr974.

24. Yu W, Clyne M, Khoury MJ, Gwinn M. Phenopedia and Genopedia: disease-centered and gene-centered views of the evolving knowledge of human genetic associations. *Bioinformatics*. 2010;26(1):145-146. doi:10.1093/bioinformatics/btp618.
25. Esteves SL, Domingues SC, da Cruz e Silva OA, Fardilha M, da Cruz e Silva EF. Protein phosphatase 1alpha interacting proteins in the human brain. *Omics*. 2012;16(1-2):3-17.
26. Esteves SL, Korrodi-Gregorio L, Cotrim CZ, et al. Protein Phosphatase 1gamma Isoforms Linked Interactions in the Brain. *J Mol Neurosci*. 2012;19:19.
27. Hamdi A, Colas P. Yeast two-hybrid methods and their applications in drug discovery. *Trends Pharmacol Sci*. 2012;33(2):109-118. doi:10.1016/j.tips.2011.10.008.
28. Gellert P, Jenniches K, Braun T, Uchida S. C-It: A knowledge database for tissue-enriched genes. *Bioinformatics*. 2010;26(18):2328-2333. doi:10.1093/bioinformatics/btq417.
29. Liu X, Yu X, Zack DJ, Zhu H, Qian J. TiGER: a database for tissue-specific gene expression and regulation. *BMC Bioinformatics*. 2008;9:271. doi:10.1186/1471-2105-9-271.
30. Yang X, Ye Y, Wang G, Huang H, Yu D, Liang S. VeryGene: linking tissue-specific genes to diseases, drugs, and beyond for knowledge discovery. *Physiol Genomics*. 2011;43(8):457-460. doi:10.1152/physiolgenomics.00178.2010.
31. Uhlen M, Oksvold P, Fagerberg L, et al. Towards a knowledge-based Human Protein Atlas. *Nat Biotechnol*. 2010;28(12):1248-1250. doi:10.1038/nbt1210-1248.
32. Wu C, Orozco C, Boyer J, et al. BioGPS: an extensible and customizable portal for querying and organizing gene annotation resources. *Genome Biol*. 2009;10(11):R130. doi:10.1186/gb-2009-10-11-r130.
33. Aitken RJ, Nixon B, Lin M, Koppers AJ, Lee YH, Baker MA. Proteomic changes in mammalian spermatozoa during epididymal maturation. *Asian J Androl*. 2007;9(4):554-564. doi:10.1111/j.1745-7262.2007.00280.x.
34. Baker MA, Aitken RJ. Proteomic insights into spermatozoa: critiques, comments and concerns. *Expert Rev Proteomics*. 2009;6(6):691-705.
35. Li J, Liu F, Liu X, et al. Mapping of the human testicular proteome and its relationship with that of the epididymis and spermatozoa. *Mol Cell Proteomics*. 2011;10(3):22.
36. Thimon V, Frenette G, Saez F, Thabet M, Sullivan R. Protein composition of human epididymosomes collected during surgical vasectomy reversal: a proteomic and genomic approach. *Hum Reprod*. 2008;23(8):1698-1707. doi:10.1093/humrep/den181.
37. Goh KI, Cusick ME, Valle D, Childs B, Vidal M, Barabasi AL. The human disease network. *Proc Natl Acad Sci U S A*. 2007;104(21):8685-8690. doi:10.1073/pnas.0701361104.
38. Guan Y, Myers CL, Lu R, Lemischka IR, Bult CJ, Troyanskaya OG. A genomewide functional network for the laboratory mouse. *PLoS Comput Biol*. 2008;4(9):e1000165. doi:10.1371/journal.pcbi.1000165.
39. Joy MP, Brock A, Ingber DE, Huang S. High-betweenness proteins in the yeast protein interaction network. *J Biomed Biotechnol*. 2005;2005(2):96-103. doi:10.1155/jbb.2005.96.
40. Kanehisa M, Goto S, Sato Y, Furumichi M, Tanabe M. KEGG for integration and interpretation of large-scale molecular data sets. *Nucleic Acids Res*. 2012;40(Database issue):D109-D114. doi:10.1093/nar/gkr988.
41. Li J, Liu F, Wang H, et al. Systematic mapping and functional analysis of a family of human epididymal secretory sperm-located proteins. *Mol Cell Proteomics*. 2010;9(11):2517-2528.
42. Okamoto T, Takeda S, Murayama Y, Ogata E, Nishimoto I. Ligand-dependent G protein coupling function of amyloid transmembrane precursor. *J Biol Chem*. 1995;270(9):4205-4208.
43. Brouillet E, Trembleau A, Galanaud D, et al. The amyloid precursor protein interacts with Go heterotrimeric protein within a cell compartment specialized in signal transduction. *J Neurosci*. 1999;19(5):1717-1727.
44. Deyts C, Vetrivel KS, Das S, et al. Novel GalphaS-protein signaling associated with membrane-tethered amyloid precursor protein intracellular domain. *J Neurosci*. 2012;32(5):1714-1729.
45. Etkovitz N, Tirosh Y, Chazan R, et al. Bovine sperm acrosome reaction induced by G-protein-coupled receptor agonists is mediated by epidermal growth factor receptor transactivation. *Dev Biol*. 2009;334(2):447-457.

46. Ward CR, Storey BT, Kopf GS. Selective activation of Gi1 and Gi2 in mouse sperm by the zona pellucida, the egg's extracellular matrix. *J Biol Chem*. 1994;269(18):13254-13258.
47. Tian XY, Sha YS, Zhang SM, et al. Extracellular domain of YWK-II, a human sperm transmembrane protein, interacts with rat Mullerian-inhibiting substance. *Reproduction*. 2001;121(6):873-880. doi:10.1530/rep.0.1210873.
48. Yin X, Ouyang S, Xu W, et al. YWK-II protein as a novel G(o)-coupled receptor for Mullerian inhibiting substance in cell survival. *J Cell Sci*. 2007;120(Pt 9):1521-1528.
49. Tseng TC, Chen SH, Hsu YP, Tang TK. Protein kinase profile of sperm and eggs: cloning and characterization of two novel testis-specific protein kinases (AIE1, AIE2) related to yeast and fly chromosome segregation regulators. *DNA Cell Biol*. 1998;17(10):823-833.
50. Berruti G, Paiardi C. Acrosome biogenesis: Revisiting old questions to yield new insights. *Spermatogenesis*. 2011;1(2):95-98.
51. Young-Pearse TL, Chen AC, Chang R, Marquez C, Selkoe DJ. Secreted APP regulates the function of full-length APP in neurite outgrowth through interaction with integrin beta1. *Neural Dev*. 2008;3(15):1749-8104.
52. Miyamoto H, Chang MC. Effects of protease inhibitors on the fertilizing capacity of hamster spermatozoa. *Biol Reprod*. 1973;9(5):533-537.
53. Phelps BM, Koppel DE, Primakoff P, Myles DG. Evidence that proteolysis of the surface is an initial step in the mechanism of formation of sperm cell surface domains. *J Cell Biol*. 1990;111(5 Pt 1):1839-1847.

4. Identification of signaling proteins as targets for diagnostic intervention in male fertility

4.1. Profiling signaling proteins in human spermatozoa: biomarker identification for sperm quality evaluation

Joana Vieira Silva[1], Maria João Freitas[1], Bárbara Regadas Correia[1], Luís Korrodi-Gregório[1], António Patrício[2], Steven Pelech[3,4], Margarida Fardilha[1]

[1] Laboratory of Signal Transduction, Department of Medical Sciences, Institute of Biomedicine – iBiMED, University of Aveiro, 3810-193 Aveiro, Portugal.

[2] Hospital Infante D. Pedro E.P.E., 3810-193 Aveiro, Portugal

[3] Kinexus Bioinformatics Corporation, Vancouver, British Columbia, Canada V6P 6T3

[4] Department of Medicine, University of British Columbia, Vancouver, British Columbia, Canada V6P 6T3

Corresponding author: Margarida Fardilha, Departamento de Ciências Médicas, Universidade de Aveiro, Campus Universitário de Santiago, Agra do Crasto – Edifício 30, 3810-193 Aveiro, Portugal. T: +351-918143947. E: mfardilha@ua.pt

Silva JV, Freitas MJ, Correia BR, Korrodi-Gregório L, Patrício A, Pelech S, Fardilha M. Profiling signaling proteins in human spermatozoa: biomarker identification for sperm quality evaluation. Fertility Sterility. 2015; 104(4):845-856.e8. doi:10.1016/j.fertnstert.2015.06.039.

4.1.1. Abstract

Objective: To determine the correlation between semen basic parameters and the expression and activity of signaling proteins. **Design:** *In vitro* studies with human spermatozoa. **Settings:** Academic research institute in collaboration with a hospital. **Patients:** Thirty-seven men provided semen samples for routine analysis. **Interventions:** None. **Main outcome measures:** Basic semen parameters tracked included sperm DNA fragmentation (SDF), the expression levels of 75 protein kinases and the phosphorylation/cleavage patterns of 18 signaling proteins in human spermatozoa. **Results:** The results indicated that the phosphorylated levels of several proteins [Bad, GSK-3β, HSP27, JNK/SAPK, mTOR, p38 MAPK and p53], as well as, cleavage of PARP (at D214), and Caspase-3 (at D175)] were significantly correlated with motility parameters. Additionally, the percentage of morphologically normal spermatozoa demonstrated a significant positive correlation with the phosphorylated levels of p70 S6 kinase and, in turn, head defects and the teratozoospermia index (TZI) showed a significant negative correlation with the phosphorylated levels of Stat3. There was a significant positive correlation between SDF and the TZI, as well as, the presence of head defects. In contrast, SDF negatively correlated with the percentage of morphologically normal spermatozoa and the phosphorylation of Akt and p70 S6 kinase. Subjects with varicocele demonstrated a significant negative correlation between head morphological defects and the phosphorylated levels of Akt, GSK3β, p38 MAPK and Stat1. Additionally, 34 protein kinases were identified as expressed in their total protein levels in normozoospermic samples. **Conclusions:** This study contributed towards establishing a biomarker "fingerprint" to assess sperm quality based on molecular parameters.

4.1.2. Introduction

Infertility is a major public health issue, especially in industrialized countries where birth rates are declining drastically below replacement levels [1]. The male factor is involved in approximately 50% of infertility cases. Male infertility may be caused by numerous factors including genetic abnormalities, acute and chronic diseases, treatments for certain conditions, lifestyle factors and exposure to environmental, occupational, and infectious agents. A common risk factor for male infertility is varicocele, which is found in about 15% of all adult males, up to 35% of men who present for infertility evaluation, and in as many as 81% of men with secondary infertility [2]. Still, many questions regarding the etiology of male infertility remain unanswered with idiopathic infertility as the most common type of male infertility [3,4].

The physiology and molecular biology of the spermatozoa has been neglected in the last decade due to the use of assisted reproduction technologies (ART) that bypassed the need for a “normal” ejaculated sperm sample. However, despite several ART improvements over the last few years,

there is still the need to increase live birth rates [5], and it is preferable to rise sperm quality and avoid ART. Identification of the male infertility factors and biomarkers will improve fertility management and even allow for conception through intercourse.

Many signaling pathways have been thoroughly investigated in somatic cells. However, limited information is available on their characterization in male germ cells. In the past few years, some studies have indicated that hormones, cytokines and growth factors regulate processes such as spermatogenesis and sperm motility and their levels differ in the genital tract secretions of fertile and infertile men [6–11]. In addition, several findings clearly demonstrate that the cellular actions of signaling pathways in spermatozoa occur through mechanisms that are distinct to those described for somatic cells [12].

Several signaling pathways that were described in somatic cells have also been documented in spermatozoa: apoptotic [13], mitogen-activated protein kinase (MAPK) [14], cAMP/PKA [15], JAK/STAT [16], among others. Despite these efforts, not much information is available on the biological significance of specific signaling pathways in human spermatozoa or their possible roles in male infertility. Additionally, the association between the activated states of these pathways and spermatozoa quality has not been established.

4.1.3. Methods

Sperm samples collection, basic semen analysis and DNA fragmentation assessment

This study was approved by the Ethics and Internal Review Board of the Hospital Infante D. Pedro E.P.E. (Aveiro, Portugal) and was conducted in accordance with the ethical standards of the Helsinki Declaration. All donors signed informed consent allowing the samples to be used for scientific purposes. A total of 37 semen samples were obtained from a randomized group of donors, by masturbation to a sterile container. Basic semen analysis was performed by qualified technicians according to World Health Organization (WHO) guidelines [17]. Briefly, after complete liquefaction of the semen samples at 37˚C, during approximately 30 minutes, a macroscopic examination was performed. The microscopic examination included the analysis of motility, concentration and morphology of the spermatozoa. DNA fragmentation was measured using a Sperm Chromatin Dispersion (SCD) test (Halosperm® kit, Halotech®, Madrid, spain) according to the manufacturer's instructions. All microscopy analysis were performed using the Zeiss ® Primo Star microscope (Zeiss ®, Jena, Germany).

Antibody array

Antibody-based arrays were carried out using the PathScan® Intracellular Signaling Array Kit (#7744, Cell Signaling Technology, Danvers, MA, USA) to determine the expression patterns of 18

well-characterized signaling molecules when phosphorylated or cleaved, in 32 semen samples obtained from a randomized group of donors. After semen liquefaction, sperm cells were washed three times in 1x phosphate buffered saline (PBS) by centrifugation (600xg for 5 minutes at 4°C) and lysed according to the manufacturer's instructions. Protein concentration was measured using bicinchoninic acid (BCA) assay (Pierce Biotechnology, USA) and final absorbance was measured at 562 nm in a microplate reader (TECAN, Genius, Männedorf, Switzerland). Each cell extract was diluted to 250 µg/ml and applied to its own multiplexed array according to the manufacturer's instructions. Fluorescence readouts from the arrays were captured digitally using LI-COR® Biosciences Odyssey® imaging system (LI-COR® Biosciences, Nebraska, USA). Pixel intensity was quantified using Odyssey software. The intensity from the negative control within each array was subtracted from all signals, and all data from each array were normalized to the internal positive control within each array.

Protein kinase screening

The total protein levels of 75 protein kinases were analyzed in normozoospermic samples by the commercial Kinetworks™ Protein Kinase Screen 1.2 (KPKS-1.2; Kinexus Bioinformatics Corporation, Vancouver, Canada) as described online at www.kinexus.ca. This involved immunoblotting of sperm lysate samples following resolution by SDS-polyacrylamide gel electrophoresis with a panel of 72 pan-specific protein kinase antibodies as described in Pelech *et al.* [18]. A pool of five normozoospermic samples (NZ) with high motility (45%–55% progressive motility) was analyzed. Samples were centrifuged at 16,000xg. Afterwards, the sperm pellet was homogenized in lysis buffer (20 mM Tris-HCl, pH 7.0, 20 mM beta-glycerophosphate, 150 mM NaCl, 3 mM EDTA, 3 mM EGTA, 1 mM Na_3VO_4, 0.5% Nonidet P-40, 1 mM dithiothreitol, 1 mM phenylmethane sulphonylfluoride (PMSF), 2 µg/mL leupeptin, 4 µg/mL aprotinin, and 1 µg/mL pepstatin A) according to Kinexus instructions. Total protein extracts were resolved on 10% SDS-PAGE gels and transferred to nitrocellulose membranes (300 µg of total lysate protein per membrane). Following the use of a 20-lane multiblotter (BioRad, Hercules, CA, USA), the membrane was incubated with mixes of up to three antibodies per lane (roughly 12 µg of total lysate protein per lane). Each protein kinase was further classified with respect to its molecular weight. Relative amounts of each protein band were quantified as counts per minute (CPM). The data were normalized following the correction for protein content.

Statistical analysis

Statistical analysis was conducted using the IBM SPSS Statistics Software 22. First, a descriptive analysis to each quantitative parameter analyzed was performed. Lastly, we calculated the Pearson correlation coefficient, r, or the Spearman's rho correlation coefficient, r_s, (a nonparametric

correlation method) to determine the relationship between two variables. We performed a test of normality (Shapiro-Wilk test) and we analyzed the box-plots to decide between a parametric or non-parametric method. The significance level was set at 0.05.

Bioinformatic analyses

The HIPPIE database was used for retrieving human protein-protein interaction (PPI) data (downloaded on April 17, 2015). This database is regularly updated by incorporating interaction data from major expert-curated experimental PPI databases (such as BioGRID, HPRD, IntAct and MINT). For the identification of testis enriched/specific proteins, proteins were searched against six tissue-expression databases: C-it [19], UniGene [20], TiGER [21], Very Gene [22], Human Protein Atlas (HPA) [23] and BioGPS [24]. The criteria used in the databases were set for maximum stringency to identify the tissue-specific proteins with a high confidence level. Only proteins that appeared in at least two databases were included as testis-enriched/specific. The protein network was build using Cytoscape V3.2.0 software [25]. Gene Ontology annotations and pathways were analyzed using the Database for Annotation, Visualization and Integrated Discovery (DAVID) v6.7 [26]. The UniProt identifiers of all proteins were used as input for the DAVID functional annotation program. The overall set of human protein-coding genes was used as background. Enrichment p-values indicated, correspond to the Bonferroni corrected retrieved by DAVID. Protein identities associated with defects in male fertility or a functional/morphological defect in the male reproductive system were obtained from the Jackson Laboratories mouse knockout database (http://www.informatics.jax.org/).

4.1.4. Results

Correlation between semen quality and signaling proteins phosphorylation and cleavage

A total of 32 semen samples, obtained from a randomized group of donors, were included in this study (Supplementary Table D.23). From those, 18.8% were diagnosed with varicocele. The dataset size was considered reasonable since based on the central limit theorem it was possible to approximate the distribution of variables to a normal distribution.

Basic semen parameters were analyzed according to the WHO's guidelines (Supplementary Table D.23). The spermatozoa DNA fragmentation was measured using a Sperm Chromatin Dispersion (SCD) test and the levels of signaling molecules (in distinct activation states) were determined with the PathScan Intracellular Signaling Array, which includes antibodies for phosphorylated or cleaved signaling proteins (Supplementary Table D.23). Initially, a descriptive analysis of the results was performed (Supplementary Table D.24). Next, to evaluate the relation between the

results obtained from the seminal parameters analysis and the PathScan array, Spearman's and Pearson correlation tests were performed (Table B.6).

The results indicated that the levels of several phosphoproteins (i.e., Bad (pS112), GSK-3β (pS9), HSP27 (pS78), JNK/SAPK (pT183/pY185), mTOR (pS2448), p38 MAPK (pT180/pY182) and p53 (pS15), as well as, the cleavages of PARP (at D214) and Caspase-3 (at D175) were negatively correlated with the percentage of motile spermatozoa. Bad (pS112) and JNK/SAPK (pT183+pY185) levels were also negatively correlated with progressive motility. In turn, phosphorylation of Bad (pS112), JNK/SAPK (pT183+pY185) and p53 (pS15) showed a positive correlation with the percentage of immotile sperm cells. Concerning sperm morphology, the percentage of normal spermatozoa positively correlated with the phosphorylation of p70 S6 kinase (pT389). In contrast, head defects and the TZI showed a negative correlation with the levels of phospho-Stat3 (pY705). The results indicated that DNA fragmentation in spermatozoa was positively correlated with the presence of head defects, the TZI and the volume, and negatively correlated with the percentage of morphologically normal spermatozoa. DNA fragmentation also presented a negative correlation with the levels of phosphorylated Akt (pT308) and p70 S6 kinase (pT389). In the subjects diagnosed with varicocele, a strong negative correlation between the percentage of head abnormalities and the levels of phosphorylated Akt (pT308+pS473), GSK3β (pS9), p38 MAPK (pT180+pY182) and Stat1 (pY701) was observed.

Protein kinases in normozoospermic sperm samples

The antibody-based KPKS-1.2 (Kinetworks^{TM} Protein Kinase Screen 1.2) was employed to investigate the presence of a large number of protein kinases in pooled human sperm samples (NZ, Supplementary Table D.25). The affinities of individual antibodies used to screen the different kinases varied; therefore, this screening approach does not provide an absolute comparison of total levels between different proteins but indicates the relative amounts of a target protein in two different samples. The KPKS screen allows the detection of 75 protein kinases (Supplementary Table D.26). From those, 34 protein kinases were detected in the sperm pool (NZ, Table B.7). Pathways analyses indicated that the top 3 overrepresented categories were: MAPK signaling pathway (44.4%, 16 proteins, p=6.1E-12); Neurotrophin signaling pathway (38.9%, 14 proteins, p=8.1E-14); and Progesterone-mediated oocyte maturation (30.6%, 11 proteins, p=3.7E-11). To determine which proteins were known to be important for normal male reproductive function our dataset was screened against the Jackson Laboratory mutant mouse DB. The analysis revealed 3 protein kinases (CDK2, RSK2 and CK2a) that are required for normal male reproductive function (Table B.7). The remainder of the targeted protein kinases screened were undetectable, either due to their absence in the sperm samples tested or because their levels were below the detection limit.

Table B.6 - Associations between the results obtained from the basic seminal analyses, sperm DNA fragmentation and the PathScan Intracellular Signaling Array. *- correlation is significant at the 0.05 level (2-tailed); **- correlation is significant at the 0.01 level (2-tailed); TZI, teratozoospermia index; SDF, sperm DNA fragmentation; NA, not applicable; rs, Spearman´s rho correlation coefficient; r, Pearson correlation coefficient. [1] Experimental data (total protein) was compared with the human sperm proteome lists published to date [70,71,74–80,83]; [2] Whenever proteins were not described in human the species is indicated; [3] Whenever the localization of the phosphorylated/cleaved status was not described, the total protein was considered ([+]). [4] Experimental data was compared to the gene knockout mice phenotypes.

Uniprot ID	Abbreviation		Recommended protein name	Previously id human sperm proteome[1]	Previously described in spermatozoa[2]	Localization in spermatozoa[3]	Function in spermatozoa	Infertility phenotype[4]	Phosphorylation/ cleavage, residue, status	Clinical correlation	Correlation Coefficient/ Sig. (2-tailed)
	Formerly	Presently									
P23443	p70 S6 kinase	RPS6KB1	Ribosomal protein S6 kinase beta-1	[70]	Yes, mouse [54]	Cytoplasm[+] [54]	Unknown		Phospho T389 Activation	Normal morphology	r_s= 0.384* p= 0.030
										SDF	r_s= -0.371* p= 0.037
P40763	Stat3	STAT3	Signal transducer and activator of transcription 3	[70,71]	Yes (47)	Head plasma membrane and flagellum cytoskeleton[+] [60]	Regulation of mitochondrial activity Capacitation? Transcription in the fertilized oocyte?	Male infertility;	Phospho Y705 Activation	Head defects	r_s= -0.458** p= 0.008
										TZI	r_s= -0.460** p= 0.008
P31749	Akt	AKT1	RAC-alpha serine/threonine-protein kinase	[70]	Yes [72]	Caudal part of the post acrosomal region and midpiece [48,49]	Sperm vitality and motility	Abnormal testis morphology; Seminiferous tubule degeneration; Abnormal spermatogenesis;	Phospho T308 Activation	SDF	r_s= -0.377* p= 0.033
										Head defects (varicocele)	r= -0.877* p= 0.022
									Phospho S473 Activation	Head defects (varicocele)	r = -0.829* p= 0.042
P42224	Stat1	STAT1	Signal transducer and activator of transcription 1-alpha/beta	[70,71]	Yes [16]	Head apical region[+] [16]; Neck region of the flagellum[+] [63]	Transcription in the fertilized oocyte?		Phospho Y701 Activation	Head defects (varicocele)	r= -0.890* p= 0.017
P42345	mTOR	MTOR	Serine/threonine -protein kinase mTOR	[70,73]	No	Unknown	Unknown		Phospho S2448 Activation	Motility	r_s= -0.370* p= 0.048
P04792	HSP27	HSPB1	Heat shock protein beta-1	[70,74–80]	No	Unknown	Unknown		Phospho S78 Activation	Motility	r_s= -0.389* p= 0.037
Q16539 Q15759 P53778	p38	MAPK14/11 /12/13	Mitogen-activated protein kinase	[70] (MAPK14/13)	Yes [34]	Upper midpiece[+] [34]	Negatively regulates motility		Phospho T180/Y182 Activation	Motility	r_s= -0.388* p= 0.038
										Head defects	r= -0.814*

Uniprot ID	Abbreviation		Recommended protein name	Previously id human sperm proteome[1]	Previously described in spermatozoa[2]	Localization in spermatozoa[3]	Function in spermatozoa	Infertility phenotype[4]	Phosphorylation/ cleavage, residue, status	Clinical correlation	Correlation Coefficient/ Sig. (2-tailed)
	Formerly	Presently									
O15264			14/11/12/13							(varicocele)	p= 0.049
P45983 P45984 P53779	SAPK/ JNK	MAPK8/9/10	Mitogen-activated protein kinase 8/9/10	[70] (MAPK9)	No	Unknown	Unknown		Phopho T183/Y185 Activation	Motility	r_s= -0.446* p= 0.015
										Progressive motility	r_s= -0.443** p= 0.016
										Immotile	r_s= 0.399* p= 0.032
P42574	Caspase-3	CASP3	Caspase-3	[70]	Yes [46]	Post acrosomal region [13] Midpiece [46]	Apoptosis		Cleavage D175 Activation	Motility	r_s= -0.392* p= 0.035
P49841	GSK-3β	GSK3B	Glycogen synthase kinase-3 beta	[70,80]	Yes, bull [38]	Posterior head and flagellum+ [39]	Motility		Phospho S9 Inhibition	Motility	r_s= -0.383* p= 0.040
										Head defects (varicocele)	r= -0.918** p= 0.010
P04637	p53	TP53	Cellular tumor antigen p53		Yes [81]	Unknown	Apoptosis	Small testis; Abnormal spermatogenesis;	Phospho S15 Activation	Motility	r_s= -0.451* p= 0.014
										Immotile	r_s= 0.424* p= 0.022
Q92934	Bad	BAD	Bcl2-associated agonist of cell death	[70]	Yes [82]	Midpiece+ [82]	Apoptosis	Abnormal reproductive system morphology and seminiferous tubule morphology;	Phospho S112 Inhibition	Motility	r_s= -0.561** p= 0.002
										Progressive motility	r_s= -0.554** p= 0.002
										Immotile	r_s= 0.512** p= 0.005
P09874	PARP	PARP1	Poly [ADP-ribose] polymerase	[70,71,79]	Yes [45]	Unknown	DNA damage repair system		Cleavage D214 Inhibition	Motility	r_s= -0.388* p= 0.038
NA	Sperm DNA Fragmentation		NA	NA	NA	NA	NA		NA	Volume	r_s= 0.391* p= 0.027
										Normal morphology	r_s= -0.535** p= 0.002
										Head defects	r_s= 0.447** p= 0.01
										TZI	r_s= 0.506** p= 0.003

Table B.7 - Protein kinases detected in the Kinetworks KPKS-1.2 Protein Kinase Screen. Protein kinases identified in the pool of 5 normozoospermic human sperm samples (NZ) and their respective detections as Counts per Minute (CPM). PTYK, protein-threonine/tyrosine kinases; PYK, protein-pyruvate kinase; PTK, protein-tyrosine kinase; AR, acrosome Reaction.

Uniprot	Abbreviation		Protein Name	Type	NZ	Previously identified in human sperm proteome[1]	Previously described in spermatozoa[2]	Localization in spermatozoa[3]	Infertility phenotype[4]
	Formerly	Presently			CPM				
P15056	RafB	BRAF	RafB proto-oncogene-encoded protein-serine kinase	PSTK	593	[70]	No		
Q9ULU4	PKCb1	ZMYND8	Protein-serine kinase C beta 1	PSTK	92	[71,79]	Yes [84]	Principal piece [84]	
Q16539	p38a MAPK	MAPK14	Mitogen-activated protein-serine kinase p38 alpha	PSTK	1968	[70]	Yes, chicken [85]	Head [85]	
P27361	Erk1	MAPK3	Extracellular regulated protein-serine kinase 1 (p44 MAP kinase)	PSTK	688	[70]	Yes [86]	Post acrosomal (before AR) and equatorial region (after AR) [86]; Midpiece [34 3]	
P28482	Erk2	MAPK1	Extracellular regulated protein-serine kinase 2 (p42 MAP kinase)	PSTK	404	[70]	Yes [86]	Post acrosomal (before AR), equatorial region (after AR) [86]; Midpiece [34 3]	
P17252	PKCa	PRKCA	Protein-serine kinase C alpha	PSTK	775	No	Yes [84]	Equatorial region [84]	
P24941	CDK2	CDK2	Cyclin-dependent protein-serine kinase 2	PSTK	378	No	Yes, bull [69]	Unknown	Abnormal spermatogenesis, spermiogenesis, male reproductive system morphology and fertility/fecundity; Small testis and seminiferous tubules; Azoospermia;
Q05655	PKCd	PRKCD	Protein-serine kinase C delta	PSTK	161	[70]	No		
P24723	PKCl	PRKCH	Protein-serine kinase C lambda/iota	PSTK	173	[70]	No		
P45983 P45984 P53779	JNK	MAPK8/9/10	Jun N-terminus protein-serine kinases (stress-activated protein kinase (SAPK)) 1/2/3	PSTK	176	[70] (MAPK9)	No		
Q05513	PKCz	PRKCZ	Protein-serine kinase C zeta	PSTK	276	[70]	Yes, mouse [87]	Acrossomal [87]	
P36507	MEK2	MAP2K2	MAPK/ERK protein-serine kinase 2	PTYK	452	[70,80]	Yes [88]	Flagellum [88]	
O75914	PAK3	PAK3	p21-activated serine kinase 3 (beta)	PSTK	2290	No	No		

Uniprot	Abbreviation		Protein Name	Type	NZ	Previously identified in human sperm proteome[1]	Previously described in spermatozoa[2]	Localization in spermatozoa[3]	Infertility phenotype[4]
	Formerly	Presently			CPM				
P49840	GSK3α	GSK3A	Glycogen synthase-serine kinase 3 alpha	PSTK	105	[70,79]	Yes, bull [89]	Posterior head and flagellum [39]	
P49841	GSK3β	GSK3B	Glycogen synthase-serine kinase 3 beta	PSTK	34	[70,80]	Yes, bull [89]	Posterior head and flagellum [39]	
Q15418	RSK1	RPS6KA1	Ribosomal S6 protein-serine kinase 1	PSTK	130	[70]	No		
P41279	COT	MAP3K8	Osaka thyroid oncogene protein-serine kinase (Tpl2)	PSTK	405	[79]	No		
P51812	RSK2	RPS6KA3	Ribosomal S6 protein-serine kinase 2	PSTK	62	[70]	No		Infertility
P19784	CK2a	CSNK2A2	Casein protein-serine kinase 2 alpha/ alpha prime	PSTK	1725	[70,74,78–80]	Yes [90]	Unknown	Abnormal spermatid morphology, male germ cell apoptosis, sperm nucleus morphology and sperm motility; Globozoospermia; Oligozoospermia; Teratozoospermia; Detached acrosome; Kinked sperm flagellum; Male infertility;
O15111	IKKa	CHUK	Inhibitor of NF-kappa-B protein-serine kinase alpha (CHUK)	PSTK	629	[70,71]	No		
Q8IVT5	Ksr1	KSR1	Protein-serine kinase suppressor of Ras 1	PSTK	402	No	No		
P51813	BMX (Etk)	BMX	Bone marrow X protein-tyrosine kinase	PSTK	45	No	Yes, bull [91]	Unknown	
P41240	Csk	CSK	C-terminus of Src tyrosine kinase	PYK	158	[70]	Yes [92]	Unknown	
P53355	DAPK1	DAPK1	Death associated protein kinase 1	PSTK	241	No	No		
P43405	Syk	SYK	Spleen protein-tyrosine kinase	PYK	403	[70]	Yes, boar [93]	Unknown	
Q13043	MST1	STK4	Mammalian STE20-like protein-serine kinase 1	PYK	121	[70]	No		
P48730	CK1d	CSNK1D	Casein protein-serine kinase 1 delta	PSTK	348	No	No		
P49674	CK1e	CSNK1E	Casein protein-serine kinase 1 epsilon	PSTK	2663	[70]	No		
Q12851	GCK	MAP4K2	Germinal centre protein-serine	PSTK	178	No	No		

Uniprot	Abbreviation		Protein Name	Type	NZ	Previously identified in human sperm proteome[1]	Previously described in spermatozoa[2]	Localization in spermatozoa[3]	Infertility phenotype[4]
	Formerly	Presently			CPM				
			kinase						
Q8IU85	CaMK1d	CAMK1D	Calcium/calmodulin-dependent protein-serine kinase 1 delta	PSTK	334	[70]	No		
P04049	Raf1	RAF1	Raf1 proto-oncogene-encoded protein-serine kinase	PSTK	1047	[70,83]	No		
P25098	GRK2	ADRBK1	G protein-coupled receptor-serine kinase 2	PSTK	319	[70]	No		
O43293	ZIPK	DAPK3	ZIP kinase (death associated protein-serine kinase 3 (DAPK3))	PSTK	582	No	No		
P23458	JAK1	JAK1	Janus protein-tyrosine kinase 1	PTK	3323	[70,73,78]	Yes [60]	Neck [60]; Equatorial region and midpiece [63]	

[1] Experimental data was compared with the human spermatozoa proteome lists published till date [70,71,74–80,83]; [2] Whenever proteins were not described in humans the species is indicated; [3] Subcellular localization is stated for the specific kinase isoform, except for Erk1 and Erk2; [4] Experimental data was compared to the gene knockout mice phenotype

Network analyses

A PPI network was constructed based on the proteins identified in the PathScan Intracellular Signaling Array (green and pink nodes in Figure B.19), the KPKS-1.2 (orange and pink nodes in Figure B.19) and the interactions between these proteins. Additionally, testis-enriched/specific interactors of those proteins were added (blue nodes and edges in Figure B.19). Only proteins identified in at least 2 tissue-expression databases were included. The total number of proteins in the PPI network is N=75 and the total number of interaction between them is L=205. In Figure B.19, node size is proportional to the number of interactions of each node (degree).

Proteins identified in the PathScan Intracellular Signaling Array and KPKS-1.2 were highly interconnected. HSPA1L, PIAS2 and PBK were, among the testis-enriched/specific proteins, the ones with higher degree of connectivity in the PPI network (Figure B.19). Testis-enriched/specific interactors were analyzed for gene ontology. Gene ontology analysis annotated 10 testis-enriched/specific proteins with biological process terms associated with reproduction (p= 1.011e-05). Several testis-enriched/specific proteins had no functional annotation and thus deserve further investigation.

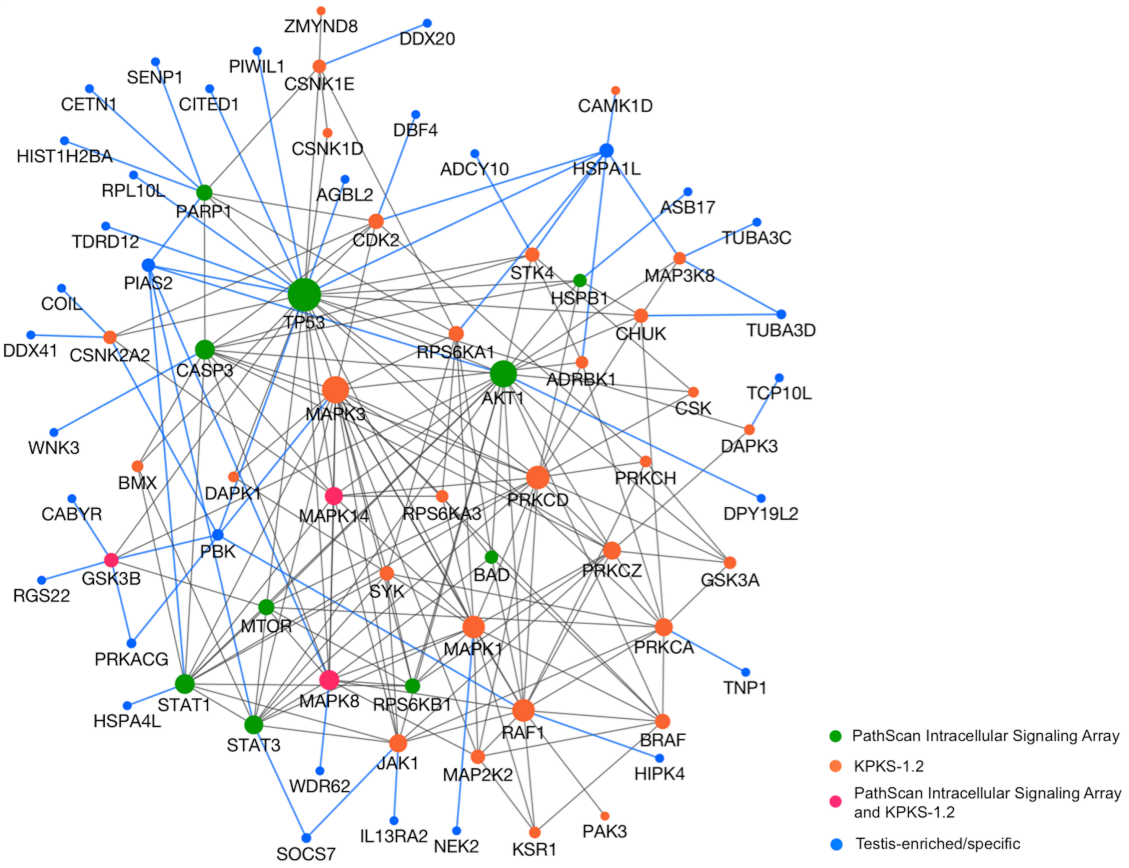

Figure B.19 - Network of the signaling proteins identified in the PathScan Intracellular Signaling Array as correlated with seminal parameters (green and pink nodes) and in the KPKS-1.2 (orange and pink nodes). Blue nodes and edges represent direct testis-enriched/specific interactors/interactions of those signaling proteins. Node sizes represent relative

degree of the nodes. Testis-enriched/specific interactors annotated for reproduction-associated gene ontology categories: PRKACG, spermatogenesis (BP) and ciliary base (CC); CABYR, sperm fibrous sheath (CC), sperm principal piece (CC) and sperm end piece (CC); HSPA1L, binding of sperm to zona pellucida (BP) and zona pellucida receptor complex (CC); RPL10L, spermatogenesis (BP); PIWIL1, spermatogenesis (BP) and spermatid development (BP); HIST1H2BA, spermatogenesis, exchange of chromosomal proteins (BP); DPY19L2, spermatid development (BP); TDRD12, spermatogenesis (BP) and fertilization (BP); TNP1, spermatogenesis (BP), spermatid development (BP), spermatid nucleus differentiation (BP), sperm motility (BP), fertilization, exchange of chromosomal proteins (BP) and male germ cell nucleus (CC); ADCY10, spermatogenesis (BP). BP, biological process; CC, cellular component.

4.1.5. Discussion

Sperm cells are incapable of genetic expression and thus highly dependent upon post-translational modifications and signal cascades to execute their function. For instance, it is well established that protein phosphorylation is essential for sperm motility [27,28]. In this study we attempted to unravel the signaling pathways involved in regulating human sperm function and to correlate them with clinical data. To gain a global understanding into spermatozoa signaling pathways, we examined eighteen well-characterized signaling proteins for their phosphorylation or cleavage status. Data was then correlated with basic semen parameters and spermatozoa DNA integrity. Additionally, we established a profile for the differential expression of a large number of protein kinases in human spermatozoa.

Motility is acquired during the spermatozoa journey through the epididymis and depends on several signaling pathways, such as cAMP/PKA, MAPK and PPP1-related signaling [29,30]. The correlation between sperm (im)motility and proteins involved in specific signaling pathways can pinpoint the problems in abnormal spermatozoa and reveal the importance of a specific protein for assessment of spermatozoa motility.

In this study a negative correlation between the levels of activated mTOR (i.e. phosphorylated at S2448) and motile spermatozoa was identified. mTOR is a protein-serine/threonine kinase, which increases translation, cell growth and proliferation in response of growth factors. In terms of tissue specificity, mTOR is expressed in numerous tissues, but has not been previously detected in spermatozoa. PI3K signaling pathway controls mTOR activity, by regulating the TSC1/2 complex, an indirect mTOR inhibitor. Chiang *et al.* showed that the p70S6 kinase can be responsible for mTOR activation by phosphorylation in S2448 [31]. Still, in human spermatozoa, the function of mTOR signaling is not yet clear.

HSP27 promotes the interaction of several proteins involved on structural integrity, membrane stability, cell cycle progression, apoptosis and thermo balance resistance [32]. HSP27 is known to be present in human testis, but was not identified in human spermatozoa [33]. This study is the first to report HSP27 in human spermatozoa and to show that the activation of HSP27 (S78) correlates negatively with motility. The well-characterized signaling pathway that activates HSP27 at S78 involves the p38 MAP kinase. p38 is a member of the MAPK family, and it is activated by

T180/Y182 phosphorylation by MKK3 and MKK6. It is a crucial participant in growth, differentiation, stress and apoptosis. In human spermatozoa, p38 is located in the tail and factors that activate p38 are still unknown [34,35]. Almog *et al.* showed that in human spermatozoa, upon phosphorylation and consequent activation, p38 inhibits forward and hyperactivated motility [34]. Our study also identified a negative association between p38 phosphorylation and spermatozoa motility. Moreover, the fact that we negatively correlated p38 and HSP27 (a p38 indirect substrate via MK2) activation with motility in human spermatozoa hints the importance of this pathway in controlling motility and reinforces the fidelity of our screen. Besides motility, we established a negative correlation between p38 phosphorylation and head abnormalities in patients with varicocele. Almog *et al.* also reported a correlation between p38 activation and human sperm morphology [34]. These results indicated that p38 has a crucial influence on spermatozoa physiology, from motility to morphology. JNK (c-Jun N-terminal kinases), another MAPK kinase, is activated by phosphorylation at T183/Y185 upon stress stimulus resulting in alterations in cell proliferation, apoptosis and migration [36,37]. In spermatozoa, the presence of JNK is still uncertain, so the fact that we identified and correlated it with motility (progressive and immotile) is another novel finding.

Glycogen synthase kinase 3 (GSK3) is a protein-serine/threonine kinase that exists in two highly related isoforms: GSK3α and GSK3β. The first report of GSK3β in spermatozoa established that after serine phosphorylation at S9, the phosphotransferase activity of this enzyme is lost. Moreover, a positive correlation was established between bull spermatozoa recovered from epididymis and GSK3β (S9) phosphorylation [38]. Interestingly, in human we found a negative correlation between phosphor-GSK3β (S9) and motility in ejaculated spermatozoa. Additionally, we identified a negative correlation of phosphor-GSK3β with spermatozoa head defects (in subjects with varicocele). To our knowledge, there is no described correlation between GSK3β and head defects in the literature. However, the fact that GSK3β is located on the posterior head region [39] can hint an association between head integrity and GSK3 activity.

We reported the association between several apoptosis-related signaling proteins and spermatozoa motility. Bad is a well-described pro-apoptotic protein. In human spermatozoa, it promotes apoptosis after significant stress [40]. Bad exerts its death- promoting effect by hetero-dimerizing with Bcl-2 in mitochondria. Upon phosphorylation, at several serine residues, Bad dissociates from Bcl-2 and is sequestered by the 14-3-3 protein. Consequently, Bcl-2 is activated and promotes cell survival [41]. Harada *et al.* identified PKA as the kinase involved in Bad phosphorylation at S112 [42]. Here, we report that Bad S112 phosphorylation is negatively correlated with progressive motility and positively correlated with immotile spermatozoa. It appears that Bad phosphorylation decreases spermatozoa motility, and it does not influence spermatozoa viability as expected. Additionally, we established a negative correlation between p53 activity and motility. In

spermatozoa, p53 is coupled with MDM2 in physiological conditions. Upon DNA damage, p53 undergoes phosphorylation at S15 (primary target) [43]. This promotes p53 uncoupling from MDM2 leading to p53 activation and consequently cell death promotion. In spermatozoa, p38 appears to be the main kinase responsible for p53 phosphorylation at S15 [43]. Since p38 phosphorylation also correlates negatively with motility (both in this study and in the literature) [34,35], we suggest that a single signaling pathway controlled by sequential phosphorylation could be involved in spermatozoa motility. Poly (ADP-ribose) polymerase (PARP) primary function is to signal DNA breaks to base excision repair and nucleotide repair pathways [44]. In human spermatozoa, it is the first line of defense against DNA breaks mostly caused by ROS. Moreover, PARP activation leads to p53 inhibition, which results in cell survival. Here, we observed a negative correlation between inactive PARP (cleaved, D214) and spermatozoa motility [44,45]. The enzyme responsible for PARP inactivation is caspase-3, a key player on apoptosis [44]. Caspase-3 activation, by cleavage at D175, is considered the no return point for apoptosis. In human spermatozoa, the presence and activation of capase-3 has been proven and extensively studied. Moreover, Weng *et al.* and Almeida *et al.* correlated caspase-3 activity with abnormal sperm concentration, morphology, and motility [46,47]. In our study, we correlated negatively caspase-3 activation (cleavage) with spermatozoa motility, which is in accordance with the literature. This reinforces the fidelity of our screen.

Akt plays a critical role in controlling survival and apoptosis in human sperm cells [48]. Recently it was suggested that phosphorylated Akt maintains the membrane integrity of ejaculated stallion spermatozoa, presumably by inhibiting caspases 3 and 7, which preserves sperm vitality [49]. Here, we report for the first time a negative correlation between phosphorylated Akt (pT308) levels and the percentage SDF, which supports a role of Akt in sperm survival. Additionally, in subjects diagnosed with varicocele, the levels of activated Akt (pT308/pT473) were negatively correlated with the percentage of head abnormalities.

p70 S6 kinase is a mitogen activated protein-serine/threonine protein kinase required for cell growth and G1 cell cycle progression [50]. Although it was originally described as being exclusively involved in cell growth and translational control [50], more recent published data described p70 S6 kinase as a multifunctional protein proposed to regulate spermatogenesis [51,52] by, for instance, regulating the actin dynamics in testis [53]. In mouse testis, p70 S6 kinase localizes in the spermatocytes' nucleus and in the cytoplasm of sperm cells, which indicated a translocation during spermatogenesis [54]. Here, we described that in human spermatozoa the levels of active p70 S6 kinase (pT389) were positively correlated with the percentage of normal spermatozoa and negatively correlated with the percentage of SDF. Phosphorylation of the T389 residue is critical for kinase function and correlates with its activity *in vivo* [50,55].

The relationship between SDF, sperm morphology and fertilization/pregnancy rates has been widely investigated, but the results are often inconsistent [56–58]. Here, we show that sperm morphology, specifically head abnormalities, and the TZI are related to elevated degree of DNA fragmentation. In contrast, the percentage of normal spermatozoa negatively correlates with the percentage of SDF. Sperm head abnormalities may, in part, be due to irregular sperm chromatin integrity. In turn, we showed that head abnormalities and the TZI are negatively correlated with the levels of activated phospho-Stat3 (pY705). Lachance and Leclerc have reported that Stat3 is present in human spermatozoa, and it is detected in the fraction containing mostly sperm head plasma membranes and in the flagellum cytoskeleton [59,60]. We reported a negative correlation between head morphological defects and the phosphorylation of Stat3 (pY705). The TZI also correlates negatively with phosphor-Stat3 (pY705) levels. Phosphorylation of Y705 is essential for Stat3 activation and has been reported in sperm [61]. Recent findings demonstrated that Stat3 function is not restricted to transcription factor activity, but is also involved in other functions through PPI [62]. Lachance and colleagues reported that Stat3-mediated signaling as significant for spermatozoa function [12].

Stat1 was previously shown to be present in human sperm in the apical region of the sperm head [16] and in the neck region of the sperm flagellum [60]. Stat1 is activated by phosphorylation at Y701 in response to the cytokines IFNα and IFNγ in human spermatozoa [16]. Capacitation-associated tyrosine phosphorylation of Stat1 was also demonstrated [59] and the JAK1-2/Stat1 pathway was shown to be activated by progesterone in human sperm [63]. However, the exact biological processes controlled by this pathway in sperm are still unknown. Here, we described that phosphorylated Stat1 (pY701) levels negatively correlate with the percentage of head abnormalities in subjects with varicocele. Previous reports have suggested a role for Stat1 in the first rounds of transcription in the fertilized oocyte [16,59]. It is already established that sperm delivers not only the male genome to the oocyte, but also crucial molecules for fertilization and embryo development [64–68]. D'Cruz and colleagues hypothesize that sperm-derived phosphorylated Stat proteins could contribute to the pool of transcription factors during sperm–oocyte fusion as well as transmit signal to the oocyte nucleus [16]. Here, we suggest that defects in Stat1- and Stat3-mediated signaling may compromise fertility.

Phosphorylation is a key mechanism for sperm motility acquisition, capacitation and acrosome reaction [27,38,39,69]. However, the players involved in the regulation of these processes are still far from being all identified. The KPKS-1.2 screen allowed the detection of 34 protein kinases (Table B.7), which include 29 PSTK, 1 PTYK, 3 PYK, and 1 PTK. From those, 8 protein kinases (CDK2, PAK3, KSR1, BMX, DAPK1, CSNK1D, MAP4K2 and ZIPK) were identified for the first time in human spermatozoa (Table B.7).

Finally, a PPI network was constructed based on the interactions between the signaling molecules examined in this study and their testis-enriched/specific interactors (Figure B.19). The key to understand how the proteins analyzed in this study are regulated in male germ cells lies in the identification and characterization of its interacting partners. Each protein interacts with a specific set of interactors according to the temporal and spatial (subcellular, cellular or tissue) context. This is particularly relevant in testis and spermatozoa since they present the largest number of enriched/specific genes leading to functional specifications [23]. For instance, TP53 interacts with 3 testis-enriched/specific proteins involved in spermatogenesis (PIWIL1, RPL10L and TDRD12) and 1 protein localized in the zona-pellucida receptor complex and involved in the binding to the zona-pellucida (HSPA1L). The recognition that GSK3β interacts with 2 testis-enriched/specific proteins localized in the sperm flagellum, specifically in the ciliary base (PRKACG) and sperm fibrous sheath (CABYR), may help to elucidate the role of this protein in sperm motility. TNP1, DPY19L2 and PIWIL1 are testis-enriched/specific proteins involved in spermatid development. They interact with PRKCA, AKT1 and TP53, respectively, suggesting a potential involvement of these proteins in the late stages of spermatogenesis. This PPI network approach may help to shed light on the function of the signaling proteins examined in the male reproductive system.

Seminal quality is a reflex of the signaling pathways occurring in the sperm cell. At the same time, spermatozoa integrity is crucial to the proper functioning of signaling cascades. We have identified several proteins that showed a high degree of differential activity and have the potential to integrate a quantitative array, which may have several applications: explain idiopathic infertility, failure in ART or repeated abortion; choice of the appropriate ART; assess the efficacy of medical interventions or treat infectious diseases and assess the efficacy of antioxidant therapies and lifestyle alterations

4.1.6. References

1. Lutz W, Leridon H, Aitken RJ, Von Eyben FE. Fertility rates and future population trends: Will Europe's birth rate recover or continue to decline? In: *International Journal of Andrology*.Vol 29.; 2006:25-33. doi:10.1111/j.1365-2605.2005.00639.x.
2. Baazeem A, Belzile E, Ciampi A, et al. Varicocele and male factor infertility treatment: A new meta-analysis and review of the role of varicocele repair. *Eur Urol*. 2011;60(4):796-808. doi:10.1016/j.eururo.2011.06.018.
3. Baker HW. Male infertility. *Endocrinol Metab Clin North Am*. 1994;23(4):783-793.
4. Hamada A, Esteves SC, Nizza M, Agarwal A. Unexplained male infertility: Diagnosis and management. *Int Braz J Urol*. 2012;38:576-594. doi:10.1590/S1677-55382012000500002.
5. Ferraretti AP, Goossens V, Kupka M, et al. Assisted reproductive technology in Europe, 2009: Results generated from European registers by ESHRE. *Hum Reprod*. 2013;28:2318-2331. doi:10.1093/humrep/det278.
6. Srivastava MD, Lippes J, Srivastava BI. Cytokines of the human reproductive tract. *Am J Reprod Immunol*. 1996;36:157-166. http://www.ncbi.nlm.nih.gov/pubmed/8874712.
7. Huleihel M, Levy A, Lunenfeld E, Horowitz S, Potashnik G, Glezerman M. Distinct expression of cytokines and mitogenic inhibitory factors in semen of fertile and infertile men. *Am J Reprod Immunol*. 1997;37:304-309.
8. Huleihel M, Lunenfeld E, Horowitz S, Levy A, Potashnik G, Glezerman M. Production of interleukin-1-like molecules by human sperm cells. *Fertil Steril*. 2000;73:1132-1137.
9. Naz RK, Kaplan P. Increased levels of interleukin-6 in seminal plasma of infertile men. *J Androl*. 15:220-227.
10. Paradisi R, Capelli M, Mandini M, Bellavia E, Focacci M, Flamigni C. Interleukin-2 in seminal plasma of fertile and infertile men. *Arch Androl*. 35:35-41.
11. Dousset B, Hussenet F, Daudin M, Bujan L, Foliguet B, Nabet P. Seminal cytokine concentrations (IL-1β, IL-2, IL-6, sR IL-2, sR IL-6), semen parameters and blood hormonal status in male infertility. *Hum Reprod*. 1997;12:1476-1479. doi:10.1093/humrep/12.7.1476.
12. Lachance C, Goupil S, Leclerc P. Stattic V, a STAT3 inhibitor, affects human spermatozoa through regulation of mitochondrial activity. *J Cell Physiol*. 2013;228:704-713. doi:10.1002/jcp.24215.
13. Paasch U, Grunewald S, Agarwal A, Glandera HJ. Activation pattern of caspases in human spermatozoa. *Fertil Steril*. 2004;81:802-809. doi:10.1016/j.fertnstert.2003.09.030.
14. Awda BJ, Buhr MM. Extracellular signal-regulated kinases (ERKs) pathway and reactive oxygen species regulate tyrosine phosphorylation in capacitating boar spermatozoa. *Biol Reprod*. 2010;83:750-758. doi:10.1095/biolreprod.109.082008.
15. Wertheimer E, Krapf D, De La Vega-Beltran JL, et al. Compartmentalization of distinct cAMP signaling pathways in mammalian sperm. *J Biol Chem*. 2013;288:35307-35320. doi:10.1074/jbc.M113.489476.
16. D'Cruz OJ, Vassilev AO, Uckun FM. Members of the Janus kinase/signal transducers and activators of transcription (JAK/STAT) pathway are present and active in human sperm. *Fertil Steril*. 2001;76:258-266. doi:10.1016/S0015-0282(01)01896-9.
17. Edition F. Examination and processing of human semen. *World Health*. 2010;Edition, F:286. http://whqlibdoc.who.int/publications/2010/9789241547789_eng.pdf.
18. Pelech S, Sutter C, Zhang H. Kinetworks protein kinase multiblot analysis. *Methods Mol Biol*. 2003;218:99-111.
19. Gellert P, Jenniches K, Braun T, Uchida S. C-It: A knowledge database for tissue-enriched genes. *Bioinformatics*. 2010;26(18):2328-2333. doi:10.1093/bioinformatics/btq417.
20. Wheeler DL, Church DM, Federhen S, et al. Database resources of the national center for biotechnology. *Nucleic Acids Res*. 2003;31(1):28-33. doi:10.1093/nar/gkg033.
21. Liu X, Yu X, Zack DJ, Zhu H, Qian J. TiGER: a database for tissue-specific gene expression and regulation. *BMC Bioinformatics*. 2008;9:271. doi:10.1186/1471-2105-9-271.
22. Yang X, Ye Y, Wang G, Huang H, Yu D, Liang S. VeryGene: linking tissue-specific genes to diseases, drugs, and beyond for knowledge discovery. *Physiol Genomics*. 2011;43(8):457-460. doi:10.1152/physiolgenomics.00178.2010.

23. Uhlén M, Fagerberg L, Hallström BM, et al. Tissue-based map of the human proteome. 2015. doi:10.1126/science.1260419.
24. Wu C, Orozco C, Boyer J, et al. BioGPS: an extensible and customizable portal for querying and organizing gene annotation resources. *Genome Biol*. 2009;10(11):R130. doi:10.1186/gb-2009-10-11-r130.
25. Saito R, Smoot ME, Ono K, et al. A travel guide to Cytoscape plugins. *Nat Methods*. 2012;9(11):1069-1076. doi:10.1038/nmeth.2212.
26. Dennis G, Sherman BT, Hosack DA, et al. DAVID: Database for Annotation, Visualization, and Integrated Discovery. *Genome Biol*. 2003;4(5):P3. doi:10.1186/gb-2003-4-9-r60.
27. Naz RK, Rajesh PB. Role of tyrosine phosphorylation in sperm capacitation / acrosome reaction. *Reprod Biol Endocrinol*. 2004;2:75. doi:10.1186/1477-7827-2-75.
28. Urner F, Sakkas D. Protein phosphorylation in mammalian spermatozoa. *Reproduction*. 2003;125:17-26. doi:10.1530/reprod/125.1.17.
29. Fardilha M, Esteves SLC, Korrodi-Gregório L, Pelech S, da Cruz e Silva OAB, da Cruz e Silva E. Protein phosphatase 1 complexes modulate sperm motility and present novel targets for male infertility. *Mol Hum Reprod*. 2011;17(8):466-477. doi:10.1093/molehr/gar004.
30. Fardilha M, Ferreira M, Pelech S, et al. "OMICS" of Human Sperm: Profiling Protein Phosphatases. *OMICS*. 2013;17(9):460-472. doi:10.1089/omi.2012.0119.
31. Chiang GG, Abraham RT. Phosphorylation of mammalian target of rapamycin (mTOR) at Ser-2448 is mediated by p70S6 kinase. *J Biol Chem*. 2005;280(27):25485-25490. doi:10.1074/jbc.M501707200.
32. Kostenko S, Moens U. Heat shock protein 27 phosphorylation: kinases, phosphatases, functions and pathology. *Cell Mol Life Sci*. 2009;66(20):3289-3307. doi:10.1007/s00018-009-0086-3.
33. Adly MA, Assaf HA, Hussein MRA. Heat shock protein 27 expression in the human testis showing normal and abnormal spermatogenesis. *Cell Biol Int*. 2008;32(10):1247-1255. doi:10.1016/j.cellbi.2008.07.009.
34. Almog T, Lazar S, Reiss N, et al. Identification of extracellular signal-regulated kinase 1/2 and p38 MAPK as regulators of human sperm motility and acrosome reaction and as predictors of poor spermatozoan quality. *J Biol Chem*. 2008;283(21):14479-14489. doi:10.1074/jbc.M710492200.
35. Ressurreição M, Rollinson D, Emery AM, Walker AJ. A role for p38 MAPK in the regulation of ciliary motion in a eukaryote. *BMC Cell Biol*. 2011;12:6. doi:10.1186/1471-2121-12-6.
36. Nishina H, Wada T, Katada T. Physiological roles of SAPK/JNK signaling pathway. *J Biochem*. 2004;136(2):123-126. doi:10.1093/jb/mvh117.
37. Stalheim L, Johnson GL. MAPK kinase kinase regulation of SAPK/JNK pathways. *Top Curr Genet*. 2008;20:1-15. doi:10.1007/4735_2007_0238.
38. Somanath PR, Jack SL, Vijayaraghavan S. Changes in sperm glycogen synthase kinase-3 serine phosphorylation and activity accompany motility initiation and stimulation. *J Androl*. 25(4):605-617. http://www.ncbi.nlm.nih.gov/pubmed/15223849.
39. Vijayaraghavan S, Mohan J, Gray H, Khatra B, Carr DW. A role for phosphorylation of glycogen synthase kinase-3alpha in bovine sperm motility regulation. *Biol Reprod*. 2000;62(6):1647-1654.
40. Aitken RJ, Bronson R, Smith TB, De Iuliis GN. The source and significance of dna damage in human spermatozoa; a commentary on diagnostic strategies and straw man fallacies. *Mol Hum Reprod*. 2013;19(8):475-485. doi:10.1093/molehr/gat025.
41. Fang X, Yu S, Eder A, et al. Regulation of BAD phosphorylation at serine 112 by the Ras-mitogen-activated protein kinase pathway. *Oncogene*. 1999;18(48):6635-6640. doi:10.1038/sj.onc.1203076.
42. Harada H, Becknell B, Wilm M, et al. Phosphorylation and inactivation of BAD by mitochondria-anchored protein kinase A. *Mol Cell*. 1999;3(4):413-422. doi:10.1016/S1097-2765(00)80469-4.
43. Karabulut S, Demiroglu-Zergeroglu A, Yilmaz E, Sagir F, Delikara N. p53 and mitogen-activated protein kinase pathway protein profiles in fresh and frozen spermatozoa. *Andrologia*. 2014. doi:10.1111/and.12200.
44. Agarwal A, Mahfouz RZ, Sharma RK, Sarkar O, Mangrola D, Mathur PP. Potential biological role of poly (ADP-ribose) polymerase (PARP) in male gametes. *Reprod Biol Endocrinol*. 2009;7:143. doi:10.1186/1477-7827-7-143.
45. Mahfouz RZ, Sharma RK, Poenicke K, et al. Evaluation of poly(ADP-ribose) polymerase cleavage

(cPARP) in ejaculated human sperm fractions after induction of apoptosis. *Fertil Steril*. 2009;91(5 SUPPL.):2210-2220. doi:10.1016/j.fertnstert.2008.02.173.

46. Weng S-L, Taylor SL, Morshedi M, et al. Caspase activity and apoptotic markers in ejaculated human sperm. *Mol Hum Reprod*. 2002;8(11):984-991.
47. Almeida C, Cardoso MF, Sousa M, et al. Quantitative study of caspase-3 activity in semen and after swim-up preparation in relation to sperm quality. *Hum Reprod*. 2005;20(5):1307-1313. doi:10.1093/humrep/deh727.
48. Aitken RJ, Baker MA. Causes and consequences of apoptosis in spermatozoa; contributions to infertility and impacts on development. *Int J Dev Biol*. 2013;57(2-4):265-272. doi:10.1387/ijdb.130146ja.
49. Gallardo Bolanos JM, Balao da Silva CM, Martin Munoz P, et al. Phosphorylated AKT preserves stallion sperm viability and motility by inhibiting caspases 3 and 7. *Reproduction*. 2014;148(2):221-235. doi:10.1530/REP-13-0191.
50. Pullen N, Thomas G. The modular phosphorylation and activation of p70(s6k). In: *FEBS Letters*.Vol 410.; 1997:78-82. doi:10.1016/S0014-5793(97)00323-2.
51. Chen L, Jia J-M, Zhong W, et al. P70S6K is involved in the inhibition of testosterone production in TM3 mouse Leydig cells overexpressing Cox7a2. *Zhonghua Nan Ke Xue*. 2011;17(4):291-295.
52. Feng LX, Ravindranath N, Dym M. Stem cell factor/c-kit up-regulates cyclin D3 and promotes cell cycle progression via the phosphoinositide 3-kinase/p70 S6 kinase pathway in spermatogonia. *J Biol Chem*. 2000;275(33):25572-25576. doi:10.1074/jbc.M002218200.
53. Ip CKM, Wong AST. p70 S6 kinase and actin dynamics: A perspective. *Spermatogenesis*. 2012;2(1):44-52. doi:10.4161/spmg.19413.
54. Yu B-Z, Song Y-T, Yu D-H, et al. Expression and immunohistochemical localization of Cdc2 and P70S6K in different stages of mouse germ cells. *Cell Biochem Funct*. 24(2):113-117.
55. Weng QP, Kozlowski M, Belham C, Zhang A, Comb MJ, Avruch J. Regulation of the p70 S6 kinase by phosphorylation in vivo. Analysis using site-specific anti-phosphopeptide antibodies. *J Biol Chem*. 1998;273:16621-16629. doi:10.1074/jbc.273.26.16621.
56. Cohen-Bacrie P, Belloc S, Ménézo YJR, Clement P, Hamidi J, Benkhalifa M. Correlation between DNA damage and sperm parameters: a prospective study of 1,633 patients. *Fertil Steril*. 2009;91(5):1801-1805. doi:10.1016/j.fertnstert.2008.01.086.
57. Dariš B, Goropevnek A, Hojnik N, Vlaisavljević V. Sperm morphological abnormalities as indicators of DNA fragmentation and fertilization in ICSI. *Arch Gynecol Obstet*. 2010;281(2):363-367. doi:10.1007/s00404-009-1140-y.
58. Cassuto NG, Hazout A, Hammoud I, et al. Correlation between DNA defect and sperm-head morphology. *Reprod Biomed Online*. 2012;24(2):211-218. doi:10.1016/j.rbmo.2011.10.006.
59. Bastián Y, Zepeda-Bastida A, Uribe S, Mújica A. In spermatozoa, Stat1 is activated during capacitation and the acrosomal reaction. *Reproduction*. 2007;134(3):425-433. doi:10.1530/REP-06-0264.
60. Lachance C, Leclerc P. Mediators of the Jak/STAT signaling pathway in human spermatozoa. *Biol Reprod*. 2011;85:1222-1231. doi:biolreprod.111.092379 [pii]\r10.1095/biolreprod.111.092379.
61. Aquila S, Rago V, Guido C, Casaburi I, Zupo S, Carpino A. Leptin and leptin receptor in pig spermatozoa: Evidence of their involvement in sperm capacitation and survival. *Reproduction*. 2008;136(1):23-32. doi:10.1530/REP-07-0304.
62. Ng DCH, Bao HL, Cheh PL, et al. Stat3 regulates microtubules by antagonizing the depolymerization activity of stathmin. *J Cell Biol*. 2006;172(2):245-257. doi:10.1083/jcb.200503021.
63. Sagare-Patil V, Modi D. Progesterone activates Janus Kinase 1/2 and activators of transcription 1 (JAK1-2/STAT1) pathway in human spermatozoa. *Andrologia*. 2013;45(3):178-186. doi:10.1111/j.1439-0272.2012.01332.x.
64. Ostermeier GC, Dix DJ, Miller D, Khatri P, Krawetz SA. Spermatozoal RNA profiles of normal fertile men. *Lancet*. 2002;360:772-777. doi:10.1016/S0140-6736(02)09899-9.
65. Ostermeier GC, Miller D, Huntriss JD, Diamond MP, Krawetz SA. Reproductive biology: delivering spermatozoan RNA to the oocyte. *Nature*. 2004;429:154. doi:10.1038/429154a.
66. Ostermeier GC, Goodrich RJ, Moldenhauer JS, Diamond MP, Krawetz SA. A suite of novel human spermatozoal RNAs. *J Androl*. 26:70-74. doi:26/1/70 [pii].

67. Saunders CM, Larman MG, Parrington J, et al. PLC zeta: a sperm-specific trigger of Ca(2+) oscillations in eggs and embryo development. *Development*. 2002;129:3533-3544.
68. Ainsworth C. Cell biology: the secret life of sperm. *Nature*. 2005;436:770-771. doi:10.1038/436770a.
69. Huang Z, Vijayaraghavan S. Increased Phosphorylation of a Distinct Subcellular Pool of Protein Phosphatase, PP1 2, During Epididymal Sperm Maturation. *Biol Reprod*. 2004;70(2):439-447. doi:10.1095/biolreprod.103.020024.
70. Wang G, Guo Y, Zhou T, et al. In-depth proteomic analysis of the human sperm reveals complex protein compositions. *J Proteomics*. 2013;79:114-122. doi:10.1016/j.jprot.2012.12.008.
71. Castillo J, Amaral A, Oliva R. Sperm nuclear proteome and its epigenetic potential. *Andrology*. 2014;2(3):326-338. doi:10.1111/j.2047-2927.2013.00170.x.
72. Aquila S, Middea E, Catalano S, et al. Human sperm express a functional androgen receptor: Effects on PI3K/AKT pathway. *Hum Reprod*. 2007;22(10):2594-2605. doi:10.1093/humrep/dem243.
73. Lefièvre L, Chen Y, Conner SJ, et al. Human spermatozoa contain multiple targets for protein S-nitrosylation: An alternative mechanism of the modulation of sperm function by nitric oxide? *Proteomics*. 2007;7(17):3066-3084. doi:10.1002/pmic.200700254.
74. De Mateo S, Martínez-Heredia J, Estanyol JM, et al. Marked correlations in protein expression identified by proteomic analysis of human spermatozoa. *Proteomics*. 2007;7(23):4264-4277. doi:10.1002/pmic.200700521.
75. Siva AB, Kameshwari DB, Singh V, et al. Proteomics-based study on asthenozoospermia: Differential expression of proteasome alpha complex. *Mol Hum Reprod*. 2010;16(7):452-462. doi:10.1093/molehr/gaq009.
76. Gu B, Zhang J, Wu Y, et al. Proteomic analyses reveal common promiscuous patterns of cell surface proteins on human embryonic stem cells and sperms. *PLoS One*. 2011;6(5). doi:10.1371/journal.pone.0019386.
77. Parte PP, Rao P, Redij S, et al. Sperm phosphoproteome profiling by ultra performance liquid chromatography followed by data independent analysis (LC-MSE) reveals altered proteomic signatures in asthenozoospermia. *J Proteomics*. 2012;75(18):5861-5871. doi:10.1016/j.jprot.2012.07.003.
78. Amaral A, Castillo J, Estanyol JM, Ballescà JL, Ramalho-Santos J, Oliva R. Human sperm tail proteome suggests new endogenous metabolic pathways. *Mol Cell Proteomics*. 2013;12(2):330-342. doi:10.1074/mcp.M112.020552.
79. Baker MA, Naumovski N, Hetherington L, Weinberg A, Velkov T, Aitken RJ. Head and flagella subcompartmental proteomic analysis of human spermatozoa. *Proteomics*. 2013;13(1):61-74. doi:10.1002/pmic.201200350.
80. Amaral A, Paiva C, Attardo Parrinello C, et al. Identification of Proteins Involved in Human Sperm Motility Using High-Throughput Differential Proteomics. *J Proteome Res*. 2014;13(12):5670-5684. doi:10.1021/pr500652y.
81. Raimondo S, Aprea G, Cuomo F, De Filippo S, Gentile T, Guida J. Quantitative evaluation of p53 as a new indicator of DNA damage in human spermatozoa. *J Hum Reprod Sci*. 2014;7(3):212. doi:10.4103/0974-1208.142490.
82. Koppers AJ, Mitchell LA, Wang P, Lin M, Aitken RJ. Phosphoinositide 3-kinase signalling pathway involvement in a truncated apoptotic cascade associated with motility loss and oxidative DNA damage in human spermatozoa. *Biochem J*. 2011;436(3):687-698. doi:10.1042/BJ20110114.
83. Nixon B, Mitchell LA, Anderson AL, Mclaughlin EA, O'bryan MK, Aitken RJ. Proteomic and functional analysis of human sperm detergent resistant membranes. *J Cell Physiol*. 2011;226(10):2651-2665. doi:10.1002/jcp.22615.
84. Rotem R, Paz GF, Homonnai ZT, et al. Ca(2+)-independent induction of acrosome reaction by protein kinase C in human sperm. *Endocrinology*. 1992;131(5):2235-2243.
85. Lemoine M, Dupont J, Guillory V, Tesseraud S, Blesbois E. Potential involvement of several signaling pathways in initiation of the chicken acrosome reaction. *Biol Reprod*. 2009;81(4):657-665. doi:10.1095/biolreprod.108.072660.
86. Luconi M, Barni T, Vannelli GB, et al. Extracellular signal-regulated kinases modulate capacitation of human spermatozoa. *Biol Reprod*. 1998;58(6):1476-1489. doi:10.1095/biolreprod58.6.1476.

87. Jungnickel MK, Sutton KA, Wang Y, Florman HM. Phosphoinositide-dependent pathways in mouse sperm are regulated by egg ZP3 and drive the acrosome reaction. *Dev Biol*. 2007;304(1):116-126. doi:10.1016/j.ydbio.2006.12.023.
88. O'Flaherty C, de Lamirande E, Gagnon C. Reactive oxygen species and protein kinases modulate the level of phospho-MEK-like proteins during human sperm capacitation. *Biol Reprod*. 2005;73(1):94-105. doi:10.1095/biolreprod.104.038794.
89. Vijayaraghavan S, Stephens DT, Trautman K, et al. Sperm motility development in the epididymis is associated with decreased glycogen synthase kinase-3 and protein phosphatase 1 activity. *Biol Reprod*. 1996;54(3):709-718. doi:10.1095/biolreprod54.3.709.
90. Xu X, Toselli PA, Russell LD, Seldin DC. Globozoospermia in mice lacking the casein kinase II alpha' catalytic subunit. *Nat Genet*. 1999;23(1):118-121. doi:10.1038/12729.
91. Lalancette C, Faure RL, Leclerc P. Identification of the proteins present in the bull sperm cytosolic fraction enriched in tyrosine kinase activity: A proteomic approach. *Proteomics*. 2006;6(16):4523-4540. doi:10.1002/pmic.200500578.
92. Lawson C, Goupil S, Leclerc P. Increased activity of the human sperm tyrosine kinase SRC by the cAMP-dependent pathway in the presence of calcium. *Biol Reprod*. 2008;79(4):657-666. doi:10.1095/biolreprod.108.070367.
93. Harayama H, Murase T, Miyake M. A cyclic adenosine 3',5'-monophosphate stimulates phospholipase Cgamma1-calcium signaling via the activation of tyrosine kinase in boar spermatozoa. *J Androl*. 26(6):732-740. doi:10.2164/jandrol.05053.

4.2. Unraveling the association between age and signaling proteins in human spermatozoa

Joana Vieira Silva[1]; Bárbara Regadas Correia[1]; António Patrício[2]; Margarida Fardilha[1]

[1] Laboratory of Signal Transduction, Department of Medical Sciences, Institute of Biomedicine – iBiMED, University of Aveiro, 3810-193 Aveiro, Portugal.

[2] Hospital Infante D. Pedro E.P.E., 3810-193 Aveiro, Portugal

Corresponding author: Margarida Fardilha, Departamento de Ciências Médicas, Universidade de Aveiro, Campus Universitário de Santiago, Agra do Crasto – Edifício 30, 3810-193 Aveiro, Portugal. T: +351-918143947. E: mfardilha@ua.pt

To be submitted to Fertility and Sterility

4.2.1. Abstract

Objective: To determine the correlation between male age and the activity of signaling proteins in human spermatozoa. **Design:** *In vitro* studies with human spermatozoa. **Settings:** Academic research institute in collaboration with a local hospital. **Patients:** Sixty-three men provided semen samples for routine analysis. **Interventions:** None **Main Outcome Measures:** Phosphorylation/cleavage patterns of 18 signaling proteins in human spermatozoa. **Results:** The volunteers for this study were Caucasian males, with ages ranging from 18 to 47 years (mean age±SD of 26±7). The results indicated that the phosphorylated levels of several proteins [p53 (S15), PRAS40 (T246), Bad (S112), p38 (T180/Y182), mTOR (S2448), HSP27 (S78), GSK-3b (S9) and Akt (S473)], as well as, cleavage of Caspase-3 (at D175) showed a significant positive correlation with age. HSP27 (S78), Bad (S112), PRAS40 (T246), p53 (S15) and p38 (T180/Y182) expression was consistently and significantly higher as early as 25 years of age. **Conclusions:** This study contributed towards understanding the molecular mechanisms underlying the age-based impact in semen quality. Furthermore, age thresholds for changes in certain spermatozoa signaling parameters were established.

4.2.2. Introduction

Infertility is a growing concern in modern society, especially in industrialized countries where birth rates are declining drastically below replacement levels. Consequences are dramatic: there will be fewer women of childbearing age, fewer family members to care for elders, pensions will increase public spending and the workforce will be older and less adaptable decreasing productivity [1]. Infertility affects ~15% of couples attempting to conceive and in half of the cases the cause is at least partly related to male reproductive issues [1]. Moreover, idiopathic infertility remains the most common type of male infertility [2,3].

The trend in parenthood at an older age is increasingly more pronounced, with the age of first child averaging 30 years in several countries. In addition to intentionally delayed childbearing due to professional activities, increased rates of obesity, sedentary lifestyle, alcohol and nicotine consumption found in reproductive-aged men and women further perpetuate the problem. The idea that "men can have children at any age" is untrue. While it is well documented that women have a decline in fecundity with age [4], the studies available regarding the effects of age on male fertility have a wider disparity of results. Most studies are mainly focused on basic semen parameters and DNA integrity (revised in [5]), many have reported lower semen volume, sperm concentration, sperm motility and proportions of sperm of normal morphology in older men; and some have, however, found semen quality to be independent from age or, even reported improvements in semen traits (revised in [5,6]). Additionally, most studies are limited to a specific study population and are

influenced by the female partner age [6,7]. Recently, Johnson and colleagues conducted a systematic review and meta-analysis to quantify the effect of male age on basic semen parameters and DNA fragmentation. Age-associated declines in semen volume, percentage motility, progressive motility, normal morphology and unfragmented cells were statistically significant and results appeared to be robust against confounding factors [5]. Stone et al reported that these parameters start to decline at 34 years of age [8]. Other age thresholds have also been established for several basic semen parameters [9–11]. Numerous studies have described adverse associations between male age and reproductive outcomes. Advanced paternal age has been associated with lower pregnancy rates, higher risk of pregnancy loss, as well as with a broad range of developmental, morphologic and neurologic disorders of the newborn, including schizophrenia, autism, X-linked recessive and autosomal dominant disorders, trisomy and some cancers (revised in [5,6,12–14]). While the molecular mechanisms are still not understood, aging is associated with an increase in oxidative stress and a decline in sperm quality has been correlated with the excessive generation of reactive oxygen species (ROS) [5].

Since the molecular mechanisms responsible for age-dependent decline in spermatozoa quality are not fully understood, in this study we evaluated the impact of aging on the human spermatozoa signaling pathways. Additionally, we determined whether age thresholds for the molecular parameters examined existed.

4.2.3. Methods

Sperm samples collection and basic semen analysis

This study was approved by the Ethics and Internal Review Board of the Hospital Infante D. Pedro E.P.E. (Aveiro, Portugal) and was conducted in accordance with the ethical standards of the Helsinki Declaration. All donors signed informed consent allowing the samples to be used for scientific purposes. A total of 63 semen samples were obtained from a randomized group of donors, by masturbation to a sterile container. Basic semen analysis was performed by qualified technicians according to World Health Organization (WHO) guidelines [15]. Briefly, after complete liquefaction of the semen sample a macroscopic examination was performed. The microscopic examination included the analysis of spermatozoa motility, concentration and morphology. All microscopy analyses were performed using the Zeiss ® Primo Star microscope (Zeiss ®, Jena, Germany).

Antibody array

Antibody-based arrays were carried out using the PathScan® Intracellular Signaling Array Kit (#7744, Cell Signaling Technology, Danvers, MA, USA) to determine the expression patterns of 18

well-characterized signaling molecules when phosphorylated or cleaved, in 63 semen samples obtained from a randomized group of donors. After semen liquefaction, sperm cells were washed three times in 1x phosphate buffered saline (PBS) by centrifugation (600xg for 5 minutes at 4°C) and lysed according to the manufacturer's instructions. Protein concentration was measured using bicinchoninic acid (BCA) assay (Pierce Biotechnology, USA) and final absorbance was measured at 562 nm in a microplate reader (TECAN, Genius, Männedorf, Switzerland). Each cell extract was diluted to 250 µg/ml and applied to its own multiplexed array according to the manufacturer's instructions. Fluorescence readouts from the arrays were captured digitally using LI-COR® Biosciences Odyssey® imaging system (LI-COR® Biosciences, Nebraska, USA). Pixel intensity was quantified using Odyssey software. The intensity from the negative control within each array was subtracted from all signals, and all data from each array were normalized to the internal positive control within each array.

Statistical analysis

Statistical analysis was conducted using the IBM SPSS Statistics Software 22. First, a descriptive analysis to each quantitative parameter analyzed was performed. Lastly, we calculated the Pearson correlation coefficient, r, or the Spearman's rho correlation coefficient, r_s, (a nonparametric correlation method) to determine the relationship between two variables. We performed a test of normality (Shapiro-Wilk test) and we analyzed the box-plots to decide between a parametric or non-parametric method. The dataset size was considered reasonable since based on the central limit theorem it was possible to approximate the distribution of variables to a normal distribution. The age brackets were set to create three consecutive subgroups and we performed the Kruskal Wallis test (grouping variable: age bracket). When differences were statistically significant between groups, they were compared by post hoc analysis. The significance level was set at 0.05.

4.2.4. Results

Correlation between age and signaling proteins in distinct states of activation

A total of 63 semen samples, obtained from a randomized group of donors, were included in this study (Supplementary Table D.27). The volunteers ages ranged from 18 to 47 years (mean age±SD of 26±7). Basic semen parameters were analyzed according to the WHO's guidelines (Supplementary Table D.27). The levels of signaling molecules were determined with the PathScan Intracellular Signaling Array, which includes antibodies for phosphorylated or cleaved signaling proteins (Supplementary Table D.27). Initially, a descriptive analysis of the results was performed (Supplementary Table D.28). Next, to evaluate the association between age and the levels of signaling molecules, Spearman's and Pearson correlation tests were performed (Table B.8). The

results indicated that the levels of several phosphoproteins positively correlates with age: p53 (S15), PRAS40 (T246), Bad (S112), p38 (T180/Y182), mTOR (S2448), HSP27 (S78), GSK-3b (S9) and Akt (S473). The cleavage, and consequently activation, of Caspase-3 (at D175) was also positively correlated with age (Table B.8).

Table B.8 – Associations between age and the phosphorylation/cleavage patterns of signaling proteins in human spermatozoa.

Uniprot ID	Abbreviation		Recommended protein name	Phosphorylation/ cleavage, residue, status	Correlation Coefficient/ Sig. (2-tailed)
	Formerly	Presently			
P04637	p53	TP53	Cellular tumor antigen p53	Phospho S15 Activation	r_s= 0.511** p= 0.000
Q96B36	PRAS40	AKT1S1	Proline-rich AKT1 substrate 1	Phospho T246 Inhibition	r_s= 0.460** p= 0.000
Q16539 Q15759 P53778 O15264	p38 MAPK	MAPK14/11/12/13	Mitogen-activated protein kinase 14/11/12/13	Phospho T180/Y182 Activation	r_s= 0.427* p= 0.000
Q92934	Bad	BAD	Bcl2-associated agonist of cell death	Phospho S112 Inhibition	r_s= 0.404** p= 0.001
P42574	Caspase-3	CASP3	Caspase-3	Cleavage D175 Activation	r_s= 0.404** p= 0.001
P42345	mTOR	MTOR	Serine/threonine-protein kinase mTOR	Phospho S2448 Activation	r_s= 0.370** p= 0.003
P04792	HSP27	HSPB1	Heat shock protein beta-1	Phospho S78 Activation	r_s= 0,346** p= 0.006
P49841	GSK-3β	GSK3B	Glycogen synthase kinase-3 beta	Phospho S9 Inhibition	r_s= 0,307* p= 0.015
P31749	Akt	AKT1	RAC-alpha serine/threonine-protein kinase	Phospho S473 Activation	r_s= 0.298* p= 0.018

*- correlation is significant at the 0.05 level (2-tailed); **- correlation is significant at the 0.01 level (2-tailed); r_s, Spearman´s rho correlation coefficient

In order to determine whether age thresholds for the molecular parameters exist, three consecutive age subgroups were created and the Kruskal Wallis test was performed. Asterisked values in Table B.9 indicate the age brackets in which average values for the measured parameters consistently and significantly increased. It was established that HSP27 (S78), Bad (S112), PRAS40 (T246), p53 (S15) and p38 (T180/Y182) expression consistently and significantly increased after 25 years (Figure B.20).

Table B.9 – Summary of statistical measures and Kruskal Wallis Test p-value.

		Age Bracket			p-value of Chi-Square [a]
		<25	[25,33]	>33	
	Frequency	35	16	12	
	Percentage	55,6%	25,4%	19,0%	
Formerly	Presently	Mean ± SD	Mean ± SD	Mean ± SD	
Erk1/2	MAPK3/1	0,12 ± 0,06	0,14 ± 0,07	0,13 ± 0,10	NS
Stat1	STAT1	0,11 ± 0,07	0,14 ± 0,09	0,14 ± 0,12	NS
Stat3	STAT3	0,10 ± 0,04	0,12 ± 0,06	0,12 ± 0,13	NS
Akt	AKT1	0,09 ± 0,03	0,10 ± 0,04	0,10 ± 0,08	NS
Akt	AKT1	0,06 ± 0,04	0,11 ± 0,07	0,11 ± 0,08	NS
AMPKa	PRKAA	0,14 ± 0,08	0,20 ± 0,11	0,19 ± 0,15	NS

		Age Bracket			p-value of Chi-Square [a]
		<25	[25,33]	>33	
	Frequency	35	16	12	
	Percentage	55,6%	25,4%	19,0%	
Formerly	**Presently**	Mean ± SD	Mean ± SD	Mean ± SD	
S6 ribosomal protein	RPS6	0,07 ± 0,04	0,12 ± 0,07	0,11 ± 0,08	NS
mTOR	MTOR	0,11 ± 0,06	0,23 ± 0,17	0,22 ± 0,16	NS
HSP27	HSPB1	0,09 ± 0,06	0,20 ± 0,17 *	0,19 ± 0,13 *	0.005
Bad	BAD	0,08 ± 0,03	0,14 ± 0,08 *	0,15 ± 0,09 *	0.002
p70 S6 Kinase	RPS6KB1	0,03 ± 0,02	0,05 ± 0,02	0,04 ± 0,03	NS
PRAS40	AKT1S1	0,06 ± 0,05	0,14 ± 0,11 *	0,14 ± 0,10 *	0.000
p53	TP53	0,03 ± 0,02	0,06 ± 0,04 *	0,07 ± 0,05 *	0.000
p38 MAPK	MAPK14	0,08 ± 0,05	0,18 ± 0,13 *	0,18 ± 0,13 *	0.001
SAPK/JNK	MAPK8/9/10	0,10 ± 0,04	0,18 ± 0,15	0,18 ± 0,13	NS
PARP	PARP	0,09 ± 0,04	0,14 ± 0,08	0,12 ± 0,08	NS
Caspase-3	CASP3	0,07 ± 0,04	0,13 ± 0,08	0,12 ± 0,08	NS
GSK-3β (S9)	GSK3B	0,14 ± 0,10	0,27 ± 0,18	0,25 ± 0,23	NS

a. Grouping variable: Age Bracket; * The average value is significantly higher than in the age bracket <25

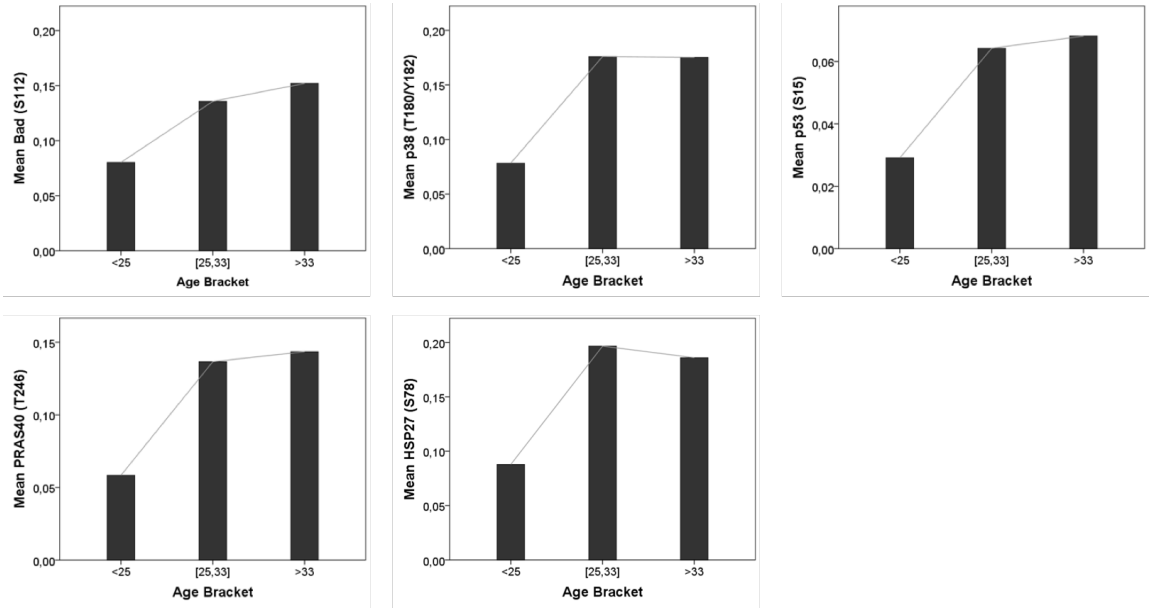

Figure B.20 – Signaling proteins consistently and significantly increased after the age bracket <25. See Table 2 for p values.

4.2.5. Discussion

Several studies have investigated age-based impact in semen parameters, such as, semen volume, sperm concentration, morphology, motility and DNA fragmentation, but the impact of paternal age on human spermatozoa signaling pathways remains unknown. Using a total of 63 semen samples, obtained from a random group of donors, we conducted a study to determine the association of male age and the activity patterns of 18 signaling proteins in human spermatozoa. The correlation between age and proteins involved in specific signaling pathways that were previously correlated with spermatozoa quality can pinpoint the age-depended alterations in sperm function.

A schematic representation of the pathways in which each of the signaling molecules examined in this study are involved is presented in Figure B.21. When known, the outcome in human spermatozoa of the signaling pathways in which the proteins are involved, is presented.

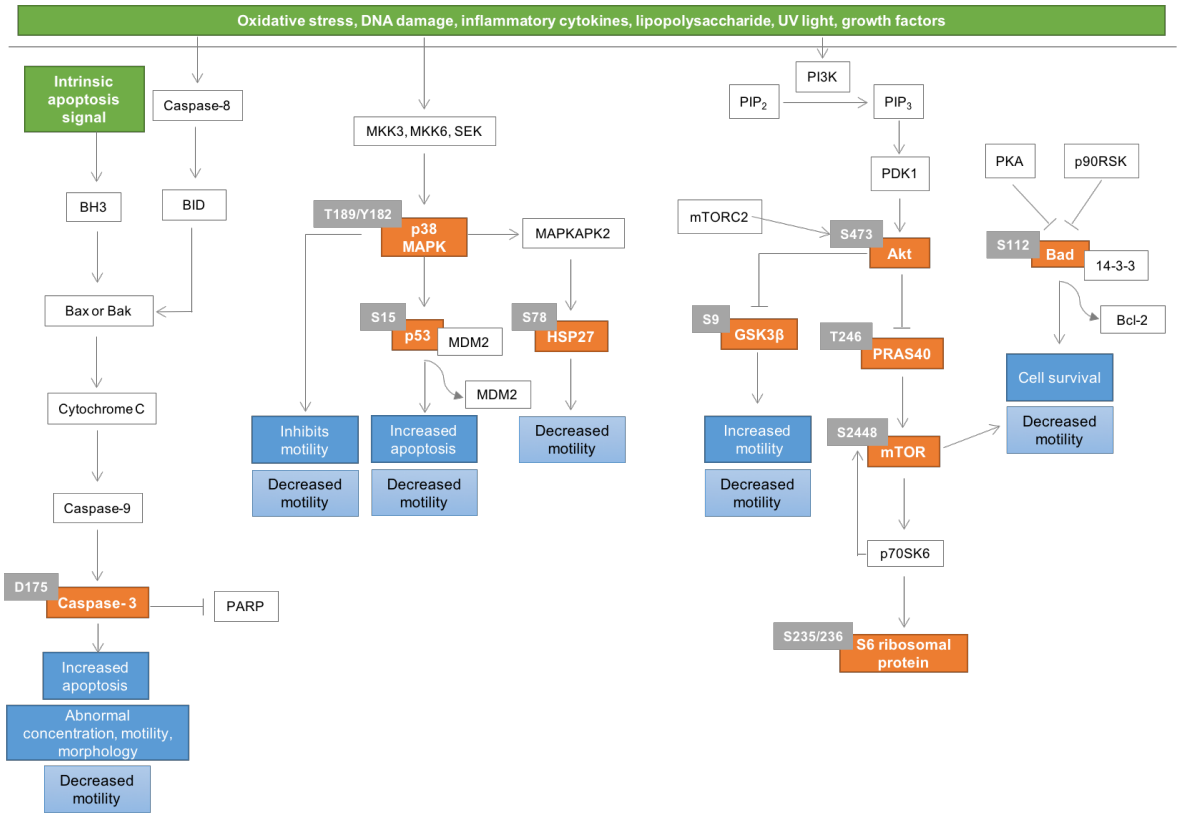

Figure B.21 – Pathways in which the signaling proteins identified as correlated with paternal age are involved (orange). Whenever the pathway output was previously described in spermatozoa it is indicated in blue boxes. Light blue boxes represent correlations between the signaling proteins and the semen parameters previously described in [16].

p38 MAPK, p53 and HSP27 activities, which correlates negatively with human spermatozoa motility [17,18,16], revealed positive associations with age. In spermatozoa, p38 MAPK appears to be the main kinase responsible for p53 phosphorylation (S15) [19], that subsequently leads to apoptosis [19]. Besides motility, a correlation between p38 MAPK activation and human sperm morphology was also previously established [17,16]. The p38 MAPK signaling pathway is also involved in the activation of HSP27 by phosphorylation at S78. We reported recently, for the first time, the presence of HSP27 and its activation in human spermatozoa. This signaling pathway appears to be involved in regulating spermatozoa apoptosis [19], motility [17,18,16] and age-dependent alterations.

Moreover, we have also shown that the activation of the PI3K/AKT1/mTOR pathway in human spermatozoa was associated with increased age. We previously reported the presence of mTOR in human spermatozoa for the first time and established a negative correlation between its activity and sperm motility.

Glycogen synthase kinase 3 (GSK3) activity has been extensively correlated with spermatozoa motility. GSK3 phosphorylation at S9 inhibits its catalytic activity. GSK3 is 6 times more active in caput than in caudal spermatozoa and its activity is correlated negatively with spermatozoa motility (bovine and mouse and macaque models) [20–22]. Recently, we reported an opposing correlation in human ejaculated spermatozoa [16]. Here we established a positive association between the levels of GSK-3β (S9) and male age.

In human spermatozoa Bad promotes apoptosis after significant stress in human spermatozoa [23]. Phospho-Bad (S99) is predominantly located in the human spermatozoa midpiece; however, when PI3K is inhibited phospho-BAD (S99) cross-reactivity is lost [24]. Upon serine phosphorylation Bad apoptotic activity is inhibited, due to dissociation from Bcl-2, and is sequestered by the 14-3-3 protein, rendering Bcl-2 active [25]. It was previously described that Bad is phosphorylated at S112 by p90RSK [26] and PKA [27]. Here we showed a positive correlation between Bad S112 phosphorylation, which was previously described as associated with decreased spermatozoa motility [16], with increased male age. Caspase-3 activation, by cleavage at D175, has been correlated with abnormal sperm concentration, morphology, and motility [28,29,16]. Caspase-3 is responsible for PARP inactivation, which is the first line of defense against DNA damage in human spermatozoa [30]. Here we demonstrated that higher amounts of activated caspase-3 are associated with increased age.

Recently, Stone and colleagues reported that semen parameters do not change before 34 years old [8]. Our analysis revealed that consistent significant increase in HSP27 (S78), Bad (S112), PRAS40 (T246), p53 (S15) and p38 (T180/Y182) appeared as soon as 25 years (Figure B.20 and Table B.9). This threshold occurs prior than the ones established for basic semen parameters, which may indicate that alterations at the molecular level occur earlier. Rising levels of ROS in semen were reported in men older than 40 years and ROS have been suggested as the causative factor for incremental sperm defects with aging [31]. Our analysis revealed alterations at the molecular level occurring before this age threshold, which may indicate other possible mechanisms for age-dependent patterns of sperm quality decline. The reduced number of individuals with more than 33 years (19% of the study population) did not allow to draw consistent conclusions for the other signaling proteins correlated with age. Further studies, to increase the number of volunteers older than 33 years, are needed in order to determine the exact age thresholds for each molecular parameter. In the future, the variables correlated with age will also be analyzed by change-point regression analysis, which will allow the definition of discrete age thresholds.

We have identified several signaling proteins that presented high correlation with aging (Table B.8, Figure B.20 and Figure B.21). The identification of the male molecular factors associated with the

age-dependent decline in seminal parameters and, consequently, in the reproductive outcomes, will improve fertility management.

4.2.6. References

1. Lutz, W., Leridon, H., Aitken, R. J. & Von Eyben, F. E. Fertility rates and future population trends: Will Europe's birth rate recover or continue to decline? in *International journal of andrology* 29, 25–33 (2006).
2. Baker, H. W. Male infertility. *Endocrinol. Metab. Clin. North Am.* 23, 783–793 (1994).
3. Hamada, A., Esteves, S. C., Nizza, M. & Agarwal, A. Unexplained male infertility: Diagnosis and management. *International Braz J Urol* 38, 576–594 (2012).
4. Crawford, N. M. & Steiner, A. Z. Age-related infertility. *Obstet. Gynecol. Clin. North Am.* 42, 15–25 (2015).
5. Johnson, S. L., Dunleavy, J., Gemmell, N. J. & Nakagawa, S. Consistent age-dependent declines in human semen quality: A systematic review and meta-analysis. *Ageing Res. Rev.* 19, 22–33 (2015).
6. Kidd, S. A., Eskenazi, B. & Wyrobek, A. J. Effects of male age on semen quality and fertility: a review of the literature. *Fertil. Steril.* 75, 237–48 (2001).
7. Zhu, Q.-X., Meads, C., Lu, M.-L., Wu, J.-Q., Zhou, W.-J. & Gao, E.-S. Turning point of age for semen quality: a population-based study in Chinese men. *Fertil. Steril.* 96, 572–6 (2011).
8. Stone, B. A., Alex, A., Werlin, L. B. & Marrs, R. P. Age thresholds for changes in semen parameters in men. *Fertil. Steril.* 100, 952–958 (2013).
9. Pasqualotto, F. F., Sobreiro, B. P., Hallak, J., Pasqualotto, E. B. & Lucon, A. M. Sperm concentration and normal sperm morphology decrease and follicle-stimulating hormone level increases with age. *BJU Int.* 96, 1087–91 (2005).
10. Levitas, E., Lunenfeld, E., Weisz, N., Friger, M. & Potashnik, G. Relationship between age and semen parameters in men with normal sperm concentration: analysis of 6022 semen samples. *Andrologia* 39, 45–50 (2007).
11. Kalyani, R., Basavaraj, P. B. & Kumar, M. L. H. Factors influencing quality of semen: a two year prospective study. *Indian J. Pathol. Microbiol.* 50, 890–5 (2007).
12. Aitken, R. J. Age, the environment and our reproductive future: bonking baby boomers and the future of sex. *Reproduction* 147, S1–S11 (2014).
13. Sartorius, G. A. & Nieschlag, E. Paternal age and reproduction. *Hum. Reprod. Update* 16, 65–79 (2010).
14. Kuhnert, B. Reproductive functions of the ageing male. *Hum. Reprod. Update* 10, 327–339 (2004).
15. Edition, F. Examination and processing of human semen. *World Health* Edition, F, 286 (2010).
16. Silva, J. V., Freitas, M. J., Correia, B. R., Korrodi-Gregório, L., Patrício, A., Pelech, S. & Fardilha, M. Profiling signaling proteins in human spermatozoa: biomarker identification for sperm quality evaluation. *Fertil. Steril.* 104, 845–856.e8 (2015).
17. Almog, T., Lazar, S., Reiss, N., Etkovitz, N., Milch, E., Rahamim, N., Dobkin-Bekman, M., Rotem, R., Kalina, M., Ramon, J., Raziel, A., Brietbart, H., Seger, R. & Naor, Z. Identification of extracellular signal-regulated kinase 1/2 and p38 MAPK as regulators of human sperm motility and acrosome reaction and as predictors of poor spermatozoan quality. *J. Biol. Chem.* 283, 14479–14489 (2008).
18. Ressurreição, M., Rollinson, D., Emery, A. M. & Walker, A. J. A role for p38 MAPK in the regulation of ciliary motion in a eukaryote. *BMC Cell Biol.* 12, 6 (2011).
19. Karabulut, S., Demiroglu-Zergeroglu, A., Yilmaz, E., Sagir, F. & Delikara, N. p53 and mitogen-activated protein kinase pathway protein profiles in fresh and frozen spermatozoa. *Andrologia* (2014). doi:10.1111/and.12200
20. Somanath, P. R., Jack, S. L. & Vijayaraghavan, S. Changes in sperm glycogen synthase kinase-3 serine phosphorylation and activity accompany motility initiation and stimulation. *J. Androl.* 25, 605–17
21. Vijayaraghavan, S., Mohan, J., Gray, H., Khatra, B. & Carr, D. W. A role for phosphorylation of glycogen synthase kinase-3alpha in bovine sperm motility regulation. *Biol. Reprod.* 62, 1647–1654 (2000).
22. Smith, G. D., Wolf, D. P., Trautman, K. C. & Vijayaraghavan, S. Motility potential of macaque epididymal sperm: the role of protein phosphatase and glycogen synthase kinase-3 activities. *J. Androl.* 20, 47–53

23. Aitken, R. J., Bronson, R., Smith, T. B. & De Iuliis, G. N. The source and significance of dna damage in human spermatozoa; a commentary on diagnostic strategies and straw man fallacies. *Mol. Hum. Reprod.* 19, 475–485 (2013).
24. Koppers, A. J., Mitchell, L. A., Wang, P., Lin, M. & Aitken, R. J. Phosphoinositide 3-kinase signalling pathway involvement in a truncated apoptotic cascade associated with motility loss and oxidative DNA damage in human spermatozoa. *Biochem. J.* 436, 687–698 (2011).
25. Fang, X., Yu, S., Eder, A., Mao, M., Bast, R. C., Boyd, D. & Mills, G. B. Regulation of BAD phosphorylation at serine 112 by the Ras-mitogen-activated protein kinase pathway. *Oncogene* 18, 6635–6640 (1999).
26. Tan, Y., Ruan, H., Demeter, M. R. & Comb, M. J. p90(RSK) blocks bad-mediated cell death via a protein kinase C-dependent pathway. *J. Biol. Chem.* 274, 34859–67 (1999).
27. Harada, H., Becknell, B., Wilm, M., Mann, M., Huang, L. J. shen, Taylor, S. S., Scott, J. D. & Korsmeyer, S. J. Phosphorylation and inactivation of BAD by mitochondria-anchored protein kinase A. *Mol. Cell* 3, 413–422 (1999).
28. Weng, S.-L., Taylor, S. L., Morshedi, M., Schuffner, A., Duran, E. H., Beebe, S. & Oehninger, S. Caspase activity and apoptotic markers in ejaculated human sperm. *Mol. Hum. Reprod.* 8, 984–991 (2002).
29. Almeida, C., Cardoso, M. F., Sousa, M., Viana, P., Gonçalves, A., Silva, J. & Barros, A. Quantitative study of caspase-3 activity in semen and after swim-up preparation in relation to sperm quality. *Hum. Reprod.* 20, 1307–1313 (2005).
30. Agarwal, A., Mahfouz, R. Z., Sharma, R. K., Sarkar, O., Mangrola, D. & Mathur, P. P. Potential biological role of poly (ADP-ribose) polymerase (PARP) in male gametes. *Reprod. Biol. Endocrinol.* 7, 143 (2009).
31. Cocuzza, M., Athayde, K. S., Agarwal, A., Sharma, R., Pagani, R., Lucon, A. M., Srougi, M. & Hallak, J. Age-Related Increase of Reactive Oxygen Species in Neat Semen in Healthy Fertile Men. *Urology* 71, 490–494 (2008).

C. CONCLUDING REMARKS AND FUTURE PERSPECTIVES

Concluding remarks

The main objective of this thesis was to identify and characterize spermatozoa proteins as targets for pharmacological and diagnostic intervention in male fertility.

To fulfill this goal, we identified, characterized and modulated key protein-complexes uniquely or selectively expressed in testis and spermatozoa in order to specifically modulate a process essential to reproduction, such as, post-meiotic events in spermatogenesis, sperm maturation in the epididymis or sperm function (**Chapters 3.1.**, **3.2.**, **3.3.** and **3.4.,** Figure C.1). Particular attention was given to two distinct proteins and its interacting partners: phosphoprotein phosphatase 1 (PPP1) and amyloid precursor protein (APP). Both proteins were shown to be involved in processes such as spermatogenesis, sperm motility and sperm-egg adhesion.

Moreover, we established biomarker "fingerprints" to assess spermatozoa quality based on molecular parameters (**Chapters 4.1.** and **4.2.,** Figure C.2).

In **Chapter 3.1.** we constructed and analyzed a testis/sperm-enriched interaction network in order to unravel the phosphoprotein phosphatase 1 catalytic subunit gamma 2 (PPP1CC2) interactome and, therefore, identify potential complexes as targets for male contraception. We showed that PPP1CC2 had 106 direct interactors in the testis/sperm-enriched network. Among those, 10 were highly specific to or strongly expressed in the testis and 19 were previously associated with male infertility phenotypes in knockout mice. Sixteen PPP1CC2 interactors were involved in spermatogenesis-related categories. Also, we recognized that PPP1CC2 had 50 direct interactors highly interconnected and associated with motility-related annotations. Analyzing the PPP1CC2-centric motility subnetwork, AKAP4 was the most appealing interactor since it was the only that fulfilled the following criteria: (1) testis/sperm-specific protein, (2) involved in all major motility-related annotations and (3) associated to a motility-related infertility phenotype. In addition to the asthenozoospermia phenotype, the *Akap4* gene knockout mice also presented a significant change in the activity and phosphorylation status of PPP1CC2. The interaction between PPP1CC2 and AKAP4 in human spermatozoa was further validated for the first time. Blocking motility-related PPP1CC2-PIP interactions during the epididymal transit, such as with AKAP4, will generate active PPP1. This, in turn, will originate dephosphorylation of a subset of substrates thereby preventing motility acquisition, representing an excellent contraceptive strategy. The mechanism of sperm motility is a perfect target for a new male contraceptive since it allows normal hormone and spermatozoa production and affects only the post-testicular sperm maturation. An attractive approach to modulate PPP1 activity is to target specific interfaces between PPP1 and tissue/event-specific PIPs, disrupting their interaction. To further address this topic, in **Chapter 3.2.**, we successfully modulated PPP1CC2-specific interactions and PPP1CC2/AKAP4 complex in

spermatozoa using cell-penetrating peptides (CPP) as a drug intracellular delivery system. PPI disruption peptides were designed, synthetized and coupled with CPP to selectively disrupt PPP1-PIPs complexes. A CPP was used to deliver a peptide sequence that mimics the unique 22 amino acid C-terminus of PPP1CC2 into spermatozoa, compromising isoform-specific interactions and, consequently, affecting sperm motility. A peptide sequence that mimics the interaction interface between PPP1CC2 and the sperm-specific PIP AKAP4 was also successfully delivered to sperm cells with an impact in sperm motility.

In **Chapter 3.3.** we characterized another PPP1 interacting protein – SARP2 – with the potential of being a target for male contraception. We demonstrated that SARP2 was highly expressed in testis and spermatozoa and interacted with PPP1CC2 in human spermatozoa. In testis, SARP2 protein was only present in the nucleus of elongating and mature spermatids. In spermatozoa, it was prominently expressed in the connecting piece and flagellum, as well as, to a lesser extent, in the acrosome. Blocking PPP1CC2-PIP interactions only expressed in post-meiotic germ cells will potentially prevent a correct sperm morphogenesis, which may also represent a good reversible contraceptive target by preserving spermatogonia and spermatocytes. Additionally, a novel SPAG9 variant, a testis and spermatozoa-specific c-Jun N-terminal kinase-binding protein, was identified by YTH and validated as a SARP2 interactor.

In **Chapter 3.4.** we provided the first report on APP interactome in human testis/spermatozoa. We constructed and analyzed the interaction network in human testis/spermatozoa of APP in order to identify sentinel proteins related to male fertility. We identified 36 novel APP interacting proteins by YTH screen using a human testis cDNA library. Those included testis/sperm-specific proteins, such as, the transmembrane serine protease TMPRSS12. The most abundant interaction detected was with SEC22C, a protein involved in vesicle transport between the ER and the Golgi complex. G-protein coupled receptor protein signaling pathway and cell adhesion were recognized as the most significantly represented biological processes among the APP interactors in human testis/sperm. Also, the majority of APP interactors in testis/spermatozoa were located at the plasma membrane. Our approach allowed the identification of novel interactions and recognition of key APP interacting proteins for male reproduction, particularly to sperm-oocyte interaction, which represent a potential mechanism for male contraception modulation.

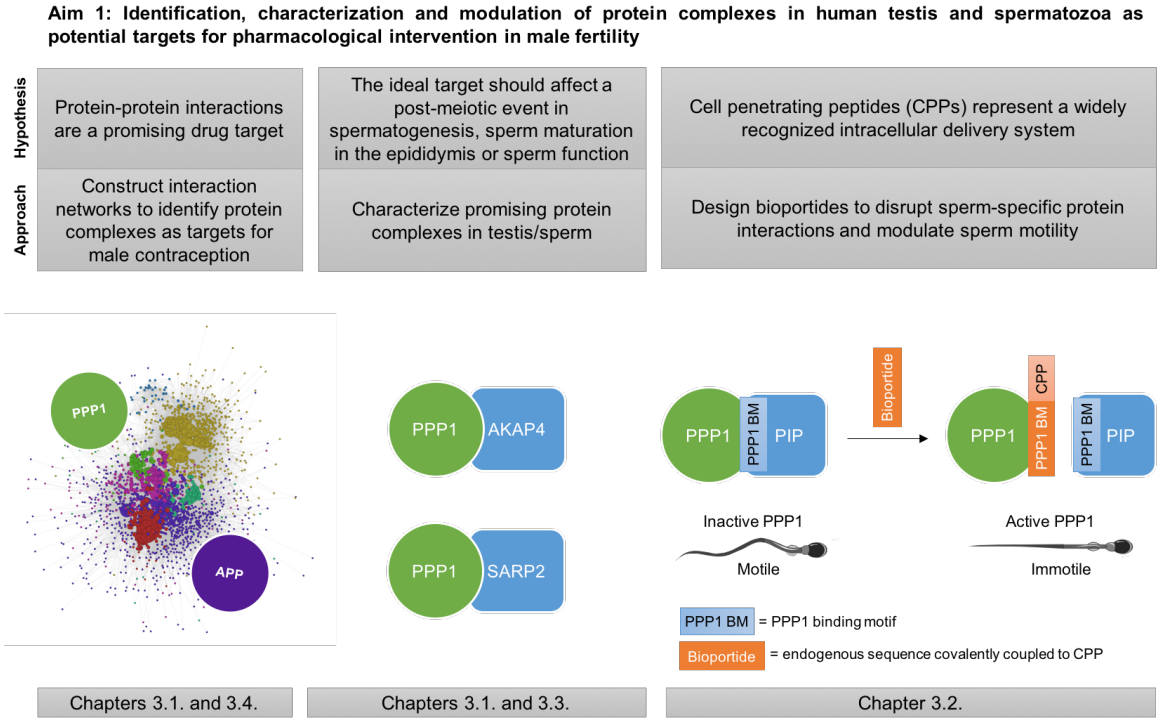

Figure C.1 – Overview of the main hypothesis and approaches used to achieve aim 1.

In **Chapters 4.1.** and **4.2.** we have identified several proteins that showed a high degree of differential activity and have the potential to integrate a quantitative array, which may have several applications: explain idiopathic infertility, failure in assisted reproductive techniques (ART) or repeated abortion; choice of the appropriate ART; assess the efficacy of medical interventions to treat, for instance, varicocele and infectious diseases; and assess the efficacy of antioxidant therapies and lifestyle alterations. Moreover, “treatments” for poor semen quality usually focus on ART that bypass the need for a normal ejaculated sperm sample. However, the success rates and elevated costs of ART demonstrate the need to increase the knowledge on the molecular processes underlying sperm function. Eventually, conditions such as poor sperm motility may be treatable by, for example, stimulating relevant signaling pathways. Though, the players involved in regulating spermatozoa function are still far from being all identified. To further address this topic, in **Chapter 4.1.** we identified 34 protein kinases expressed in normozoospermic samples. From those, 8 (CDK2, PAK3, KSR1, BMX, DAPK1, CSNK1D, MAP4K2 and ZIPK) were identified for the first time in human spermatozoa. Additionally, the activity patterns of 13 signaling proteins in human spermatozoa revealed significant correlations with specific semen parameters (concentration, motility, morphology or sperm DNA fragmentation). Besides the potential to integrate a biomarker "fingerprint" to assess sperm quality, those molecules have the potential to allow the recognition of the signaling pathways accountable for regulating specific spermatozoa

functions.

Several studies have investigated age-based impact in basic semen parameters, but the molecular mechanisms responsible for age-dependent decline in spermatozoa quality are poorly understood. The identification of the molecular factors associated with the age-dependent decline in sperm quality and, consequently, in the reproductive outcomes, will improve fertility management. In **Chapter 4.2.** we established the association between age and proteins involved in specific signaling pathways that were previously correlated with spermatozoa quality. The activity of 9 signaling proteins in human spermatozoa revealed significant positive correlations with male age: p53 (S15), PRAS40 (T246), Bad (S112), p38 (T180/Y182), mTOR (S2448), Hsp27 (S78), GSK-3β (S9) and Akt (S473) and Caspase-3 (D175). Additionally, we determined that consistent and significant alterations in molecular parameters were observed as early as 25 years of age.

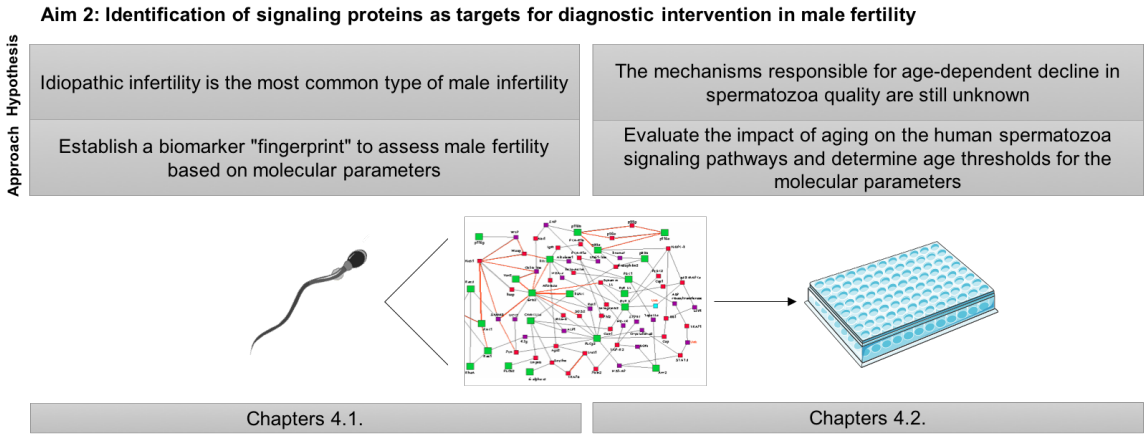

Figure C.2 – Overview of the main hypothesis and approaches used to achieve aim 2.

Concluding, the work described in this thesis identified, characterized and modulated protein complexes in human testis and spermatozoa as potential targets for contraceptive intervention and identified spermatozoa signaling proteins which may incorporate a diagnostic platform.

Future Perspectives

The testis/sperm-enriched/specific protein interaction networks constructed in this study offered us a platform to identify potential contraceptive targets. Furthermore, we demonstrated that rationally-designed bioportides can modulate spermatozoa complexes and, consequently, motility. Future efforts will focus upon the identification of novel bioportides likely to possess highly efficient uptake and pharmacodynamic parameters. The interactions of bioportides on their target interfaces will be modelled *in silico* and the most promising candidates will be redesigned to achieve better affinity, activity and specificity. High throughput peptide synthesis will support the production of small number libraries of potential protein-protein interaction modulatory bioportides. The most promising bioportide candidates will be selected for validation in heterogeneous human sperm samples and detailed *in vivo* studies. *In vivo* studies will allow, for instance, to assess the ability of these compounds to cross the blood-epididymis barrier. Collaborations with international experts in molecular pharmacology (John Howl, Molecular Pharmacology Group, University of Wolverhampton, UK), biomolecular simulations/computational chemistry (Giorgio Colombo, Biomolecular Simulations and Computational Chemistry Group, Italy) and human reproduction (Steve Publicover, School of Biosciences, The University of Birmingham, UK), as well as with a local hospital (António Patrício, Urology Unit, Infante D. Pedro Hospital, Portugal) are already established and will be essential in the next steps proposed.

Additionally, this study holds promising results for the development of novel, clinically useful male fertility biomarkers. Further studies will need to establish the thresholds (basal level *versus* pathological levels) for each molecular parameter identified and address the design and cost‑effectiveness of an array of biomarkers to assess male fertility, in which the collaboration established with a fertility clinic (Ferticentro – Centre for Fertility Studies, Portugal) will be crucial.

D. SUPPLEMENTARY DATA

Supplementary Table D.1 – Proteins identified in at least 2 databases (DB) as testis-enriched/specific.

Supplementary Table D.2 – Gene ontology categories of the testis-enriched proteins. Enriched categories are identified as those with p value <0.01.

Supplementary Table D.3 – PPP1CC interactors obtained from the different sources.

Supplementary Table D.4 – (A). Topological properties of proteins in testis/sperm specific network. (B) Topological clusters of proteins in testis/sperm specific network. The number in Module is the index of topologically clustered groups. (C) Topological clusters of proteins in sub-networks for spermatogenesis and motility. The number in Module is the index of topologically clustered groups. Blue colored proteins are overlapped in both sub-networks.

Supplementary Table D.5 – PPP1CC interactors from the testis-enriched network associated with male infertility-related phenotypes in knockout mice.

Supplementary Table D.6 – Gene ontology and KEGG categories of the different modules of the testis-enriched network. Enriched GO categories are identified as those with p value <0.01. Only the top 3 KEGG categories are presented.

Supplementary Table D.7 – (A). Proteins from the testis-enriched network associated with spermatogenesis-related biological processes. Gene ontology data obtained from the "GO Term Enrichement" tool of the AmiGO database. GO, gene ontology. (B) Proteins from the testis-enriched network associated with motility-related biological processes (BP) and cellular components (CC). Gene ontology data obtained from the "GO Term Enrichement" tool of the AmiGO database. GO, gene ontology.

Due to the extent of **Supplementary Table D.1** to **D.7** and until the paper is available online the information is available on

https://www.dropbox.com/s/73f0nfcfbmj35tf/Supplementary%20Information.xlsx?dl=0

Supplementary Table D.8 – Quantitative analysis of peptide translocation into bovine and human spermatozoa. Bovine and human spermatozoa were incubated with TAMRA-labeled bioportides (10 μM) for 1 h at 37°C. Data are expressed as fluorescence (minus negative control). Three independent experiments were performed in quadriplicate.

Human												
	Experiment 1				**Experiment 2**				**Experiment 3**			
TAMRA-PPP1CC2-CT	37166	37225	36603	36992	30614	30534	30065	30168	43443	44051	42722	43266
TAMRA-AKAP4-BM	25581	25175	24616	25222	41315	40612	41028	40596	22868	22593	22201	22461
TAMRA-AKAP4-BM M	9228	9271	9506	9066	12619	12780	12634	12487	9055	8675	8565	8887
Bovine												
	Experiment 1				**Experiment 2**				**Experiment 3**			
TAMRA-PPP1CC2-CT	6616	6441	6714	6616	5571	5336	5350	5421	6108	6061	6318	6146
TAMRA-AKAP4-BM	21247	20923	20930	20852	14760	14390	14580	14588	19320	18946	19170	19362
TAMRA-AKAP4-BM M	2774	2616	2703	2789	2204	2201	2282	2284	3523	3400	3442	3539

Supplementary Table D.9 – Descriptive analysis; Statistical measures: Mean and standard deviation (SD) associated with PPP1CC2 CT peptides treatments in bovine spermatozoa. NC, negative control; PM, progressive motility; NPM, non-progressive motility; IM, immotile spermatozoa; V, viability. Data are expressed as mean of three independent experiments performed in triplicate.

		1h						**2h**					
		PPP1CC2-CT		**TAMRA-PPP1CC2-CT**		**NC**		**PPP1CC2-CT**		**TAMRA-PPP1CC2-CT**		**NC**	
		10 μM	20 μM	10 μM	20 μM	10 μM	20 μM	10 μM	20 μM	10 μM	20 μM	10 μM	20 μM
PM fast (%)	Mean	17,10	13,68	9,71	10,61	37,07	38,14	21,51	24,04	16,79	7,47	46,83	44,03
	SD	11,87	6,37	7,24	8,05	13,47	15,18	10,78	5,00	6,04	2,37	13,28	9,52
PM slow (%)	Mean	4,29	4,19	3,83	4,81	13,82	6,37	6,79	8,07	8,08	6,17	10,88	10,56
	SD	1,82	2,17	2,45	3,25	8,21	1,96	2,91	2,43	3,00	2,89	4,33	2,87
NPM (%)	Mean	14,39	16,13	11,57	13,21	15,99	16,30	13,56	12,48	13,03	10,03	13,69	12,38
	SD	4,68	5,69	3,63	4,16	5,94	6,39	4,46	2,62	3,68	2,92	4,33	3,62
IM (%)	Mean	64,19	65,12	74,84	71,38	38,47	39,24	58,21	56,37	68,00	76,32	28,64	33,01
	SD	11,66	6,54	6,46	13,78	10,23	12,77	15,13	5,95	9,79	4,76	10,42	8,62
V (%)	Mean	80,17	77,03	76,97	72,57	80,77	76,43	77,97	75,83	76,53	72,83	78,63	84,10
	SD	3,78	8,28	6,14	5,56	9,12	9,46	5,49	4,92	5,22	6,12	4,97	2,50

Supplementary Table D.10 – Descriptive analysis; Statistical measures: Mean and standard deviation (SD) associated with AKAP4-BM peptides treatments in bovine spermatozoa. NC, negative control; PM, progressive motility; NPM, non-progressive motility; IM, immotile spermatozoa; V, viability. Data are expressed as mean of three independent experiments performed in triplicate

		10 μM						**20 μM**					
		1h			**2h**			**1h**			**2h**		
		AKAP4-BM	**AKAP4-BM M**	**NC**	**AKAP4-BM**	**AKAP4 BM M**	**NC**	**AKAP4-BM**	**AKAP4-BM M**	**NC**	**AKAP4-BM**	**AKAP4-BM M**	**NC**
PM fast (%)	Mean	23,02	39,13	46,93	22,88	40,97	45,92	1,54	30,60	42,76	0,42	27,18	34,44
	SD	9,48	10,47	9,05	7,57	7,44	10,57	1,96	6,17	9,58	0,74	5,13	12,30
PM slow (%)	Mean	5,52	8,28	7,66	4,17	6,29	7,53	0,33	8,28	7,36	0,42	6,30	6,83
	SD	2,81	4,10	1,92	1,85	1,78	2,29	0,38	2,33	2,23	0,41	2,80	2,39
NPM (%)	Mean	23,30	19,21	18,97	20,89	21,72	18,51	9,10	25,20	18,54	9,07	24,78	23,57
	SD	8,20	5,89	4,02	4,79	5,73	4,29	1,72	3,97	2,76	2,14	3,97	5,85
IM (%)	Mean	48,14	33,38	26,49	51,9	31,03	27,32	89,04	30,90	31,58	90,02	41,54	35,46
	SD	7,89	7,8	5,64	8,38	5,42	4,64	2,79	6,53	10,57	2,98	7,75	13,03
V (%)	Mean	76,83	82,07	80,90	79,03	82,67	87,13	83,77	67,67	79,67	80,10	77,80	43,33
	SD	1,27	1,72	5,34	6,67	6,86	4,62	5,40	1,90	8,2	3,6	1,65	2,84

Supplementary Table D.11 – Inferential statistics; Test for difference between means of two independent groups associated with PPP1CC2-CT peptides treatments in bovine spermatozoa. NC, negative control; PM, progressive motility; NPM, non-progressive motility; IM, immotile spermatozoa; V, viability.

Variable	**Groups** 10 µM	**Test**	**Sig (2-tailled)**	**Interpretation Unilateral Test** *% of spermatozoa (variable) is significantly higher in*
PM fast (1h)	PPP1CC2-CT/ NC	Mann-Whitney	0,007	NC
PM fast (2h)		T-student	0.000	NC
PM slow (1h)		Mann-Whitney	0,004	NC
PM slow (2h)		T-student	0.032	NC
NPM (1h)		T-student		-
NPM (2h)		T-student		-
IM (1h)		T-student	0.000	PPP1CC2-CT
IM (2h)		T-student	0.000	PPP1CC2-CT
V (1h)		T-student		-
V (2h)		T-student		-
Variable	**Groups** 20 µM	**Test**	**Sig (2-tailled)**	**Interpretation Unilateral Test** *% of spermatozoa (variable) is significantly higher in*
PM fast (1h)	PPP1CC2-CT/ NC	T-student	0.000	NC
PM fast (2h)		T-student	0.000	NC
PM slow (1h)		T-student	0.040	NC
PM slow (2h)		T-student		-
NPM (1h)		T-student		-
NPM (2h)		T-student		-
IM (1h)		T-student	0.000	PPP1CC2-CT
IM (2h)		T-student	0.000	PPP1CC2-CT
V (1h)		T-student		-
V (2h)		T-student		-
Variable	**Groups** 10 µM	**Test**		**Interpretation Unilateral Test** *% of spermatozoa (variable) is significantly higher in*
PM fast (1h)	TAMRA-PPP1CC2-CT / NC	Mann-Whitney	0,001	NC
PM fast (2h)		T-student	0.000	NC
PM slow (1h)		Mann-Whitney	0,003	NC
PM slow (2h)		T-student		-
NPM (1h)		T-student		-
NPM (2h)		T-student		-
IM (1h)		Mann-Whitney	0,000	TAMRA-PPP1CC2-CT
IM (2h)		T-student	0.000	TAMRA-PPP1CC2-CT
V (1h)		T-student		-
V (2h)		T-student		-
Variable	**Groups** 20 µM	**Test**	**Sig (2-tailled)**	**Interpretation Unilateral Test** *% of spermatozoa (variable) is significantly higher in*
PM fast (1h)	TAMRA-PPP1CC2-CT / NC	T-student	0.000	NC
PM fast (2h)		T-student	0.000	NC
PM slow (1h)		T-student		-
PM slow (2h)		Mann-Whitney	0,019	NC
NPM (1h)		T-student		-
NPM (2h)		T-student		-
IM (1h)		T-student	0.000	TAMRA-PPP1CC2-CT
IM (2h)		T-student	0.000	TAMRA-PPP1CC2-CT
V (1h)		T-student		-
V (2h)		T-student	0.000	NC

Supplementary Table D.12 – Inferential statistics; Test for difference between means of two independent groups associated with AKAP4 peptides treatments in bovine spermatozoa. NC, negative control; PM, progressive motility; NPM, non-progressive motility; IM, immotile spermatozoa; V, viability.

Variable	**Conditions** 10 µM	**Test**	**Sig (2-tailled)**	**Interpretation Unilateral Test**
				% of spermatozoa (variable) is significantly higher in
PM fast (1h)	AKAP4-BM/ NC	T-student	0.000	NC
PM fast (2h)		T-student	0.000	NC
PM slow (1h)		T-student		-
PM slow (2h)		T-student	0.003	NC
NPM (1h)		Mann-Whitney		-
NPM (2h)		T-student		-
IM (1h)		T-student	0.000	AKAP4-BM
IM (2h)		Mann-Whitney	0,000	AKAP4-BM
V (1h)		T-student		-
V (2h)		T-student		-
Variable	**Conditions** 20 µM	**Test**		**Interpretation Unilateral Test**
				% of spermatozoa (variable) is significantly higher in
PM fast (1h)	AKAP4-BM/ NC	Mann-Whitney	0,000	NC
PM fast (2h)		Mann-Whitney	0,000	NC
PM slow (1h)		Mann-Whitney	0,000	NC
PM slow (2h)		T-student	0.000	NC
NPM (1h)		T-student	0.000	NC
NPM (2h)		T-student	0.000	NC
IM (1h)		T-student	0.000	AKAP4-BM
IM (1h)		T-student	0.000	AKAP4-BM
V (1h)		T-student		-
V (2h)		T-student	0.000	NC
Variable	**Conditions** 10 µM	**Test**	**Sig (2-tailled)**	**Interpretation Unilateral Test**
				% of spermatozoa (variable) is significantly higher in
PM fast (1h)	AKAP4-BM M /NC	Mann-Whitney		-
PM fast (2h)		T-student		-
PM slow (1h)		T-student		-
PM slow (2h)		T-student		-
NPM (1h)		Mann-Whitney		-
NPM (2h)		T-student		-
IM (1h)		T-student	0,047	AKAP4-BM M
IM (1h)		Mann-Whitney		-
V (1h)		Mann-Whitney		-
V (2h)		Mann-Whitney		-
Variable	**Conditions** 20 µM	**Test**	**Sig (2-tailled)**	**Interpretation Unilateral Test**
				% of spermatozoa (variable) is significantly higher in
PM fast (1h)	AKAP4-BM M /NC	T-student	0,000	NC
PM fast (2h)		T-student		
PM slow (1h)		T-student		
PM slow (2h)		T-student		
NPM (1h)		T-student	0,001	AKAP-BM M
NPM (2h)		T-student		
IM (1h)		T-student		
IM (1h)		T-student		
V (1h)		T-student		
V (2h)		T-student		
Variable	**Conditions** 10 µM	**Test**	**Sig (2-tailled)**	**Interpretation Unilateral Test**
				% of spermatozoa (variable) is significantly higher in
PM fast (1h)	AKAP4-BM/ AKAP4-	Mann-Whitney	0,002	AKAP-BM M

Variable	Conditions 10 µM	Test	Sig (2-tailled)	Interpretation Unilateral Test
				% of spermatozoa (variable) is significantly higher in
PM fast (2h)	BM M	T-student	0,000	AKAP-BM M
PM slow (1h)		T-student		-
PM slow (2h)		T-student	0,024	AKAP-BM M
NPM (1h)		T-student		-
NPM (2h)		T-student		-
IM (1h)		T-student	0,001	AKAP-BM
IM (2h)		T-student	0,000	AKAP-BM
V (1h)		Mann-Whitney	0,05	AKAP-BM M
V (2h)		Mann-Whitney		-
Variable	**Conditions 20 µM**	**Test**	**Sig (2-tailled)**	**Interpretation Unilateral Test**
				% of spermatozoa (variable) is significantly higher in
PM fast (1h)	AKAP4-BM/ AKAP4-BM M	Mann-Whitney	0,000	AKAP-BM M
PM fast (2h)		Mann-Whitney	0,000	AKAP-BM M
PM slow (1h)		Mann-Whitney	0,000	AKAP-BM M
PM slow (2h)		T-student	0,000	AKAP-BM M
NPM (1h)		T-student	0,000	AKAP-BM M
NPM (2h)		T-student	0,000	AKAP-BM M
IM (1h)		T-student	0,000	AKAP-BM
IM (2h)		T-student	0,000	AKAP-BM

Supplementary Table D.13 – Descriptive analysis; Statistical measures: Mean and standard deviation (SD) associated with PPP1CC2 CT and AKAP4-BM peptides treatments in human spermatozoa. NC, negative control; PM, progressive motility; NPM, non-progressive motility; IM, immotile spermatozoa; Data are expressed as mean of two independent experiments performed in triplicate.

20µM		1h				2h			
		PM fast (%)	PM slow (%)	NPM (%)	IM (%)	PM fast (%)	PM slow (%)	NPM (%)	IM (%)
PPP1CC2-CT	N Valid	6	6	6	6	6	6	6	6
	Mean	9,50	11,23	18,32	60,93	7,25	8,63	27,67	56,43
	SD	5,73	7,46	4,25	16,34	1,43	3,70	12,25	14,30
AKAP4-BM	N Valid	6	6	6	6	6	6	6	6
	Mean	1,27	1,82	9,60	87,30	1,28	1,73	9,10	87,97
	SD	0,71	1,09	3,36	3,91	1,76	1,18	2,50	1,92
AKAP4-BM M	N Valid	6	6	6	6	6	6	6	6
	Mean	9,72	11,90	18,18	60,23	6,82	10,03	19,90	62,55
	SD	3,43	2,84	4,85	8,64	1,42	1,39	4,00	6,17
NC	N Valid	6	6	6	6	6	6	6	6
	Mean	14,65	13,65	15,05	55,08	11,18	13,05	23,80	51,98
	SD	5,11	3,12	5,04	10,08	1,68	3,75	7,21	10,73

Supplementary Table D.14 – Inferential statistics; Test for difference between means of two independent groups associated with PPP1CC2-CT peptide treatment in human spermatozoa. NC, negative control; PM, progressive motility; NPM, non-progressive motility; IM, immotile spermatozoa;

Time	Variable	Test	Sig (2-tailled)	Interpretation Unilateral Test
				Statistically significant
				% of spermatozoa (variable) is significantly higher in
1h	PM fast	Mann-Whitney U	U=8; W=29; sig=0,109	-
	PM slow	Mann-Whitney U	U=15; W=36; sig=0,631	-
	NPM	Mann-Whitney U	U=12; W=33; sig=0,337	-
	IM	Mann-Whitney U	U=12; W=33; sig=0,337	-
2h	PM fast	Mann-Whitney U	U=0; W=21; sig=0,004	NC
	PM slow	Mann-Whitney U	U=8; W=29; sig=0,109	-
	NPM	Mann-Whitney U	U=15; W=36; sig=0,631	-
	IM	Mann-Whitney U	U=14; W=35; sig=0,520	-

Supplementary Table D.15 – Inferential statistics; Test for difference between means of two independent groups associated with AKAP4-BM peptides treatment in human spermatozoa. NC, negative control; PM, progressive motility; NPM, non-progressive motility; IM, immotile spermatozoa;

Time	Variable	Condition	Test	Sig (2-tailled)	Interpretation Unilateral Test ***Statistically significant*** *% of spermatozoa (variable) is significantly higher in*
1h	PM fast	AKAP4-BM/ NC	Mann-Whitney U	U=0; W=21; sig=0,004	NC
	PM slow		Mann-Whitney U	U=0; W=1; sig=0,004	NC
	NPM		Mann-Whitney U	U=7; W=28; sig=0,078	NC
	IM		Mann-Whitney U	U=0; W=21; sig=0,004	AKAP4 BM
2h	PM fast		Mann-Whitney U	U=0; W=21; sig=0,004	NC
	PM slow		Mann-Whitney U	U=0; W=21; sig=0,004	NC
	NPM		Mann-Whitney U	U=0; W=21; sig=0,004	NC
	IM		Mann-Whitney U	U=0; W=21; sig=0,004	AKAP4 BM
1h	PM fast	AKAP4-BM M/ NC	Mann-Whitney U	U=6; W=27; sig=0,054	NC
	PM slow		Mann-Whitney U	U=12; W=33; sig=0,337	-
	NPM		Mann-Whitney U	U=14; W=35; sig=0,522	-
	IM		Mann-Whitney U	U=11; W=32; sig=0,262	-
2h	PM fast		Mann-Whitney U	U=0; W=21; sig=0,004	NC
	PM slow		Mann-Whitney U	U=11; W=32; sig=0,262	-
	NPM		Mann-Whitney U	U=11; W=32; sig=0,262	-
	IM		Mann-Whitney U	U=8,5; W=29,5; sig=0,128	-
1h	PM fast	AKAP4-BM/ AKAP4-BM M	Mann-Whitney U	U=0; W=21; sig=0,004	AKAP4 BM M
	PM slow		Mann-Whitney U	U=0; W=21; sig=0,004	AKAP4 BM M
	NPM		Mann-Whitney U	U=1; W=22; sig=0,006	AKAP4 BM M
	IM		Mann-Whitney U	U=0; W=21; sig=0,004	AKAP4 BM
2h	PM fast		Mann-Whitney U	U=0; W=21; sig=0,004	AKAP4 BM M
	PM slow		Mann-Whitney U	U=0; W=21; sig=0,004	AKAP4 BM M
	NPM		Mann-Whitney U	U=0; W=21; sig=0,004	AKAP4 BM M
	IM		Mann-Whitney U	U=0; W=21; sig=0,004	AKAP4 BM

Supplementary Table D.16 – Primers used for cellular markers and housekeeping genes in qRT-PCR analysis (Mus musculus).

Housekeeping genes	Gene	Sequence	Position	Acc. No
Glyceraldehyde-3-phosphate dehydrogenase	*Gapdh*	TGTCCGTCGTGGATCTGAC	763-781	NM_008084
		CCTGCTTCACCACCTTCTTG	818-837	
Hypoxanthine guanine phosphoribosyl transferase 1	*Hprt1*	TCCTCCTCAGACCGCTTTT	104-122	NM_013556
		CCTGGTTCATCATCGCTAATC	173-193	
Marker for spermatogonia				
Tumor-associated calcium signal transducer 1 (= Ep-CAM)	*Tacstd1*	CAGAATACTGTCATTTGCTCCA	615-637	NM_008532
		GTTCTGGATCGCCCCTTC	708-725	
Kit oncogene	*c-kit*	GGTTGTCCAACTTATTGAGAAGC	2813-2835	BC075716
		GCAGTTTGCCAAGTTGGAGT	2863-2882	
Marker for spermatocytes				
Stathmin 1 (= Phosphoprotein p19)	*Stmn1*	CTGCAGAAGAAAGACGCAAGT	246-266	NM_019641
		TGCTGAAGTTGTTGTTCTCCTC	341-362	
Synaptonemal complex protein 3	*Sycp3*	GGACAGCGACAGCTCACC	106-123	NM_011517
		TTCCCAGATTTCCCAGAATG	170-189	
Marker for spermatids				
Transition protein 1	*Tpn1*	AGCCGCAAGCTAAAGACTCA	19-38	NM_009407
		CGGTAATTGCGACTTGCAT	146-164	
Protamine 2	*Prmn2*	CAGAAGGCGGAGGAGACAC	309-327	NM_008933
		CTCCTCCTTCGGGATCTTCT	364-383	
Marker for Leydig cells				
Hydroxysteroid (17-beta) dehydrogenase 3	*Hsd17b3*	AATATGTCACGATCGGAGCTG	813-833	NM_008291
		GAAGGGATCCGGTTCAGAAT	872-891	
Marker for Sertoli cells				
Androgen receptor	*Ar*	CCAGTCCCAATTGTGTCAAA	1513-1532	NM_013476
		TCCCTGGTACTGTCCAAACG	1584-1603	
Marker for peritubular cells				
Actin alpha 2	*Acta2*	ACTCTCTTCCAGCCATCTTTCA	854-875	NM_007392
		ATAGGTGGTTTCGTGGATGC	894-913	

Supplementary Table D.17 – Primers used for the target genes in qRT-PCR analysis (Mus musculus).

Target genes	Gene	Sequence	Position	Acc. No
Phosphoprotein phosphatase 1 alpha isoform	*Ppp1ca*	TGTTCCTTCCAGATCCTCAAGCCC	914-937	NM_031868
		TGGCTTTGGCAGAATTGCGGG	1008-1028	
Phosphoprotein phosphatase 1 beta isoform	*Ppp1cb*	AGCTCATCAGGTGGTGGAAGACG	1121-1143	NM_172707
		GGTGGATTAGCTGTTCGAGGCG	1336-1357	
Phosphoprotein phosphatase 1 gamma 1 isoform	*Ppp1cc*	GAGCCCATCAGGTGGTTGAAGATG	1019-1042	NM_013636
		AGTCCCAACCAGGCAGTGTCAAG	1261-1283	
Phosphoprotein phosphatase 1 gamma 2 isoform	*Ppp1cc*	CCACGGGGTTGGATCAGGC	1219-1237	NM_013636
		CCGGTGGACGGCAAGTTAGTTC	2287-2308	
Phosphoprotein phosphatase 1 gamma isoform	*Ppp1cc*	GCCCATCAGGTGGTTGAAGATGGC	1021-1044	NM_013636
		TGTGACAGGTCTCGTGGCGTTG	1194-1215	
Ankyrin repeat domain 42 (=SARP)	*Ankrd42*	TCCCAGCGTGACTGACAAGAGAG	1408-1430	NM_028665
		GGCTGCTAAATGAACCGGGAGG	1534-1555	
Ankyrin repeat domain 42 isoform 2 (=SARP2)	*Ankrd42*	GCTGGATGAGTATCGAGTGGAAGTG	2341-2365	NM_028665
		GTCATCTTCCATAGCCGCGACAC	2406-2428	

Supplementary Table D.18 – – Enriched GO categories of the APP interactors identified by YTH. Enriched categories are identified as those with $p<0.05$

Supplementary Table D.19 – Distribution of APP interacting proteins in human testicular, epididymal and sperm proteomes, and their overlap. The human epididymis proteome includes both epididymal tissue and fluid proteomes. The secretory vesicular (epididymosome) part of the human epididymosome proteome was also considered. In bold are the APP interactors identified in the YTH screen.

Supplementary Table D.20 – Statistics of collected protein-protein interaction data.

Supplementary Table D.21 – Topological properties of 457 proteins in local APP/APLP2 network. (a) Rank of degree, clustering coefficient, betweenness centrality, and closeness centrality. (b) k-core and community that proteins are involved. Note that the number in community column is only index of the community.

Supplementary Table D.22 – Topological properties of proteins in extended APP/APLP2 network. (a) Top 1000 rank of degree, clustering coefficient, betweenness centrality, and closeness centrality. Note that proteins with clustering coefficient 0 are neglected. (b) kcore and community that proteins are involved. The number in the community column is only index of the community. (c) Topological properties of APP partners identified by YTH in the extended APP/APLP2 network. Proteins with prominent topological properties are indicated with purple color.

Due to the extent of **Supplementary Table D.18** to **D.22** the information is available on **http://bmcbioinformatics.biomedcentral.com/articles/10.1186/s12859-014-0432-9**.

Supplementary Table D.23 – Basic semen parameters, sperm DNA fragmentation (SDF) and expression patterns of 18 well-characterized signaling molecules when phosphorylated or cleaved (PathScan Intracellular Signaling Array) of 32 random men providing semen samples for routine analysis. MP, Midpiece.

Volunteer	Age (years)	Volume (ml)	Concentration ($x10^6$/ml)	No. spermatozoa ($x10^6$)	Motility (%)				Morphology (%)						SDF (%)	Varicocele
					Total	Progressive	Non-progressive	Immotile	Normal	Head	MP	Tail	ERC	TZI		
1	35	7,70	20,00	158,00	89,00	82,00	7,00	11,00	6,00	99,00	67,00	4,00	16,00	1,86	14,00	No
2	36	2,50	91,00	228,00	89,00	73,00	16,00	11,00	9,00	100,00	56,00	16,00	8,00	1,80	23,00	No
3	33	7,00	18,00	129,00	81,00	62,00	19,00	19,00	9,00	91,00	37,00	16,00	12,00	1,57	12,00	No
4	33	4,00	24,00	97,00	39,00	32,00	7,00	61,00	4,00	99,00	60,00	22,00	17,00	1,99	41,00	No
5	35	3,20	20,00	64,00	70,00	53,00	17,00	30,00	5,00	99,00	65,00	21,00	5,00	1,91	16,00	No
6	35	7,00	2,00	14,00					3,00	89,00	49,00	37,00	0,00	1,80	30,00	Yes
7	36	5,10	49,00	250,00	56,00	30,00	26,00	44,00	6,00	90,00	52,00	23,00	0,00	1,80	49,00	No
8	39	3,20	9,00	29,00	44,00	18,00	26,00	56,00	3,00	70,00	40,00	27,00	1,00	1,42	13,00	No
9	32	3,30	95,00	314,00	41,00	23,00	18,00	59,00	6,00	58,00	39,00	19,00	3,00	1,27	10,00	No
10	36	3,00	13,00	39,00	49,00	32,00	17,00	51,00	10,00	84,00	41,00	19,00	3,00	1,58	7,00	No
11		5,40	140,00	756,00	76,00	66,00	10,00	24,00	13,00	60,00	25,00	6,00	3,00	1,18	23,00	No
12	31	4,70	9,00	42,00	37,00	27,00	10,00	63,00	16,00	43,00	34,00	23,00	0,00	1,17	13,00	No
13	35	3,20	29,00	93,00	58,00	35,00	23,00	42,00	5,00	79,00	33,00	24,00	3,00	1,45	13,00	No
14	29	1,50	2,00	3,00					6,00	70,00	45,00	39,00	1,00	1,64	9,00	No
15	25	3,00	59,00	177,00	82,00	69,00	13,00	18,00	7,00	79,00	32,00	30,00	0,00	1,52	10,00	Yes
16	20	4,00	24,00	96,00	76,00	60,00	16,00	24,00	4,00	76,00	40,00	49,00	2,00	1,73	18,00	No
17	36	0,90	2,00	1,80					2,00	80,00	45,00	40,00	0,00	1,68	34,00	No
18	34	4,00	8,00	32,00	44,00	30,00	14,00	56,00	7,00	78,00	40,00	20,00	3,00	1,51	17,00	No
19	47	4,00	94,00	376,00	78,00	72,00	6,00	22,00	11,00	50,00	32,00	49,00	0,00	1,39	11,00	No
20	32	3,00	197,00	591,00	81,00	76,00	5,00	19,00	18,00	44,00	31,00	24,00	1,00	1,00	9,00	No
21	39	0,70	57,00	40,00	65,00	45,00	20,00	35,00	12,00	73,00	44,00	20,00	0,00	1,37	9,00	No
22	32	4,20	4,00	17,00	54,00	39,00	15,00	46,00	5,00	79,00	39,00	27,00	5,00	1,60	36,00	No
23	19	4,30	22,00	95,00	62,00	50,00	12,00	38,00	5,00	72,00	31,00	21,00	0,00	1,25	12,00	Yes
24	29	2,30	30,00	69,00	57,00	48,00	9,00	43,00	6,00	77,00	47,00	39,00	7,00	1,57	7,00	Yes
25	28	3,00	90,00	270,00	62,00	52,00	10,00	38,00	7,00	64,00	39,00	28,00	3,00	1,31	20,00	Yes
26	26	2,20	13,00	29,00	44,00	33,00	11,00	66,00	4,00	84,00	43,00	40,00	0,00	1,67	24,00	Yes
27	22	1,70	67,00	114,00	85,00	76,00	9,00	15,00	14,00	75,00	6,00	28,00	1,00	1,28	9,00	No
28	21	3,00	140,00	420,00	83,00	68,00	15,00	17,00	5,00	81,00	44,00	29,00	3,00	1,65	17,00	No
29	24	2,50	110,00	275,00	87,00	75,00	12,00	13,00	6,00	80,00	47,00	21,00	1,00	1,59	9,00	No
30	20	1,00	60,00	60,00	64,00	43,00	21,00	36,00	5,00	78,00	32,00	37,00	2,00	1,57	16,00	No
31	20	2,10	58,00	122,00	115,0	65,00	50,00	15,00	12,00	60,00	30,00	21,00	0,00	1,26	10,00	No
32	28	2,50	86,00	215,00	79,00	72,00	7,00	21,00	12,00	54,00	31,00	30,00	0,00	1,31	8,00	No

Supplementary Table D.23 – (continuation) Basic semen parameters, sperm DNA fragmentation (SDF) and expression patterns of 18 well-characterized signaling molecules when phosphorylated or cleaved (PathScan Intracellular Signaling Array) of 32 random men providing semen samples for routine analysis.

Volunteer	PathScan® Intracellular Signaling Array																	
	Erk1/2 (T202/ Y204)	Stat1 (Y701)	Stat3 (Y705)	Akt (T308)	Akt (S473)	AMPKa (T172)	S6 Ribosomal Protein (S235/236)	mTOR (S2448)	HSP27 (S78)	Bad (S112)	p70 S6 Kinase (T389)	PRAS40 (T246)	p53 (S15)	p38 (T180/Y182)	SAPK/JNK (T183/Y185)	PARP Asp214 Cleavage	Caspase-3 Asp175 Cleavage	GSK-3b (S9)
1	0,05	0,05	0,05	0,04	0,04	0,05	0,04	0,07	0,07	0,07	0,02	0,07	0,03	0,06	0,06	0,06	0,05	0,08
2	0,13	0,19	0,09	0,11	0,15	0,27	0,15	0,35	0,25	0,17	0,06	0,20	0,08	0,27	0,23	0,16	0,16	0,30
3	0,09	0,10	0,07	0,07	0,09	0,11	0,10	0,21	0,09	0,06	0,04	0,05	0,04	0,15	0,08	0,07	0,08	0,15
4	0,13	0,14	0,11	0,09	0,17	0,29	0,18	0,34	0,34	0,25	0,06	0,23	0,09	0,29	0,31	0,22	0,19	0,35
5	0,05	0,06	0,06	0,12	0,05	0,08	0,06	0,10	0,08	0,10	0,02	0,07	0,05	0,07	0,07	0,07	0,06	0,09
6	0,16	0,09	0,07	0,07	0,09	0,21	0,10	0,20	0,17	0,15	0,03	0,14	0,05	0,16	0,18	0,10	0,10	0,16
7	0,06	0,08	0,06	0,05	0,06	0,09	0,06	0,12	0,11	0,11	0,02	0,09	0,05	0,11	0,11	0,08	0,08	0,17
8	0,09	0,11	0,09	0,08	0,09	0,18	0,09	0,21	0,20	0,17	0,03	0,12	0,05	0,15	0,29	0,12	0,12	0,17
9	0,10	0,14	0,09	0,11	0,09	0,18	0,09	0,23	0,14	0,12	0,04	0,09	0,05	0,16	0,12	0,11	0,10	0,18
10	0,25	0,32	0,18	0,18	0,25	0,39	0,27	0,61	0,49	0,38	0,09	0,42	0,13	0,44	0,49	0,26	0,31	0,58
11	0,08	0,08	0,08	0,06	0,06	0,11	0,06	0,13	0,09	0,09	0,02	0,04	0,04	0,09	0,09	0,09	0,08	0,15
12	0,29	0,35	0,29	0,19	0,28	0,45	0,29	0,70	0,66	0,37	0,10	0,44	0,16	0,50	0,63	0,35	0,32	0,70
13	0,11	0,09	0,10	0,09	0,10	0,14	0,09	0,21	0,16	0,16	0,04	0,15	0,06	0,14	0,15	0,11	0,10	0,18
14	0,26	0,23	0,14	0,13	0,18	0,40	0,17	0,38	0,30	0,17	0,06	0,22	0,09	0,32	0,26	0,18	0,21	0,34
15	0,05	0,07	0,06	0,06	0,06	0,14	0,06	0,15	0,12	0,11	0,03	0,07	0,04	0,09	0,09	0,08	0,06	0,14
16	0,41	0,18	0,13	0,09	0,12	0,27	0,12	0,29	0,25	0,19	0,05	0,20	0,07	0,16	0,24	0,13	0,15	0,27
17	0,03	0,04	0,04	0,02	0,03	0,05	0,03	0,06	0,06	0,06	0,02	0,04	0,02	0,05	0,05	0,04	0,04	0,04
18	0,14	0,16	0,11	0,12	0,14	0,23	0,15	0,29	0,26	0,23	0,07	0,19	0,08	0,23	0,22	0,15	0,15	0,25
19	0,05	0,06	0,06	0,05	0,03	0,07	0,04	0,06	0,05	0,06	0,02	0,04	0,03	0,05	0,06	0,05	0,04	0,19
20	0,12	0,09	0,11	0,09	0,06	0,10	0,07	0,09	0,07	0,07	0,06	0,07	0,06	0,09	0,07	0,07	0,07	0,24
21	0,39	0,44	0,51	0,31	0,28	0,53	0,26	0,34	0,33	0,16	0,12	0,19	0,19	0,38	0,25	0,27	0,25	0,82
22	0,13	0,14	0,09	0,10	0,12	0,18	0,12	0,23	0,21	0,21	0,04	0,16	0,07	0,19	0,19	0,14	0,15	0,38
23	0,15	0,19	0,14	0,14	0,14	0,36	0,13	0,24	0,22	0,11	0,06	0,13	0,08	0,23	0,16	0,15	0,13	0,44
24	0,11	0,12	0,08	0,09	0,10	0,20	0,10	0,18	0,16	0,11	0,04	0,13	0,06	0,17	0,16	0,12	0,11	0,27
25	0,21	0,30	0,20	0,17	0,23	0,31	0,22	0,39	0,43	0,18	0,08	0,28	0,12	0,34	0,31	0,25	0,28	0,59
26	0,07	0,07	0,07	0,06	0,05	0,11	0,05	0,10	0,06	0,08	0,05	0,06	0,06	0,07	0,05	0,07	0,07	0,14
27	0,25	0,29	0,19	0,20	0,24	0,41	0,24	0,26	0,27	0,10	0,09	0,24	0,13	0,29	0,19	0,25	0,25	0,25
28	0,07	0,07	0,05	0,05	0,06	0,11	0,05	0,11	0,08	0,08	0,03	0,06	0,04	0,09	0,09	0,07	0,06	0,08
29	0,08	0,09	0,07	0,07	0,08	0,12	0,08	0,16	0,13	0,13	0,04	0,08	0,04	0,12	0,11	0,10	0,11	0,20
30	0,08	0,11	0,09	0,07	0,08	0,15	0,08	0,17	0,14	0,11	0,03	0,10	0,05	0,14	0,15	0,11	0,10	0,15
31	0,07	0,09	0,08	0,06	0,06	0,13	0,05	0,12	0,10	0,07	0,02	0,07	0,03	0,10	0,10	0,08	0,05	0,08
32	0,16	0,21	0,15	0,14	0,18	0,22	0,16	0,34	0,30	0,16	0,07	0,22	0,09	0,23	0,25	0,19	0,19	0,36

Supplementary Table D.24 – Descriptive statistics of the human sperm samples used in the PathScan Intracellular Signaling Array and the intensity patterns of the 16 phosphorylated signaling proteins and cleavage of the 2 apoptosis proteins analyzed. The intensity from the negative control within each PathScan Intracellular Signaling array was subtracted from all signals, and all data from each array were normalized to the internal positive control within each array.

Parameter	N	Minimum	Maximum	Mean	Std. Dev.
Age (years)	30	19	47	30.6	6.9
Varicocele (presence/absence)	32	0	1	0.19	0.40
Sexual Abstinence (days)	32	1	10	4	2.1
Volume (ml)	32	0.7	7.7	3.4	1.7
Concentration ($x10^6$/ml)	32	2	197	51	49
Total Number of Spermatozoa ($x10^6$)	32	2	756	163	175
Motility (%)	29	37	115	67	19
Progressive Motility (%)	29	18	82	52	19
Non-Progressive Motility (%)	29	5	50	15	8.8
Immotile (%)	29	11	66	34	18
Normal morphology (%)	29	3	18	8	4
Head Defects (%)	29	43	100	75	16
Midpiece Defects (%)	29	6	67	40	12
Tail Defects (%)	29	4	49	25	10
Teratozoospermia índex (TZI)	32	1	1.99	1.52	0.24
Sperm DNA Fragmentation (SDF) (%)	32	7	49	17.16	10.54
Erk1/2 (T202/Y204)	32	0.03	0.41	0.14	0.10
Stat1 (Y701)	32	0.04	0.44	0.15	0.10
Stat3 (Y705)	32	0.04	0.51	0.115	0.09
Akt (T308)	32	0.02	0.31	0.10	0.06
Akt (S473)	32	0.03	0.28	0.12	0.07
AMPKa (T172)	32	0.05	0.53	0.21	0.13
S6 Ribosomal Protein (S235/236)	32	0.03	0.29	0.12	0.07
mTOR (S2448)	32	0.06	0.70	0.23	0.15
HSP27 (S78)	32	0.05	0.66	0.20	0.14
Bad (S112)	32	0.06	0.38	0.14	0.08
p70 S6 Kinase (T389)	32	0.02	0.12	0.05	0.03
PRAS40 (T246)	32	0.04	0.44	0.145	0.10
p53 (S15)	32	0.02	0.19	0.07	0.04
p38 (T180/Y182)	32	0.05	0.50	0.185	0.12
SAPK/JNK (T183/Y185)	32	0.05	0.63	0.18	0.13
PARP D214 Cleavage	32	0.04	0.35	0.135	0.08
Caspase-3 D175 Cleavage	32	0.04	0.32	0.13	0.08
GSK3b (S9)	32	0.04	0.82	0.27	0.19

Supplementary Table D.25 – Characterization of the human sperm samples used in the Kinetworks™ Protein Kinase Screen 1.2 (KPKS-1.2). NZ, Normozoospermic.

Sample	Concentration ($x10^6$/mL)	Motility		
		Progressive (%)	Non-progressive (%)	Immotile (%)
NZ	125	45	16	39
	112	44	7	49
	258	43	17	40
	68	55	10	35
	127	43	9	48

Supplementary Table D26 – Proteins analyzed by the Kinetworks™ Protein Kinase Screen 1.2 (KPKS-1.2).

ABBREVIATION	FULL NAME	ANTIBODY	SITE	TYPE	REACTIVITY			MW		REFERENCE LINKS	
Target Protein Name	Full Target Protein Name	Code	Pan (Human Site)	Ab (species)	H	M	R	Predicted UniProt	Kinexus Target Size	Refseq	Swissprot
Aurora A (AIK)	Aurora Kinase A (serine/threonine protein kinase 6)	NK008-2	Pan-specific	RpAb	T	T	F	39,28	45-50	NP_940835	O14965
BMX (Etk)	Bone marrow X protein-tyrosine kinase	NK012	Pan-specific	MmAb	T	T	T	78,011	69-75	NP_001712	P51813
Btk	Bruton's agammaglobulinemia tyrosine kinase	NK014	Pan-specific	RpAb	T	T	F	76,281	63-69	NP_000052	Q06187
CaMK1d	Calcium/calmodulin-dependent protein-serine kinase 1 delta	NK016-2	Pan-specific	GpAb	T	T	T	40,189	39-45	NP_003647	Q8IU85
CaMK4	Calcium/calmodulin-dependent protein-serine kinase 4	NK021	Pan-specific	RpAb	T	T	T	52		NP_001735	Q16566
CaMKK (CaMKK2)	Calcium/calmodulin-dependent protein-serine kinase kinase	NK022	Pan-specific	RpAb	T	T	T	55,736	50-55	NP_006540	Q8N5S9
CDK1 (CDC2)	Cyclin-dependent protein-serine kinase 1	NK025-2	Pan-specific	MmAb	T	T	T	34,095	24-28	NP_001777	P06493
CDK2	Cyclin-dependent protein-serine kinase 2	NK026-3	Pan-specific	MmAb	T	T	T	33,93	24-29	NP_001789	P24941
CDK4	Cyclin-dependent protein-serine kinase 4	NK027	Pan-specific	MmAb	T	T	T	33,73	23-29	NP_000066	P11802
CDK5	Cyclin-dependent protein-serine kinase 5	NK028-1	Pan-specific	RpAb	T	T	T	33,305	22-28	NP_004926	Q00535
CDK6	Cyclin-dependent protein-serine kinase 6	NK029	Pan-specific	MmAb	T	T	T	37	32-37	NP_001250	Q00534
CDK7	Cyclin-dependent protein-serine kinase 7	NK030-2	Pan-specific	MmAb	T	T	T	39,038	34-38	NP_001790	P50613
CDK9	Cyclin-dependent protein-serine kinase 9	NK032	Pan-specific	RpAb	T	T	T	42,792	33-37	NP_001252	P50750
CK1d	Casein protein-serine kinase 1 delta	NK036	Pan-specific	GpAb	T	T	T	47,33	37-43	NP_001884	P48730
CK1e	Casein protein-serine kinase 1 epsilon	NK037	Pan-specific	MmAb	T	T	T	47,315	32-37	NP_001885	P49674
CK2a	Casein protein-serine kinase 2 alpha/ alpha prime	NK041	Pan-specific	RpAb	T	T	T	45 + 41	32-36 + 34-38 + 36-40	NP_001887	P68400
COT	Osaka thyroid oncogene protein-serine kinase (Tpl2)	NK042	Pan-specific	RpAb	T	T	T	52,898	50-56	NP_005195	P41279
Csk	C-terminus of Src tyrosine	NK044	Pan-specific	MmAb	T	T	T	50,704	41-47	NP_004374	P41240

ABBREVIATION	FULL NAME	ANTIBODY	SITE	TYPE	REACTIVITY			MW		REFERENCE LINKS	
Target Protein Name	Full Target Protein Name	Code	Pan (Human Site)	Ab (species)	H	M	R	Predicted UniProt	Kinexus Target Size	Refseq	Swissprot
	kinase										
DNAPK	DNA-activated protein-serine kinase	NK048	Pan-specific	RpAb	T	T	T	469,14	215-300	NP_008835	P78527
eEF2K	Elongation factor-2 protein-serine kinase	NK051	Pan-specific	RpAb	T	T	T	82,172	100-106	NP 037434	O00418
Erk2	Extracellular regulated protein-serine kinase 2 (p42 MAP kinase)	NK056	Pan-specific	RpAb	T	T	T	41,39	36-41 + 38-43	NP_002736	P28482
Erk3	Extracellular regulated protein-serine kinase 3	NK057-2	Pan-specific	RpAb	T	T	T	82,681	51-55 + 53-58	NP_002739	Q16659
FAK	Focal adhesion protein-tyrosine kinase	NK060	Pan-specific	RpAb	T	T	T	119,233	112-126	NP_005598	Q05397
Fyn	Fyn proto-oncogene-encoded protein-tyrosine kinase	NK065	Pan-specific	MmAb	T	T	T	60,631	43-48 + 45-50	NP_002028	P06241
GCK	Germinal centre protein-serine kinase	NK066	Pan-specific	GpAb	T	T	T	91,586	80-89	NP_004570	Q12851
GRK2 (BARK1)	G protein-coupled receptor-serine kinase 2	NK067	Pan-specific	RpAb	T	T	T	79,668	71-79	NP_001610	P25098
GSK3a + GSK3b	Glycogen synthase-serine kinase 3 alpha + Glycogen synthase-serine kinase 3 beta	NK069-NK070	Pan-specific	MmAb	T	T	T	51 + 47	40-45 + 34-37	NP_063937 + NP_002084	P49840 + P49841
GSK3a + GSK3b	Glycogen synthase-serine kinase 3 alpha + Glycogen synthase-serine kinase 3 beta	NK069-NK070-2	Pan-specific	MmAb	T	T	T	51 + 47	40-45 + 34-37	NP_063937 + NP_002084	P49840 + P49841
Hpk1	Hematopoetic progenitor protein-serine kinase 1	NK072	Pan-specific	GpAb	T	T	T	91,296	83-95	NP_009112	Q92918
IKKa	Inhibitor of NF-kappa-B protein-serine kinase alpha (CHUK)	NK075-3	Pan-specific	RpAb	T	T	T	84,654	80-90	NP_001269	O15111
IKKb	Inhibitor of NF-kappa-B protein-serine kinase beta	NK076-1	Pan-specific	RpAb	T	T	T	86,564	83-90	NP_001547	O14920
JAK1	Janus protein-tyrosine kinase 1	NK084-2	Pan-specific	RpAb	T	T	T	131,957	115-124	NP_002218	P23458
JAK2	Janus protein-tyrosine kinase 2	NK085	Pan-specific	RpAb	T	T	T	130,674	105-124	NP_004963	O60674
JNK1/2/3	Jun N-terminus protein-serine kinases (stress-activated protein kinase (SAPK)) 1/2/3	NK088-1	Pan-specific	RpAb	T	T	T	44+48+53	36-42 + 43-49	NP_002741	P45983
Ksr1	Protein-serine kinase suppressor of Ras 1	NK090	Pan-specific	RpAb	T	T	T	71,671	90-97	AAC50354.1	Q8IVT5
Lck	Lymphocyte-specific protein-	NK092-2	Pan-specific	MmAb	T	T	T	57,869	41-47	NP_005347	P06239

ABBREVIATION	FULL NAME	ANTIBODY	SITE	TYPE	REACTIVITY			MW		REFERENCE LINKS	
Target Protein Name	Full Target Protein Name	Code	Pan (Human Site)	Ab (species)	H	M	R	Predicted UniProt	Kinexus Target Size	Refseq	Swissprot
	tyrosine kinase										
Lyn	Yes-related protein-tyrosine kinase	NK095	Pan-specific	MmAb	T	T	T	58,443	44-48	NP_002341	P07948
MEK1 (MAP2K1)	MAPK/ERK protein-serine kinase 1 (MKK1)	NK099-1	Pan-specific	MmAb	T	T	T	43,308	37-43	NP_002746	Q02750
MEK2 (MAP2K2)	MAPK/ERK protein-serine kinase 2 (MKK2)	NK100-1	Pan-specific	MmAb	T	T	T	44,424	37-43	AAH00471.1	P36507
MEK4 (MAP2K4)	MAPK/ERK protein-serine kinase 4 (MKK4)	NK103	Pan-specific	RpAb	T	T	T	44,288	34-40	NP_003001	P45985
MEK6 (MAP2K6)	MAPK/ERK protein-serine kinase 6 (MKK6)	NK105-1	Pan-specific	RpAb	T	T	T	37+ 31	31-36	NP_002749	P52564
Mnk2	MAP kinase-interacting protein-serine kinase 2 (calmodulin-activated)	NK111	Pan-specific	GpAb	T	F	F	46,615	51-56	NP_060042	Q9HBH9
MST1	Mammalian STE20-like protein-serine kinase 1 (KRS2)	NK113-2	Pan-specific	MmAb	T	T	T	55,63	57-59	NP_006273	Q13043
p38a MAPK	Mitogen-activated protein-serine kinase p38 alpha	NK120-3	Pan-specific	RpAb	T	T	T	41,293	36-41	NP_001306	Q16539
p38g MAPK (Erk6)	Mitogen-activated protein-serine kinase p38 gamma (MAPK12)	NK059-1	Pan-specific	RpAb	T	T	T	41,94	38-40	NP_002960	P53778
PAK1	p21-activated kinase 1 (alpha) (serine/threonine-protein kinase PAK 1)	NK122	Pan-specific	RpAb	T	T	T	60,661	63-69	NP_002567	Q13153
PAK3	p21-activated kinase 3 (beta) (serine/threonine-protein kinase PAK 3)	NK123	Pan-specific	GpAb	T	T	T	60,693	58-63	NP_002569	O75914
PDK1	3-phosphoinositide-dependent protein-serine kinase 1	NK126-2	Pan-specific	GpAb	T	T	T	63,152	48-55	NP_002604	O15530
PKA Ca/b	cAMP-dependent protein-serine kinase catalytic subunit alpha/beta	NK127-1	Pan-specific	MmAb	T	T	T	40/ 40	35-40	NP_002721	P17612
PKBa (Akt1)	Protein-serine kinase B alpha	NK129	Pan-specific	MmAb	T	T	T	55,716	56-60 + 58-63	NP_005154	P31749
PKCa	Protein-serine kinase C alpha	NK132	Pan-specific	MmAb	T	T	T	76,764	73-82	NP_002728	P17252
PKCb1	Protein-serine kinase C beta 1	NK133	Pan-specific	RpAb	T	T	T	76,869	74-82	NP_002729	P05771
PKCd	Protein-serine kinase C delta	NK135	Pan-specific	RpAb	T	T	T	77,477	70-74	NP_006245	Q05655
PKCe	Protein-serine kinase C epsilon	NK136	Pan-specific	RpAb	T	T	T	83,674	88-95 + 93-101	NP_005391	Q02156
PKCg	Protein-serine kinase C gamma	NK137	Pan-specific	RpAb	T	T	T	78,448	72-80	NP_002730	P05129

ABBREVIATION	FULL NAME	ANTIBODY	SITE	TYPE	REACTIVITY			MW		REFERENCE LINKS	
Target Protein Name	Full Target Protein Name	Code	Pan (Human Site)	Ab (species)	H	M	R	Predicted UniProt	Kinexus Target Size	Refseq	Swissprot
PKCl/i	Protein-serine kinase C lambda/iota	NK138	Pan-specific	RpAb	T	T	T	67,258	74-80	NP_002731	P41743
PKCm (PKD)	Protein-serine kinase C mu (Protein kinase D)	NK142	Pan-specific	RpAb	T	T	T	101,888	106-112 + 110-117	NP_002733	Q15139
PKCq	Protein-serine kinase C theta	NK140	Pan-specific	MmAb	T	T	T	81,865	69-76	NP_006248	Q04759
PKCz	Protein-serine kinase C zeta	NK141	Pan-specific	RpAb	T	T	T	67,718	74-84 + 79-86	NP_002735	Q05513
PKG1	Protein-serine kinase G1 (cGMP-dependent protein kinase)	NK143	Pan-specific	RpAb	T	T	T	76 + 79	69-74	NP_006249	Q13976
PKR1	Double stranded RNA dependent protein-serine kinase	NK144-1	Pan-specific	MmAb	T	T	T	62,094	75-76	NP_002750	P19525
Pyk2	Protein-tyrosine kinase 2	NK154	Pan-specific	GpAb	T	T	T	115,875	110-113	NP_004094	Q14289
Raf1	Raf1 proto-oncogene-encoded protein-serine kinase	NK155-3	Pan-specific	RpAb	T	N/A	T	73,052		NP_002871	P04049
RafB (Braf)	RafB proto-oncogene-encoded protein-serine kinase	NK156	Pan-specific	RpAb	T	T	T	84,491	93-98	NP_004324	P15056
ROKa (ROCK2)	RhoA protein-serine kinase alpha	NK159-1	Pan-specific	MmAb	T	T	T	160,913	149-163	NP_004841	O75116
RSK1	Ribosomal S6 protein-serine kinase 1	NK164	Pan-specific	RpAb	T	T	T	82,723	72-84 + 79-88	NP_002944	Q15418
RSK2	Ribosomal S6 protein-serine kinase 2	NK165	Pan-specific	RpAb	T	T	T	83,736	69-78 + 75-83	NP_004577	P51812
S6Ka (p70 S6Ka) + S6Ka (p85 S6Ka)	p70 ribosomal protein-serine S6 kinase alpha + p85 ribosomal protein-serine S6 kinase alpha	NK168-NK169-1	Pan-specific	MmAb	T	T	T	70	60-72 + 78-83	NP_003152	P23443
Src	Src proto-oncogene-encoded protein-tyrosine kinase	NK172	Pan-specific	MmAb	T	T	T	59,704	45-50	NP_005408	P12931
Syk	Spleen protein-tyrosine kinase	NK174	Pan-specific	MmAb	T	T	T	72,066	65-68	NP_003168	P43405
Yes	Yamaguchi sarcoma proto-oncogene-encoded tyrosine kinase	NK186	Pan-specific	MmAb	T	T	T	60,801	52-57	NP_005424	P07947
ZAP70	Zeta-chain (TCR) associated protein-tyrosine kinase, 70 kDa	NK187	Pan-specific	MmAb	T	T	T	69,872	61-65	NP_003168	P43403
ZIPK	ZIP kinase (death associated protein-serine kinase 3 (DAPK3))	NK188-2	Pan-specific	RpAb	T	T	T	52,536	41-46 + 44-49	NP_001339	O43293

Supplementary Table D.27 – Age, basic semen parameters and expression patterns of 18 signaling molecules when phosphorylated or cleaved of 63 random men.

Volunteer	Age (years)	Volume (ml)	Concentration ($x10^6$/mL)	No. Spermatozoa ($x10^6$)	Motility (%)				Morphology (%)			
					Total	Progressive	Non-progressive	Immotile	Normal	Head	Middpiece	Tail
1	35	7,70	20,00	158,00	89,00	82,00	7,00	11,00	6,00	99,00	67,00	4,00
2	36	2,50	91,00	228,00	89,00	73,00	16,00	11,00	9,00	100,00	56,00	16,00
3	33	7,00	18,00	129,00	81,00	62,00	19,00	19,00	9,00	91,00	37,00	16,00
4	33	4,00	24,00	97,00	39,00	32,00	7,00	61,00	4,00	99,00	60,00	22,00
5	35	3,20	20,00	64,00	70,00	53,00	17,00	30,00	5,00	99,00	65,00	21,00
6	35	7,00	2,00	14,00					3,00	89,00	49,00	37,00
7	36	5,10	49,00	250,00	56,00	30,00	26,00	44,00	6,00	90,00	52,00	23,00
8	39	3,20	9,00	29,00	44,00	18,00	26,00	56,00	3,00	70,00	40,00	27,00
9	32	3,30	95,00	314,00	41,00	23,00	18,00	59,00	6,00	58,00	39,00	19,00
10	36	3,00	13,00	39,00	49,00	32,00	17,00	51,00	10,00	84,00	41,00	19,00
11	31	4,70	9,00	42,00	37,00	27,00	10,00	63,00	16,00	43,00	34,00	23,00
12	35	3,20	29,00	93,00	58,00	35,00	23,00	42,00	5,00	79,00	33,00	24,00
13	29	1,50	2,00	3,00					6,00	70,00	45,00	39,00
14	25	3,00	59,00	177,00	82,00	69,00	13,00	18,00	7,00	79,00	32,00	30,00
15	20	4,00	24,00	96,00	76,00	60,00	16,00	24,00	4,00	76,00	40,00	49,00
16	36	0,90	2,00	1,80					2,00	80,00	45,00	40,00
17	34	4,00	8,00	32,00	44,00	30,00	14,00	56,00	7,00	78,00	40,00	20,00
18	47	4,00	94,00	376,00	78,00	72,00	6,00	22,00	11,00	50,00	32,00	49,00
19	32	3,00	197,00	591,00	81,00	76,00	5,00	19,00	18,00	44,00	31,00	24,00
20	39	0,70	57,00	40,00	65,00	45,00	20,00	35,00	12,00	73,00	44,00	20,00
21	32	4,20	4,00	17,00	54,00	39,00	15,00	46,00	5,00	79,00	39,00	27,00
22	19	4,30	22,00	95,00	62,00	50,00	12,00	38,00	5,00	72,00	31,00	21,00
23	29	2,30	30,00	69,00	57,00	48,00	9,00	43,00	6,00	77,00	47,00	39,00
24	28	3,00	90,00	270,00	62,00	52,00	10,00	38,00	7,00	64,00	39,00	28,00
25	26	2,20	13,00	29,00	44,00	33,00	11,00	66,00	4,00	84,00	43,00	40,00
26	22	1,70	67,00	114,00	85,00	76,00	9,00	15,00	14,00	75,00	6,00	28,00
27	21	3,00	140,00	420,00	83,00	68,00	15,00	17,00	5,00	81,00	44,00	29,00
28	24	2,50	110,00	275,00	87,00	75,00	12,00	13,00	6,00	80,00	47,00	21,00
29	20	1,00	60,00	60,00	64,00	43,00	21,00	36,00	5,00	78,00	32,00	37,00
30	20	2,10	58,00	122,00	115,00	65,00	50,00	15,00	12,00	60,00	30,00	21,00
31	28	2,50	86,00	215,00	79,00	72,00	7,00	21,00	12,00	54,00	31,00	30,00
32	22	0,70	35,00	24,50	74,00	37,00	37,00	50,00	9,00	59,00	49,00	42,00
33	22	1,00	90,00	90,00	61,00	49,00	12,00	39,00	17,00	50,00	49,00	37,00
34	20	2,20	35,00	77,00	39,00	28,00	11,00	51,00	18,00	71,00	38,00	28,00
35	20	3,00	35,00	105,00	63,00	49,00	14,00	37,00	17,00	63,00	39,00	18,00
36	24	3,10	31,00	96,10	27,00	16,00	11,00	73,00	4,00	79,00	60,00	51,00
37	24	5,00	61,00	305,00	41,00	18,00	23,00	59,00	4,00	83,00	69,00	60,00

Volunteer	Age (years)	Volume (ml)	Concentration ($x10^6$/mL)	No. Spermatozoa ($x10^6$)	Motility (%)				Morphology (%)			
					Total	Progressive	Non-progressive	Immotile	Normal	Head	Middpiece	Tail
38	24	3,60	50,00	180,00	36,00	30,00	6,00	63,00	6,00	65,00	43,00	43,00
39	25	1,20	19,00	22,80	19,00	4,00	15,00	81,00	5,00	77,00	34,00	39,00
40	25	3,30	26,00	85,80	29,00	14,00	15,00	71,00	6,00	71,00	52,00	44,00
41	25	3,80	20,00	76,00	40,00	24,00	16,00	60,00	7,00	60,00	49,00	32,00
42	18	3,10	56,00	173,60	69,00	41,00	28,00	31,00	13,00	60,00	44,00	21,00
43	18	7,00	74,00	518,00	40,00	15,00	25,00	60,00	4,00	90,00	40,00	33,00
44	18	3,80	95,00	361,00	68,00	59,00	9,00	32,00	8,00	80,00	34,00	12,00
45	20	2,80	113,00	316,40	89,00	51,00	38,00	11,00	18,00	70,00	47,00	38,00
46	20	2,10	194,00	407,40	82,00	46,00	36,00	17,00	18,00	60,00	41,00	30,00
47	20	3,50	120,00	420,00	69,00	56,00	13,00	31,00	19,00	71,00	36,00	15,00
48	25	2,60	27,00	70,20	41,00	26,00	15,00	59,00	10,00	69,00	50,00	39,00
49	23	5,50	23,00	115,00	42,00	12,00	30,00	58,00				
50	23	4,00	55,00	220,00	26,00	6,00	20,00	74,00				
51	23	1,60	46,00	73,60	44,00	33,00	11,00	56,00	10,00	65,00	39,00	45,00
52	23	4,00	25,00	100,00	60,00	39,00	21,00	40,00	12,00	51,00	39,00	30,00
53	23	2,10	42,00	88,20	42,00	31,00	11,00	58,00				
54	20	5,00	40,00	200,00	78,00	71,00	7,00	22,00				
55	20	2,00	74,00	148,00	51,00	31,00	20,00	49,00				
56	22	0,70	35,00	24,50	74,00	37,00	37,00	50,00	9,00	59,00	49,00	42,00
57	22	6,00	29,00	174,00	68,00	50,00	18,00	32,00	13,00	70,00	51,00	29,00
58	22	5,50	67,00	368,50	78,00	59,00	19,00	22,00	22,00	60,00	42,00	20,00
59	20	1,30	111,00	144,30	84,00	80,00	4,00	16,00	7,00	63,00	42,00	21,00
60	22	2,50	28,00	70,00	38,00	24,00	14,00	62,00	10,00	74,00	36,00	20,00
61	22	3,20	23,00	73,60	29,00	20,00	9,00	71,00	9,00	81,00	34,00	29,00
62	23	5,60	24,00	134,40	85,00	56,00	29,00	15,00	3,00	88,00	30,00	19,00
63	23	6,80	19,00	129,20	45,00	26,00	19,00	55,00	2,00	91,00	51,00	20,00

Volunteer	PathScan® Intracellular Signaling Array																	
	Erk1/2 (T202/Y204)	Stat1 (Y701)	Stat3 (Y705)	Akt (T308)	Akt (S473)	AMPKa (T172)	S6 Ribosomal Protein (S235/236)	mTOR (S2448)	HSP27 (S78)	Bad (S112)	p70 S6 Kinase (T389)	PRAS40 (T246)	p53 (S15)	p38 (T180/Y182)	SAPK/JNK (T183/Y185)	PARP (D214)	Caspase-3 (D175)	GSK-3b (S9)
1	0,05	0,05	0,05	0,04	0,04	0,05	0,04	0,07	0,07	0,07	0,02	0,07	0,03	0,06	0,06	0,06	0,05	0,08
2	0,13	0,19	0,09	0,11	0,15	0,27	0,15	0,35	0,25	0,17	0,06	0,20	0,08	0,27	0,23	0,16	0,16	0,30
3	0,09	0,10	0,07	0,07	0,09	0,11	0,10	0,21	0,09	0,06	0,04	0,05	0,04	0,15	0,08	0,07	0,08	0,15
4	0,13	0,14	0,11	0,09	0,17	0,29	0,18	0,34	0,34	0,25	0,06	0,23	0,09	0,29	0,31	0,22	0,19	0,35
5	0,05	0,06	0,06	0,12	0,05	0,08	0,06	0,10	0,08	0,10	0,02	0,07	0,05	0,07	0,07	0,07	0,06	0,09
6	0,16	0,09	0,07	0,07	0,09	0,21	0,10	0,20	0,17	0,15	0,03	0,14	0,05	0,16	0,18	0,10	0,10	0,16
7	0,06	0,08	0,06	0,05	0,06	0,09	0,06	0,12	0,11	0,11	0,02	0,09	0,05	0,11	0,11	0,08	0,08	0,17
8	0,09	0,11	0,09	0,08	0,09	0,18	0,09	0,21	0,20	0,17	0,03	0,12	0,05	0,15	0,29	0,12	0,12	0,17
9	0,10	0,14	0,09	0,11	0,09	0,18	0,09	0,23	0,14	0,12	0,04	0,09	0,05	0,16	0,12	0,11	0,10	0,18
10	0,25	0,32	0,18	0,18	0,25	0,39	0,27	0,61	0,49	0,38	0,09	0,42	0,13	0,44	0,49	0,26	0,31	0,58
11	0,29	0,35	0,29	0,19	0,28	0,45	0,29	0,70	0,66	0,37	0,10	0,44	0,16	0,50	0,63	0,35	0,32	0,70
12	0,11	0,09	0,10	0,09	0,10	0,14	0,09	0,21	0,16	0,16	0,04	0,15	0,06	0,14	0,15	0,11	0,10	0,18
13	0,26	0,23	0,14	0,13	0,18	0,40	0,17	0,38	0,30	0,17	0,06	0,22	0,09	0,32	0,26	0,18	0,21	0,34
14	0,05	0,07	0,06	0,06	0,06	0,14	0,06	0,15	0,12	0,11	0,03	0,07	0,04	0,09	0,09	0,08	0,06	0,14
15	0,41	0,18	0,13	0,09	0,12	0,27	0,12	0,29	0,25	0,19	0,05	0,20	0,07	0,16	0,24	0,13	0,15	0,27
16	0,03	0,04	0,04	0,02	0,03	0,05	0,03	0,06	0,06	0,06	0,02	0,04	0,02	0,05	0,05	0,04	0,04	0,04
17	0,14	0,16	0,11	0,12	0,14	0,23	0,15	0,29	0,26	0,23	0,07	0,19	0,08	0,23	0,22	0,15	0,15	0,25
18	0,05	0,06	0,06	0,05	0,03	0,07	0,04	0,06	0,05	0,06	0,02	0,04	0,03	0,05	0,06	0,05	0,04	0,19
19	0,12	0,09	0,11	0,09	0,06	0,10	0,07	0,09	0,07	0,07	0,06	0,07	0,06	0,09	0,07	0,07	0,07	0,24
20	0,39	0,44	0,51	0,31	0,28	0,53	0,26	0,34	0,33	0,16	0,12	0,19	0,19	0,38	0,25	0,27	0,25	0,82
21	0,13	0,14	0,09	0,10	0,12	0,18	0,12	0,23	0,21	0,21	0,04	0,16	0,07	0,19	0,19	0,14	0,15	0,38
22	0,15	0,19	0,14	0,14	0,14	0,36	0,13	0,24	0,22	0,11	0,06	0,13	0,08	0,23	0,16	0,15	0,13	0,44
23	0,11	0,12	0,08	0,09	0,10	0,20	0,10	0,18	0,16	0,11	0,04	0,13	0,06	0,17	0,16	0,12	0,11	0,27
24	0,21	0,30	0,20	0,17	0,23	0,31	0,22	0,39	0,43	0,18	0,08	0,28	0,12	0,34	0,31	0,25	0,28	0,59
25	0,07	0,07	0,07	0,06	0,05	0,11	0,05	0,10	0,06	0,08	0,05	0,06	0,06	0,07	0,05	0,07	0,07	0,14
26	0,25	0,29	0,19	0,20	0,24	0,41	0,24	0,26	0,27	0,10	0,09	0,24	0,13	0,29	0,19	0,25	0,25	0,25
27	0,07	0,07	0,05	0,05	0,06	0,11	0,05	0,11	0,08	0,08	0,03	0,06	0,04	0,09	0,09	0,07	0,06	0,08
28	0,08	0,09	0,07	0,07	0,08	0,12	0,08	0,16	0,13	0,13	0,04	0,08	0,04	0,12	0,11	0,10	0,11	0,20
29	0,08	0,11	0,09	0,07	0,08	0,15	0,08	0,17	0,14	0,11	0,03	0,10	0,05	0,14	0,15	0,11	0,10	0,15
30	0,07	0,09	0,08	0,06	0,06	0,13	0,05	0,12	0,10	0,07	0,02	0,07	0,03	0,10	0,10	0,08	0,05	0,08
31	0,16	0,21	0,15	0,14	0,18	0,22	0,16	0,34	0,30	0,16	0,07	0,22	0,09	0,23	0,25	0,19	0,19	0,36
32	0,09	0,13	0,09	0,09	0,05	0,11	0,07	0,07	0,10	0,07	0,02	0,04	0,02	0,05	0,07	0,06	0,04	0,23
33	0,09	0,13	0,08	0,10	0,05	0,10	0,06	0,07	0,09	0,06	0,03	0,03	0,02	0,04	0,07	0,06	0,04	0,23

Volunteer	PathScan® Intracellular Signaling Array																	
	Erk1/2 (T202/Y204)	Stat1 (Y701)	Stat3 (Y705)	Akt (T308)	Akt (S473)	AMPKa (T172)	S6 Ribosomal Protein (S235/236)	mTOR (S2448)	HSP27 (S78)	Bad (S112)	p70 S6 Kinase (T389)	PRAS40 (T246)	p53 (S15)	p38 (T180/Y182)	SAPK/JNK (T183/Y185)	PARP (D214)	Caspase-3 (D175)	GSK-3b (S9)
34	0,12	0,07	0,09	0,08	0,05	0,07	0,06	0,06	0,05	0,05	0,03	0,04	0,01	0,04	0,12	0,06	0,04	0,07
35	0,15	0,07	0,10	0,10	0,06	0,09	0,07	0,07	0,04	0,06	0,04	0,03	0,02	0,04	0,10	0,05	0,04	0,05
36	0,09	0,07	0,12	0,09	0,05	0,12	0,06	0,08	0,04	0,06	0,03	0,03	0,02	0,04	0,10	0,09	0,08	0,10
37	0,14	0,08	0,20	0,12	0,06	0,20	0,09	0,13	0,09	0,09	0,06	0,05	0,02	0,07	0,13	0,09	0,06	0,23
38	0,09	0,07	0,08	0,06	0,04	0,05	0,06	0,05	0,04	0,05	0,03	0,04	0,01	0,04	0,09	0,06	0,04	0,08
39	0,13	0,08	0,19	0,14	0,05	0,19	0,08	0,12	0,12	0,09	0,04	0,04	0,02	0,05	0,11	0,09	0,05	0,17
40	0,14	0,06	0,08	0,07	0,05	0,09	0,05	0,06	0,05	0,06	0,01	0,05	0,02	0,05	0,12	0,08	0,05	0,09
41	0,09	0,06	0,07	0,07	0,06	0,08	0,07	0,07	0,06	0,08	0,03	0,04	0,03	0,06	0,11	0,09	0,07	0,07
42	0,10	0,08	0,13	0,11	0,05	0,12	0,07	0,10	0,07	0,07	0,03	0,04	0,02	0,05	0,11	0,08	0,04	0,17
43	0,11	0,07	0,10	0,09	0,05	0,10	0,05	0,08	0,07	0,06	0,04	0,04	0,01	0,05	0,09	0,07	0,04	0,37
44	0,14	0,14	0,10	0,12	0,07	0,10	0,10	0,09	0,13	0,13	0,03	0,08	0,03	0,06	0,17	0,11	0,06	0,21
45	0,12	0,30	0,10	0,10	0,05	0,13	0,06	0,07	0,05	0,05	0,02	0,03	0,01	0,03	0,07	0,04	0,03	0,10
46	0,07	0,23	0,09	0,09	0,03	0,13	0,06	0,08	0,06	0,03	0,02	0,03	0,01	0,03	0,11	0,05	0,03	0,12
47	0,13	0,27	0,11	0,12	0,06	0,21	0,07	0,08	0,06	0,06	0,03	0,05	0,03	0,06	0,10	0,08	0,05	0,08
48	0,09	0,05	0,07	0,08	0,03	0,10	0,05	0,08	0,05	0,06	0,01	0,03	0,02	0,05	0,07	0,08	0,05	0,08
49	0,08	0,05	0,07	0,07	0,03	0,09	0,04	0,07	0,05	0,06	0,02	0,03	0,02	0,04	0,07	0,07	0,04	0,09
50	0,16	0,09	0,13	0,13	0,05	0,16	0,09	0,13	0,11	0,11	0,04	0,08	0,04	0,10	0,11	0,13	0,09	0,23
51	0,07	0,07	0,06	0,05	0,03	0,07	0,05	0,06	0,04	0,05	0,03	0,04	0,02	0,05	0,07	0,06	0,06	0,06
52	0,13	0,07	0,11	0,11	0,05	0,15	0,08	0,11	0,07	0,09	0,04	0,05	0,03	0,08	0,09	0,13	0,09	0,09
53	0,09	0,10	0,10	0,08	0,04	0,18	0,05	0,09	0,06	0,08	0,02	0,02	0,02	0,07	0,07	0,11	0,08	0,07
54	0,15	0,13	0,10	0,10	0,07	0,13	0,09	0,10	0,09	0,12	0,03	0,08	0,03	0,09	0,11	0,14	0,09	0,13
55	0,11	0,05	0,06	0,06	0,04	0,07	0,05	0,07	0,05	0,06	0,03	0,03	0,02	0,06	0,06	0,07	0,07	0,06
56	0,10	0,05	0,06	0,06	0,04	0,06	0,04	0,06	0,04	0,05	0,01	0,03	0,02	0,05	0,07	0,08	0,05	0,05
57	0,12	0,08	0,10	0,12	0,05	0,13	0,06	0,10	0,05	0,08	0,04	0,03	0,02	0,07	0,10	0,11	0,09	0,08
58	0,10	0,05	0,10	0,10	0,05	0,14	0,06	0,10	0,06	0,09	0,02	0,05	0,03	0,06	0,08	0,10	0,06	0,08
59	0,13	0,05	0,04	0,04	0,02	0,07	0,04	0,04	0,02	0,04	0,01	0,01	0,00	0,07	0,04	0,07	0,06	0,04
60	0,10	0,06	0,14	0,14	0,04	0,16	0,08	0,13	0,12	0,11	0,03	0,06	0,03	0,08	0,12	0,13	0,08	0,10
61	0,08	0,05	0,07	0,07	0,03	0,08	0,05	0,08	0,08	0,07	0,02	0,03	0,02	0,05	0,08	0,10	0,05	0,09
62	0,06	0,04	0,04	0,04	0,03	0,03	0,04	0,04	0,04	0,06	0,02	0,04	0,02	0,05	0,07	0,08	0,06	0,05
63	0,09	0,07	0,16	0,12	0,04	0,22	0,08	0,14	0,08	0,09	0,03	0,05	0,04	0,07	0,06	0,11	0,07	0,06

Supplementary Table D.28 – Descriptive statistics of the intensity patterns of the 16 phosphorylated signaling proteins and cleavage of the 2 apoptosis proteins analyzed. The intensity from the negative control within each PathScan Intracellular Signaling array was subtracted from all signals, and all data from each array were normalized to the internal positive control within each array.

Parameter	Minimum	Maximum	Mean	SD
Age	18	47	26	7
Erk1/2 (T202/Y204)	0,05	0,41	0,12	0,07
Stat1 (Y701)	0,04	0,44	0,12	0,09
Stat3 (Y705)	0,04	0,51	0,11	0,07
Akt (T308)	0,04	0,31	0,10	0,05
Akt (S473)	0,02	0,28	0,08	0,06
AMPKa (T172)	0,03	0,50	0,16	0,10
S6 Ribosomal Protein (S235/236)	0,04	0,29	0,09	0,06
mTOR (S2448)	0,04	0,70	0,16	0,13
HSP27 (S78)	0,02	0,66	0,13	0,12
Bad (S112)	0,03	0,38	0,11	0,07
p70 S6 Kinase (T389)	0,01	0,12	0,04	0,02
PRAS40 (T246)	0,01	0,44	0,09	0,09
p53 (S15)	0,00	0,19	0,05	0,04
p38 (T180/Y182)	0,03	0,50	0,12	0,10
SAPK/JNK (T183/Y185)	0,04	0,63	0,14	0,10
PARP (D214)	0,04	0,35	0,11	0,06
Caspase-3 (D175)	0,03	0,32	0,09	0,07
GSK-3b (S9)	0,04	0,82	0,19	0,16